Probing the Mechanism of the Cytochrome P-450 Catalysed Dealkylation of Amides

Thesis

UNRESTRICTED

PROBING THE MECHANISM OF THE CYTOCHROME P-450 CATALYSED DEALKYLATION OF AMIDES

A thesis submitted by:

Roberto Tolando

in partial fulfilment of the requirements

for the Degree of Doctor of Philosophy

of the Open University

DEPARTMENT OF CHEMISTRY

THE OPEN UNIVERSITY

OCTOBER 1997

Date of submission: 27th October 1997
Date of award: 5th February 1998

ACKNOWLEDGEMENTS

I would like to thank Dr. Jim Iley for his endless encouragement and advice during my three year post-graduate study and in the writing the this thesis.

I would like also thanks Dr. Charlie Harding of the Open University and Prof. Aldo Tomasi of the University of Modena for their help and advice on the ESR experiments. My thanks also to Dr. Maurizio Manno and Dr. Roberta Ferrara of the University of Padua for their kindness on the supplying the microsomes and for the useful discussion on the results of the DMF studies. I would also thanks the Open University of the financial support over the period of my research.

My thanks are also extended to the technical staff of the Chemistry Department of the Open University for the help and advice.

Finally, I would like say thank-you to Kika for the patience and encouragement all over these three years and to my parents and my brother for their endless support throughout my academic career.

Abstract

Cytochrome P-450 (P450) metabolises N,N-dialkylamides to their corresponding N-dealkylated products *via* formation of an N-hydroxyalkyl-N-alkylamide intermediate. The first-step of these oxidative dealkylations, has been studied both by the use of probe substrates able to trap intramolecularly the reactive intermediate, and also by the use of the intermolecular spin trapping agent PBN, together with ESR analysis. The results obtained indicate that oxidative dealkylation of amides occurs *via* hydrogen atom abstraction from the alkyl carbon atom α- to the amide nitrogen leading to the formation of a carbon-centred radical intermediate. Such an intermediate can subsequently undergo hydroxyl group insertion, from the activated haem-oxygen complex of P450, to give the N-hydroxyalkyl intermediate. No evidence for an iminium ion intermediate was obtained. Dealkylation of chiral substrates reveals little stereoselectivity in the dealkylation reactions. In contrast, by using fixed-conformation probe substrates, a regioselectivity for the oxidation of the Z- group was observed. Comparison of these results with those of a biomimetic system and with semi-empirical M.O. calculations suggests that these reactions are kinetically rather than thermodynamically driven. Finally, the effects of the generation of a carbon-centred radical intermediate during amide metabolism on the P450 enzyme system were analysed. Oxidation of N,N-dimethylformamide and N,N-dimethylacetamide results in the inactivation of the metabolising enzyme. PBN, but not ascorbic acid or glutathione, protects against this inactivation. Such inactivation is due to the carbon-centred radical species attacking the prosthetic haem group of the enzyme, resulting in the formation of a modified haem that retains its tetrapyrrolic structure. The modified haem can be synthesised from haemin by reaction with a chemically-generated α-carbon-centred radical. The full characterisation of the structure of the modified haem requires further work, but preliminary studies reveal it to be the result of attack at the vinyl or meso positions of the haem rather than at the pyrrolic nitrogen atoms.

CONTENTS

ABBREVIATIONS

AIBN	Azobis(cyclohexane-carbonitrile)
AMCC	N-acetyl-(S-(N-methylcarbamoyl))cysteine
BMB	N-benzyl-N-methylbenzamide
Bu	Butyl
DMAC	N,N-Dimethylacetamide
DMB	N,N-Dimethylbenzamide
DMF	N,N-Dimethylformamide
ΔH_f	Heat of formation
$\Delta\Delta Hf$	Differences of heats of formation
ESR	Electron spin resonance
FAD	Flavin adenine dinucleotide, oxidised form
$FADH_2$	Flavin adenine dinucleotide, reduced form
FMN	Flavin adenine nucleotide, oxidised form
$FMNH_2$	Flavin adenine nucleotide, reduced form
GC	Gas chromatography
GCMS	Gas chromatography mass spectroscopy
GSH	Glutathione, reduced form
HPLC	High performance liquid chromatography

IR	Infra-red spectroscopy
K_m	Michaelis -Menten constant
M.O.	Molecular orbital
m.p.	Melting point
MS	Mass spectroscopy
MTBSTFA	N-methyl-N-*tert*-butyldimethylsilyltrifluoroacetamide
NADP	Nicotine adenine dinucleotide phosphate, oxidised form
NADPH	Nicotine adenine dinucleotide phosphate, reduced form
NMF	N-methylformamide
PBN	N-*tert*-butyl-α-phenylnitrone
$P450_{cam}$	Bacterial cytochrome P450 responsible for the metabolism of camphor
SMG	S-(N-methylcarbamoyl)glutathione
SOD	Superoxide dismutase
$TPPFe^{(III)}$	tetraphenylporphirinatoiron (III) chloride
UV	Ultra-violet spectroscopy
V_{max}	Maximum reaction velocity

CHAPTER 1

Introduction

In this introduction the following will be discussed:

- the constitution of the cytochrome P450-containing monooxygenase system (P450)
- characteristics of substrate binding
- biomimetic system of P450
- mechanistic features of some reactions catalysed by P450
- amides as substrates for P450

The utilisation of oxygen is a function that most living organisms, both unicellular prokaryotic or large multicellular eukaryotics, must be able to perform. Such organisms must be capable of oxygen insertion into a wide variety of molecules in order both to anabolize the compounds necessary for structure building and energy utilisation and catabolize noxious compounds for ready disposal. Well over 200 enzymes are known to utilise dioxygen as substrate.[1; 2] Many such reactions are carried out by enzymes containing a haem prosthetic group at their active site.

Oxygen utilising enzymes have been divided into two categories based on whether oxygen atoms from dioxygen are directly incorporated into the substrate (the oxygenases) or whether the substrate is oxidised without oxygen incorporation (the oxidases). The oxygenases have been further subdivided into the dioxygenases, which incorporate both dioxygen atoms into the organic substrate, and the mono-oxygenases, which only incorporate one oxygen atom with the other being concomitantly reduced to water.

The group of mono-oxygenase enzymes known as the cytochromes P-450 monooxygenase system has been the subject of intense investigation over the last 30

years, due primarily to the important role play in a wide variety of living process, as well as to particular features of their structures and of the chemistry they carry out.

1.1 Constitution of the cytochrome (P450)-containing mono-oxygenase system

P450s are a class of lipophilic enzymes located in the endoplasmic reticulum of cells. Most methods used to elucidate the constitution of the P450-containing oxygenase system have followed three main steps: purification of mammalian liver subcellular preparation (microsomes), solubilization of the enzyme system and experiments involving reconstitution of the oxygenase activity. It is generally agreed that two membrane-bound protein components, the haem P450 and an NADPH-dependent flavin containing P450 reductase are needed for reconstituting the NADPH-linked oxidation activity.

1.1.1 Cytochrome P450

In mammals, cytochrome P450 enzymes are found mainly in the endoplasmic reticulum of the liver and in the mitochondria of the adrenal cortex. However, they are also present in many other organs and tissues including the lung, kidney, testes, ovary, brain, placenta, pancreas, spleen, intestine, skin and nasal epithelium. Other than the liver, kidney and adrenal cortex, the role of P450 in many of these organs is poorly understood. As a group P450 operates on an apparently unlimited number of compounds, being responsible, more than any other enzyme system, for initiating biotransformation.

P450s are members of a large family of haem-containing enzymes that are the terminal monooxygenases for the metabolism of a large number and variety of endogenous substrates and xenobiotics.[3; 4] P450 is recognised as a superfamily of monooxygenases displaying wide substrate acceptability. Recent updates on new sequences list 146 members of the P450 superfamily.[5] This is consistent with the diversity observed in biological compartmentalisation: in most bacteria, the forms are soluble; in eukaryotic organisms, most are membrane bound. The term "cytochrome

P450" refers to a family of isomeric enzymes (or isozymes) constituted by a polypeptide chain with an approximate molecular weight of 50 kDa that contains an iron^{III} protophorphyrin IX prosthetic group (Figure 1.1). A cysteine residue of the polypeptide presents a thiolate ion that can ligate to the haem iron in one of the axial positions, while the other axial position is usually occupied by a molecule of water.

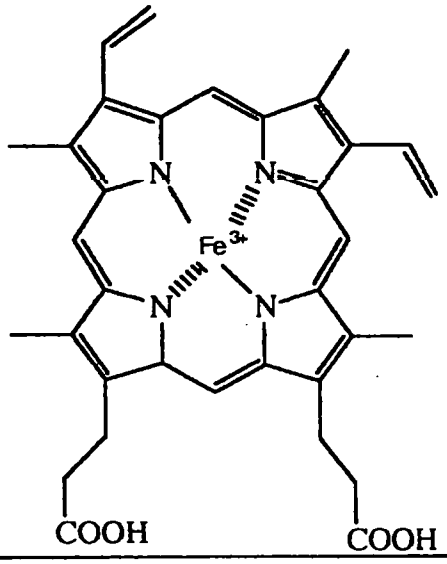

Figure 1.1 Haem group (protoporphyrin IX).

The common characteristic of these isozymes is the absorption in the UV spectrum at 450 nm of the reduced P450-carbon monoxide (CO) complex. Indeed, the prefix "P" refers to their pigment-like nature. In fact, many P450 isozymes form CO complexes that absorb at wavelengths slightly shifted from 450 nm, with an overall range lying between 447 and 452 nm. The absorption maximum at around 450 nm (known as the Soret peak) in these cytochromes is due to an $n \rightarrow \pi^*$ electronic transition in the haemoprotein caused by the ligation of the sulfur-containing residue to the haem prosthetic group.[6]

The unusual diversity of distribution of P450s is matched by their ability to catalyse a considerable array of reactions (shown in Figure 1.2) including C-, N- and S-oxygenation, dealkylations, deaminations and dehalogenations. It is believed that the

electron-donating character of the sulfur ligand triggers the unique chemical reactivity of this enzyme system, especially the reductive cleavage of molecular oxygen and the insertion into non-activated C-H bonds.[7] This ability to oxidise a wide range of substrates has given rise to the term "mixed-function oxidases" to describe the P450 activity.

A simplified mechanism for the monoxygenase activity of P450 is as follows:

$$RH + NADPH + H^+ + O_2 \longrightarrow ROH + NADP^+ + H_2O$$

In addition to their ability of metabolise foreign compounds, their endogenous role lies in the metabolism of lipids, eicosanoids and the steroid hormones. [8]

P450 is known as an enzyme that plays a central role in either detoxification or activation of xenobiotics. Over the last twenty years it has become apparent that there are many distinct forms of P450 in liver microsomes, each of which possess overlapping but distinguishable specificity to foreign substrates.[9; 10]

The detoxification pathway is characterised by the conversion of lipid soluble foreign compounds to products that are more water soluble. This is achieved by the insertion of a polar functionality. These metabolites are then subjected to second phase conjugation reactions that generate even more polar products which are subsequently excreted *via* the urine and faeces. The P450-dependent metabolism of xenobiotics usually leads to the formation of biologically inactive metabolites. However, in certain cases such metabolism may lead to the activation of previously harmless chemicals to reactive species that may possess toxic effects

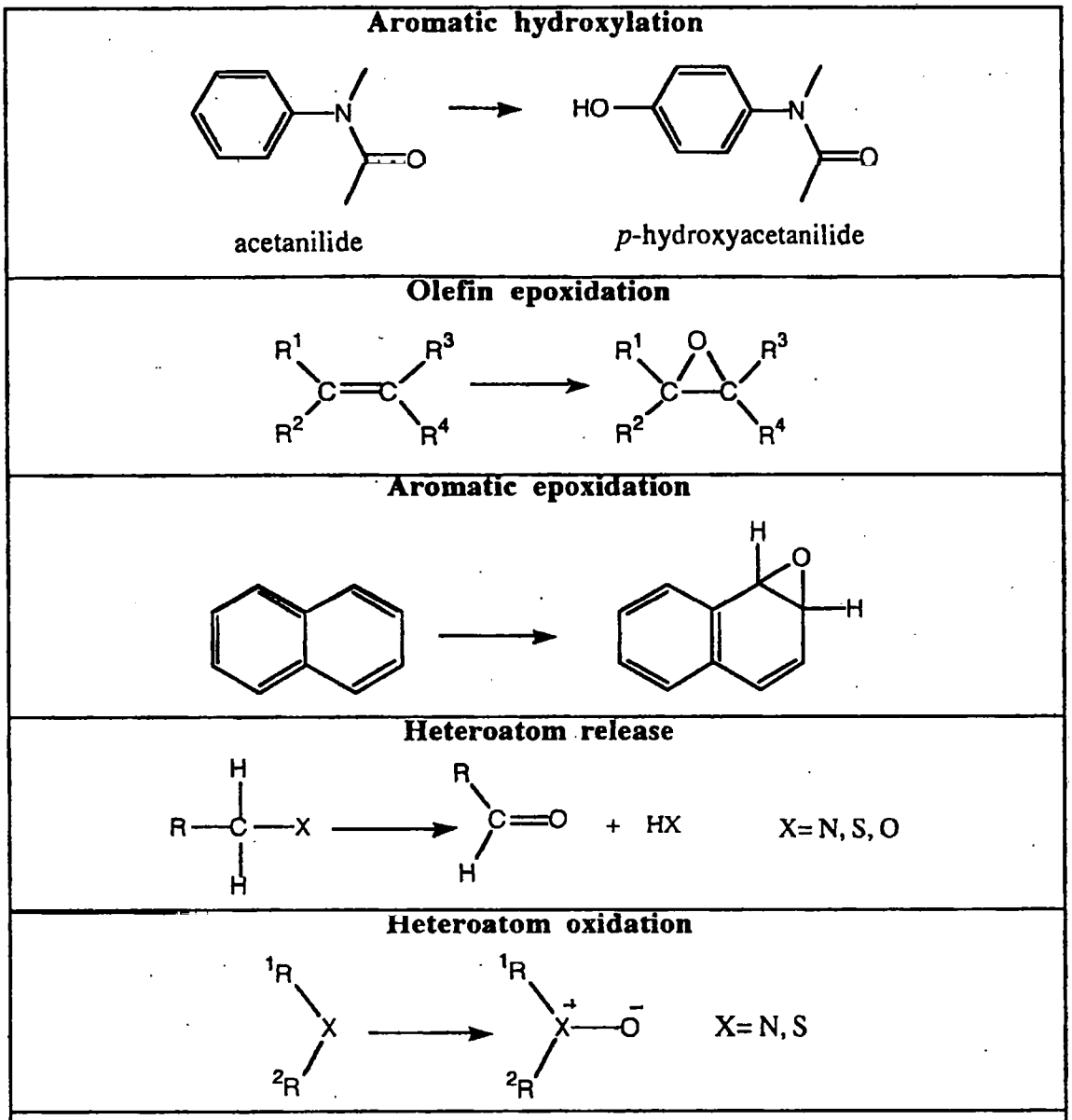

Figure 1.2 Some representative examples of P450-dependent metabolism of drugs and industrial chemicals

Though there exists, even for a single substrate, a range of P450-catalysed metabolic fates it is generally accepted that the mechanism of bioactivation to toxic metabolites involves the formation of an electrophilic species. Such species can react with cellular nucleophiles such as proteins or nucleic acids leading to an abnormal physiological state.

The basal-level P450 contents of cells may be drastically affected by a wide range of factors, including diet, living habit, physiological state and exposure to chemicals. Most, if not all, of the P450 isozymes are inducible by chemicals such as phenobarbital, 3-methylcholanthrene (3MC), pregnenolone 16-α-carbonitrile (PCN), ethanol, polychlorinated biphenyls (PCB), isosafrole and clofibrate. Such induction is of prime importance in the potentiation of the P450 dependent bioactivation of toxic chemicals. It is also of relevance regarding the presence of P450 isoforms in particular tissues, especially P450 I and P450 IIE and, to a lesser extent P450 IVA1, all which are known to be involved in activation-dependent toxicological responses.

1.1.2 The catalytic cycle of P450

An overall scheme for the P450 catalytic cycle is presented in Figure 1.3. To clarify the oxidation state of P450, the oxidised and the reduced forms are represented by Fe^{3+} and Fe^{2+}, respectively. The scheme shows seven representative states of P450, but does not include every possible state.

In the resting state P450 is in the oxidised form. The P450-catalysed reaction is considered to be initiated by substrate binding to the enzyme (step 1). Substrate binding induces conformational changes around the haem and increases the redox potential of the haem iron from -300 mV to -170 mV. Substrate-bond P450 therefore becomes more easily reduced.[11] Electrons are transferred to P450 in the substrate-bound form (step 2) from the specific electron carrier proteins that coexist with the P450s.

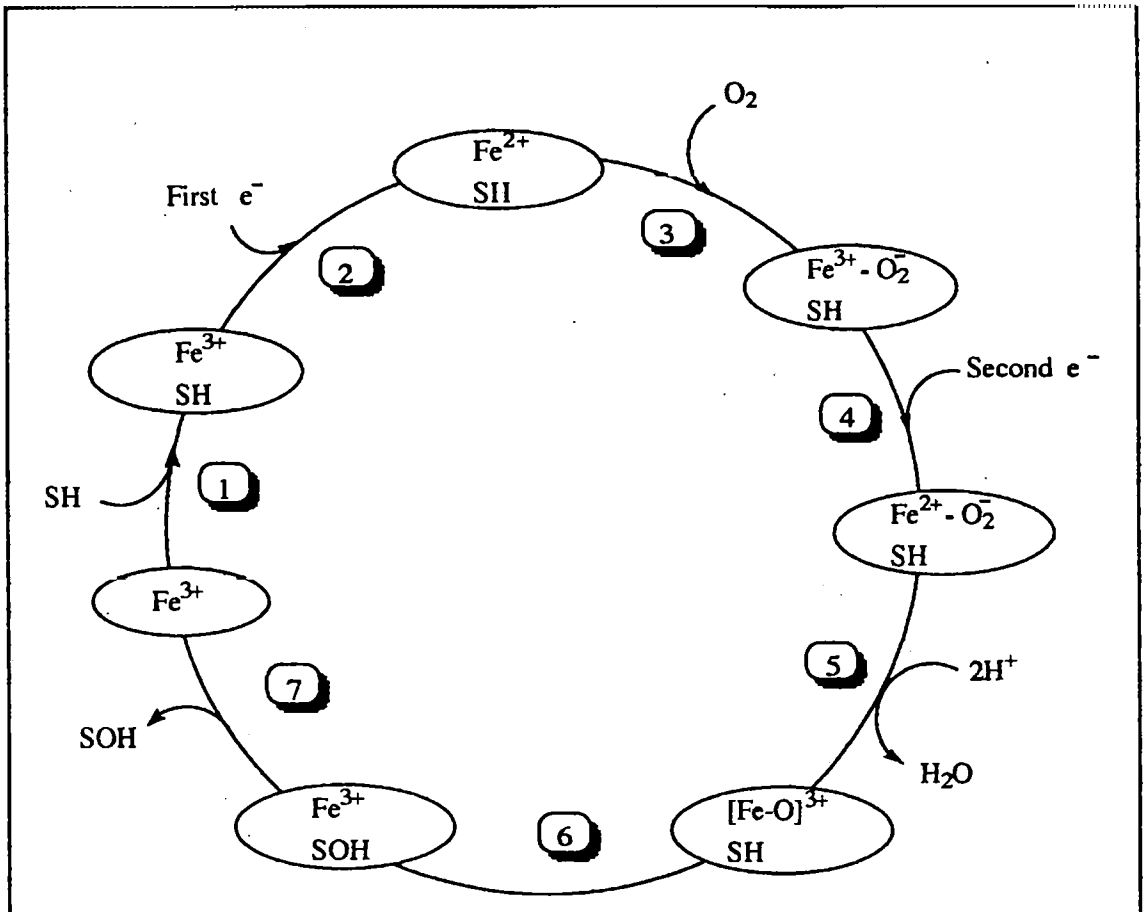

Figure 1.3. Schematic diagram of cytochrome P-450 monooxygenase reaction. SH represents a substrate and SOH is the product.

P450 in the oxidised state (SH-Fe^{3+}) has low affinity for dioxygen but in the reduced state (SH-Fe^{2+}) it has high affinity, like other haem proteins.[12] A dioxygen molecule binds to the reduced haem iron at the sixth coordination position, *trans* to the thiolate anion (step **3**). The substrate-haem-dioxygen complex may be considered as the Fe^{3+}-superoxide complex SH-Fe^{3+}-O_2^-, formally the product of intramolecular electron transfer from the Fe^{2+} centre to the dioxygen ligand. Oxygenated P450 is easily autooxidised into SH-Fe^{3+} with O_2 release.[13] However, if a second electron transfer to P450 is faster than autooxidation (step **4**), the result is the formation of SH-Fe^{2+}-O_2^-. Subsequently, step **5**, it is widely accepted that Fe^{2+}-O_2^- reacts with two protons, liberating H_2O while forming an active iron-oxo, Fe^{3+}=O, centre. The activated oxygen

atom in this functionality may react with a substrate molecule residing in close proximity, step **6**. This forms an oxygenated product that may be released, step **7**, to regenerate the initial state of P450.[14-20] Each reaction cycle usually takes 1-10 seconds in membrane-bound P450, but in some case it can take less than 0.05 seconds.[21]

1.1.3 NADPH-dependent flavin containing P450 reductase

The NADPH-cytochrome P-450 reductase is a flavoprotein, with a molecular weight of about 76 kDa, containing two prosthetic groups: FAD and FMN. The FAD group is the acceptor of the initial electron from NADPH, while the FMN group is the electron donor to P450 as summarised in Figure 1.4.[22]

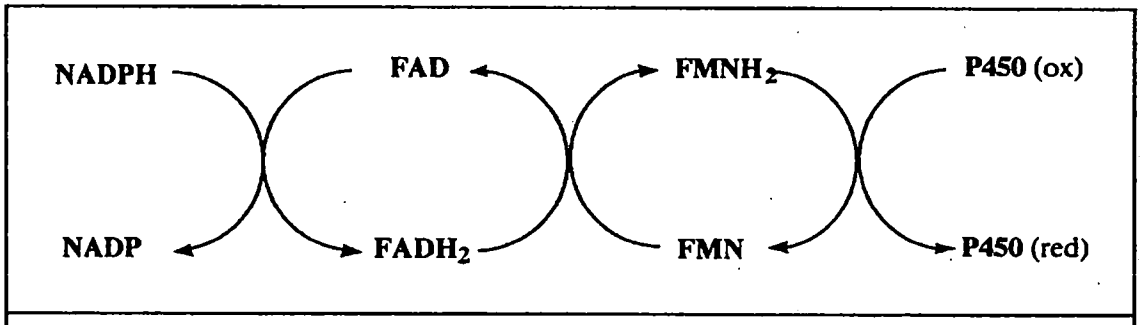

Figure 1.4 Schematic representation of the transport of electrons to P450.

However, it is also known that cytochrome b_5 can supply electrons to P450. This contribution of cytochrome b_5 appears to be different from one form of P450 to another, and also is dependent upon the characteristics of the substrates.[23]

It has been confirmed that the first electron for the reduction of ferric ion in P450 is always supplied from NADPH-cytochrome P-450 reductase, whereas the second electron for the activation of the haem-bound oxygen atoms can come from either the reductase or from the reduced cytochrome b_5, as shown in Figure 1.5.

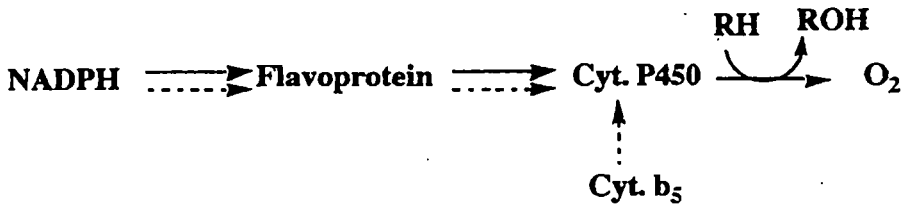

Figure 1.5 Electron transfers to the P450 mono-oxygenase system of mammalian liver microsomes. The pathway of first and second electrons are indicated by solid and broken arrows, respectively. The mono-oxygenase reaction is shown by the transformation of a substrate (RH) into its oxygenated product (ROH).

Thus, the overall characteristics of the liver mammalian cytochrome P450-mono oxygenase systems can be summarised as follows: they are (i) always found in association with the membrane of the endoplasmic reticulum (microsomes), (ii) constituted by NADPH-cytochrome P-450 reductase and cytochrome P-450, and (iii) supported by NADH cytochrome *b5* reductase and cytochrome *b5*.

1.2 Substrate-cytochrome P-450 interactions

The interaction of a substrate with P450 produces observable changes in the UV/visible spectrum arising from characteristic perturbations of the haem iron. These changes are normally determined as differences between the spectrum of oxidised microsomes plus xenobiotic agent and that of oxidised microsomes alone.[27; 28] Generally three major types of difference spectra are observed. Type I spectra, produced by compounds such as benzphetamine, biphenyl and aminopyrine,[29] are characterised by a peak at 385 nm and a trough around 420 nm. Type II spectra, produced by compounds such as aniline, *n*-octylamine and imidazole,[30] are characterised by a peak at 430 nm and a broad trough between 390 and 430 nm. Finally reverse type I spectra, produced by compounds containing an alcoholic OH group,[31] are the mirror image of type I spectra.

The importance of hydrophobic interactions between the substrate and the groups in the binding site of P450 has been demonstrated. Optical studies on substrate binding to

P450 in hepatic microsomes have shown that more lipophilic substrates bind more tightly to the enzyme.[32] Moreover, hydrophobic interactions have been shown to be a predominant force in the binding to P450 of the various substituted aryl hydroperoxides that have been used as artificial oxygen donors.[33]

1.3 Biomimetic systems of cytochrome P-450

In recent years, significant effort has been devoted to developing simple synthetic models of the active site of P450. A major requirement of such systems is the ability to perform the broad spectrum of P450-catalysed reactions, namely hydroxylation of aromatic rings, including the NIH-shift, the hydroxylation of non-activated C-H bonds, the epoxidation of double bonds and the oxidative cleavage of non-activated C-C bonds in a regio-and stereospecific manner. Synthetic tetraarylporphyrins (Figure 1.6) are recognised as one of the most efficient biomimetic systems. They are readily prepared, bind a variety of metals (M= Fe, Co, Cr, Mn, Ru and so on), and have been used extensively to model the natural haem prosthetic group protoporphyrin IX.[34; 35;36]

In these tetraarylporphyrin derivatives, bulky substituents in the *ortho*-position of the aryl rings reduce the tendency of the natural haem to agglomerate in solution and also help protect the *meso*-carbons (that is those carrying the aryl substituents) from oxidation. In addition, the inclusion of aryl groups possessing variety of substituents provides porphyrins with varying solubilities and substrate specificity. Currently, the metal$^{(III)}$ 5,10,15,20-tetraphenylporphyrines, and their aryl analogues are extensively used for modelling the reactions performed by P450s, peroxidases and catalases. A variety of metals can be used; most commonly Fe$^{(III)}$ and Mn$^{(III)}$ complexes have met with considerable success[37]

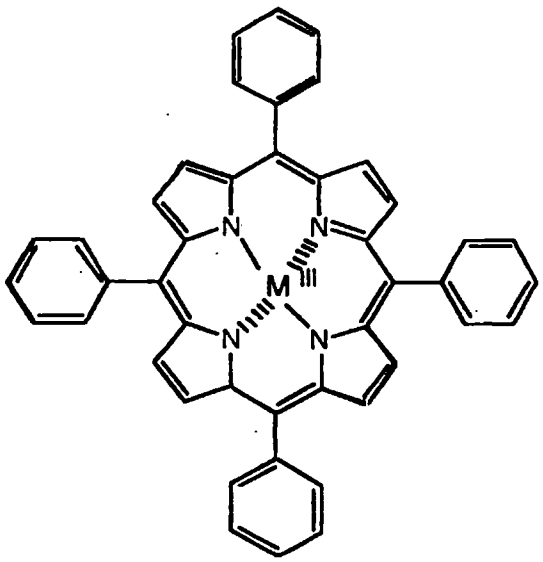

Porphines	M^{III}	Phenyl substituent		
		o	*m*	*p*
$(TPP)Fe^{III}(Cl)$	Fe	H	H	H
$(TPP)Cr^{III}(Cl)$	Cr	H	H	H
$(TPP)Mn^{III}(Cl)$	Mn	H	H	H
$(F_{20}TPP)Co^{III}(Cl)$	Co	F	F	F
$(Cl_8TPP)Fe^{III}(Cl)$	Fe	Cl	H	H
$(Cl_8TPP)Mn^{III}(Cl)$	Mn	Cl	H	H

Figure 1.6 Some examples of biomimetic metalloporphines (TTP = tetraphenylporphine; M = metal).

The success of these biomimetic systems may be judged by their ability to effect the hydroxylation of unactivated alkanes (Figure 1.7), the most difficult of P450-mediated oxidations.[38; 39; 40]

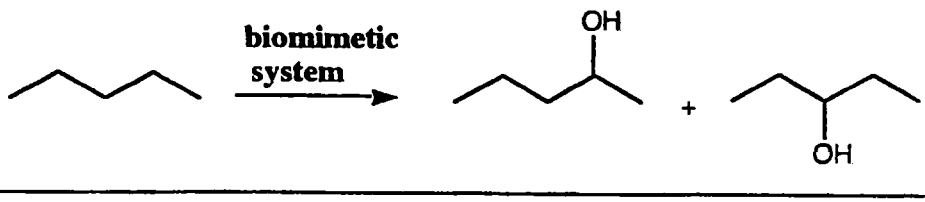

Figure 1.7 Example of hydroxylation of unactivated alkanes.

1.3.1 The porphyrin-iodosobenzene system

Groves[41] has shown that the oxidation reactions carried out by synthetic porphyrins in the presence of iodosobenzene presents similar mechanistic features to those of P450. The proposed mechanism for hydrocarbon hydroxylation involves an oxoiron (IV) porphyrin radical (Figure 1.8). This is expected to have considerable oxy radical character, allowing the abstraction of a hydrogen atom from a carbon-hydrogen bond approaching parallel to the porphyrin plane (Figure 1.9).

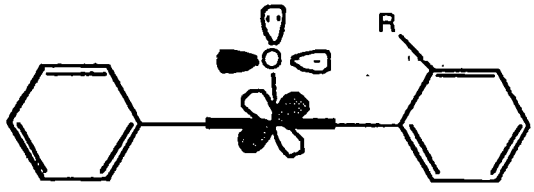

Figure 1.8 Structure of the postulated oxoiron(IV) porphyrin radical.

The shape-selectivity of the hydroxylations, and the sensitivity of these reactions to relatively small changes in the steric environment of the porphyrin periphery, were considered to be consistent with such an approach. Recombination of the Fe(IV)OH complex with the alkyl radical gives rise to the product alcohol, while occasional escape of the radical rationalises the formation of brominated products in the presence of $BrCCl_3$.

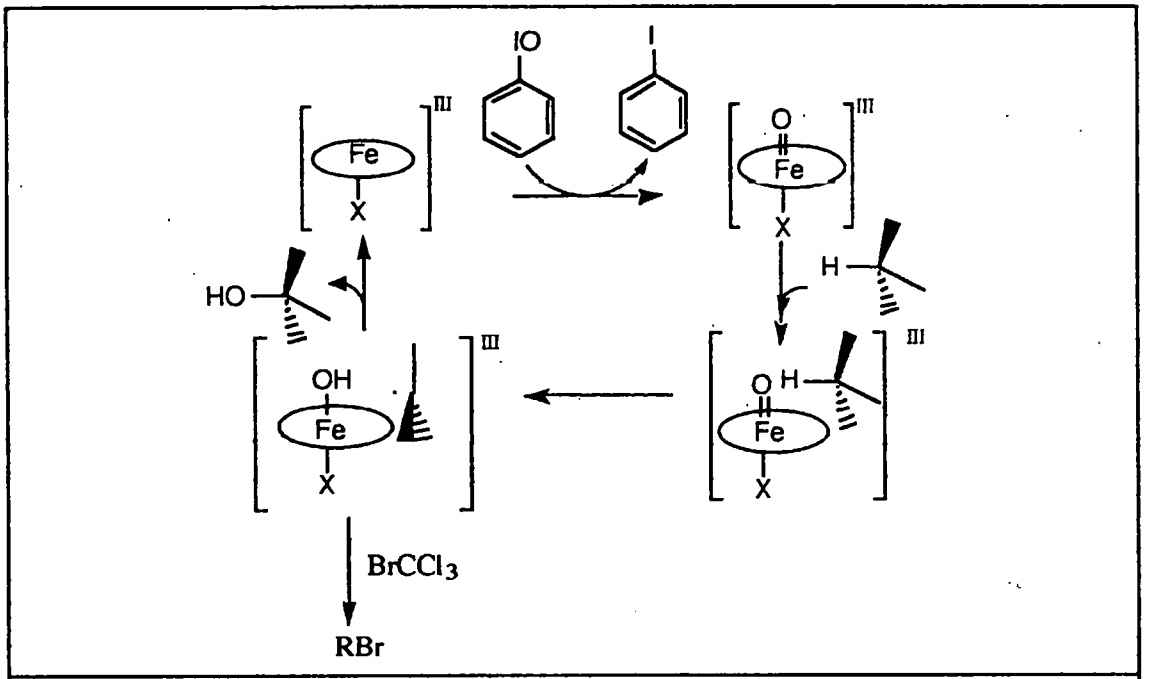

Figure 1.9 Mechanism of alkane hydroxylation catalysed by ferric porphyrins.

However, for amine dealkylation an alternative mechanism has been proposed. The presence of an intramolecular isotope effect < 3 together with the electronic effects of the R group, is interpreted as an indication that the mechanism involves the abstraction of an electron from the substrate, followed by deprotonation (Figure 1.10).[42; 43]

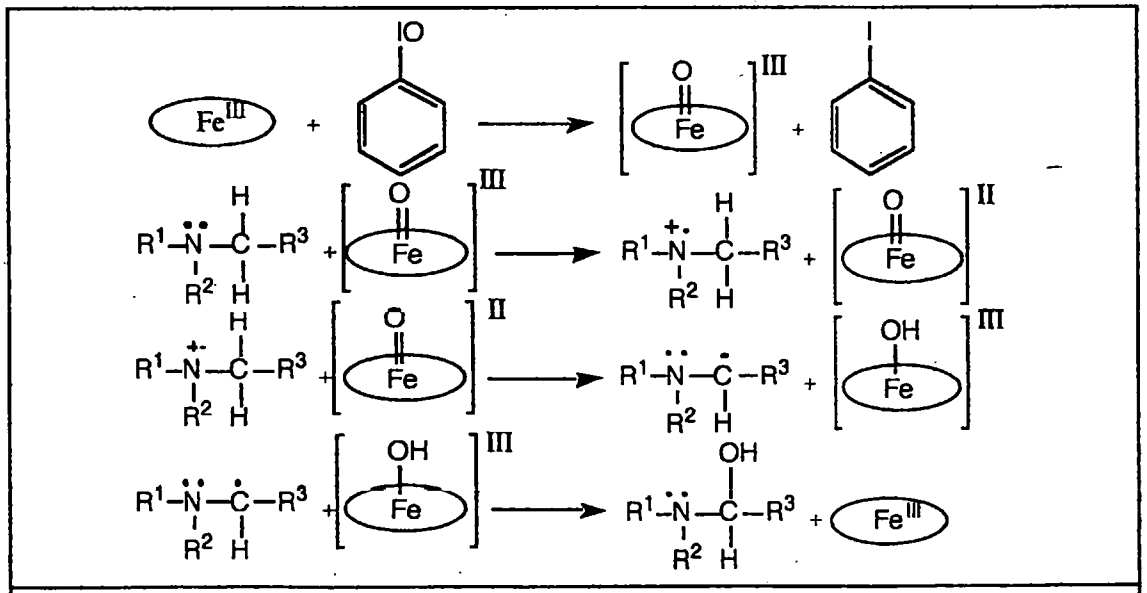

Figure 1.10 Proposed mechanism for the biomimetic oxidation reaction of amines using iodosobenzene as source of oxygen.

1.3.2 The porphyrin-alkylhydroperoxide system

Alkanes are easily hydroxylated in presence of $TPPFe^{(III)}$ and *tert*-butyl hydroperoxide,[44] whereas the epoxidation of alkenes is more difficult when compared with oxidation by $TPPFe^{(III)}$ and iodosobenzene.[45;46] Alkylhydroperoxides are also efficient oxygen sources for the metalloporphyrin-mediated oxidation of alkanes, though marked differences are observed.[47]

Unfortunately one of the major issues, namely whether the breakdown of the O-O bond in the metal-hydroperoxide complex is homolytic or heterolytic, has yet to be clarified with certainty. Homolytic breakdown will form an $[Fe{=}O]^{II}$ complex, while the heterolytic breakdown will result in the formation of an $[Fe{=}O]^{III}$ complex[44; 48; 49] (Figure 1.11).

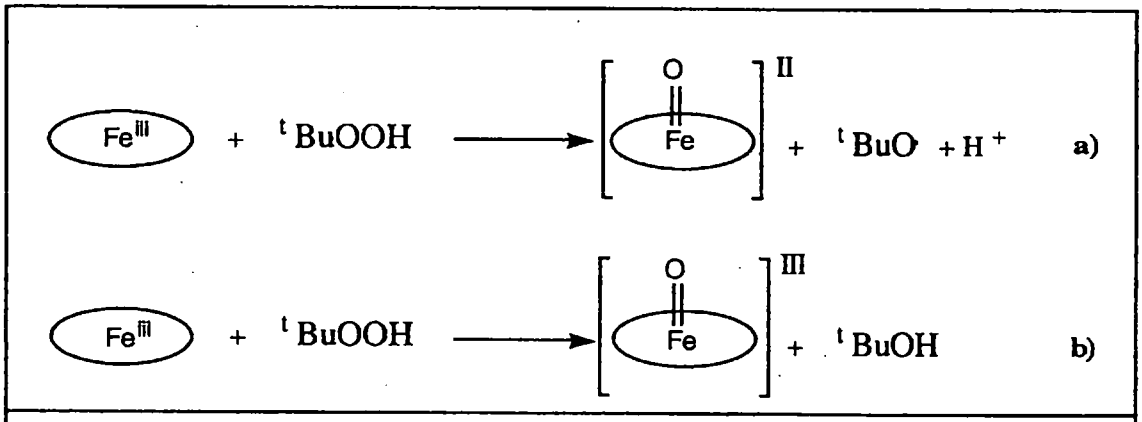

Figure 1.11 Homolytic (a) and heterolytic (b) breakdown of alkylhydroperoxides in the presence of porphyrin.

This is an important point, because the $[Fe{=}O]^{III}$ complex is able to abstract a hydrogen atom from the substrate forming an $[Fe\text{-}OH]^{II}$ species that hydroxylates the carbon-centred radical so-formed.[50; 51] Alternatively, the $[Fe\text{-}OH]^{II}$ complex is not able to abstract a hydrogen atom, but its formation, via homolytic breakdown of *tert*-butylhydroperoxide, leads to the formation of the *tert*-butoxyl radical species. This species is then able to abstract a hydrogen atom from the substrate.[52;47]

Conflicting reports exist relating to the formation of the iron-oxo species from the reaction of porphyrins with alkyl- and acylhydroperoxides (ROOH). On the one hand, Bruice[53;54] has reported that the pKa of the leaving group (RO^-) affects the reaction more for the acyl analogues. This would imply a heterolytic breakdown for acyl hydroperoxides and homolytic for alkyl hydroperoxides. On the other hand, Traylor [55] observed that in the reaction between peracids and porphyrin the cleavage of the O-O bound is heterolytic. With this assumption they compared the isotope effect and the acidity of the solvent on the reactions of porphyrins with peroxides and peracids.[48;55] Both types of peroxy compound present similar sensitivities indicating that a similar heterolytic mechanism operates for both. Moreover, these authors found that the acidity of the leaving group displays similar effects for hydroperoxides and peracids.[48; 55]

Traylor [50] has proposed a mechanism that can rationalise the heterolytic cleavage of the O-O bond with the difficulties in the oxidation of alkenes and the presence of an alkoxyl radical. Thus, heterolytic cleavage of the O-O bond generate the $[Fe{=}O]^{III}$ complex which subsequently can react with the hydroperoxide:

$$Fe^{3+} + ROOH \longrightarrow [Fe{=}O]^{III} + ROH$$

$$[Fe{=}O]^{III} + ROOH \longrightarrow [Fe\text{-}OH]^{III} + ROO$$

The system therefore generates the products anticipated from homolytic breakdown of the hydroperoxide.

Whatever the mechanistic characteristics of the cleavage of the O-O bond, it is generally accepted that in the presence of compounds like imidazole, that can bind to the centre of the porphyrin, the cleavage is heterolytic. [51; 56; 57; 58] Traylor [48] has also reported that the heterolytic mechanism can be promoted by the presence of water and alcohols. It is believed that binding of an extra ligand to the metal of the porphyrin increases the electron density of the metal.[59]

1.4 Mechanism of the P450-mediated mono-oxygenation of xenobiotics

P450 carries out oxidative reactions with typical mixed-function oxidase stoichiometry:

$$R + NAD(P)H + H^+ + O_2 \longrightarrow RO + H_2O + NAD(P)^+$$

Five types of oxidative reactions will be discussed:

- aliphatic hydroxylation,
- olefins epoxidation,
- aromatic hydroxylation,
- heteroatom release,
- heteroatom oxygenation.

During the catalytic cycle of substrate oxidation by P450 it is believed that the transfer of the oxygen atom from the enzyme to the substrate occurs from an activated iron-oxygen complex that several authors refer to as a perferryl oxygen, formally $(Fe=O)^{3+}$.[60] It has been suggested that this complex acts like an electrode, able to abstract a hydrogen atom, or electron, from the substrate.[14] The species so-generated in the porphyrin then transfers a hydroxyl group to the radical centre generated in the substrate. After oxygen addition, the oxygenated product dissociates to leave the iron in its original ferric state. The initial hydrogen atom abstraction or the electron transfer is identified as the rate-determining step of the reaction.[61]

An exception to this mechanism is represented by the situation in which the oxygen atom in the haem is unable to interact with the newly-formed substrate radical because of a rearrangement or aromatization of the substrate, as reported for 4,4-dialkyl-1,4-dihydropyridines[62] (Figure 1.12).

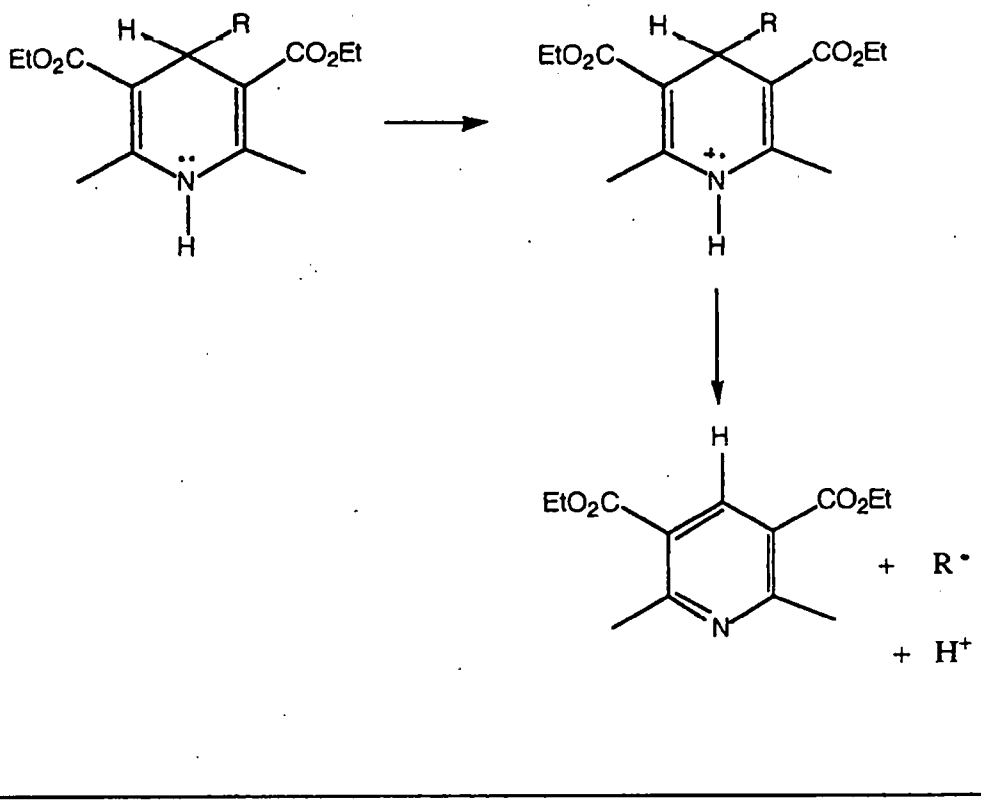

Figure 1.12. The rearrangement of intermediate cation radicals during the microsomal oxidation of 4,4-dialkyl-1,4-dihydropyridines.

1.4.1 Aliphatic hydroxylation

The hydroxylation of unactivated carbon atoms is one of the more remarkable reactions performed by P450. It is also one that has received a great deal of attention due to the critical role this transformation plays in the metabolism of numerous essential physiological as well as xenobiotic compounds. Groves,[63] in his studies on the hydroxylation of norbornane, observed large isotope effects (k_H/k_D =11.5) together with a loss of stereochemistry (postulated to be a result of radical epimerization). Isotope effects for other aliphatic hydroxylation reactions have been reported to lie in a range between 7 and 14.[63; 64]

These data suggest that alkane hydroxylation proceeds by a stepwise process involving the formation of a carbon-centred free-radical via hydrogen atom abstraction (Figure 1.13). Such a scheme is supported by mechanistic probes, as for example bicyclo [2.1.0.] pentane[65; 66] and alkylcyclopropanes,[67] able to give rearrangement after an H• abstraction.

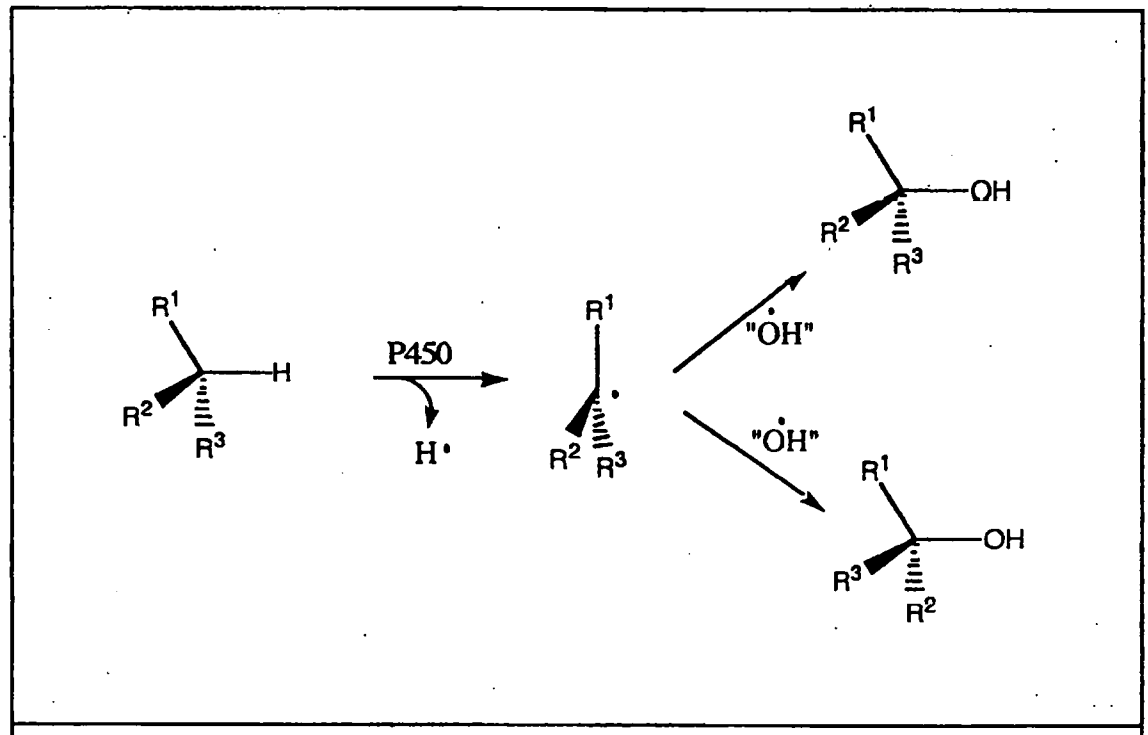

Figure 1.13. Mechanism for the P450-mediated aliphatic hydroxylation.

The slow step in the oxygen-transfer sequence is thought to be abstraction of the hydrogen atom from the alkane carbon by the perferryl oxygen. Collapse of the intermediate alkyl and iron-hydroxyl radical pair is presumably a cage reaction with a low-energy barrier. Radical reactions involve a planar radical centre. Thus, hydroxylation of aliphatic systems would be expected to involve loss of stereochemical integrity. Therefore, the stereospecificity often observed during P450-catalysed hydroxylations probably reflects physical factors associated with substrate binding in the enzyme active centre.

1.4.2 Olefin epoxidation

The transfer of oxygen to carbon-carbon π bonds proceeds with retention of olefin stereochemistry. Such retention does not unambiguously differentiate concerted from non-concerted mechanisms. However, studies on the suicide inactivation of P450 that occurs during the metabolism of unsaturated compounds, as well as on the rearrangements that accompany the metabolism of certain olefins, indicates the presence of a non-concerted mechanism in this reaction.[68] For example, synthetic epoxides were shown not to destroy the haem of P450 in cases where the destruction of P450 was observed during the oxidative metabolism of the parent olefin.[69; 70] Ortiz de Montellano has deduced the structures of several haem-olefin adducts,[71; 72; 73] which correspond to the structures expected from attack of the porphyrin pyrrolic nitrogen upon the epoxide. However, since epoxides have been shown not be involved, the adduct can only be explained by attack at the pyrrolic nitrogen of a transient enzyme intermediate.

The rearrangements observed during the oxidation of trichloroethylene to trichloroacetaldehyde, first thought to result from acid-catalysed rearrangement of the epoxide metabolite, appears to occur during the oxygen transfer reaction because synthetic trichloroethylene oxide does not rearrange to trichloroacetaldehyde, except under non physiological conditions.[74; 75]

Despite the consistent evidence for a non-concerted mechanism in the P450-dependent oxidation of olefins, the precise nature of the oxidation mechanism is still not clear. Guengerich and collaborators have postulated the mechanism summarised in Figure 1.14.[14; 76]

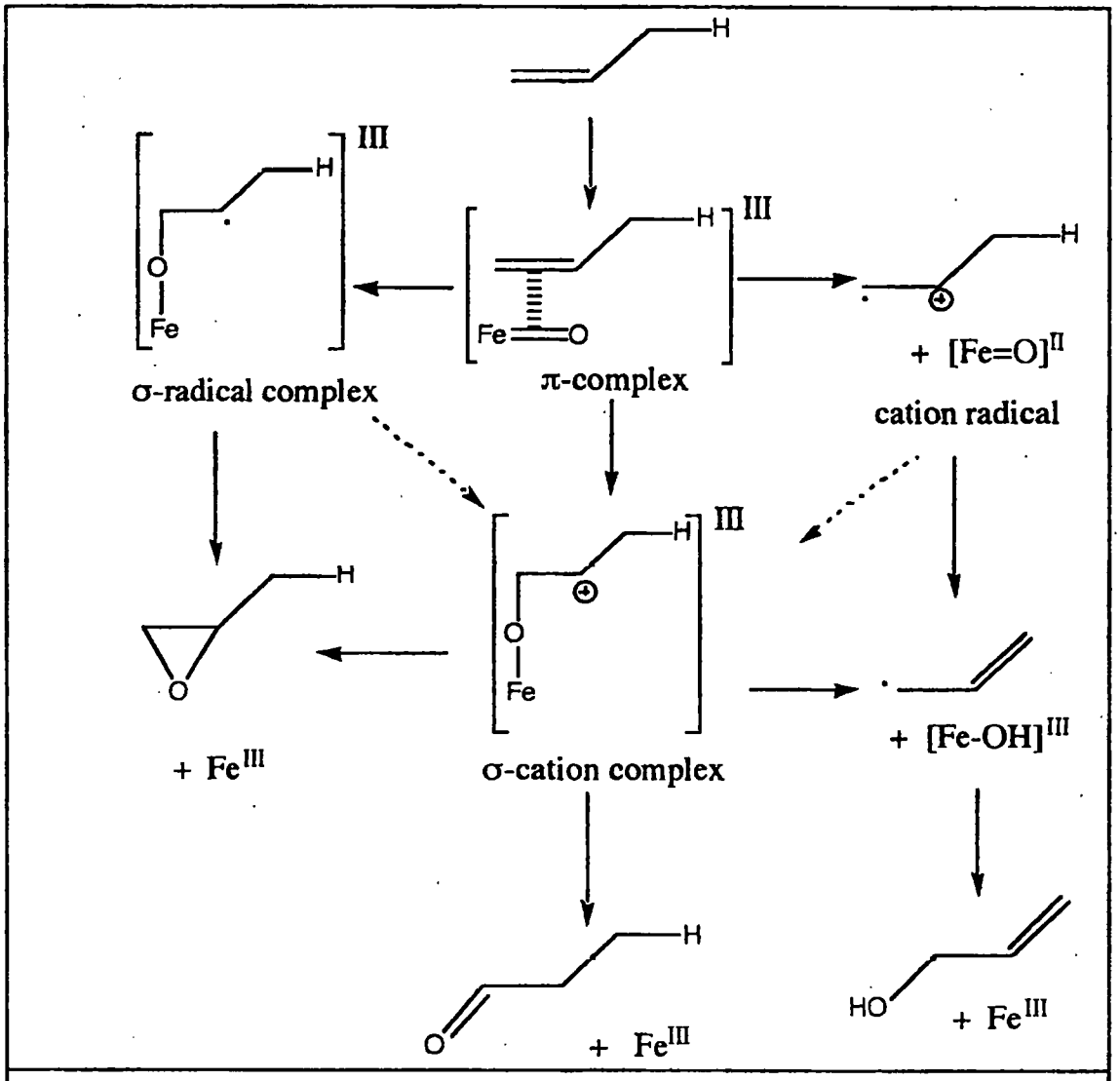

Figure 1.14 Proposed mechanism for P450-mediated oxidation of olefins

The Fe^{V}=O form of P450 forms an initial π-complex with the double bond. This can undergo either electron transfer to generate a transient olefin radical cation, or radical attack to generate a σ-radical complex. The radical cation itself can subsequently collapse to generate the σ-cation complex or, alternatively lose a proton to form an allylic radical, which is then trapped by the haem hydroxyl species.

The σ-radical complex can collapse to form an epoxide or undergo an electron transfer to form the σ–cation complex. The σ-cation complex may collapse to generate the epoxide or the corresponding aldehyde or ketone.

1.4.3 Aromatic hydroxylation

The introduction of an OH group into an aromatic ring by P450 reflects, with few exceptions, initial epoxidation of the aromatic ring followed by (i) chemical opening of the epoxide ring, (ii) migration of a hydride to the vicinal carbon, the "NIH shift" [77] and (iii) keto-enol tautomerism (Figure 1.15). Only a fraction of the hydrogen that shifts, H^a, is retained in the product because upon migration it becomes equivalent to H^b and only one of the hydrogens is lost in the tautomerization step. Deuterium substitution alters the proportion of the shifted hydrogen in the product due to isotope effects on the cleavage of the C-H/C-D bonds, but it does not effect the hydroxylation rate since the tautomerization occurs after the rate-determining epoxidation step.[77]

Two mechanisms are possible, a non-concerted mechanism in which the epoxide is formed from an intermediate (Figure 1.15 A), and a concerted mechanism by which the oxygen atom is inserted directly (Figure 1.15 B). Moreover, the intermediate of the non-concerted pathway can produce a ketone directly without formation of the epoxide.

However, for hydroxylation *para* to a halogen substituent quantitative loss of hydrogen at the hydroxylated carbon coupled with small deuterium kinetic isotope effects has been interpreted as possible insertion of oxygen directly into the C-H bond (Figure 1.15 C).[78; 79]

The non-concerted mechanism for the epoxidation of olefins suggests, by analogy, that aromatic rings are also oxidised by a non-concerted mechanism. However, experimental evidence for the non-concerted mechanism in these reactions is relatively weak.

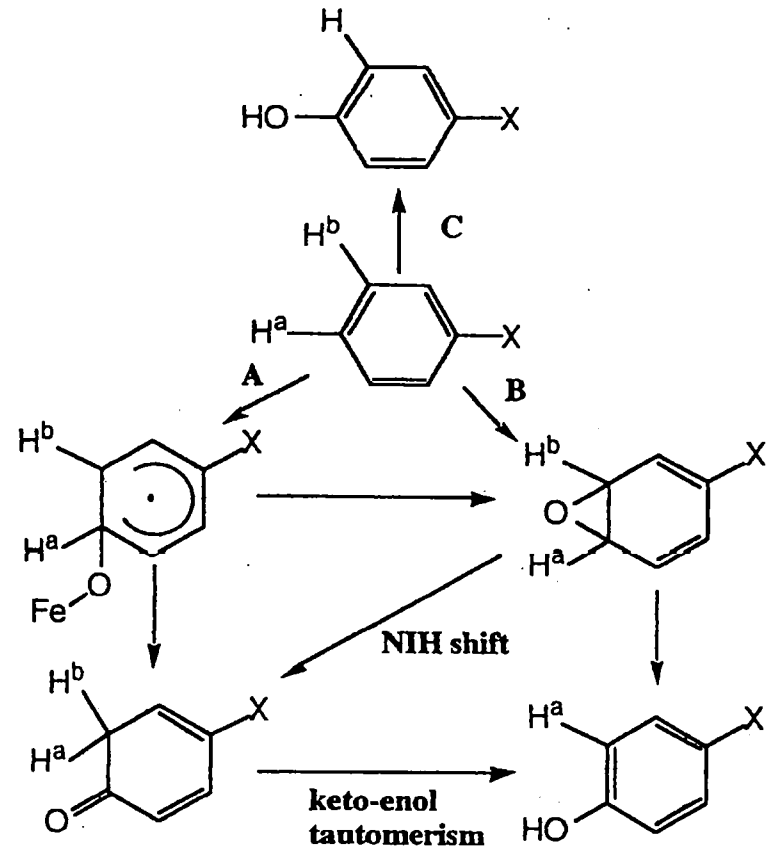

Figure 1.15 Alternative mechanisms for the hydroxylation of aromatic rings.

A reaction pathway that reconciles the observations consistent with both of a non-concerted mechanism and a concerted mechanism, has been proposed (Figure 1.16).[14; 77] In this, the first step is rate-determining and involves one-electron oxidation of the aromatic ring to give an aromatic radical cation and the one-electron reduced oxygenated haem intermediate $[Fe{=}O]^{II}$ (which has σ-radical cation character). Deprotonation of the aromatic cation radical and subsequent hydroxylation generates the hydroxylated products without formation of epoxide intermediates. Alternatively, a σ-cation complex can originate epoxides that subsequently undergo rearrangement or alkylation of the porphyrin.

The presence of a cation radical intermediate is compatible with the observed correlation between the kinetic parameters (V_{max}/K_m) of the hydroxylation reactions and the Hammett σ^+ parameter of the substituent,[80] indicating the presence of a transition

state in which a positive charge is developed. Moreover, correlation between the rate of oxidation of substituted halobenzenes and toluenes and the oxidation potential of the arenes has been noted.[74]

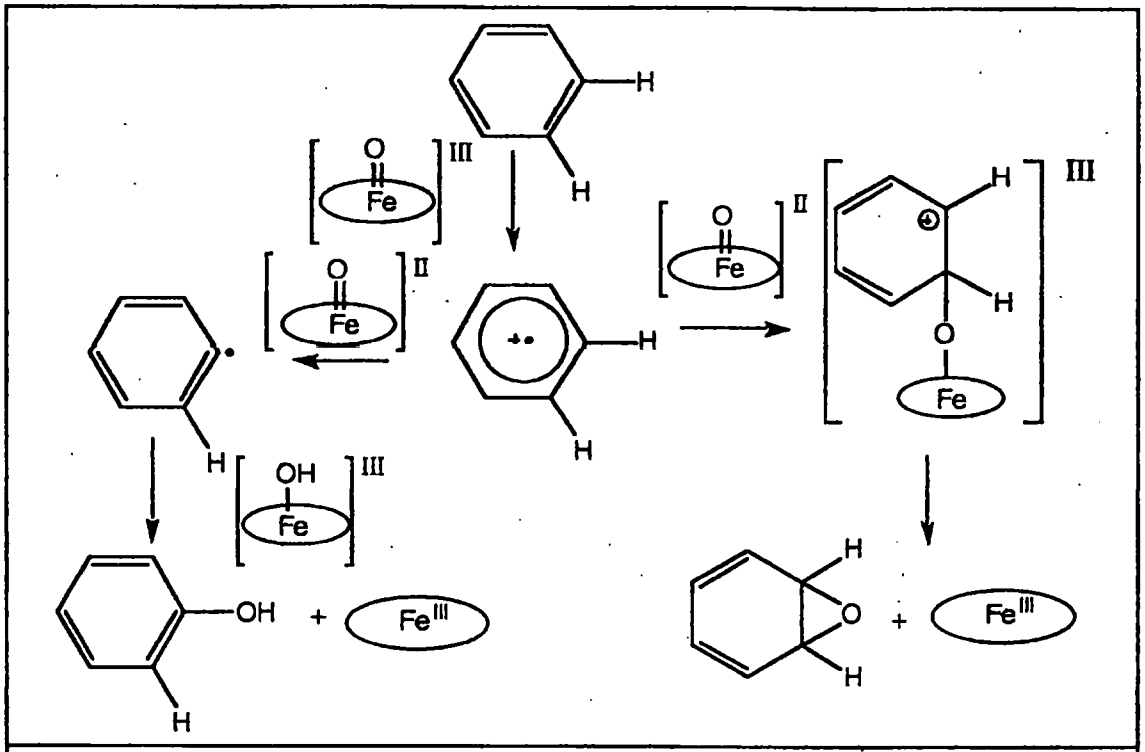

Figure 1.16. Proposed mechanism for the hydroxylation of aromatic rings.

1.4.4 Heteroatom release

In heteroatom release, oxygen is transferred to the carbon adjacent (α) to the heteroatom. Hydroxylation of heteroatom-containing substrates normally demonstrates a marked regioselectivity for the α-position as compared with β–, γ– or more distant positions.[81] Such reactions are observed for compounds containing nitrogen, sulfur, oxygen and halogens. The present discussion focuses on amines because of their structural similarities to amides, the subject of this thesis.

For amines, the explanation of the regioselectivity in these reactions invokes a pathway in which P450 initially abstracts an electron from the nitrogen atom.[82] The aminium cation radical so-formed can then undergo one of the two possible reactions,

loss of a hydrogen atom or loss of a proton. Both pathways lead to heteroatom loss. Comparison of the electrochemical and enzymic oxidation of amines reveals similar patterns of regioselectivity and kinetic deuterium isotope effects.[83] Because electrochemical oxidation of amines involve one-electron transfer from nitrogen,[84; 85] enzymic N-dealkylation presumably follows a similar pathway.[86; 87]

N-cyclopropyl probes have been used to investigate further the mechanism of these reactions. Cyclopropyl radicals are known to rearrange rapidly ($k > 10^8$ s^{-1}) upon formation.[88; 89] If formed in an active site of an enzyme, such species are highly reactive and destructive. Indeed, these compounds have been used as diagnostic suicide inactivators of P450.[90;91] The mechanism-based inactivation of P450 by cyclopropylamine is reported to be due to a single electron transfer followed by ring opening (Figure 1.17).[92; 93]

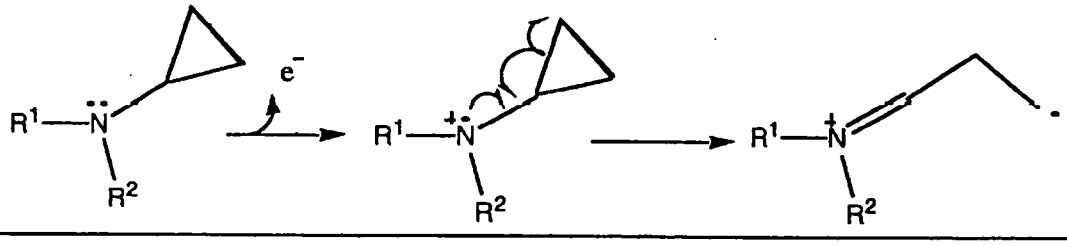

Figure 1.17 Proposed mechanism for the suicide inactivation of P450 by cyclopropylamines.

This mechanism accords with the results of Guengerich and MacDonald [14] who observed a correlation between the log of the rate constant for the inactivation of P450 and the single-electron transfer-cyclopropane ring opening sequence.

Thus, the evidence reported so-far indicates that one-electron oxidation is the first step in the P450 catalysed oxidation of heteroatom-containing compounds. In most cases, such an electron transfer results in overall α-hydroxylation and subsequent heteroatom release (Figure 1.18).

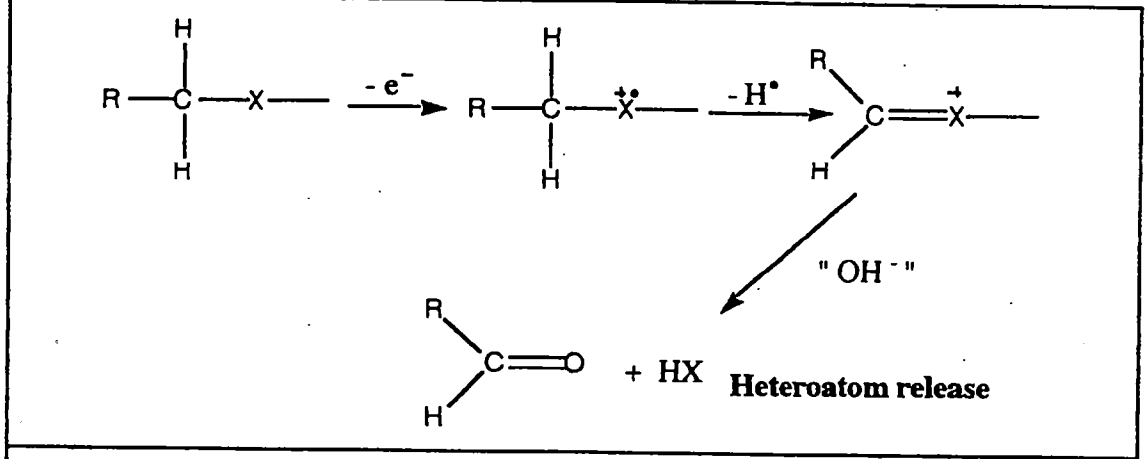

Figure 1.18 Mechanism of the oxidation of heteroatom-containing compounds.

1.4.5 Heteroatom oxygenation

Many heteroatom oxygenation reactions, that in the literature are reported to be catalysed by P450, can be attributed to another mixed-function oxidase, the flavin-containing monoxygenase.[62] Several examples of sulfur oxidation and of the oxygenation of trivalent phosphorus are known.[94; 95; 96] While many N- oxygenations are also attributed to P450, there are very few cases in which strong evidence exists for the involvement of this enzyme in these reactions.[97-101]

Heteroatom oxygenation reactions are conceptually related to the heteroatom release reaction. In heteroatom oxygenation, an oxygen atom becomes bonded to the heteroatom, whereas in heteroatom release, the oxygen atom is transferred to the carbon atom adjacent (α) to the heteroatom. The relationship between these two biotransformations is further underscored by the observation that for an isoelectronically substituted series of compounds, e.g. amines and phosphines, the predominant metabolic process tends to favour heteroatom oxygenation over heteroatom release as the elements progress down a group in the periodic table. Thus alkylamines produce predominantly intermediate α-hydroxyamines, whereas the isoelectronic alkylphosphines generate phosphine oxides. Alkyl ethers produce putative α-hydroxyethers, whereas the isoelectronic alkyl sulfides generate sulfoxides.[14]

Guengerich and MacDonald[14] have suggested that the first step in heteroatom oxygenation is one-electron oxidation of the heteroatom, as for heteroatom release. If α-hydrogens are available, they will tend to be abstracted before oxygen rebound can occur to give heteroatom oxygenation, and heteroatom release will result. Heteroatom oxygenation is favoured under two conditions, where (1) no α-hydrogens are available, as in the cases of aromatic amides[102] and certain primary amines[98], or (2) the radical system has properties that render it relatively stable, as in the case of sulfides[94] or phosphines.[96]

Studies in which the ionisation potentials of the heteroatom towards for one-electron oxidation were correlated with the rate of enzymic oxidation indicated that an order $R_3P>R_3N>R_2S>RI\approx R_2O>RBr>RCl>RF$ holds for close structural analogues.[80; 102; 103]

In summary, heteroatom oxygenation preferentially occurs for those heteroatoms that have relatively low first-electron ionisation potentials and that form thermodynamically stable heteroatom oxides. The primary reason for this metabolic preference is the stability of the heteroatom radical cation (e.g. $RCH_2\overset{+\bullet}{X}R$) relative to the carbon centred radical (e.g., $R\dot{C}HXR$). Heteroatom release occurs preferentially for those atoms in which the α-carbon radical is more stable than the corresponding heteroatom radical cation.

1.5 Amides

1.5.1 Biological relevance of the amides

Many toxic and carcinogenic compounds do not themselves produce a toxic response. Rather they need to be activated, usually to an electrophilic form capable of reacting with biological nucleophiles. Similarly, many existing drugs require activation to exercise their therapeutic action. Liver P450s play a strategic role in these biotransformations of foreign organic compounds.

Many of the xenobiotic compounds that are exposed to P450 metabolism are based on the dialkylamino functionality, R^1R^2N-, whether as tertiary amines (e.g.. nicotine, 1-(1-phenylcyclohexyl)piperidines, the tricycle antidepressants), dialkylamides (e.g. benzodiazepine anxiolytics, industrial solvents, insects repellents, barbiturates) or related groups such as dialkylnitrosoamines (environmental carcinogens) and dialkyltriazenes (anticancer agents). The amide group is present in a wide variety of compounds that are extensively used as drugs , cosmetics and pesticides. Various amines and amides are known, or suspected, mutagenic compounds.[103;104] N,N-Dialkylamides possess a range of biological activities. For example, N,N-diethylnicotinamide is a respiratory stimulant,[105] N,N-diethyl-3-toluamide is the most used insect repellent worldwide,[103] cotinine is the major tobacco metabolite,[107] N,N-dimethylformamide is an industrial solvent suspected to be carcinogenic[108] while miscellaneous N-alkyl and N,N-dialkylamides show activity against same forms of cancer.[109; 110] All these compounds are known to undergo oxidative N-dealkylation or oxidation upon liver metabolism *in vivo*. Thus, a study of the details of the mechanism of these P450-dependent reactions ought to provide useful information that should further the understanding of both their hazard and utility.

1.5.2 Chemical properties of amides of relevance to their metabolism

In contrast to amines, P450-dependent metabolism of amides has received little mechanistic attention. Since both compounds undergo P450-dependent metabolism to generate N-dealkylation products through the formation either a carbinolamine or carbinolamide, it is tempting to suggest that they follow the same pathway. However, there are some important differences between the two that must be taken into account.

Aliphatic amines are relatively strong bases due to the fact that the non-bonded electron pair in the sp^3 orbital is readily available for the formation of a new covalent bond. In amides, however, the presence of the carbonyl moiety causes resonance delocalization of the electron pair, resulting in these electrons being less available. Indeed,

the protonation of amides takes place at the oxygen atom rather than at the nitrogen.[111] Moreover, the presence of the electron-withdrawing carbonyl group results in amides having much higher ionisation potentials than the corresponding amines.

Another interesting difference between amides and amines is seen in UV/visible spectra generated upon interaction of the substrate with P450. Under reducing conditions, amines typically give type II spectra.[28] This is believed to be due to the nucleophilicity of the electron pair, allowing these compounds to bind to the haem. Amides are known to give type I spectra.[28] It is thought that the interaction of amides with the haem group takes place through the carbonyl oxygen rather than the nitrogen atom. Numerous examples are reported on the formation of complexes of amides in which the carbonyl group is bound to a variety of metals.[111; 112; 113]

A complex formed between N,N-dimethylformamide and the Fe^{IV}=O species generated during oxidation of 5,10,15,20-tetrabis(2,6-dichlorophenylporphyrinato) Fe^{III} in the presence of dimethylformamide and *m*-chloroperoxybenzoic acid has been characterised.[114]

1.5.3 Comparison of the P450-dependent metabolism of amines and amides

The oxidative N-dealkylation of amines by P450 has been extensively investigated and considerable indirect evidence can be found in support of a mechanism involving initial and rate-limiting electron abstraction from amine nitrogen. This evidence can be summarised as follows:

- oxidations of 1,4-dihydropyridines results in loss of alkyl radicals from the 4-position,[62]

- cyclopropylamines are suicide substrates for P450,[92; 93]

- kinetic deuterium isotope effects observed for N-dealkylation of N,N-dimethylanilines,[64] dihydropyridine dehydrogenation[115] and several other amines [116; 117] are small; this is in contrast to the large kinetic isotope deuterium effects often observed for O-dealkylation[118;119] and carbon hydroxylation.[121;122]

These results have been interpreted[64; 92; 93; 122] as implying that the mechanism of the P450-mediated N-dealkylation reaction proceeds *via* an initial one-electron abstraction (Figure 1.19; *path b*).

In contrast, P450-dependent N-dealkylation of amides shows a large kinetic isotope deuterium effects.[123] Moreover, the P450-mediated metabolism of N-cyclopropylamides does not lead to suicide inactivation of the enzyme, despite the fact that N-dealkylation occurs.[124; 125] These, together with the higher ionisation potential of amides, suggest that the N-dealkylation of amides occurs via hydrogen atom abstraction with the formation of a carbon-centred radical intermediate (Figure 1.19; *path a*).

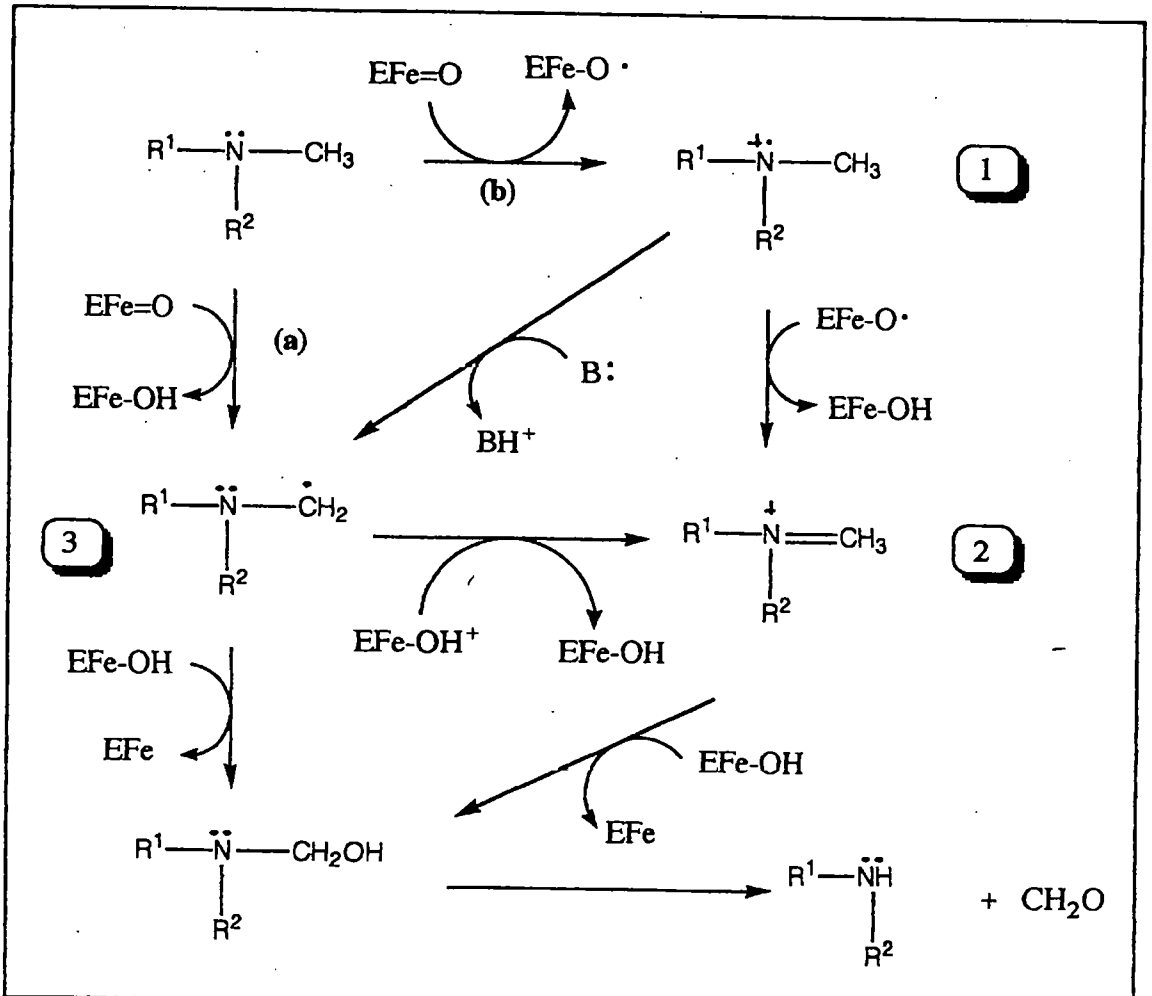

Figure 1.19 Pathways for N-dealkylation of amides and amides. *Path a* involves the rate-limiting hydrogen atom abstraction and should show large kinetic deuterium isotope effects, while *path b* involves rate-limiting electron abstraction and should show small kinetic deuterium isotope effects. For amines R_1 and R_2 can be alkyl or aryl. For amides R_1 is RCO or ArCO and R_2 can be alkyl or aryl.

The postulated formation of a carbon-centred radical species in amide metabolism was investigated by Iley and Constantino.[125] The strategy adopted involved the use of two substrate probes (shown in Figure 1.20) that were designed to intercept two of the possible intermediates, i.e. the cation radical (1 of Figure 1.10) and the carbon centred radical (3 of Figure 1.20).

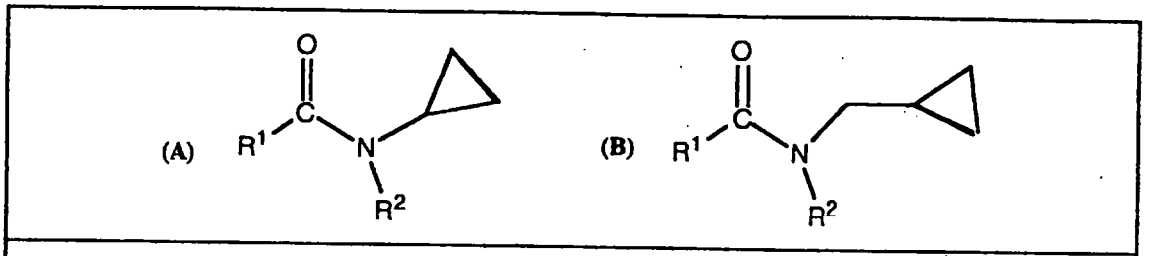

Figure 1.20 Substrates used for the trapping of reactive intermediates formed during the microsomal metabolism of amides. A) the cyclopropylamide designed to trap the radical cation B) the N-methylcyclopropylamide designed to trap the carbon-centred radical.

The hypothesis is that a cyclopropyl ring adjacent to a radical centre, either the amide cation radical or a carbon-centred radical, can potentially intercept the intermediates, diverting them to rearranged products, as indicated in Figure 2.21. However, neither compound resulted in any ring opening product, even though N-dealkylation was observed.[125]

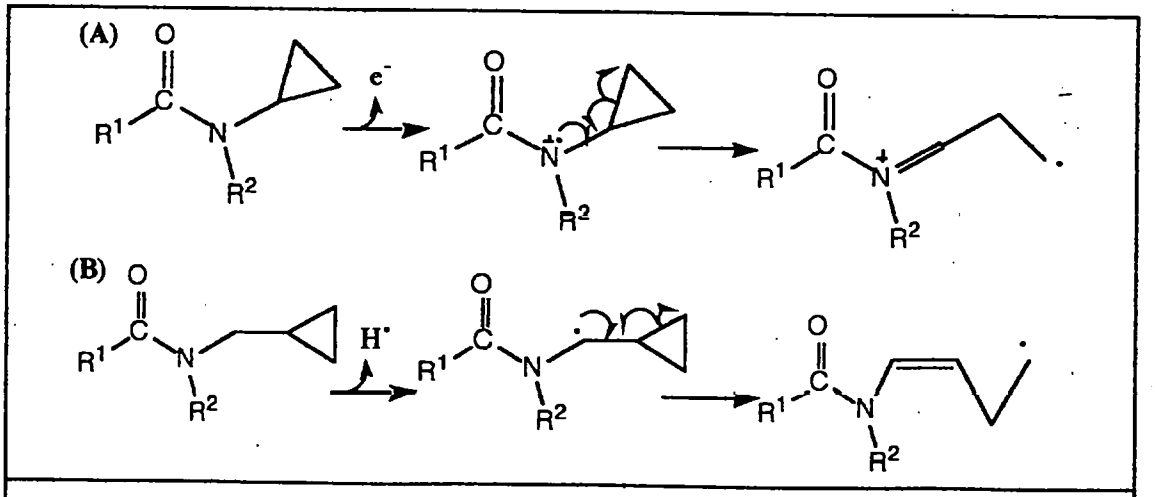

Figure 1.21 Potential mechanism of the microsomal metabolism of (A) cyclopropyl amide and (B) methylcyclopropylamide.

Thus although kinetic data strongly suggest a mechanism for amide metabolism involving hydrogen atom abstraction as the rate-determining step, direct experimental evidence for the presence of a carbon-centred radical intermediate has yet to be produced.

1.6 Scope of the thesis

This thesis reports an investigation that attempts to elucidate further the mechanism of the oxidative metabolism of N,N-dialkylamides by P450. The first section is concerned with methods directed at trapping reaction intermediates using two different approaches, namely direct trapping by functional groups present in the substrate (Chapter II) and the use of a spin trapping ESR technique to detect the postulated carbon-centred radical (Chapter III). In the second part of the thesis, the investigation is concerned with two structural aspects of the N-dealkylation reactions, regioselectivity (Chapter IV) and stereoselectivity (Chapter V). The strategy employs a comparison of the kinetic parameters of the microsomal P450-catalysed reactions with both the $TPPFe^{(III)}$/*tert*Bu.OOH biomimetic system and theoretical molecular orbital calculations. In the third and final part, the effects of the reactive intermediates on the enzyme itself were investigated. In this section, attention is focused on the industrial solvents N,N-dimethylformamide and N,N-dimethylacetamide in an attempt to obtain more information relating to their metabolism-based toxicity.

1.7 References

1 Keevil T. and Mason H.S., In: *Methods in Enzymology* (Fleischer S. and Packer L. eds.) Academic Press, New York, (1978), **52**, 3-

2 Malmstrom B.G., (1982) *Annu. Rev. Biochem.*, **51**, 21-

3 Alexander L.S. and Goff H.M, (1982), *J. Chem. Educ.*, **59**, 179-

4 Park B.K. and Kitteringham N.M., (1988), *Prog. Drug Metab.*, **11**, 1-

5 Nerberth D.W., Nelson D.R., Coon M.J., Estarbrook R.W., Feyereisen R., Kuriyama Y.,Gonzales F.J., Guengerich F.P., Gunsalus I.C., Johnson E.F, Loper J.C., Sato R., Waterman M.R. and Waxman D.J., (1991), *DNA and Cell Biology*, **10**, 1-

6 Hanson L.K., Sligar S.G. and Gunsalus I.C., (1977), *Croat. Chem. Acta*, **49**, 237-

7 Dawson J.H., Holm R.H., Trudell J.R., Barth G., Linder R.E., Bunnenberg E. and Djerass C., (1976), *J. Am. Chem. Soc.*, **98**, 3707-

8 Walsh C., in: *Enzymic Reaction Mechanism*, Freeman, New York. (1979).

9 Astrom A. and Depierre J.W., (1989), *Biochem. Biophys. Acta*, **853**, 1-

10 Lu A.Y.H. and West S.B., (1988), *Pharmacol. Ther.*, **2**, 337-

11 Sligar S.G. and Gunsalus I.C., (1976), *Proc. Natl. Acad. Sci. U.S.A.*, **73**, 1078-

12 Ishimura Y., Ullrich I.C. and Peterson J.A., (1971), *Biochem. Biophys. Res. Commun.*, **42**, 140-

13 Sligar S.G., Lipscomb J.D., Debrinner P.G. and Gunsalus I.G., (1974), *Biochem. Biophys. Res. Commun.*, **61**, 290-

14 Guengerich F. P and MacDonald T.L., (1984), *Acc. Chem. Res.*, **17**, 9-

15 Lewis D.F.V., (1986), *Drug Metab. Rev.*, **17**, 1-

16 Stellwagen E., (1978), *Nature*, **275**, 73-

17 Blanck J., Rein H., Sommer H., Ristau O., Smettan G. and Ruckpaul K, (1983), *Biochem. Pharm.*, **32**, 1683-

18 Hasinoff B.B., (1985), *Biochim. Biophys. Acta*, **829**, 1-

19 Ortiz de Montellano P.R., Kunze K.L. and Beilan, (1983), *J. Biol. Chem.*, **258**, 45-

20 Matthew J.B., Weber P.C., Salemore I.R. and Richards F.M., (1983), *Nature*, **301**, 169-

21 Narhi L.O. and Fulco A.J., (1986), *J. Biol. Chem.*, **261**, 7160-

22 Vermilion, J.L., Coon M.J., (1978), *J. Biol. Chem.*, **253**, 8812-

23 Miki N., Sugiyama T. and Yamano Y., (1980) *J. Biochem.*, **88**, 307-

24 Lu A.Y.H., Levin W., Selander H. and Jerina D.M.; (1974); *Biochem. Biophys. Res. Commun.*; **61**: 1348-

25 Imai Y. and Sato R.; (1977); *Biochem Biophys. Res. Commun.*; **88**: 420-

26 Mike N., Sugiyama T. and Yamano T.; (1980); *J. Biochem.*; **88**: 307-

27 Schenkmann J.B., Remmer H. and Estabrook R.W., (1967), *Mol. Pharmacol.*, **3**, 113-

28 Schenkmann J.B., Sliger S.G. and Cinti D.L., (1981), *Pharmacol. Ther.*, **12**, 43-

29 Narasimhulu S., (1971), *Arch. Biochem. Biophys.*, **147**, 384-

30 Yoshida Y., Imai Y. and Hashimoto-Yutsudo C., (1982), *J. Biochem.*, **91**, 1651-.

31 Imai Y. and Sato R., (1966), *Biochem. Biophys. Res. Commun.*, **22**, 620-

32 Perkonen O., and Viano H., (1975), *FEBS Lett.*, **51**, 11-

33 Blake R.C. and Coon M.J., (1980), *J.Biol. Chem.*, **255**, 4100-

34 Mansuy D., Battioni F and Battioni J.P., (1989), *Eur. J. Biochem.*, **184**: 267-

35 Masumoto H., Takeuchi K.; Ohta S. and Hirobe M., (1989), *Chem. Pharm. Bull.*, **37**: 1788-

36 Masumoto H., Ohta S. and Hirobe M., (1991), *Drug Metab. Dispos.*, **19**: 768-

37 McMurry T.J. and Groves J.T., (1986), in: *Cytochrome P-450: Structure, Mechanism and Biochemistry* (P.R. Ortiz de Montellano, Ed.) Plenum Press, New York 1-

38 Hill C.L and Schardt B.C., (1980), *J. Am. Chem. Soc.*, **102**,, 6374-

39 Lindsay Smith J.R. and Sleath P.R.,(1983), *J. Chem. Soc. Perkin Trans 2*, 1165-

40 Battioni P., Renaud J.P., Bartoli J.F. and Mansuy D., (1986), *J.Chem. Soc. Chem. Commum.*, 341-

41 Groves J.T., Nemo T.E. and Myers R.S., (1979), *J. Am. Chem. Soc.*, **101**, 1032-

42 Lindsay-Smith J.R. and Mortimer D.N., (1985), *J. Chem. Soc. Chem. Commun.*, 64-

43 Lindsay-Smith J.R. and Mortimer D.N., (1986), *J. Chem. Soc. Perkin Trans 2*, 1743-

44 Labeque R. and Marnett L.J., (1989), *J. Am. Chem. Soc.*, **111**, 6621-

45 Arasasingham R.D. and Bruice T.C., (1991), *J. Am. Chem. Soc.*, **113**, 6095-

46 Battioni P., Renaud J.P., Bartoli J.F., Reina-Artiles M., Fort M. and Mansuy D., (1988), *J. Am. Chem. Soc.*, **110**, 8462-

47 Mansuy D., Bartoli J.F. and Momenteau M., (1982), *Tetrahedron Lett.*, **23**, 2781-

48 Traylor T.G. and Xu F, (1990), *J. Am. Chem. Soc.*, **112**, 178-

49 Arasasingham R,D., Cornman C.R. and Balch A.L.,(1989), *J. Am. Chem. Soc.*, **111**, 7800-

50 Traylor T.G. and Ciccone J.P., (1989), *J. Am. Chem. Soc.*, **111**, 8413-

51 Groves J.T. and Watanabe Y., (1988), *J.Am. Chem. Soc.*, **110**, 8443-

52 Lindsay-Smith J.R. and Lower R.J, (1991), *J.Chem. Soc. Perkin Tras II*, 31-

53 Lee W.A. and Bruice T.C., (1985), *J. Am. Chem. Soc.*, **107**, 513-

54 Bruice T.C., Balasubramaian P.N., Lee R.W. and Lindsay-Smith J.R., (1988), *J. Am. Chem. Soc.*, **110**, 7890-

55 Traylor T.G., Lee W.A. and Stynes D.V., (1984), *J. Am. Chem. Soc.*, **106**, 755-

56 Lindsay-Smith J.R. and Lower R.J., (1991), *J. Chem. Soc. Perkin Trans 2*, 31-

57 Mansuy D., Battioni P. and Renaud J.P., (1984), *J. Chem. Soc. Chem. Commun.*, 1255-

58 Labeque R. and Marnett L.J., (1989), *J. Am. Chem. Soc.*, **111**, 6621-

59 Traylor T.G. and Popovitz-Biro R., (1988), *J. Am. Chem. Soc.*, **110**, 239-

60 Groves J.T., Haushalter R.C., Nakamura M., Nemo T.E. and Evans B.J., (1981), *J. Am. Chem Soc.*, **103**, 2884-

61 White W.E. and Coon M.J., (1980), *Annu. Rev. Biochem.*, **49**, 315-

62 Augusto O., Beilan H.S. and Ortiz de Montellano.P.R., (1982), *J. Biol. Chem.*, **257**, 11288-

63 Groves J.T., McClusky G.A., White R.E. and Coon M.J., (1978), *Biochem. Biophys. Res. Commun.*, **81**, 154-

64 Miwa G.T., Walsh J.S. and Lu A.Y.H., (1984), *J. Biol. Chem.*, **259**, 3000-

65 Ortiz de Montellano P.R. and SteamsR.A, (1987), *J. Am. Chem. Soc.*, **109**, 3414-

66 Bowry V.W., Lusztyk J. and Ingold K.U., (1991), *J. Am. Chem. Soc.*, **113**, 5687-

67 Bowry V.W. and Ingold K.U., (1991), *J. Am. Chem. Soc.*, **113**, 5699-

68 Ortiz de Montellano P.R., Mangold B.L.K., Wheeler C., Kunze K.L., Reich N.O., (1983), *J. Biol. Chem.*, **258**, 4202-

69 Miller R.E. and Guengerich F.P., (1983), *Cancer Res.*, **43**, 11445- .

70 Ortiz de Montellano P.R., Yost G.S., Mico B.A., Dinizo S.E., Correia M.A. and Kumbara H., (1979), *Arch. Biochem. Biophys.*, **197**, 524-

71 Ortiz de Montellano P.R., Beilan H.S., Kunze K.L. and Mico B.A., (1981), *J. Biol. Chem.*, **256**, 4395-

72 Ortiz de Montellano P.R., Kunze K.L., Beilan H.S. and Wheeler C., *Biochemistry*, **21**, 1331-

73 Ortiz de Montellano P.R., Mangold B.L.K., Wheeler C., Kunze K.L. and Reich N.O., (1983), *J. Biol. Chem.*, **258**, 4208-

74 Henscheleer D., Hoos W.R., Fetz H., Dallmeier E. and Metzler M., (1979), *Biochem. Pharmacol.*, **28**, 543-

75 Miller R.E. and Guengerich F.P., (1982), *Biochemistry*, **21**, 1090-

76 Guengerich F.P. and MacDonald J.L, (1990), *FASEB J.*, **4**, 2453-

77 Jerina D.M. and Daly J.W., (1974), *Science*, **185**, 573-

78 Tomaszewski J.E., Jerina D.M. and Daly J.W., (1975), *Biochemistry*, **14**, 2024-

79 Preston B.D., Miller J.A. and Miller E.C., (1983), *J. Biol. Chem.*, **258**, 8304-

80 Burka L.T., Plucinsky T.M. and McDonald T.L., (1983), *Proc. Natl. Acad. Sci. USA*, **80**, 6680-

81 Testa B. and Mihailova D.M.J., (1978), *J. Med. Chem*, **21**, 683-

82 Griffin B.W., March Y., Yasukochi Y. and Masters B.S.S., (1980), *Arch. Biochem. Biophys.*, **205**, 543-

83 Shono T., Toda T. and Oshino N., (1982), *J. Am. Chem. Soc.*, **104**, 2639-

84 Shono T., Hamaguchi H. and Matsumara Y., (1975), *J. Am. Chem. Soc.*, **97**, 4264-

85 Lindsay-Smith J.R and Mascheder D.J., (1976), *J. Chem. Soc. Perkin Trans. Trans. 2*, 47-

86 McMahon R.E., Cilp H.W. and Occolowitz J.C., (1969), *J. Am. Chem. Soc.*, **91**, 3389-

87 Shea J.P., Valentine G.L. and Nelson S.D., (1982), *Biochem. Biophys. Res. Commun.*, **109**, 231-

88 Griller D. and Ingold K.V., (1980), *Acc. Chem. Rec.*, **13**, 317-

89 Martinez A.M., Cushamac G.E. and Rocek J., (1975), *J. Am. Chem. Soc.*, **97**, 6503-

90 Sailer N., Jung M.J. and Koch-Weser J., (1978), in: "*Enzyme-activated Irreversible Inhibitors*" Elsevier-North Holland, New York.

91 Hanzlik R.P., Kishore V. and Tullman R., (1979), *J. Med. Chem.*, **22**, 759-

92 MacDonald T.L., Zirvi K., Burka L.T., Peyman P. and Guengerich F.P., (1982), *J. Am. Chem. Soc.*, **104**, 2050-

93 Hanzlik R.P. and Tullman R.H., (1982), *J. Am. Chem. Soc.*, **104**, 2048-

94 Guengerich F.P., (1979), *Pharmacol. Ther.* Part. A, **6**, 99-

95 Lu A.Y. H. and West S.B., (1980), *Pharmacol. Rev.*, **31**, 277-

96 Wiley R.A., Sterson L.A., Sesame H.A. and Gillette J.R., (1972), *Biochem. Pharmacol.*, **21**,3235-

97 Johnson E.F., Levitt D.S., Muller-Eberhard U. and Thorgeirsson S.S., (1980), *Cancer Res.*, **40**, 4456-

98 Frederick C.B.Mays J.B., Ziegler D.M., Guengerich F.P. and Kudlubar F.F., (1982), *Cancer Res.*, **42**, 2671-

99 Duncan J.D. Cho A.K., (1982), *Mol. Pharmacol.*, **22**, 235-

100 Mita S., Ishii K., Yamazoe Y., Kamataki T., Kato R. and Sugimura T., (1981), *Cancer Res.*, **41**, 3610-

101 Cummings S.W., Guengerich F.P. and Prough R.A., (1982), *Drug Metab. Dispos.*, **10**, 459-

102 MacDonald T.L., (1982), *CRC Crit. Rev. Toxicol.*, **11**, 85-

103 Weisburger E.K., (1981), *Natl. Cancer Inst. Monogr.*, **58**, 1-

104 Miller J.A, (1970), *Cancer Res.*, **30**, 559-

105 Reynolds J.E.F., (1989), *Martindale, The Extra Pharmacopoeia*, 29th ed., The Pharmaceutical Press, London.

106 Robbins P.J. and ChemiackM.C., (1986), *J. Toxicol. Envirom. Health*, **18**,503-

107 Hucker H.B., Gillette J.R. and Brodie B.B., (1960), *J. Pharm. Exp. Ther.*, **129**, 94-

108 Gescher A., (1990), *Chemistry in Britain*, **26**, 435-

109 Kestel P., Gill M.H., Threadgill M.D., Gescher A., Howard O. and Curazon E.H., (1986), *Life Sci.*, **38**, 719-

110 Kestel P., Threadgill M.D., Gescher A., Gledhill A.P., Shaw A.J. and Farmer P.B., (1987), *J. Pharmacol. Ther.*, **240**, 265-

111 Homer R.B. and Johnson C.D., (1970), In: *The Chemistry of Amides* (Ed. Zabicky J., Patais series). Interscience Publischer, London.

112 Bull W.E., Madan S.K. and Willis J.E., (1963), *Inorg. Chem.*, 2: 303-

113 Tokasaki B.K., Kim J.H., Rubin E. and Chin E.J., (1993), *J. Am. Chem. Soc.*, **115**, 1157-

114 Gold A., Jayaraj K., Dopplet P., Weiss R., Chottard G., Bill E., Ding X. and Trantwein A.X., (1988), *J. Am. Chem. Soc.*, **110**, 5736-

115 Bocker R.H. and Guengerich F.P, (1986), *J. Med. Chem.*, **29**, 1596-

116 Nelson S.D., Pohl L.R. and Trager W.F., (1975), *J. Med. Chem.*, **18**, 1062-

117 Miwa G.T., Garland W.A., Hodston B.J., Lu A.Y.H. and Northrop D.B., (1980), *J. Biol. Chem.*, **265**, 6049-

118 Guengerich F.P., (1987), *J. Biol. Chem.*, **262**, 8459-

119 Foster A.B., Jarman M., Stevens J.D., Thomas P. and Westwood J.H., (1974), *Chem-Biol. Inter.*, **9**, 327-

120 Dagne E., Gruencke L. and Castagnoli N.Jr., (1974), *J. Med. Chem.*, **17**, 1350-

121 Shono T., Ohmizu Y., Toda T. and Oshimo N., (1981), *Drug Metab. Dispos.*, **9**, 476-

122 Tullman R.N and Hanzlick R.B., (1984), *Drug Metab. Dispos.*, **15**, 1163-

123 Hall L.R. and Hanzlick R.P, (1990), *J. Biol. Chem.*, **265**, 12349-

124 Hall L.R. and Hanzlick R.P., (1991), *Xenobiotica*, **21**, 1127-

125 Iley J. and Constantino L., (1994), *Biochem. Pharmacol.*, **47**, 275-

CHAPTER 2

Trapping of the reactive intermediates of the P450-dependent metabolism of N,N-dialkylamides

The present chapter describes the following studies related to the mechanism of the microsomal oxidation of tertiary amides:

- attempts to intramolecularly trap iminium species
- attempts to intermolecularly trap iminium species
- intramolecular trapping of carbon-centred radical intermediates using C- and N-alkenyl substrates.

2.1 Introduction

As discussed in Chapter 1, the metabolism of tertiary amides is believed to occur *via* rate-determining hydrogen atom abstraction from the α-carbon, with the formation of a carbon-centred radical intermediate. This intermediate can undergo insertion of an activated hydroxyl group from the P450-haem oxoiron complex, leading to the formation of a relatively stable carbinolamide product.[1-4]

Despite the kinetic data supporting this hypothesis,[1-4] the formation of such an intermediate remains speculative. One previous attempt to trap the carbon-centred-radical intermediates proved unsuccessful.[3] The system employed involved a probe substrate characterised by the presence of an N-cyclopropylmethyl group; the postulated carbon-centred radical, if formed, should be trapped following the mechanism in Figure 2.1.

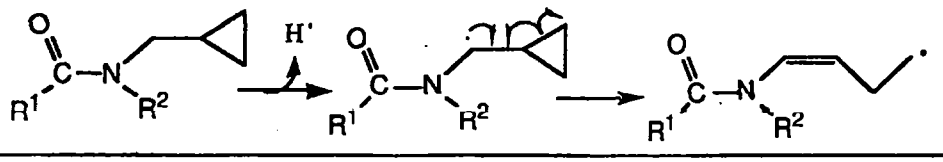

Figure 2.1 Postulated ring opening reaction due to the formation of a carbon-centred radical during the microsomal metabolism of N-cyclopropylmethyl amide.

However, although the substrate underwent metabolism of the cyclopropylmethyl group, it did so without any detectable ring opening.[3] The authors suggested that the formation of the carbon-centred radical cannot be ruled out, as it may be that such a radical is trapped by the haem-hydroxyl moiety of the enzyme faster than it can rearrange. This situation has certainly been observed for saturated hydrocarbons substrates.[5] Thus it may be that the failure to detect the carbon-centred radical intermediate results from either (i) such a species not being formed, or (ii) the probe substrate used not being ideal for the intramolecular trapping. Clearly, further investigation into the nature of the reactive intermediates formed during the microsomal oxidation of tertiary amides is needed in order to obtain a better understanding of the mechanistic aspects of these reactions.

From mechanistic point of view, tertiary amides may undergo P-450-mediated metabolism through the mechanism illustrated in Figure 2.2.

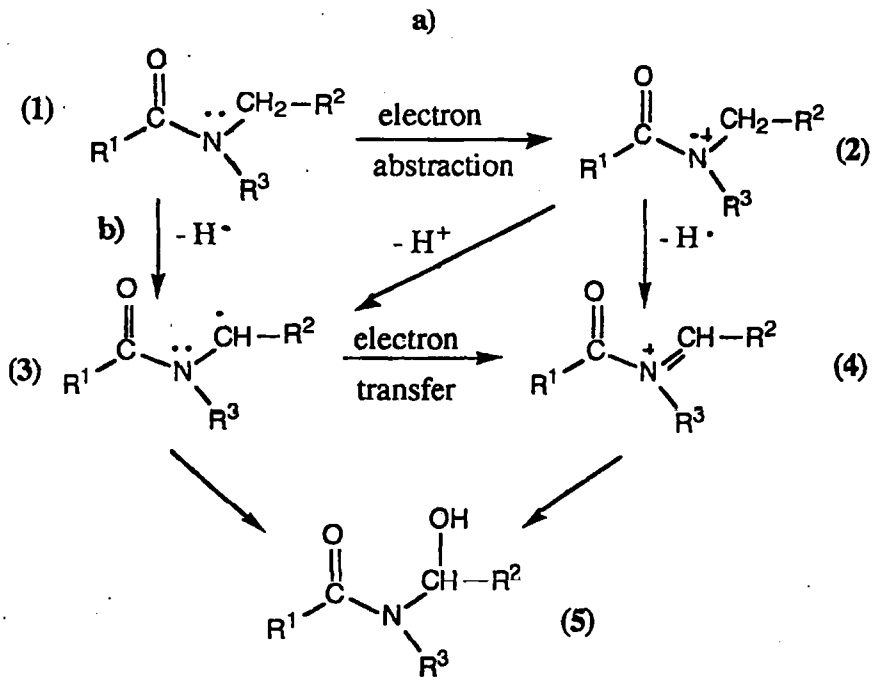

Figure 2.2 Potential pathways for the oxidative N-dealkylation of N,N-dialkylamides.

Amide (**1**), can undergo two alternative first step reactions, namely electron abstraction, leading to the formation of the cation radical intermediate (**2**) (path, a), and hydrogen atom abstraction (path b), leading to the formation of the carbon-centred radical intermediate (**3**). Intermediate (**3**), may then undergo loss of a hydrogen atom to form the iminium ion intermediate (**4**) or, alternatively, the loss of a proton to generate the carbon-centred radical (**3**). Both (**3**) and (**4**) can subsequently form the carbinolamide product (**5**), by hydroxyl group insertion from the P450 haem-hydroxyl complex. Alternatively, the carbon centred radical (**3**) can undergo electron abstraction to generate the iminium ion (**4**), or insertion of hydroxyl group to lead to the formation of the carbinolamide product (**5**). Moreover it is worth noting that the carbinolamine product from tertiary amine metabolism is reported to exist in equilibrium with the iminium ion species.[6-8] Indeed, formation of iminium ion species from the rearrangement of carbinolamines in solution is reported.[9] This latter mechanism is believed to be responsible for the toxic effects observed upon metabolism of tertiary amines.[9] Formation of an iminium ion from carbinolamides under the same conditions is not reported. This different result can be rationalised by considering the electron availability at the nitrogen atoms in the carbinol compounds obtained from these two class of substrates. The electron delocalising effect of the carbonyl group in the carbinolamide probably results in the OH group being much less likely to be expelled.

In this part of the thesis, the attempts to identify two of the possible intermediates of the P450-mediated oxidation of N,N-dialkylamides, namely the carbon-centred radical intermediate (**3**) and the iminium ion (**4**) will be presented and discussed. The main goal is, actually, the identification of the carbon-centred radical (**3**), largely because of the strong indirect indications, reported in the literature,[1-4] that it is the more probable intermediate in these metabolic oxidations. However, due to the potential formation of an iminium ion species even from carbon-centred radical, attempts to identify this intermediate were also carried out.

Intermolecular trapping of carbon-centred radical intermediates will be described in detail in the next chapter. However, the basic approach involves the use of a spin trapping agent capable of stabilising short-lived carbon-centred radicals and rendering them detectable by electron spin resonance (ESR).

Intramolecular trapping of the potential carbon-centred radical intermediates involves the use of various unsaturated groups inserted in the substrate molecules, as illustrated in Figure 2.3. These unsaturated groups should be able to trap the unpaired electron of the radical to generate a rearranged product, in this case a cyclic compound.

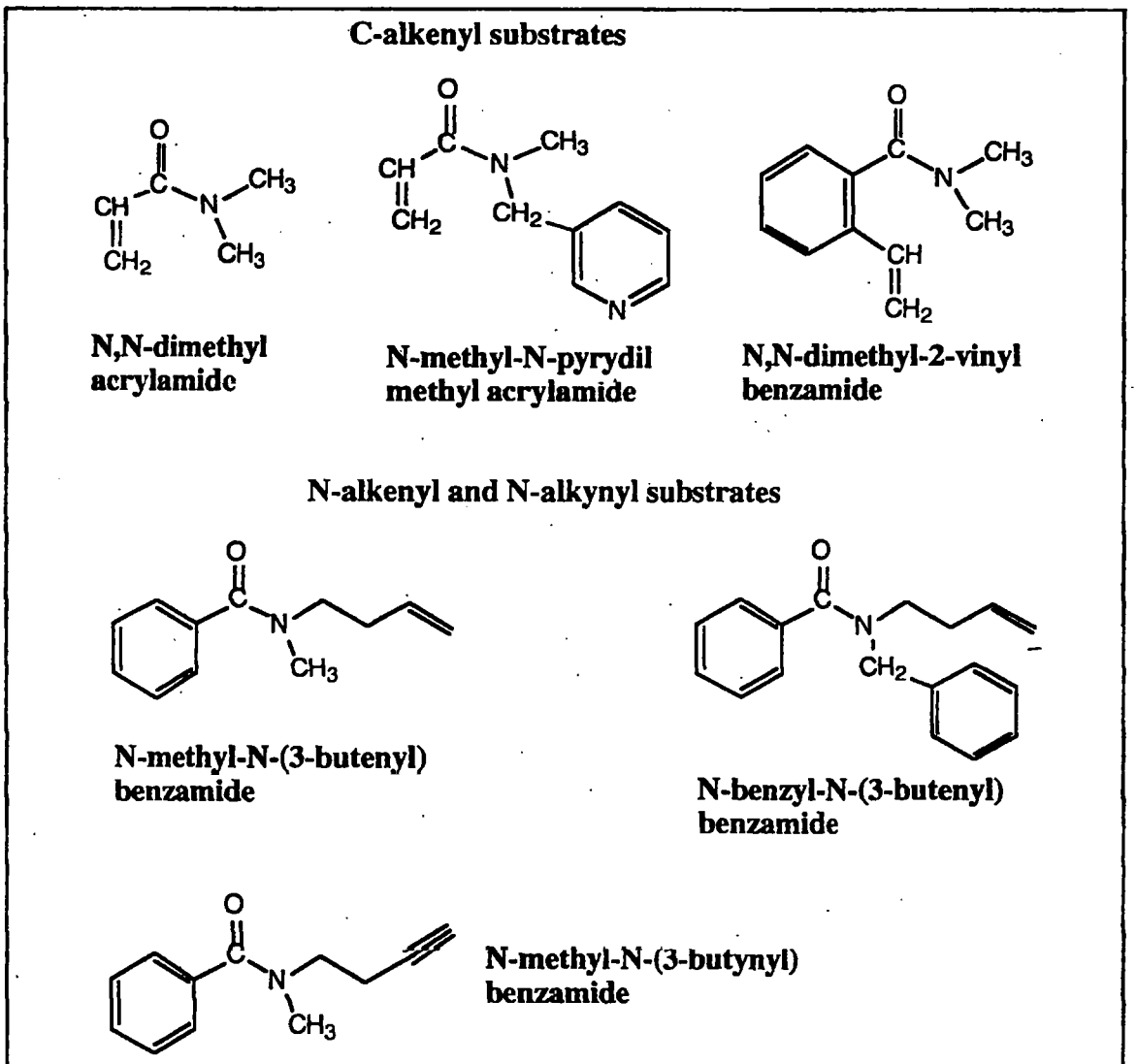

Figure 2.3 Substrate probes for the intramolecular trapping of carbon-centred radical intermediates.

The probe substrates can be divided into two classes: the C-alkenyl compounds, in which the alkenyl group is attached to the carbonyl carbon atom, and the N-alkenyl compounds, in which the alkenyl group is attached to the amide nitrogen atom. The proposed pathway for the trapping of any carbon-centred radical intermediates produced by these substrates is shown in Figure 2.4.

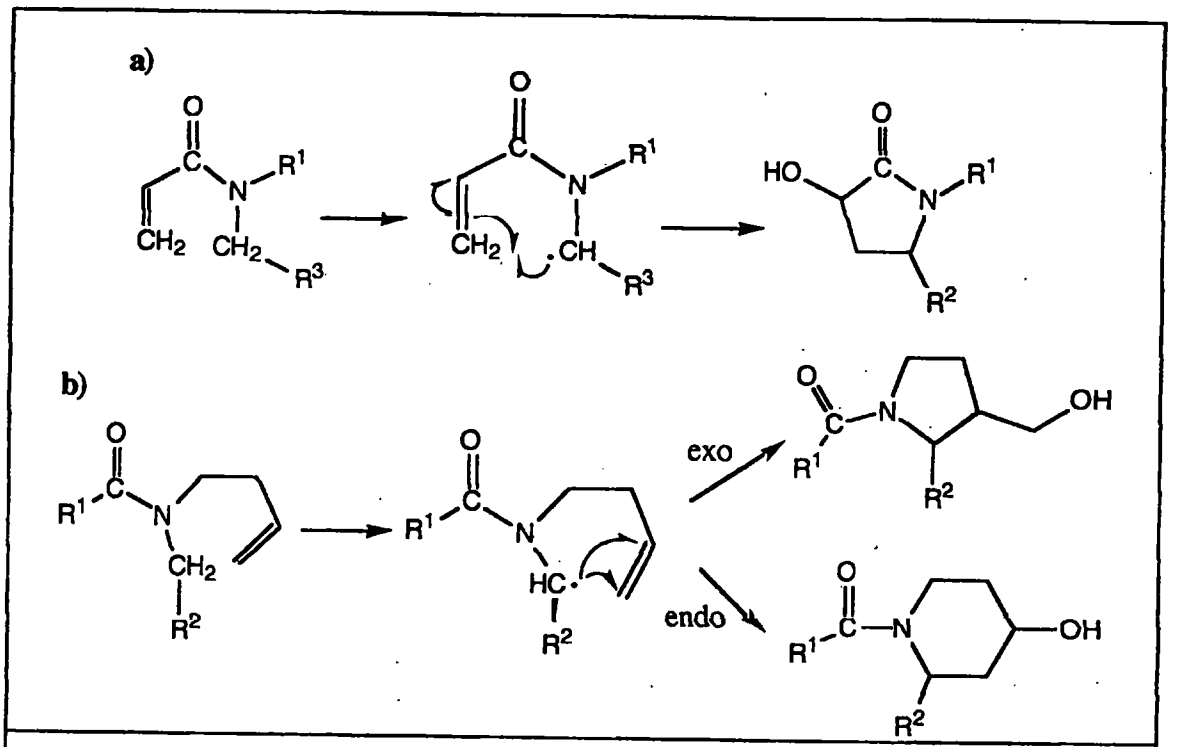

Figure 2.4 Proposed mechanism for the trapping of carbon-centred radical intermediate.

Intramolecular trapping should present kinetic advantages over the intermolecular counterpart. Intermolecularly trapping will have kinetic constants comparable with those of the insertion of the hydroxyl group from the P450-haem-hydroxyl complex. In contrast, the internal trapping of the radical intermediate has time constants reported to be generally much smaller than insertion of a hydroxyl group,[5; 10] making cyclisation the favoured reaction.

Attempts to trap the iminium ion intermediate centred on two strategies, intermolecularly using the nucleophiles ^{-}CN and $^{-}BD_4$, and intramolecularly using a substrate containing a nucleophilic group able to capture the electrophilic intermediate.

The substrate used for the intramolecular trapping on iminium ion is illustrated in Figure 2.5.

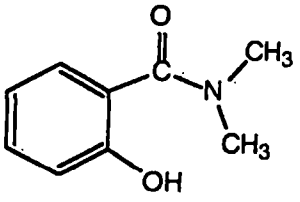

N,N-dimethyl-2-hydroxybenzamide

Figure 2.5 Substrate probe used for the intramolecular trapping of iminium ion intermediates

The use of $^{-}$CN as an intermolecular trap for iminium ion species is reported to have been successful in the microsomal P450 metabolism of tertiary amines such as nicotine. [6; 10; 11] Reaction with $^{-}$CN therefore should lead to the formation of an N-cyanomethylamide derivative, easily identifiable by normal analytical procedures (Figure 2.6). The use of sodium borodeuteride as a trap follows the same principle. Reaction between the iminium ion intermediate, if formed, and the borodeuteride ion should lead to the formation of deuterated substrate (Figure 2.4) which should be identifiable by mass spectroscopic analysis.

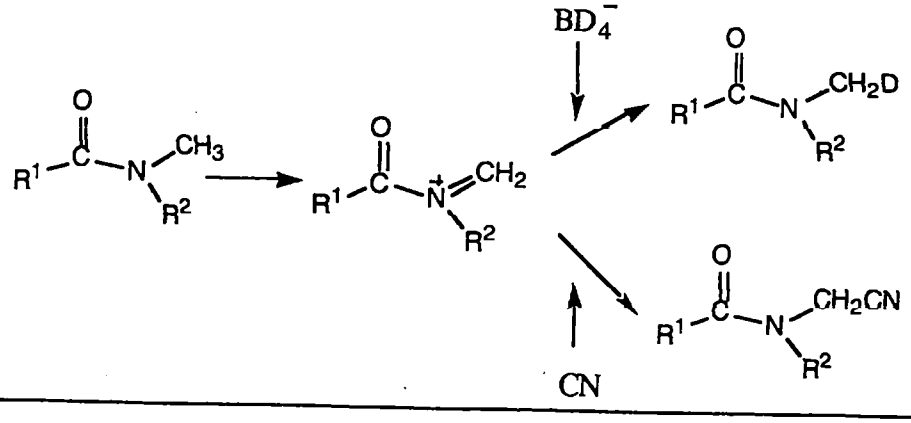

Figure 2.6 Scheme for the intermolecular trapping of iminium ion species by $^{-}$CN and $^{-}$BD$_4$.

Intramolecular trapping of the iminium ion intermediate relies upon the presence of the hydroxyl group in the *ortho* position. If formed, the iminium ion should lead to cyclisation (Figure 2.7) alongside concomitant demethylation.

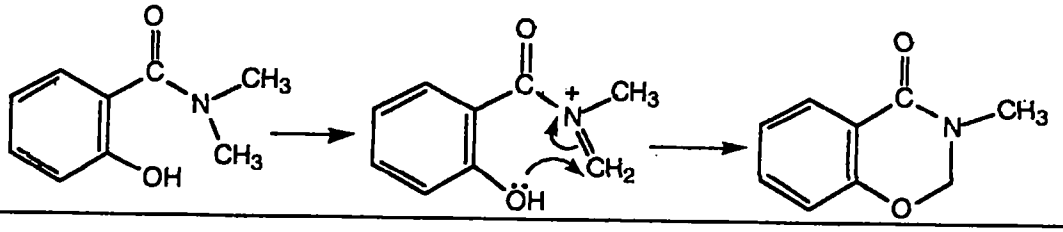

Figure 2.7 Cyclic trapping of an iminium ion intermediate.

2.2. Iminium ion trapping

2.2.1 Trapping of iminium ion by ^{-}CN

As a preliminary to the study of the intermolecular trapping during metabolism of N,N-dimethylbenzamide, oxidation of N,N-dimethylaniline was performed in the presence of either NaCN or $NaBD_4$. This substrate was chosen because it has been reported that metabolism occurs via iminium ion formation.[11; 12] Due to the structural similarity to N,N-dimethylbenzamide, this amine is an ideal positive control for these experiments.

- **Identification of the products**

Since CN^- is a well known P450 inhibitor, optimum conditions for the metabolism incubations in the presence of NaCN were established by varying both the concentration of N,N-dimethylaniline between 0.5 and 10 mM and also of sodium cyanide between 1 and 10 mM. The best experimental conditions were found to be a substrate concentration of 10 mM and a sodium cyanide concentration of 1 mM. At that concentration sodium cyanide does not appreciably inhibit the P450-dependent metabolism of N,N-dimethylaniline.

A typical gas chromatogram/mass spectral (GCMS) analysis of a sample obtained after 30 minutes incubation of 10 mM N,N-dimethylaniline in the presence of 1 mM sodium cyanide is reported in Figure 2.8. The products of the reactions were identified by comparison of their mass spectra and chromatographic profile with those obtained from pure synthetic standards. The identified products are reported in Table 2.1. Clearly sodium cyanide is an efficient trap for the iminium ion species. Moreover, formation of the expected N-demethylated metabolite is strong evidence that P450 oxidation of the substrate is not inhibited by the trap at these concentrations.

Having optimised the experimental conditions for trapping the iminium ion formed by N,N-dimethylaniline, attention was directed towards the possible involvement of the iminium ion intermediate in the metabolism of N,N-dimethylbenzamide. Microsomal incubations using 10 mM N,N-dimethylbenzamide were performed in the presence of 1 mM sodium cyanide. A typical GCMS analysis obtained after 30 minutes microsomal incubation is shown in Figure 2.9. The products of the reaction were identified, as before, by comparison of their mass spectra and gas chromatographic data with those obtained from pure synthetic standards. The identified products of the reaction are given in Table 2.2. Microsomal metabolism of N,N-dimethylbenzamide in the presence of sodium cyanide results in the formation of only one metabolite, N-methylbenzamide. No evidence for the formation of N-cyanomethyl-N-methylbenzamide was obtained under any experimental conditions. To ascertain whether sodium cyanide interferes with the metabolism of the substrate, and therefore with iminium ion formation, incubations using increased concentrations of N,N-dimethylbenzamide were performed. All incubations failed to show any detectable formation of N-cyanomethyl-N-methylbenzamide. Synthetic N-cyanomethyl-N-methylbenzamide was analysed under the same conditions to determine if it would degrade under the analytical conditions. The GCMS (result (c) of Figure 2.9) indicates that such an intermediate, if formed, would be clearly detectable. Thus the P450-dependent metabolism of N,N-dimethylbenzamide does not occur *via* the formation of ^{-}CN trappable iminium ion intermediates.

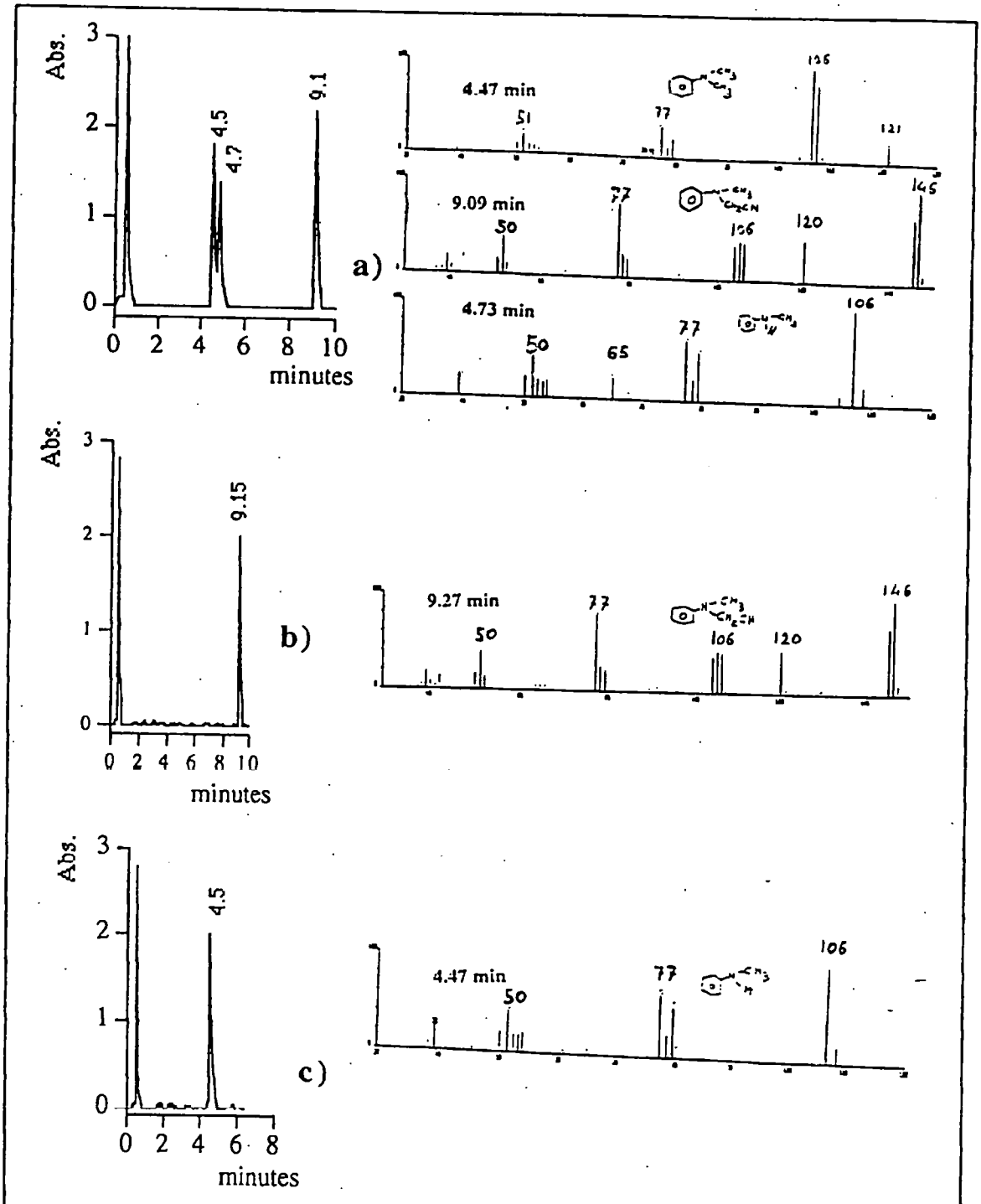

Figure 2.8 GCMS from microsomal incubation of (a) 10 mM N,N-dimethylaniline in the presence of 1 mM sodium cyanide, and of synthetic standards (b) N-cyanomethyl-N-methylaniline and (c) N-methylaniline.

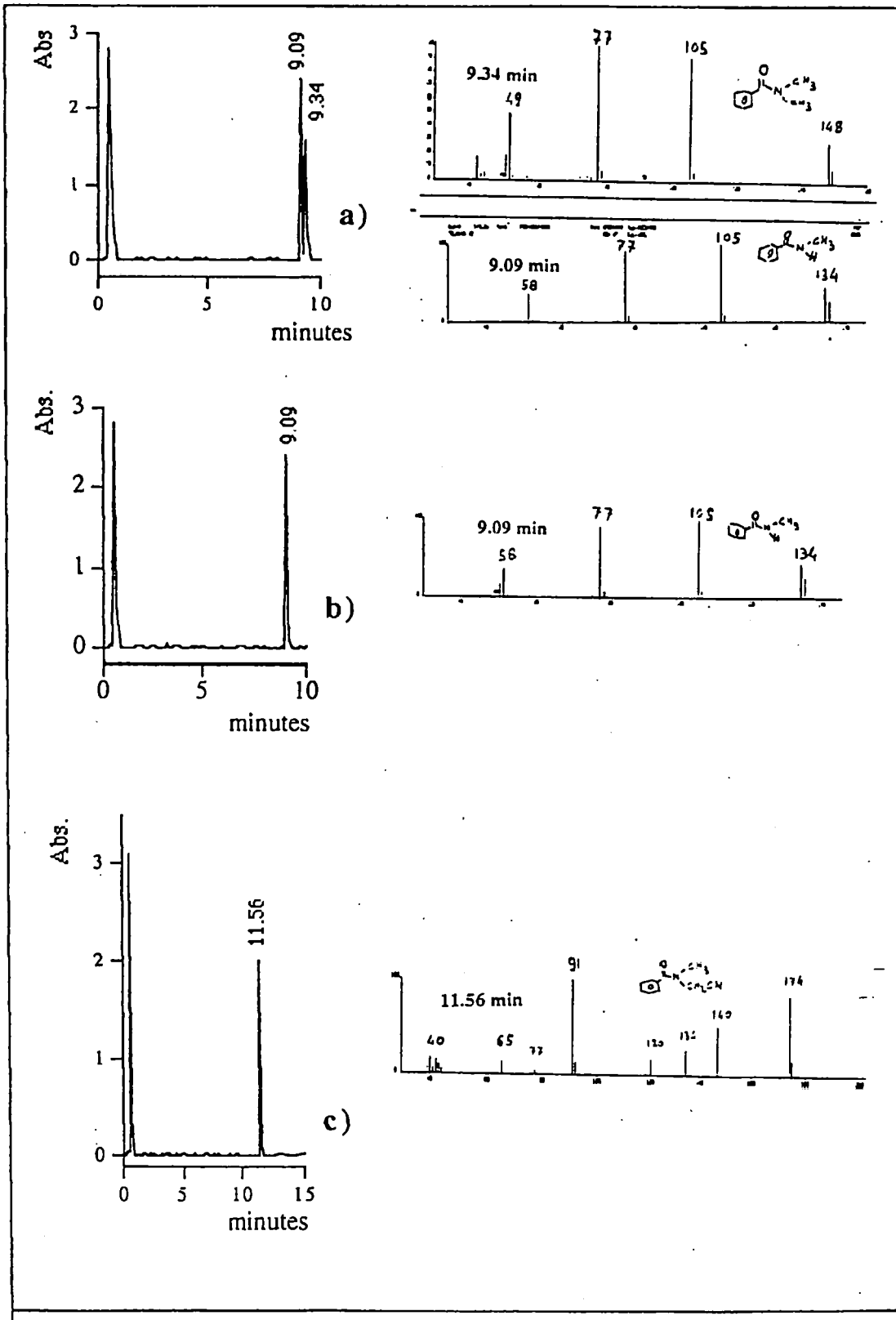

Figure 2.9 GCMS from microsomal incubation of (a) 10 mM N,N-dimethylbenzamide in the presence of 1 mM sodium cyanide, and of synthetic standards (b) N-methylbenzamide and (c) N-cyanomethyl-N-methylbenzamide.

Peak	Compound identified
Retention Time: 4.47 minutes	N,N-dimethylaniline
Retention Time: 4.73 minutes	N-methylaniline
Retention Time: 9.16 minutes	N-cyanomethyl-N-methylaniline

Table 2.1 Products identified from the microsomal oxidation of N,N-dimethylaniline in the presence of sodium cyanide.

Peak	Compound identified
Retention Time: 9.09 minutes	N-methylbenzamide
Retention Time: 9.34 minutes	N,N-dimethylbenzamide

Table 2.2 Products identified from the microsomal oxidation of N,N-dimethylbenzamide in the presence of sodium cyanide.

- **Quantitative study of the microsomal oxidation of N,N-dimethylbenzamide and N,N-dimethylaniline in the presence of sodium cyanide**

As CN^- has a high affinity for the haem iron, the effect of 1 mM NaCN as a competitive inhibitor upon the metabolism of N,N-dimethylbenzamide and N,N-dimethylaniline was examined. The results obtained, expressed as the initial rates for the total metabolism of the substrates, together with the derived kinetic constants, V_{max} and K_m, are reported in Table 2.3. The results indicate that the presence of sodium cyanide has no effect on the metabolism of the substrates.

	v_i for total metabolism (mM/h/nmol P450)			
[Substrate] (mM)	**N,N-dimethyl benzamide**	**N,N-dimethyl benzamide and 1 mM NaCN**	**N,N-dimethyl aniline**	**N,N-dimethyl aniline and 1 mM NaCN**
0.5	0.60 ± 0.03	0.55 ± 0.04	0.92 ± 0.04	0.88 ± 0.05
1.0	1.01 ± 0.06	0.94 ± 0.06	1.38 ± 0.09	1.31 ± 0.07
3.0	1.84 ± 0.11	1.75 ± 0.08	2.04 ± 0.16	1.98 ± 0.11
10.0	2.19 ± 0.16	2.18 ± 0.06	2.46 ± 0.11	2.44 ± 0.07
20.0	2.81 ± 0.07	2.78 ± 0.11	2.55 ± 0.05	2.57 ± 0.11
V_{max} (mM/h/nmol P450)	3.10 ± 0.21	3.07 ± 0.11	2.7 ± 0.06	2.68 ± 0.05
K_m (mM^{-1})	2.06 ± 0.12	2.66 ± 0.08	0.96 ± 0.04	1.07 ± 0.03
V_{max}/K_m	1.50	1.15	2.81	2.51

Table 2.3 Initial rates and derived kinetic parameters for the microsomal oxidation of N,N-dimethylbenzamide and N,N-dimethylaniline.

2.2.2. Trapping of iminium ion by sodium borodeuteride ($NaBD_4$)

- **Identification of the products**

Optimal experimental conditions were obtained by using N,N-dimethylaniline as substrate. Incubations involved substrate concentrations between 0.5 and 10 mM, while sodium borodeuteride concentrations ranged from 1 to 10 mM. Analysis of the products was achieved by GCMS. Figure 2.10 illustrates typical GCMS results while Table 2.4 reports the identified products after 30 minutes of microsomal oxidation of 10 mM N,N-dimethylaniline in the presence of 5 mM sodium borodeuteride. These are the optimum experimental conditions resulting from this study.

Products of the metabolism were identified by comparison of their mass spectra with those obtained from synthetic standards. Comparison of the mass spectrum of N,N-dimethylaniline obtained from the microsomal incubations with that obtained from pure N,N-dimethylaniline (Figure 2.11) clearly reveals that deuterium incorporation into the substrate has taken place.

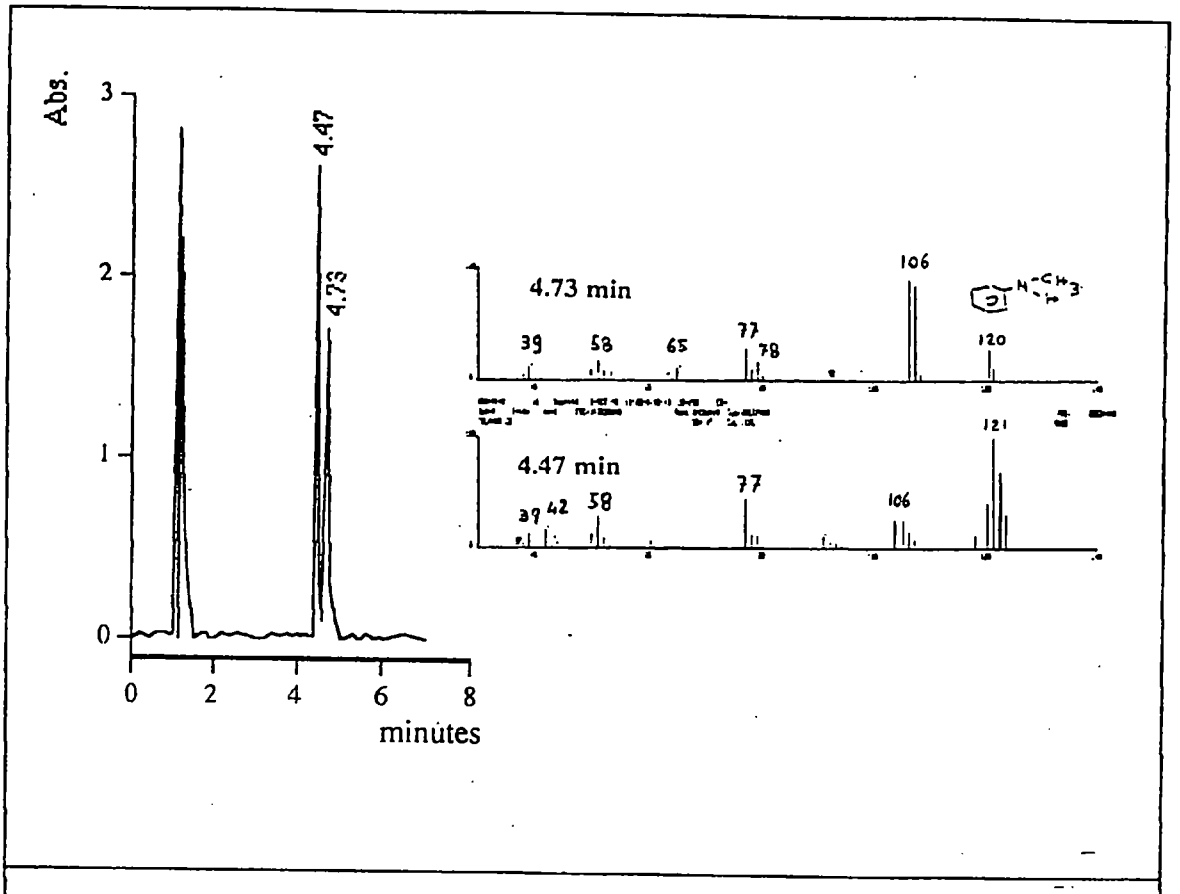

Figure 2.10 GCMS results of microsomal incubation of 10 mM N,N-dimethylaniline in the presence of 5 mM sodium borodeuteride.

Peak	Compound identified
Retention Time: 4.47 minutes	N,N-dimethylaniline
Retention Time: 4.73 minutes	N-methylaniline

Table 2.4 Identified products of the microsomal metabolism of N,N-dimethylaniline.

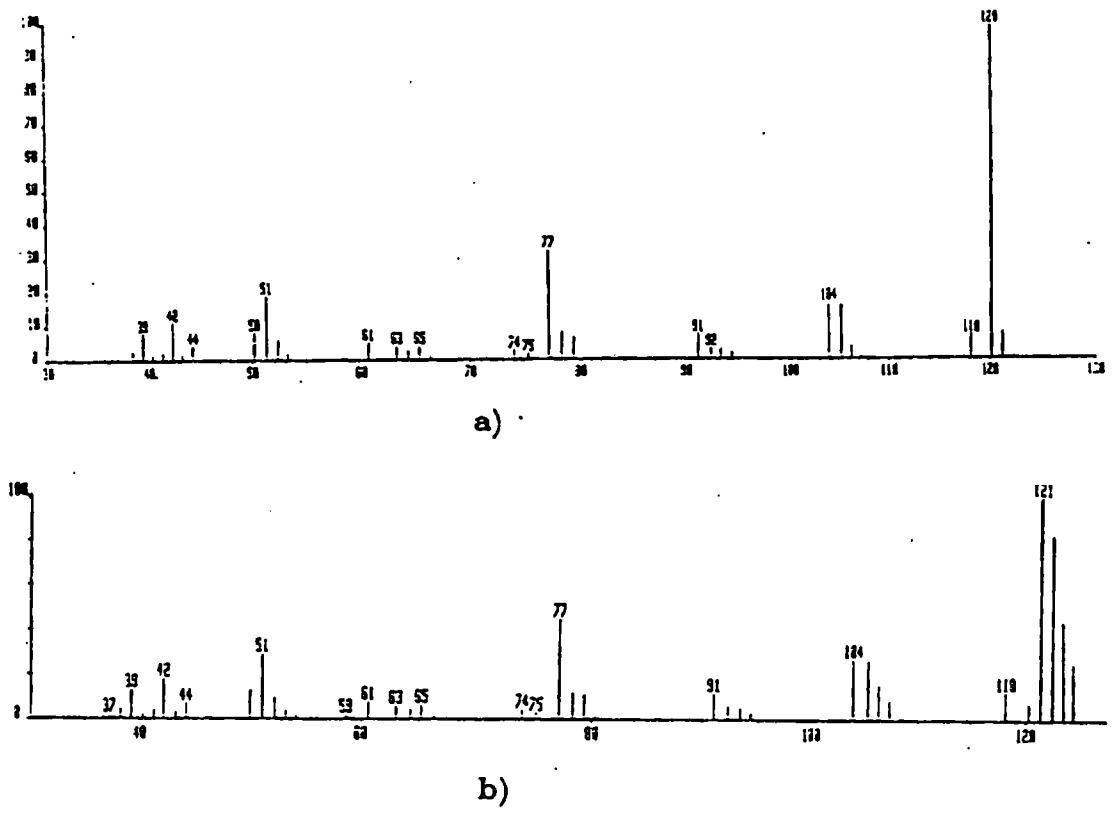

Figure 2.11 Mass spectra of (a) pure N,N-dimethylaniline and (b) N,N-dimethylaniline obtained from microsomal incubation in the presence of sodium borodeuteride.

These results are good evidence for the formation of an iminium ion intermediate which is reduced by the sodium borodeuteride present in the solution, leading to the formation of deuterated starting material. Since the major peak in the mass spectrum of N,N-dimethylaniline is the (M-1) peak at M/Z 120, the M/Z 121 peak in the spectrum obtained from microsomal metabolism can be assigned to the incorporation of one D atom. The presence of M/Z 123 and 124 peaks thus signify the incorporation of two, three and four deuterium atoms, respectively, into the product. The presence of these higher mass species suggests that the deuterated N,N-dimethylanilines undergo further P450 oxidation via iminium ion formation. This is quite surprising because two successive metabolic cycles of the same substrate molecule would be expected to be an unlikely process.

Given the efficient trapping of the iminium ion intermediate by sodium borodeuteride, identical experimental conditions were employed for the microsomal metabolism of N,N-dimethylbenzamide.

Figure 2.12 and Table 2.5 report the GCMS of a typical microsomal incubation of 10 mM N,N-dimethylbenzamide in presence of 5 mM sodium borodeuteride.

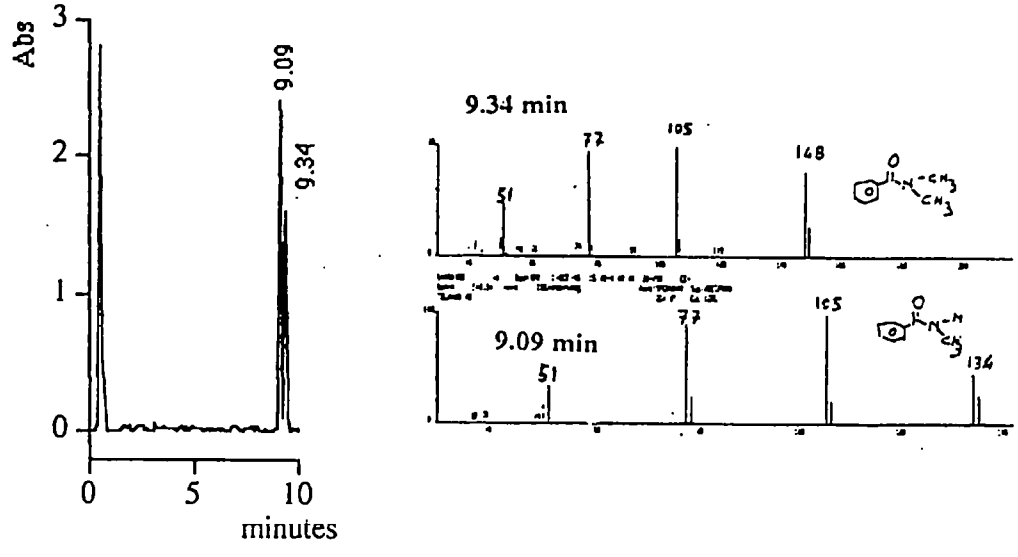

Figure 2.12 GCMS results from the microsomal incubation of 10 mM N,N-dimethylbenzamide in the presence of 5 mM sodium borodeuteride.

Peak	Compound identified
Retention Time: 9.34 minutes	**N,N-dimethylbenzamide**
Retention Time: 9.09 minutes	**N-methylbenzamide**

Table 2.5 Products identified after 30 minutes microsomal oxidation of 10 mM N,N-dimethylbenzamide in presence of sodium borodeuteride.

Comparison of the mass spectra of the products obtained from metabolism of N,N-dimethylbenzamide with those of synthetic standards reveals that no deuterated N,N-dimethylbenzamide was detected under any of the experimental conditions. This result can be interpreted either as indicating that microsomal metabolism of tertiary amides does not occur *via* iminium ion formation or that intermolecular trapping of such an

intermediate is not efficient. This latter possibility seems unlikely, given the effective trapping of iminium ion intermediates during the metabolism of N,N-dimethylaniline. The conclusion is that during the microsomal P450-dependent metabolism of tertiary amides iminium ion species are not formed.

- **Quantitative study of the microsomal metabolism of N,N-dimethylaniline and N,N-dimethylbenzamide in the presence of sodium borodeuteride**

To obtain further information on the effects of sodium borodeuteride on the microsomal oxidation of the amine and amide substrates, a quantitative analysis of these reactions was carried out. Microsomal incubations were performed with the substrate concentration varying between 1 and 10 mM in the presence of 5 mM of sodium borodeuteride. The measured rates for the microsomal oxidations of N,N-dimethylaniline and N,N-dimethylbenzamide, together with the derived kinetic parameters, are presented in Table 2.6.

	v_i **total metabolism** (mM/h/nmol P450)			
[Substrate] (mM)	**N,N-dimethylaniline**	**N,N-dimethylaniline and $NaBD_4$**	**N,N-dimethyl benzamide**	**N,N-dimethyl benzamide and $NaBD_4$**
0.5	0.92 ± 0.03	0.69 ± 0.03	0.60 ± 0.05	0.60 ± 0.04
1.0	1.38 ± 0.08	1.02 ± 0.07	1.00 ± 0.06	1.03 ± 0.03
3.0	2.04 ± 0.06	1.57 ± 0.07	1.84 ± 0.09	1.82 ± 0.10
5.0	2.26 ± 0.11	1.81 ± 0.06	1.91 ± 0.11	1.94 ± 0.05
10.0	2.46 ± 0.12	1.99 ± 0.09	2.19 ± 0.06	2.21 ± 0.07
V_{max} (mM/h/nmol P450)	2.70 ± 0.11	2.20 ± 0.09	3.10 ± 0.12	3.08 ± 0.13
K_m (mM^{-1})	0.96 ± 0.06	1.15 ± 0.08	2.06 ± 0.14	2.07 ± 0.09
V_{max}/K_m	2.81	1.91	1.50	1.48

Table 2.6 Observed rates for the microsomal metabolism of N,N-dimethylaniline and N,N-dimethylbenzamide in the presence and in absence of 5 mM sodium borodeuteride.

These data indicate that metabolism of N,N-dimethylbenzamide is not effected by the presence of sodium borodeuteride. In contrast, the metabolism of N,N-dimethylaniline is significantly inhibited by the presence of the BD_4^- ion. Analysis of the kinetic parameters for the N,N-dimethylaniline reaction indicates that V_{max} is reduced while K_m remains relatively constant. This is consistent with non-competitive inhibition, in which the rate of product formation from the reaction intermediates is reduced. Clearly, this must be the case if the intermediate iminium ion is reduced back to starting material.

The kinetic data, together with the qualitative analysis of the products of the reactions, indicate that in the case of N,N-dimethylaniline microsomal oxidation occurs *via* formation of an iminium ion, whereas in the case of N,N-dimethylbenzamide microsomal oxidation does not lead to the formation of any trappable iminium ion species.

2.2.3 Attempts to trap an iminium ion intramolecularly

As illustrated in Figure 2.7, N,N-dimethyl-2-hydroxybenzamide has the potential to trap, intramolecularly, iminium ion intermediates. Such trapping should result in the formation of the cyclic product, 3-methyl-4-oxobenz-1,3-oxazinane. Typical GCMS results obtained from microsomal oxidation of 10 mM N,N-dimethyl-2-hydroxybenzamide are shown in Figure 2.13. Identification of the products was achieved by comparison with synthetic standards (Table 2.6).

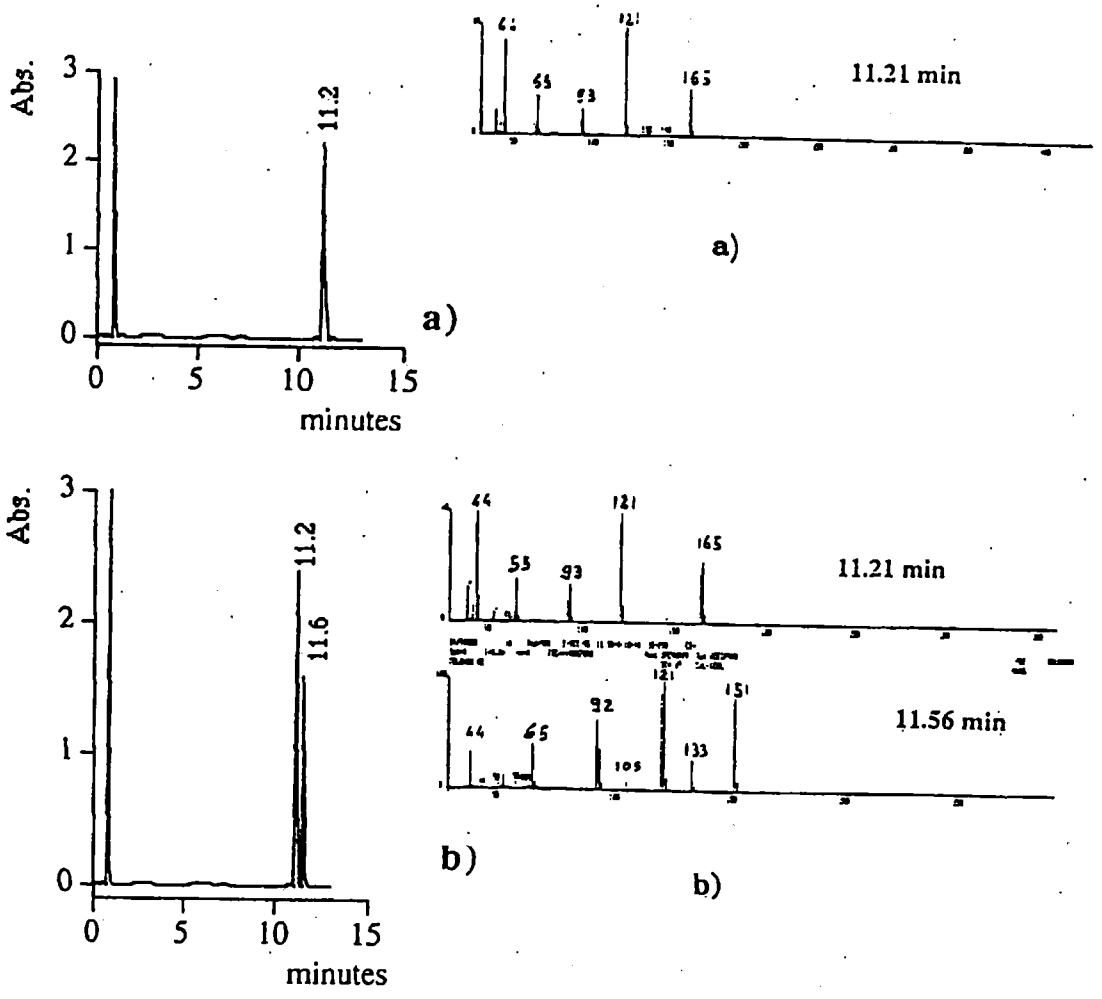

Figure 2.13 GCMS of the ethyl acetate extracts from microsomal oxidation of 10 mM N,N-dimethyl-2-hydroxy benzamide at (a) time 0 and (b) time 30 minutes.

Peak	Compound identified
Retention Time: 11.21 minutes	**N,N-dimethyl-2-hydroxybenzamide**
Retention Time: 11.56 minutes	**N-methyl-2-hydroxybenzamide**

Table 2.6 Products identified from the microsomal oxidation of 10 mM N,N-dimethyl-2-hydroxybenzamide.

No cyclic product was identified under any experimental condition. A synthetic standard of 3-methyl-4-oxobenz-1,3-oxazinane was analysed using the same analytical conditions, to verify that such a compound is not formed in any of the experiments. Analysis of the incubations by HPLC, to avoid any possibility that extraction was inefficient, also revealed that no cyclisation product was present. Thus, it would appear that microsomal metabolism of the amide does not occur via iminium ion formation.

Finally, the initial rates of metabolism and the derived kinetic parameters K_m and V_{max} were determined and compared with those for the microsomal oxidation of N,N-dimethyl benzamide. The results are presented in Table 2.7. The results confirm that the increasing of polarity of the substrate affects metabolism as illustrated by a comparison of the V_{max}/K_m values of the two substrates tested. The smaller value for the 2-hydroxy derivative previous reports that rates increase with increasing lipophilicity.[13; 14]

	v_i (mM/h/nmol P450)	
[Substrate] (mM)	**From N,N-dimethyl benzamide**	**From N,N-dimethyl-2-hydroxy benzamide**
0.5	0.60 ± 0.05	0.28 ± 0.02
1.0	1.01 ± 0.06	0.51 ± 0.05
3.0	1.84 ± 0.11	0.96 ± 0.03
5.0	1.91 ± 0.10	1.34 ± 0.09
10.0	2.18 ± 0.14	1.62 ± 0.15
V_{max} (mM/h/nmolP450)	3.1 ± 0.20	2.57 ± 0.09
K_m (mM^{-1})	2.06 ±0.12	4.06 ± 0.31
V_{max}/K_m	1.50	0.63

Table 2.7 Initial rates of formation and derived kinetic parameters for the microsomal oxidation of N,N-dimethylbenzamide and N,N-dimethyl-2-hydroxybenzamide.

2.3. Trapping of carbon centred radicals

2.3.1 Using the N,N-dimethylacrylamide system

The potential pathway for microsomal oxidation of N,N-dimethylacrylamide involving carbon-centred radicals is illustrated in Figure 2.14. The carbon-centred radical intermediate **2** can undergo direct insertion of the hydroxyl group from the activated P450 haem-oxygen complex, leading to the N-demethylated product **3**. Alternatively it can be trapped by the double bond of the acryloyl functionality, giving, *via* cyclisation, the N-methyl-3-hydroxy pyrrolidinone product, **4** (Figure 2.14).

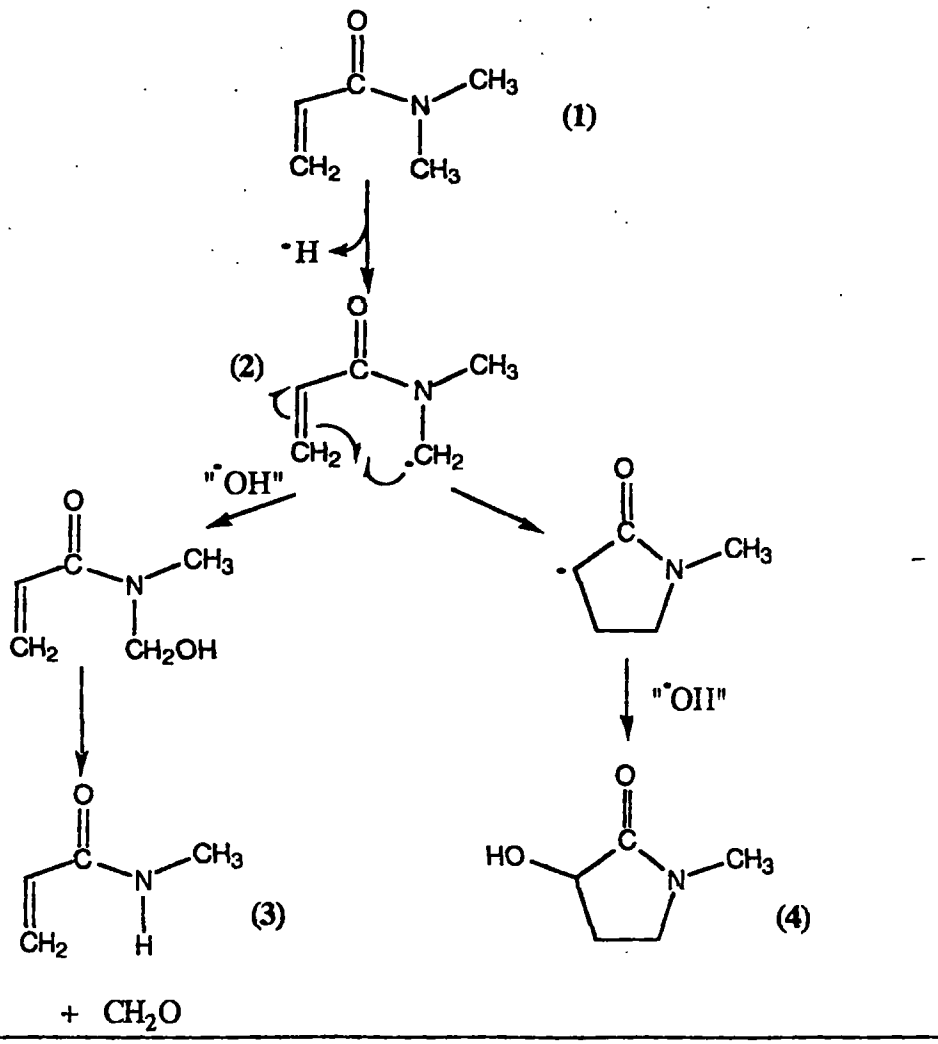

Figure 2.14 Potential P450-dependent oxidation pathway of N,N-dimethyl acrylamide.

2.3.1.1 Chemical cyclisation and AM1 semi-empirical molecular orbital calculations

Semi-empirical M.O. calculated heats of formation for the species in Table 2.8 were obtained using the AM1 self-consistent field model. Interestingly, the difference between the heats of formation of N,N-dimethylcrylamide and its carbon-centred radical, 98.1 kJ mol^{-1}, is comparable to the analogous difference reported for N,N-dimethylbenzamide, 119.9 kJ mol^{-1}.[3] Thus there is relatively little energetic difference in the formation of the carbon-centred radical for acrylamide. Furthermore, the cyclisation of the carbon-centred radical seems to be an energetically favoured process, as indicated from the difference, 9.2 kJ mol^{-1}, between the heats of formation of the open chain/cyclised carbon-centred radicals.

Compound	ΔH_f (Kj/mol.)
N,N-dimethylacrylamide	- 58.6
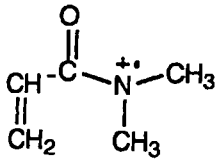	775.9
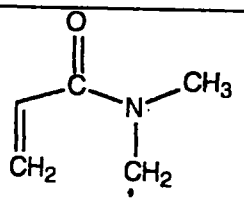	39.5
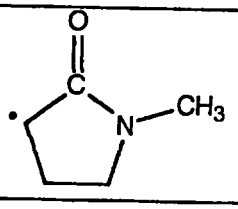	30.3

Table 2.8 Heats of formation (ΔH_f) calculated by the AM1 model for N,N-dimethyl acrylamide and its postulated radical intermediates.

The efficiency of the acryloyl system for trapping the carbon-centred radical was tested by chemically generating the carbon-centred radical intermediate **2** of Figure 2.14 from N-chloromethyl-N-methylacrylamide.

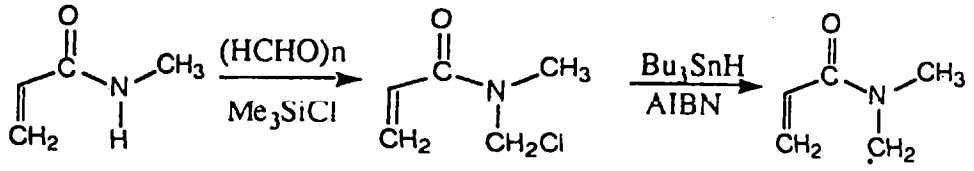

The GC results are illustrated in Figure 2.15, and identified by comparison of their mass spectra with that obtained from synthetic standards reported in Table 2.9.

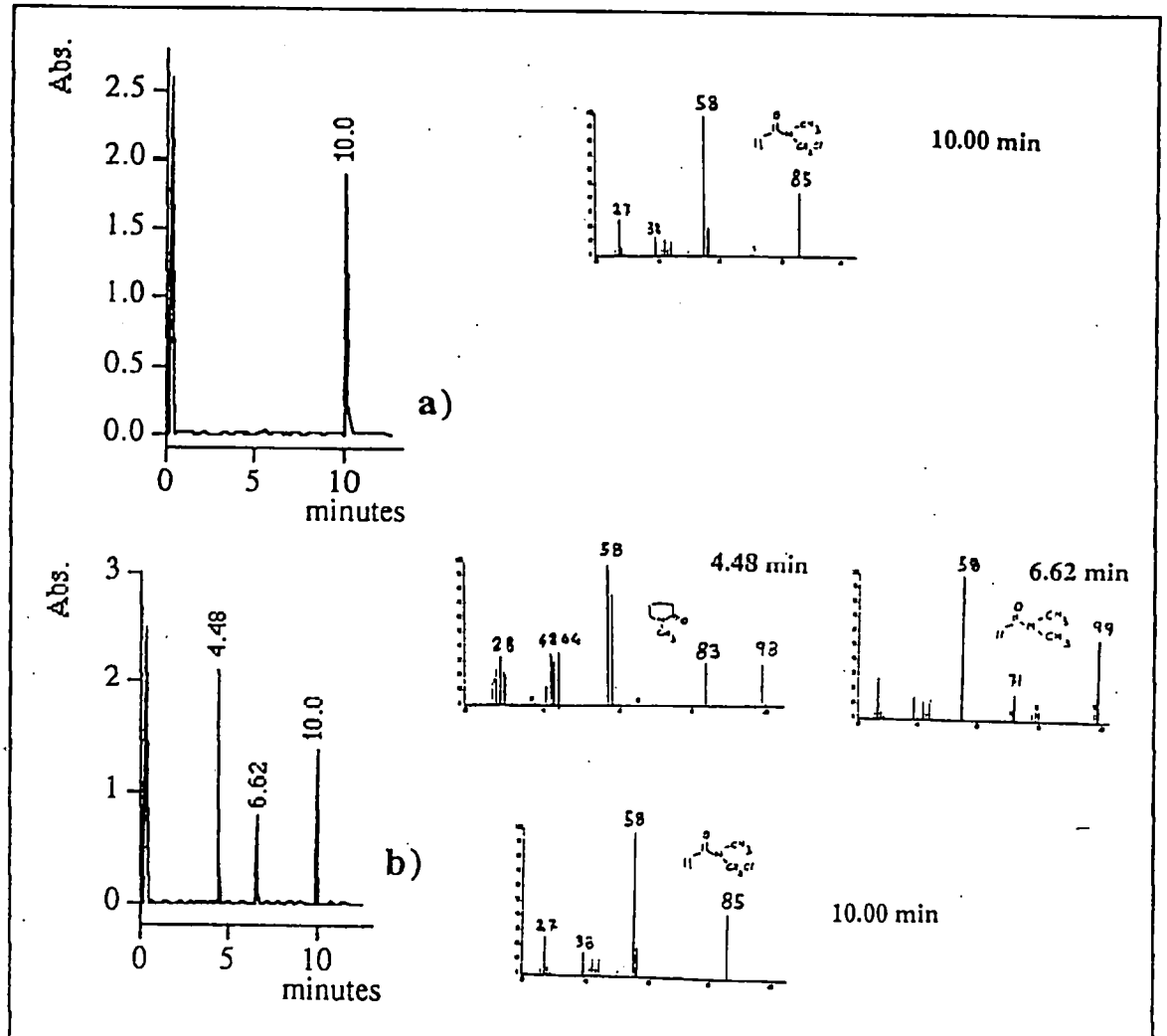

Figure 2.15 GCMS traces obtained from the reaction involving chemical generation of the carbon-centred radical **2** of figure 2.17.

Peak	Compound identified
Retention Time: 10.00 minutes	N-chloromethyl-N-methylacrylamide
Retention Time: 4.48 minutes	N-methylpyrrolidinone
Retention Time: 6.62 minutes	N,N-dimethylacrylamide

Table 2.9 Products identified from the cyclisation of the chemically generated carbon centred-radical **2** of Figure 2.17.

In this chemical system, the carbon-centred radical can either abstract a hydrogen atom directly from Bu_3SnH to form N,N-dimethylacrylamide, or it can cyclise and then abstract a hydrogen atom to form N-methyl-2-pyrrolidinone. Both products are formed and quantification indicates that cyclisation is favoured by 4 to 1 over N,N-dimethylacrylamide formation.

2.3.1.2 Trapping of carbon-centred radicals during the P450-dependent metabolism of N,N-dimethyl acrylamide

A typical HPLC analysis of a microsomal incubation of 10 mM N,N-dimethyl acrylamide after 30 minutes is illustrated in Figure 2.19. The products of the reaction were identified by comparison of their retention times and diode array spectra with those of synthetic standards and are summarised in Table 2.10.

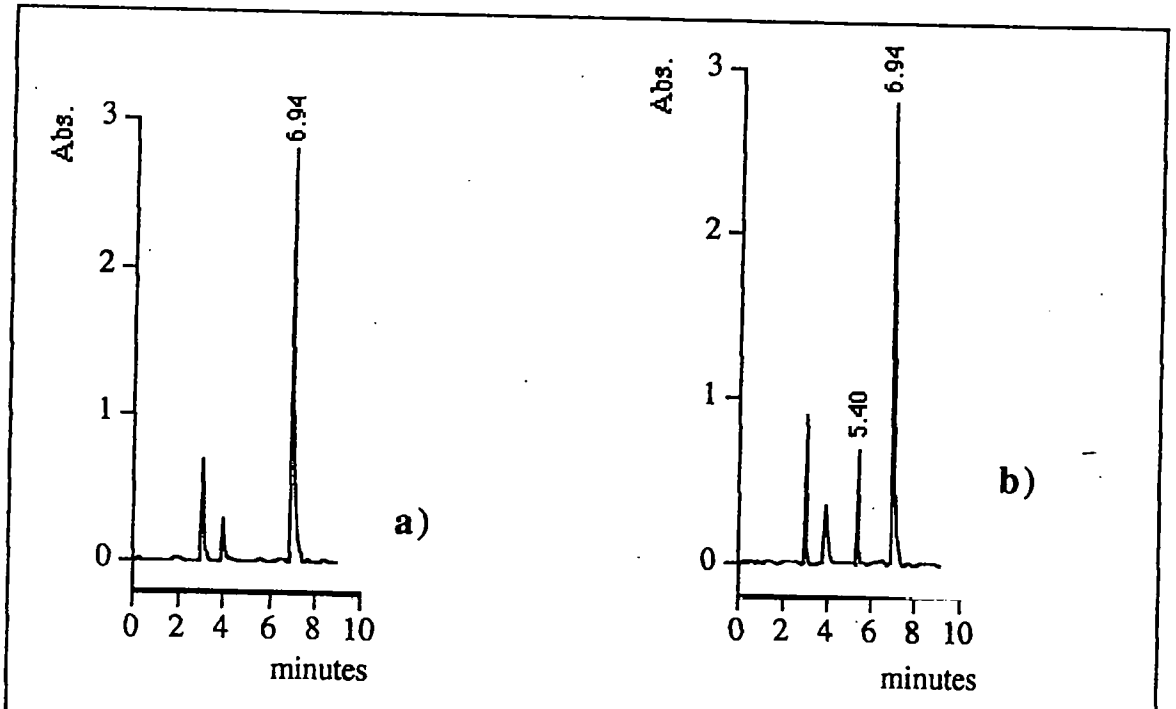

Figure 2.16 Typical HPLC chromatograms from the microsomal oxidation of 10 mM N,N-dimethylacrylamide, at time of (a) 0 and (b) 30 minutes.

Peak	Product identified
Retention Time: 6.94 minutes	**N,N-dimethylacrylamide**
Retention Time: 5.40 minutes	**N-methyl-3-hydroxylpyrrolidinone**

Table 2.10 Products identified from the microsomal metabolism of N,N-dimethyl acrylamide.

It is interesting to note that no N-demethylated product was found. The results are consistent with the formation of a carbon-centred radical intermediate which is then intramolecularly trapped to give the cyclic metabolite N-methyl-3-hydroxy-2-pyrrolidinone. The absence of the N-demethylated product indicates that cyclisation is the favoured reaction with respect to hydroxylation. Given that cyclisation is more favoured in the case of microsomal oxidation than in the case of analogous chemical system. It is possible that interactions between the enzyme and the substrate influence the proximity of the radical centre to the double bond. Further investigation of this aspect of the reaction was not undertaken.

The results of a kinetic analysis of the microsomal metabolism of N,N-dimethyl acrylamide are reported in Table 2.11.

[Substrate] (mM)	**v_i for formation of N-methyl-3-hydroxy-2-pyrrolidinone** (mM/h/nmol P450)
0.5	0.23 ± 0.02
1.0	0.37 ± 0.05
3.0	0.66 ± 0.06
5.0	0.78 ± 0.08
10.0	0.90 ± 0.11
V_{max} (mM/h/nmol P450)	1.07 ± 0.08
K_m (mM^{-1})	1.85 ± 0.09
V_{max}/K_m	0.58

Table 2.11 Initial rates and kinetic parameters for the microsomal oxidation of N,N-dimethylacrylamide.

These are unremarkable, but reveal a rate α one-third of that for N,N-dimethylbenzamide. This probably reflects the greater hydrophilicity of the acrylamide.

2.3.2 N-methyl-N-pyridylmethylacrylamide

Having verified that the acryloyl system is an effective trap for carbon-centred radical intermediates in amide dealkylation, a further substrate was investigate, namely N-

methyl-N-pyridylmethylacrylamide. The presence of the aryl ring should favour hydrogen atom abstraction from the carbon atom α-to the ring due to resonance stabilisation of the carbon-centred radical intermediate. A potential pathway for this substrate is illustrated in Figure 2.20. Hydrogen abstraction can theoretically occur from both α-carbon atoms, leading to the formation of two carbon-centred intermediates, **2** and **3** (Figure 2.17). These can then undergo intramolecular cyclisation to give compound, **4** and **6** (Figure 2.17).

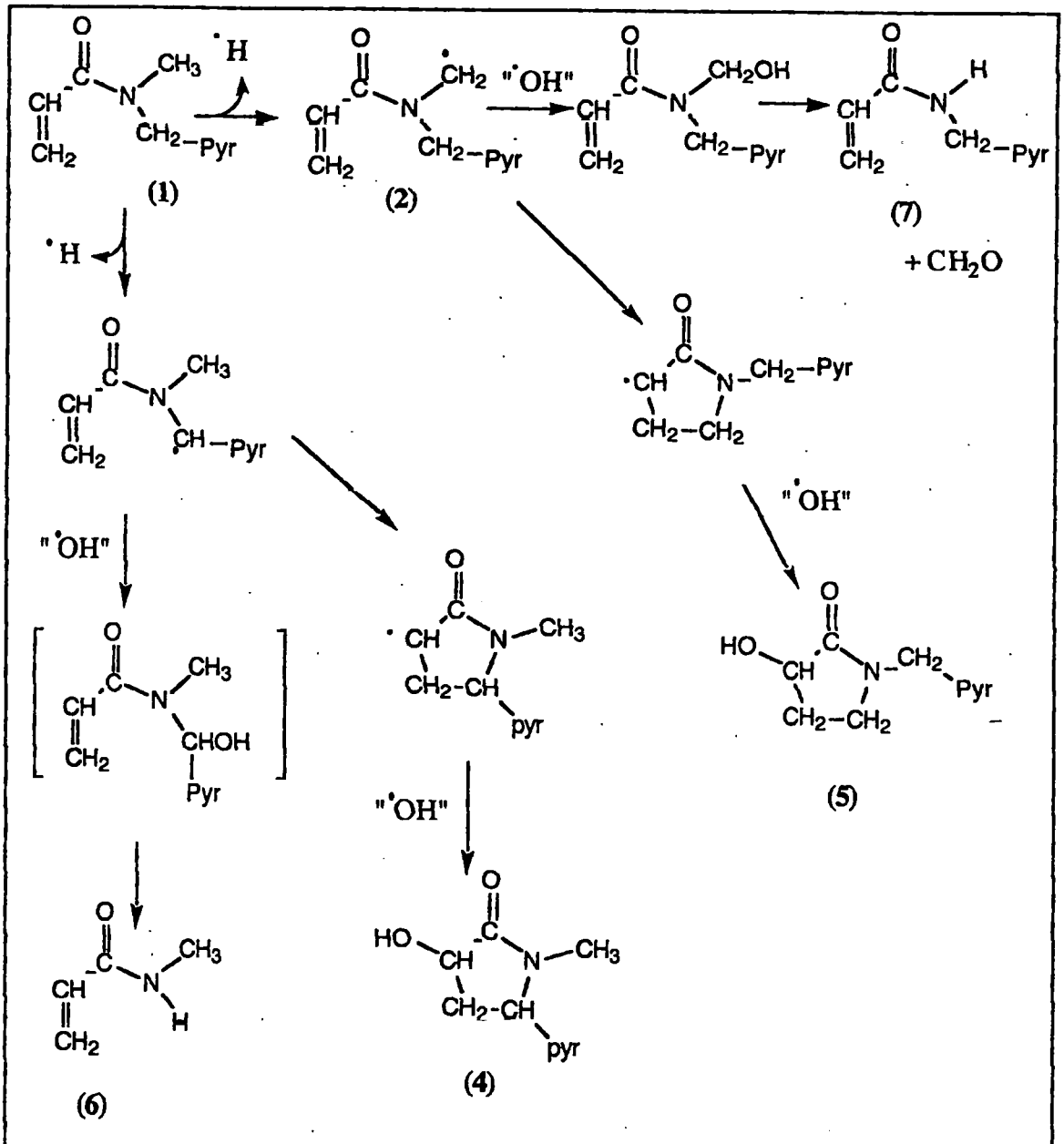

Figure 2.17 Potential pathway for the microsomal oxidation of N-methyl-N-pyridylmethylacrylamide.

HPLC analysis of the microsomal incubation of 10 mM N-methyl-N-pyridylmethylacrylamide gave the chromatogram illustrated in Figure 2.18. Table 2.12 reports the products of the reaction, identified by comparison of their UV spectra with those of synthetic standards.

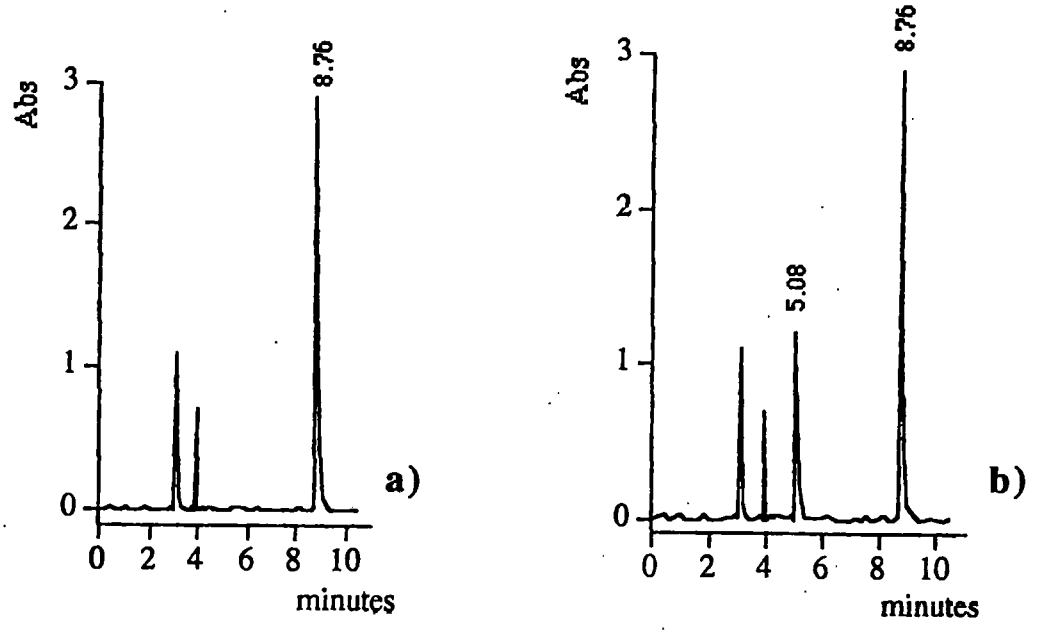

Figure 2.18 HPLC chromatograms of the microsomal oxidation of 10 mM N-methyl-N- pyridylmethylacrylamide, at time (a) 0 and (b) 30 minutes.

Peak	Compound identified
Retention Time: 8.76 minutes	**N-methyl-N-pyridylmethylacrylamide**
Retention Time: 5.08 minutes	**3-hydroxycotinine**

Table 2.12 Products of the microsomal oxidation of N-methyl-N-pyridylmethylacrylamide.

Significantly, reaction occurs exclusively in the N-alkyl group to form the cyclic product 3-hydroxycotinine, and no N-dealkylated product is observed. Moreover, no

reaction at the N-methyl group could be detected. These results indicate that substrate metabolism occurs *via* hydrogen atom abstraction to form a carbon-centred radical intermediate. The presence of the aromatic ring directs the reaction toward N-alkyl rather than N-methyl oxidation.

Kinetic parameters for this reaction are reported in Table 2.13. Comparison of these data with those obtained for the metabolism of N,N-dimethylacrylamide, indicate that the N-pyridylmethyl compound is metabolised 2-3 times faster, further supporting a reaction mechanism involving hydrogen atom abstraction from the α-carbon.

	v_i (mM/h/nmol P450)
[substrate] (mM)	**3-hydroxycotinine**
0.5	0.55 ± 0.03
1.0	0.86 ± 0.08
3.0	1.41 ± 0.06
5.0	1.61 ± 0.10
10.0	1.80 ± 0.12
V_{max} (mM/h/nmol P450)	2.05 ± 0.12
K_m (mM^{-1})	1.36 ± 0.06
V_{max}/K_m	1.51

Table 2.13 Initial rates of formation and kinetic parameters of the microsomal oxidation of N-methyl-N-pyridylmethylbenzamide.

2.3.3 Using N,N-dimethyl- 2-vinylbenzamide

A potential pathway for the microsomal oxidation of N,N-dimethyl-2-vinylbenzamide is shown in Figure 2.19. Formation of the carbon-centred radical intermediate **2** can lead either to insertion of the hydroxyl group from P450 to give the

carbinolamide and, subsequently, the N-demethylated product **3**, or to cyclisation and the formation of product **4**.

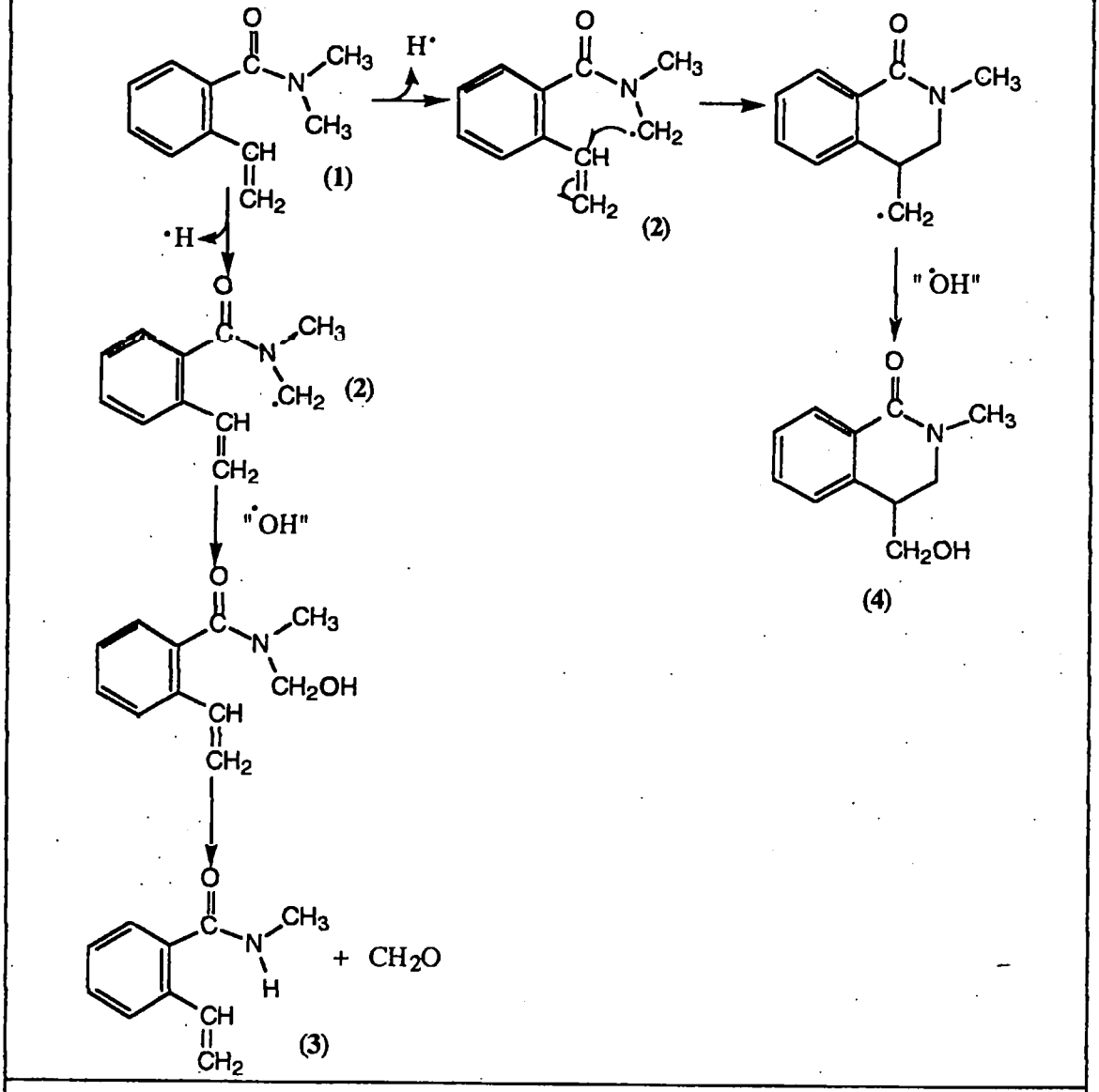

Figure 2.19 Potential pathways for the microsomal oxidation of N,N-dimethyl-2-vinylbenzamide.

A typical GCMS analysis of the microsomal incubation of 10 mM N,N-dimethyl-2-vinylbenzamide obtained after 30 minutes is shown in Figure 2.20.

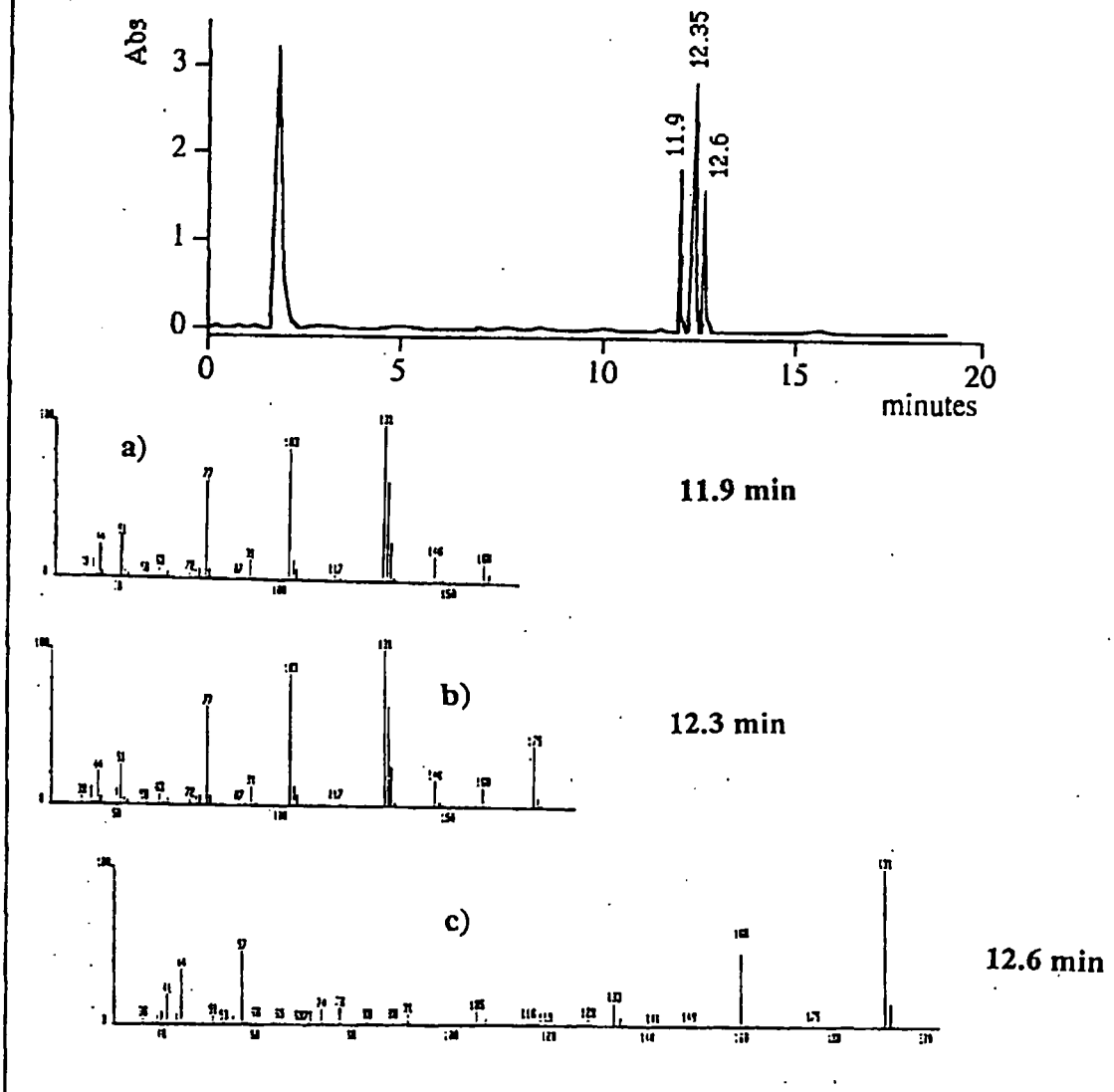

Figure 2.20 GCMS analysis of the microsomal incubation of 10 mM N,N-dimethyl-2-vinylbenzamide, spectrum a) N-methyl-2-vinylbenzamide, spectrum b) N,N-dimethyl-2-vinylbenzamide and spectrum c) metabolite resulting to insertion of an oxygen atom to N,N-dimethyl-2-vinylbenzamide.

The peak with retention time of 12.45 minutes was identified as the substrate, by comparison of the mass spectrum with that of the synthetic standard. The 11.95 minute peak has a mass spectral profile of which the major features are

- an M/Z value of 191, equivalent to the mass of the substrate plus an oxygen atom
- the loss of a fragment of mass 31, equivalent to the group M-CH_2OH.

This mass spectral profile is consistent with the three compounds illustrated in Figure 2.21.

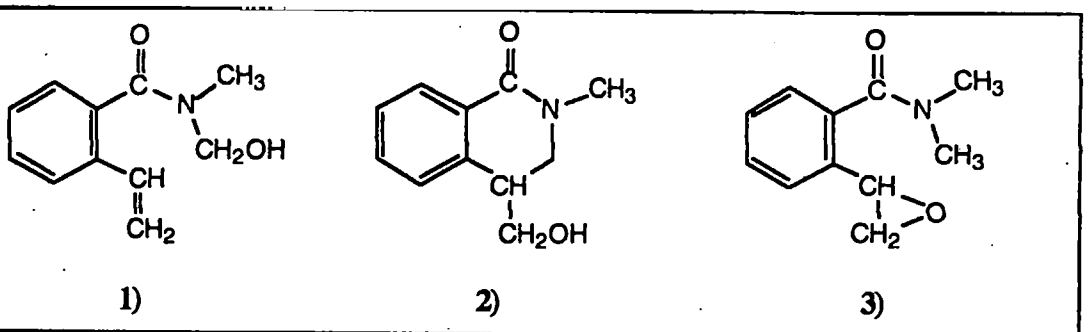

Figure 2.21 Potential structure of the oxygenated metabolite formed upon metabolism of N,N-dimethylbenzamide.

N-hydroxymethyl-N-methyl-2-vinylbenzamide (compound **1**), is an unlikely candidate since treatment of the sample by base (which is carried out prior to analysis) would result in the N-demethylated product.[3; 4]

To further clarify the structure of the 11.95 minutes metabolite ethyl acetate extracts from the base treated incubation mixture were divided in two aliquots; one was subjected to treatment by strong base (5 M KOH; 1 hour), the other to acylation by trifluoroacetic acid.

Compound **2**) of Figure 2.21 would be expected to undergo acylation

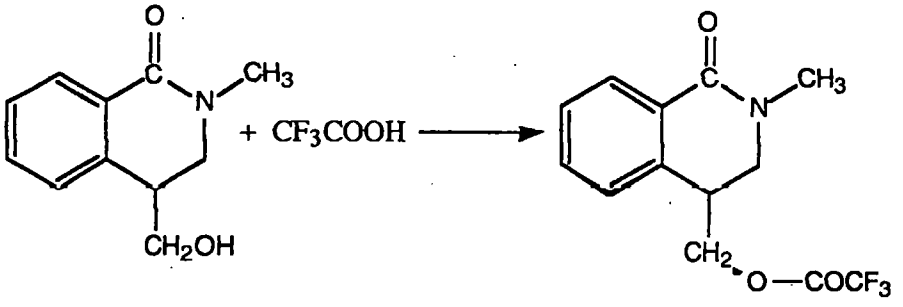

Thus if the 11.95 minute peak corresponds to compound **2**) it should disappear after trifluoroacetic treatment. Alternatively, compound **1**) should disappear after basic treatment to form N-methyl-2-vinylbenzamide, whereas if it corresponds to compound **3**) treatment with strong base should lead to a diol via opening of the epoxide. Figure 2.22 reports the typical GC traces of these samples.

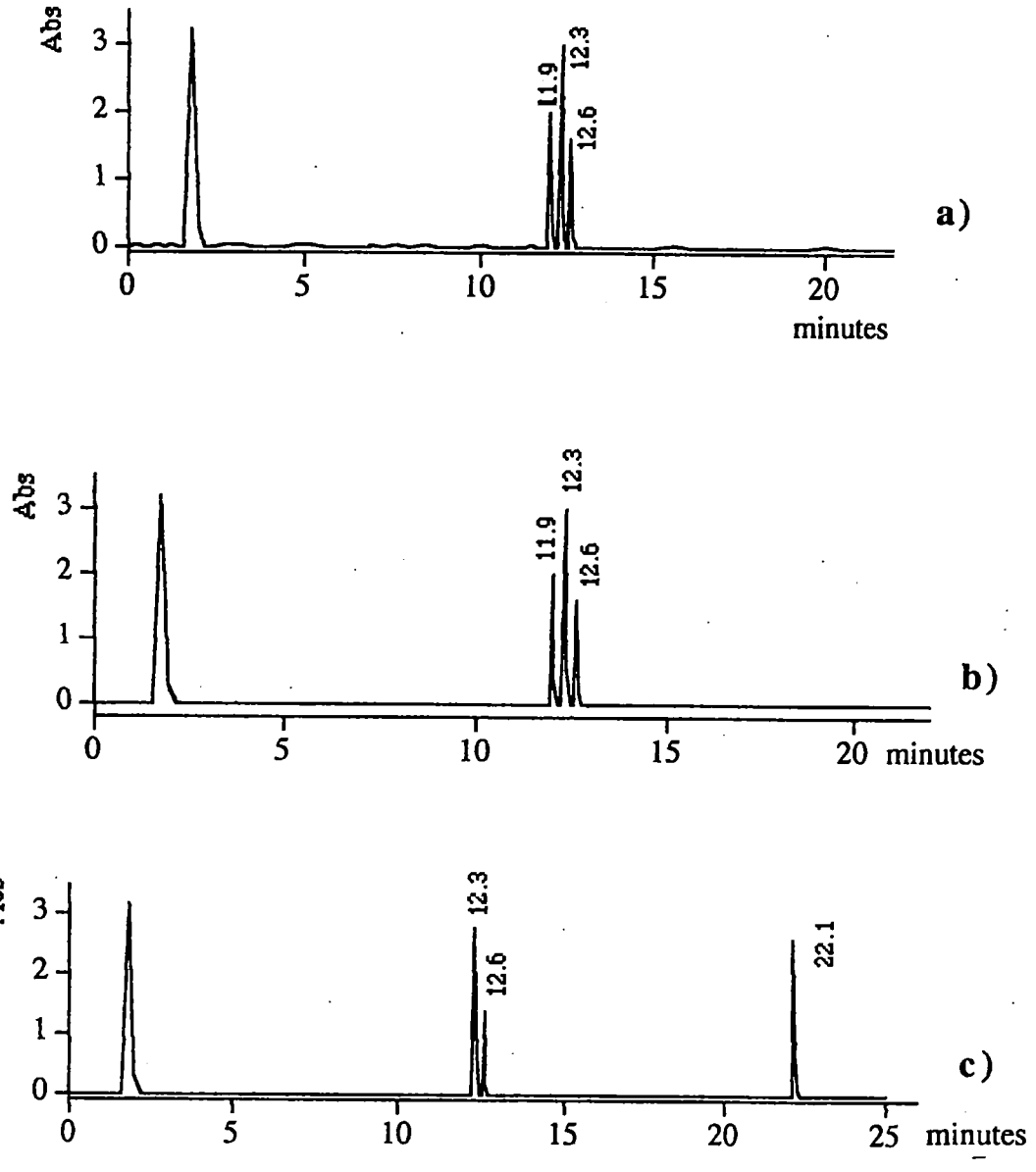

Figure 2.22 GC traces of the extracts of microsomal incubation of 10 mM N,N-dimethyl-2-vinyl benzamide, after a) normal base treatment, b) 5 M NaOH 1 hour treatment and c) after trifluoroacetic acid treatment.

The 11.95 minute peak is not affected by base but disappears as a consequence of the acylation reaction. Moreover, upon trifluoroacetic acid a new peak appears, with a retention time of 22.26 minutes, consistent with an acylated product. The results point to the 11.95 minutes peak as corresponding to compound **2)** of Figure 2.21.

2.4 Using N-alkenyl and N-alkynyl substrates

The N-alkenyl and N-alkynyl substrate probes used in this study are the compounds illustrated in Figure 2.3. It has been reported that double and triple bonds are able to intramolecularly trap a carbon-centred radical to generate cyclic products through rearrangement. [15; 16; 17] This being so, the potential microsomal oxidative pathways for N-(3-butenyl)-N-methylbenzamide and N-(3-butynyl)-N-methylbenzamide are illustrated in Figures 2.23 and 2.24.

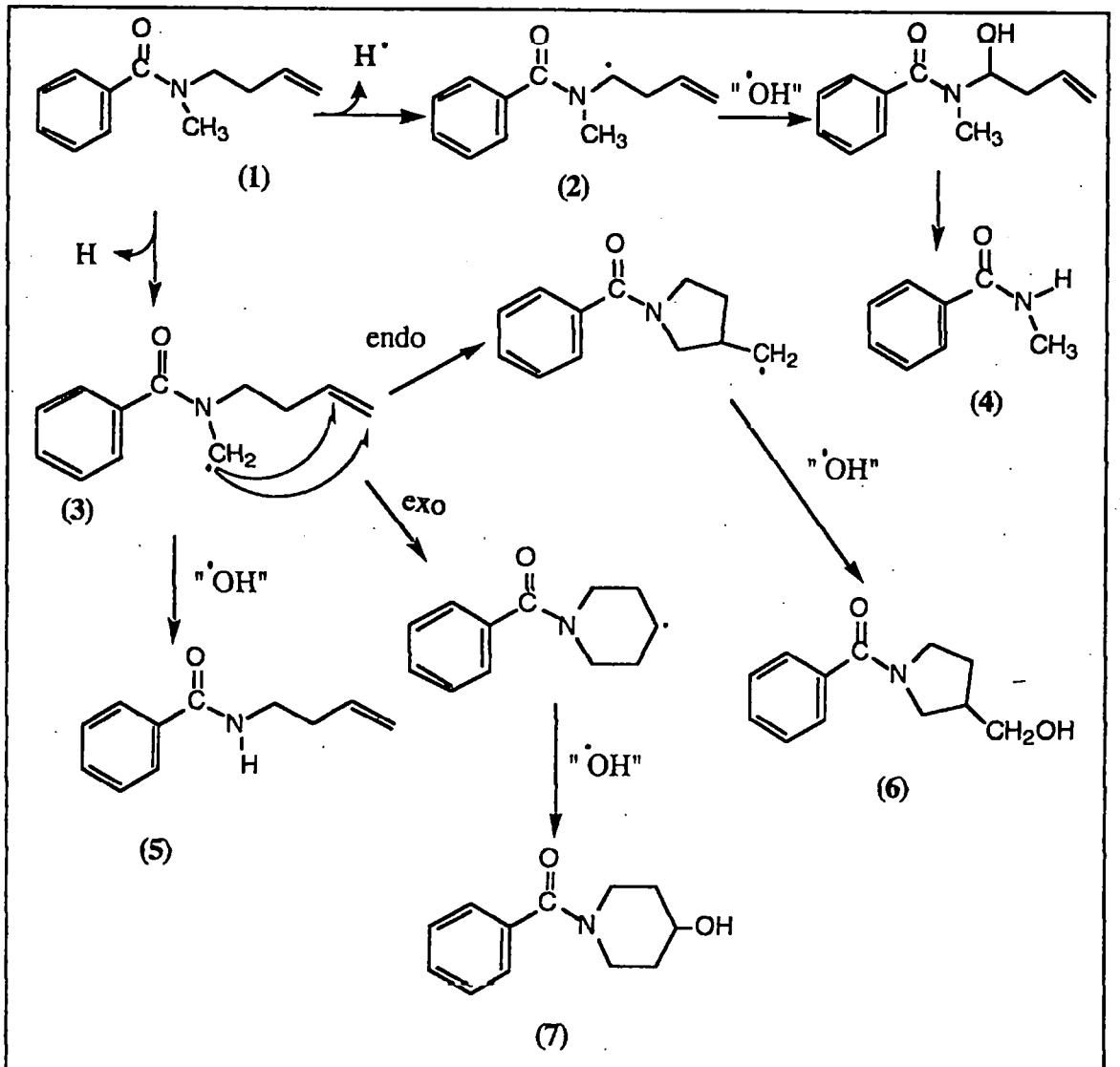

Figure 2.23 Potential pathways for the microsomal oxidation of N-(3-butenyl)-N-methylbenzamide.

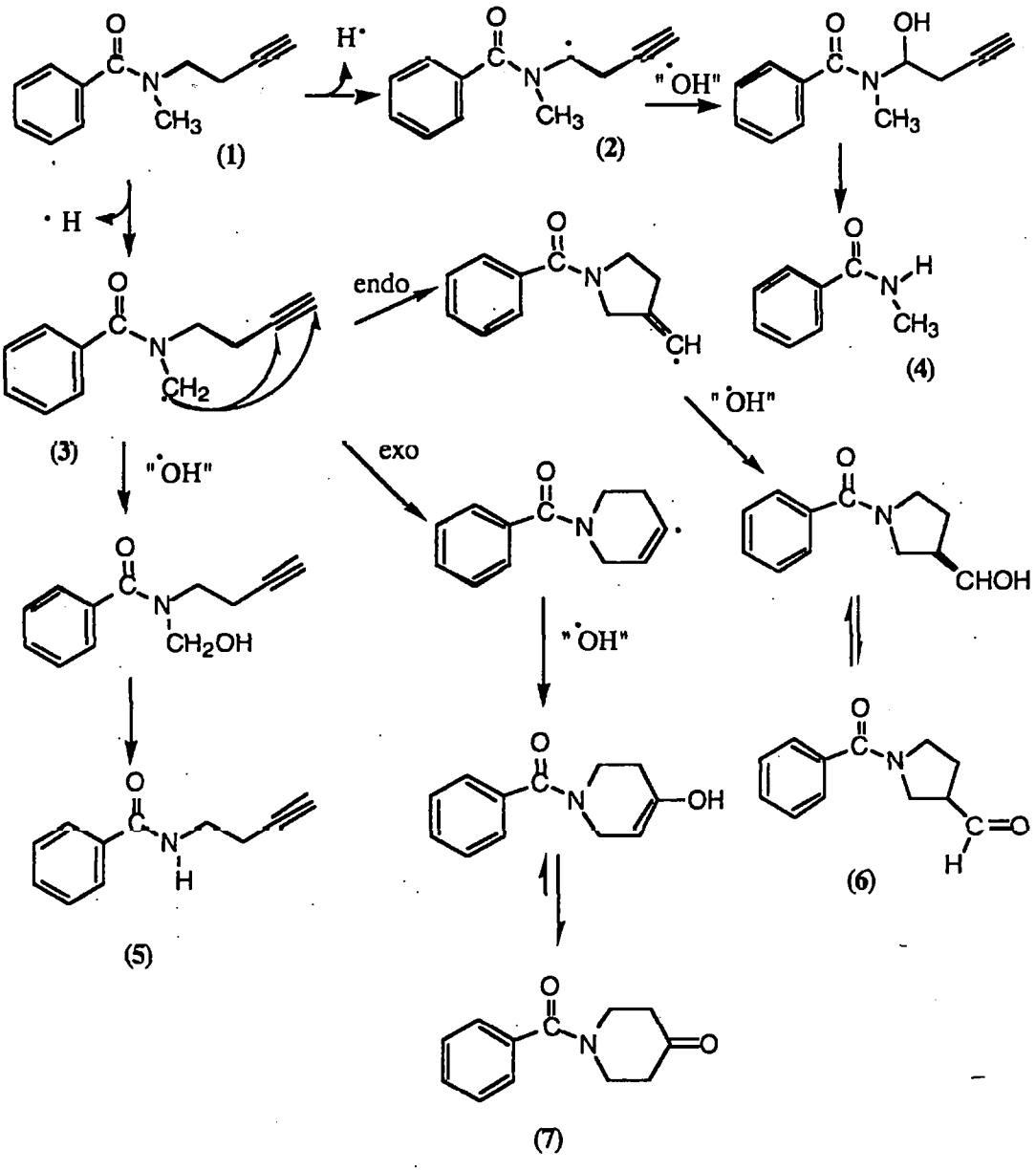

Figure 2.24 Potential pathways for the microsomal oxidation of N-(3-butynyl)-N-methylbenzamide.

Hydrogen atom abstraction from the carbon α- to the nitrogen can lead to the formation of two potential carbon-centred radical intermediates, **2** and **3** of Figures 2.23 and 2.24. Both radical intermediates can undergo hydroxyl group insertion from the P450 haem-oxoiron complex to give the dealkylated metabolites **4** and **5**. Alternatively, the

carbon-centred radical derived from the N-methyl group can undergo intermolecular trapping by either endo- or exo- cyclisation to yield the metabolites **6** and **7** (Figures 2.26 and 2.24).

Initially AM1 semi-empirical calculations of the heats of formation of the radical species illustrated in Figure 2.23 and 2.24, were calculated. These were accompanied by reactions involving the chemical formation of the carbon-centred radicals. Subsequently, microsomal oxidation of the substrate was performed.

2.4.1 AM1 semi-empirical molecular orbital calculations and cyclisation of chemically generated radicals

The heats of formation of the postulated carbon-centred radical intermediates of the reactions illustrated in Figure 2.23 and 2.24 were calculated by the self-consistent field semi-emphirical AM1 model (Table 2.14). The results indicate the oxidation of the N-methyl is disfavoured with respect to the N-alkyl group. Moreover, cyclisation, from thermodynamic considerations, should lead to the formation of the six-membered ring compound. This contrast with reports that similar radical cyclisation reactions result in the formation of a five- rather than six-membered ring product,[18; 19; 20; due to a less strained transition state in the formation of the five membered ring product. However, the ratio of the five- to six- membered rings depends upon the substituents attached to the olefinic bond. Systems containing amido groups are reported to yield a considerable amount of the larger ring product.[21; 22] Moreover, the situation changes when radical cyclisation is reversible; under thermodynamic conditions, six-membered ring products are reported to be formed predominantly.[23; 24]

Compound	ΔH_f (kJ/mol.)
N-(3-butenyl)-N-methylbenzamide	**30**
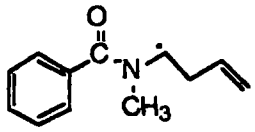	**130**
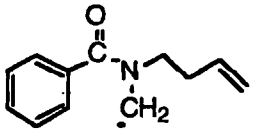	**133**
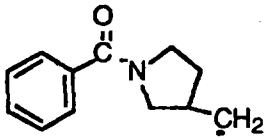	**85**
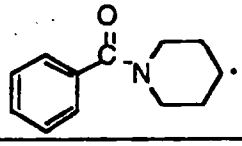	**75**
N(3-butynyl)-N-methylbenzamide	**187**
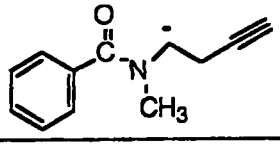	**276**
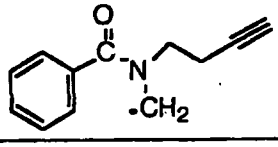	**291**
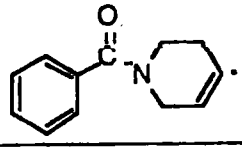	**243**
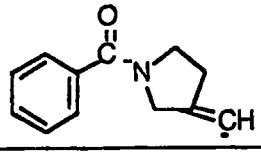	**250**

Table 2.14 Heats of formation (ΔH_f) of N-(3-butenyl)-N-methylbenzamide, N-(3-butynyl)-N-methylbenzamide and the postulated carbon-centred radicals formed during their microsomal oxidation.

To ascertain the efficiency of the intramolecular trapping systems adopted, the cyclisation of the chemically generated N-methylene carbon-centred radical 3 (Figure 2.23 and 2.24) was studied. Figures 2.25 and 2.26 report typical GCMS obtained from the reaction of the N-(3-butenyl)-N-chloromethylbenzamide and N-(3-butynyl)-N-chloromethylbenzamide respectively, with Bu_3SnH/AIBN. Tables 2.15 and 2.16 detail the products of reactions identified by comparison with those of synthetic standards.

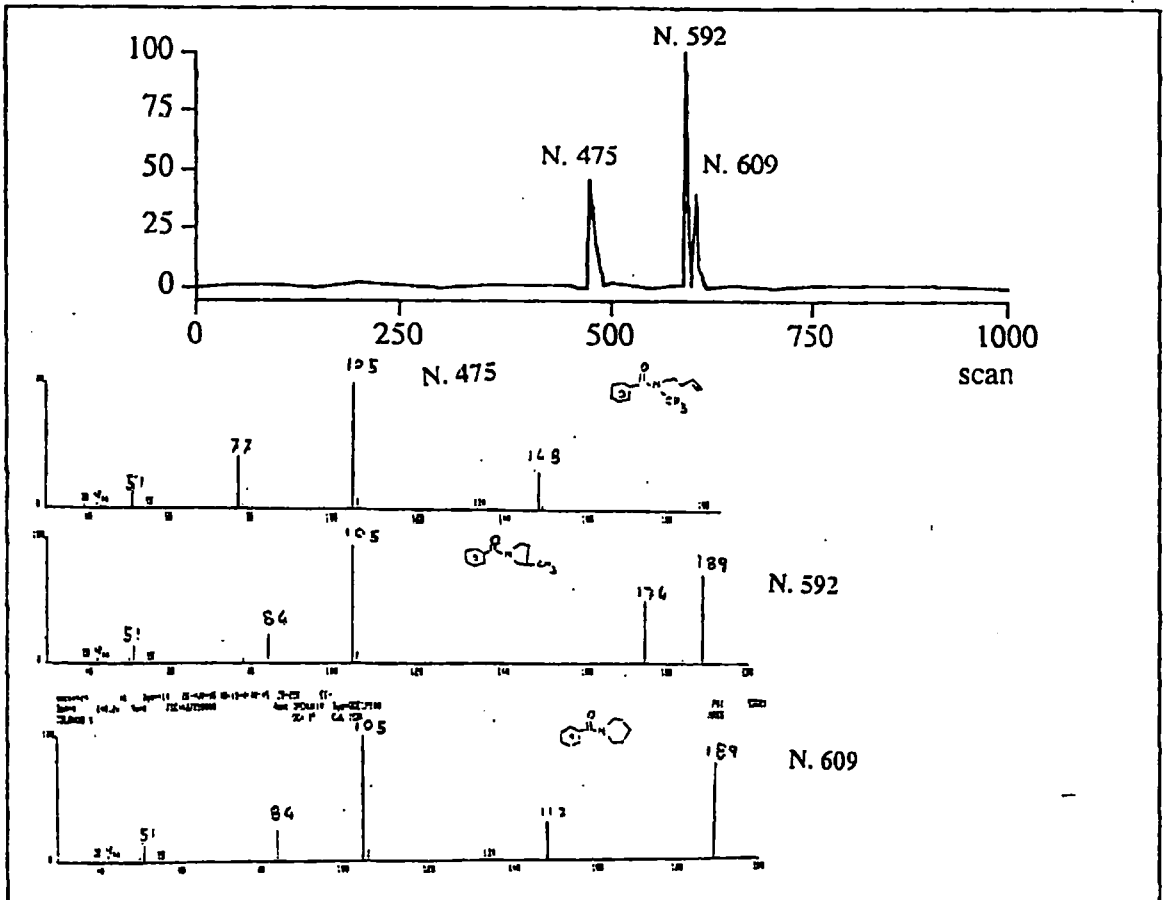

Figure 2.25 GSMS obtained from the cyclisation of the chemically generated N-methyl radical from N-(3-butenyl)-N-chloromethylbenzamide.

Peak	Compound identified	Yield
N. 475	N-(3-butenyl)-N-methylbenzamide	2
N. 592	N-benzoyl-3-methylpyrrolidin	5
N. 609	N-benzoylpiperidine	1

Table 2.15 Products identified from the cyclisation of the chemically generated N-methyl radical from N-(3-butenyl)-N-chloromethylbenzamide.

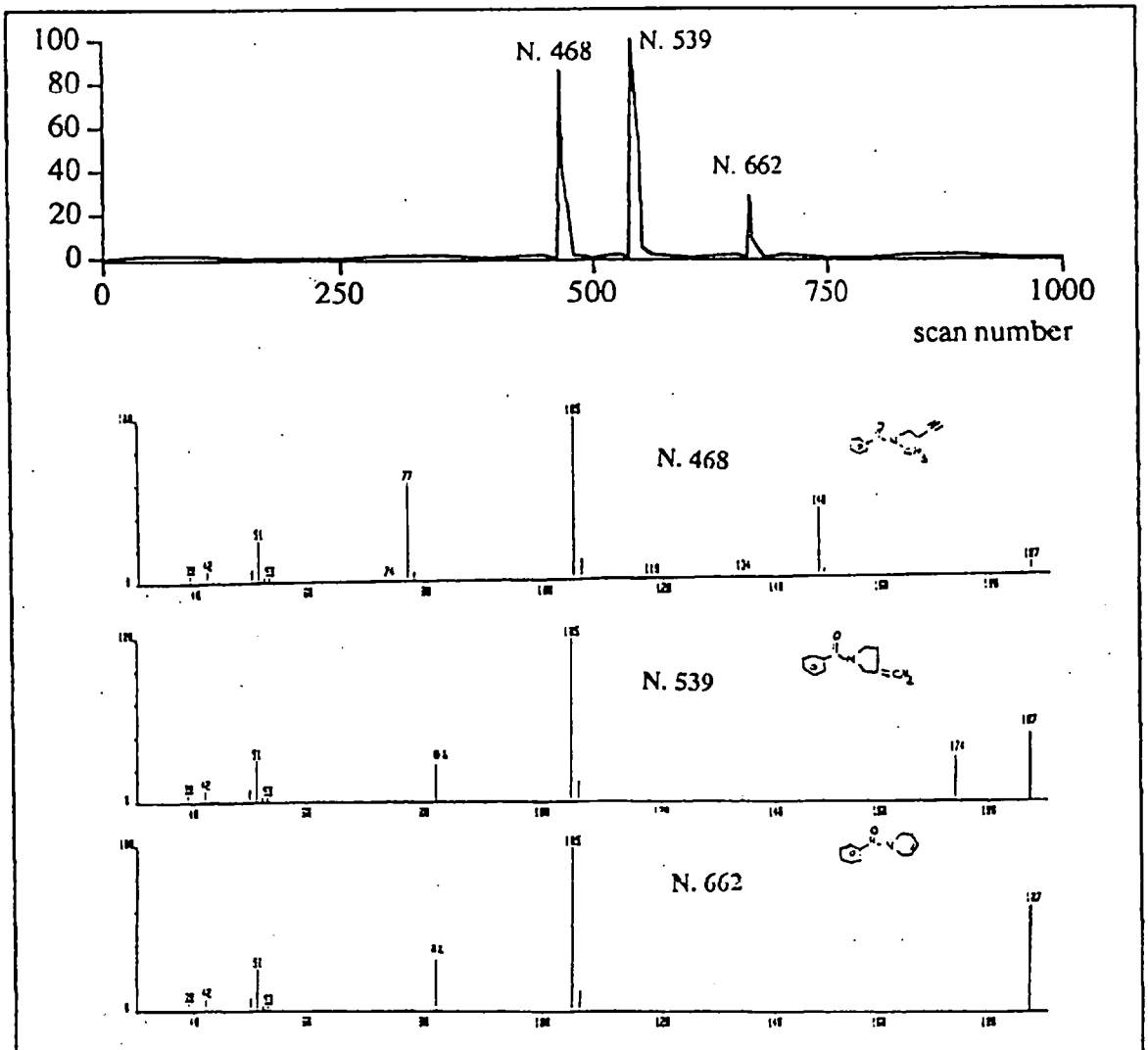

Figure 2.26 GSMS obtained from the cyclisation of the chemically generated N-methylene radical from N-(3-butynyl)-N-chloromethylbenzamide

Peak	Compound identified	Yield
N. 468	N-(3-butynyl)-N-methylbenzamide	2.5
N. 539	N-benzoyl-3-methylenepyrrolidine	5.0
N. 662	N-benzoyl-1,2,5,6-tetrahydropyridine	0.5

Table 2.16 Products identified from the cyclisation of the chemically generated N-methylene radical from N-(3-butynyl)-N-chloromethylbenzamide.

The carbon-centred radical so-generated cyclises *via* both endo and exo pathways. The ratio of five- versus six-membered compounds was then calculated; the results indicate that formation of the five-membered ring product is favoured by a factor of 5 and 10 for N-butenyl and N-butynyl amide, respectively. Furthermore, cyclisation of the carbon-centred radical appears to be favoured over hydrogen atom insertion from Bu_3SnH by a factor of 2 for both compounds.

The results indicate that this alternative intramolecular trapping system is potentially very effective. They also suggest that the more probable products of the radical cyclisation will contain a five-membered ring, resulting from exo cyclisation. Moreover, given that cyclisation is likely to be more rapid than P450-dependent insertion of a hydroxyl group, these cyclic products are anticipated to be the main metabolites of these reactions.

2.4.2 Microsomal oxidation of N-(3-butenyl)-N-methylbenzamide and N-(3-butynyl)-N-methylbenzamide

Typical GCMS obtained after 30 minutes of microsomal incubation of 10 mM N-(3-butenyl)-N-methylbenzamide or N-(3-butynyl)-N-methylbenzamide are reported in Figures 2.27 and 2.28, respectively. Again, the products of the reactions were identified by comparison of their mass spectra with those of synthetic standards analysed under similar conditions (Tables 2.17 and 2.18).

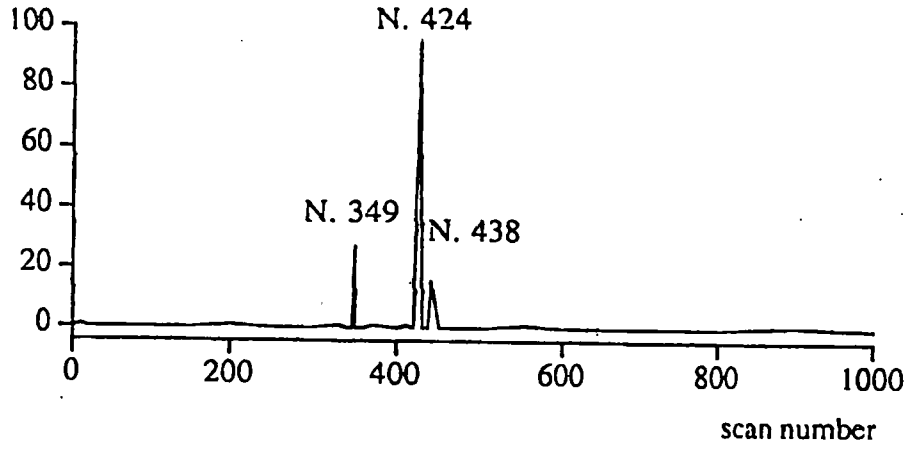

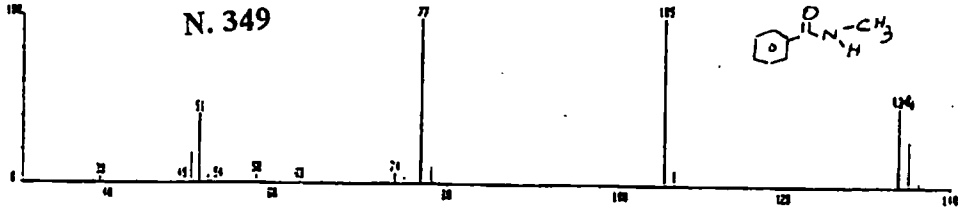

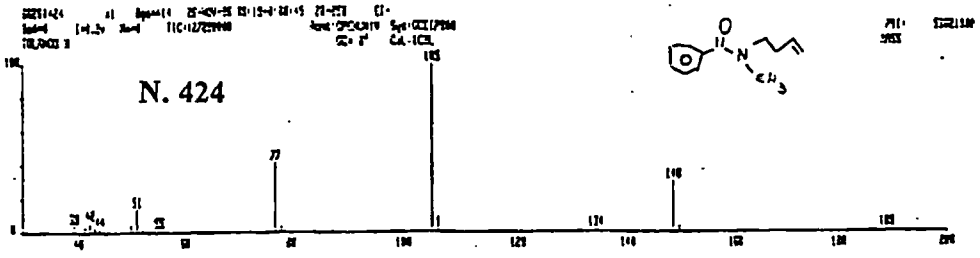

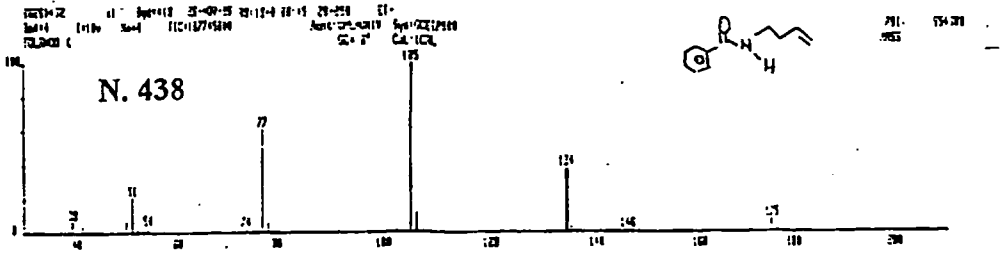

Figure 2.27 GCMS trace obtained after 30 minutes from microsomal oxidation of 10 mM N-(3-butenyl)-N-methylbenzamide.

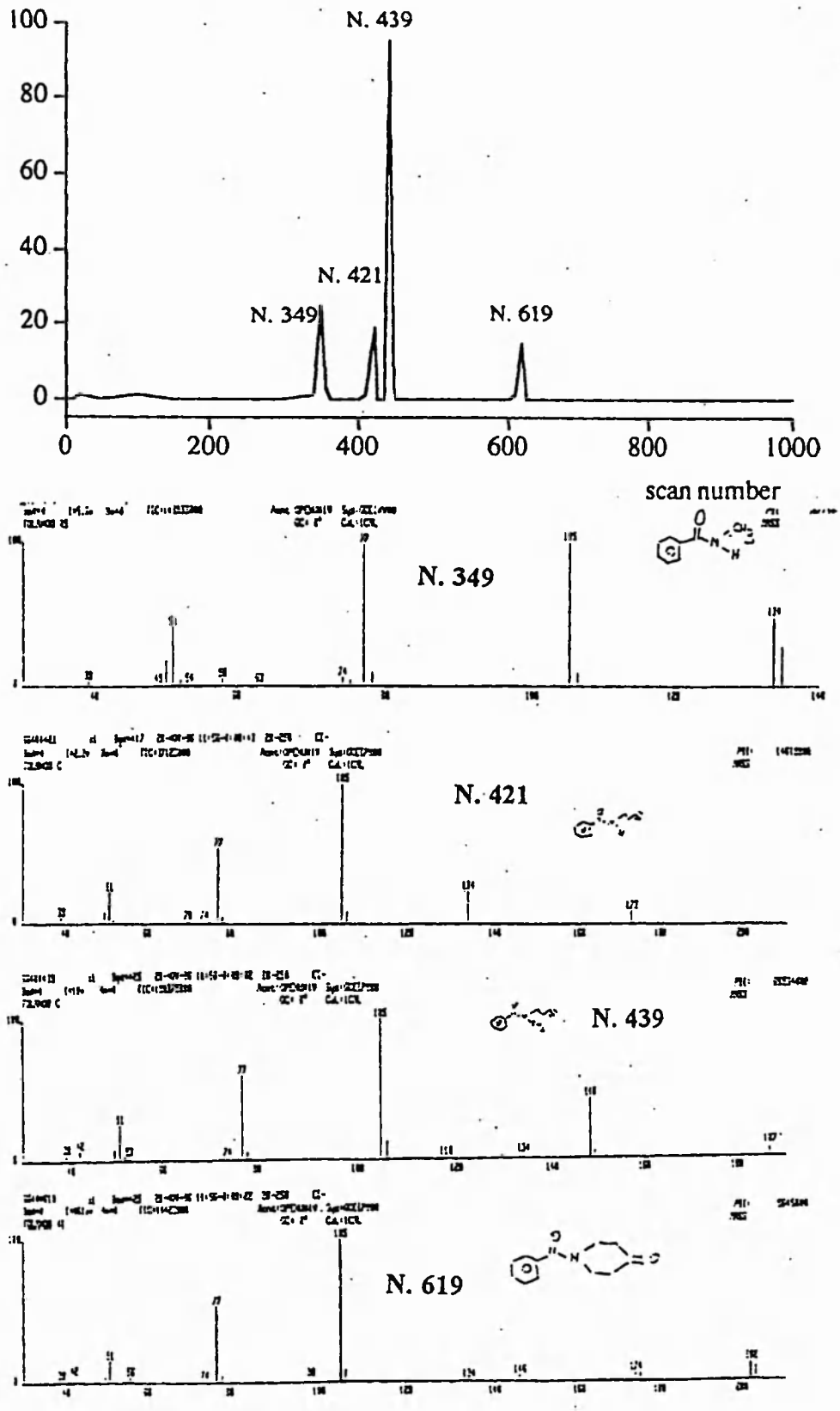

Figure 2.28 GCMS trace obtained after 30 minutes from microsomal oxidation of 10 mM N-(3-butynyl)-N-methylbenzamide.

Peak	Compound identified
Retention Time: 9.18 minutes	N-(3-butenyl)-N-methylbenzamide
Retention Time: 7.39 minutes	N-methylbenzamide
Retention Time: 9.30 minutes	N-(3-butenyl)benzamide

Table 2.17 Products identified after 30 minutes microsomal oxidation of 10 mM N-(3-butenyl)-N-methylbenzamide.

Peak	Compound identified
Retention Time: 9.43 minutes	N-(3-butynyl)-N-methylbenzamide
Retention Time: 7.40 minutes	N-methylbenzamide
Retention Time: 9.29 minutes	N-(3-butynyl)benzamide
Retention Time: 13.45 minutes	1-benzoylpiperidone

Table 2.18 Products identified after 30 minutes microsomal oxidation of 10 mM N-(3-butynyl)-N-methylbenzamide.

The results point to some unexpected features of these microsomal P450-dependent reactions. First, the metabolism of N-methyl-N-(butenyl)benzamide does not result in the formation of any cyclic metabolite. Indeed, the only two products of the reactions are those due to N-demethylation or N-dealkylation. Second, the metabolism of N-methyl-N (3-butynyl)benzamide leads to the formation of a single cyclic compound, other than the two products of the N-demethylation and N-dealkylation. Quite surprisingly, this metabolite is the six-membered ring product, arising from the less favoured endo cyclisation.

The rates of formation and the derived kinetic parameters for these reactions are presented in Tables 2.19 and 2.20.

	v_i (mM/h/nmol P450)		
[Substrate] (mM)	**Total metabolism**	**N-methyl benzamide**	**N-(3-butenyl) benzamide**
0.5	1.42 ± 0.04	0.45 ± 0.03	0.91 ± 0.04
1.0	1.91 ± 0.06	0.64 ± 0.07	1.19 ± 0.06
5.0	2.61 ± 0.16	1.00 ± 0.10	1.59 ± 0.11
10.0	2.74 ± 0.14	1.07 ± 0.08	1.65 ± 0.15
V_{max} (mM/h/nmol P450)	2.88 ± 0.1	1.16 ± 0.06	1.73 ± 0.09
K_m (mM^{-1})	0.51 ± 0.03	0.80 ± 0.04	0.45 + 0.03
V_{max}/K_m	5.65	1.45	3.81

Table 2.19 Initial rates of metabolism and kinetic parameters for the microsomal oxidation of N-(3-butenyl)-N-methylbenzamide.

	v_i (mM/h/nmol P450)			
[Substrate] (mM)	**Total metabolism**	**N-methyl benzamide**	**N-(3-butenyl) benzamide**	**1-benzoyl-4-piperidone**
0.5	1.52 ± 0.12	0.39 ± 0.06	0.27 ± 0.05	0.21 ± 0.03
1.0	2.02 ± 0.15	0.58 ± 0.05	0.70 ± 0.06	0.33 ± 0.04
5.0	2.74 ± 0.21	0.93 ± 0.07	0.89 ± 0.07	0.60 ± 0.04
10.0	2.86 ± 0.31	1.00 ± 0.06	1.03 ± 0.08	0.66 ± 0.07
V_{max} (mM/h/nmol P450)	3.01 ± 0.11	1.10 ± 0.06	1.20 ± 0.08	0.75 ±0.03
K_m (mM^{-1})	0.49 ± 0.04	0.90 ± 0.05	1.71 ± 0.09	1.25 ± 0.06
V_{max}/K_m	6.10	1.22	0.70	0.60

Table 2.20 Initial rates of metabolism and kinetic parameters for the microsomal oxidation of N-(3-butynyl)-N-methylbenzamide.

These results confirm that metabolism of N-methyl-N-(butenyl) benzamide leads to the formation of only the N-demethylated and N-dealkylated products. Quantitative analysis of the metabolism of N-methyl-N-(3-butynyl)benzamide indicates that cyclisation occurs at a comparable rate with respect to the hydroxyl group insertion at the carbon-centred radical intermediate. This observation is quite surprising since cyclisation should be more favoured. This difference between the theoretical prediction, and also the results from the microsomal metabolism of the C-alkenyl substrates, and with the present observations for the oxidation of these N-alkenyl substrates, can be ascribed to greater freedom of motion in the N-alkenyl system. The differences observed between the chemical cyclisation and the microsomal oxidations, are probably due to interactions between the substrate and enzyme in the active site imposing a constrained spatial conformation on the substrate.

To explore further the failure of the trapping of the radical by the N-butenyl system, the metabolism of the N-benzyl-N-(3-butenyl)benzamide was examined. This substrate was chosen because the presence of the aromatic ring should enhance hydrogen atom abstraction by P450 and stabilise the carbon-centred radical intermediate so-formed.

2.4.3 Microsomal oxidation of N-benzyl-N-(3-butenyl) benzamide

Typical GCMS results after 30 minutes of metabolism of 10 mM N-benzyl-N-(3-butenyl)benzamide are reported in Figure 2.29. The products of the microsomal metabolism of the substrate were identified by comparison of their mass spectra with those of synthetic standards (Table 2.21).

Microsomal metabolism of the substrate does not result in the formation of any cyclic product. The kinetic parameters of the reaction are reported in Table 2.22.

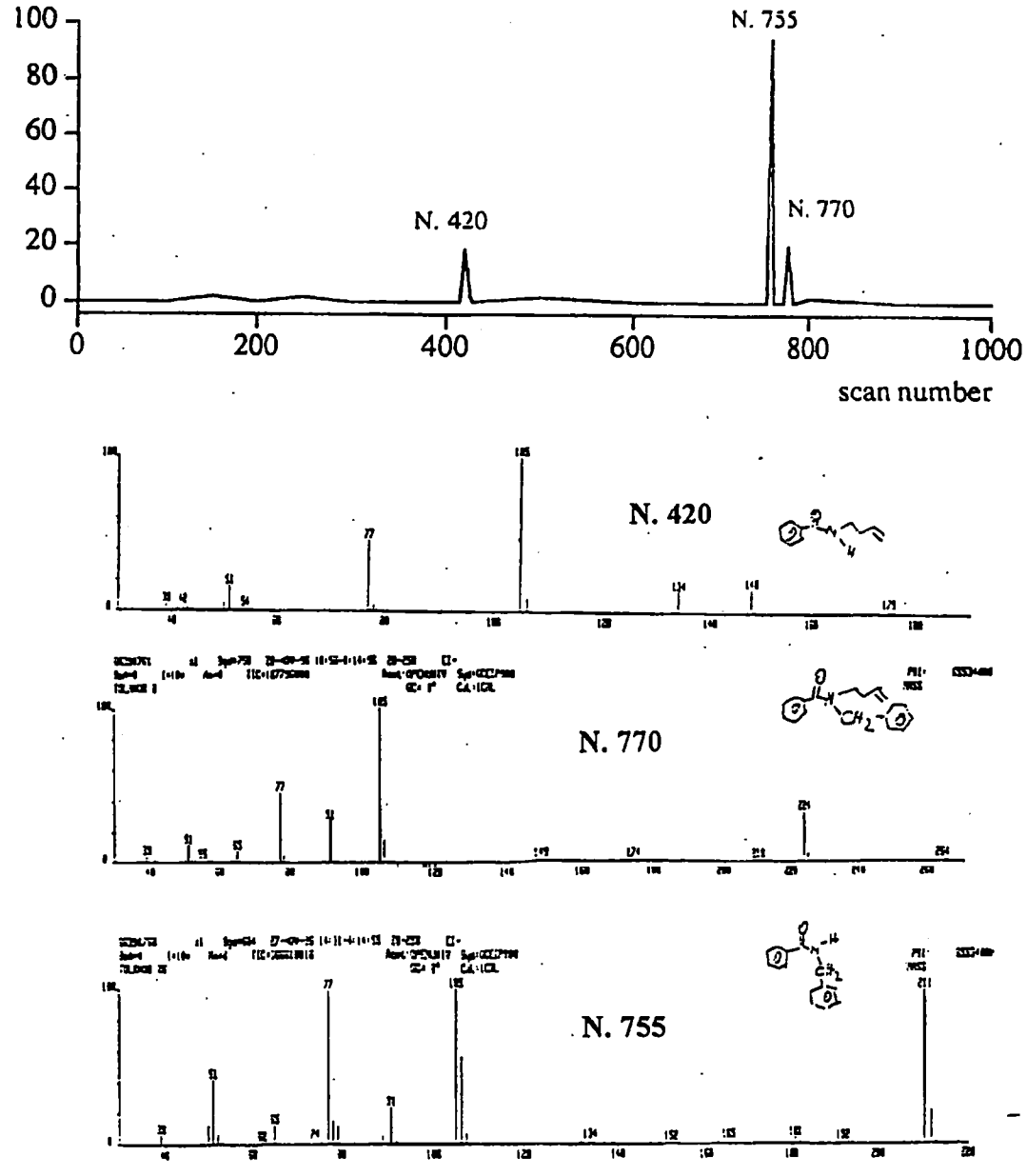

Figure 2.29 Typical GCMS profile of samples obtained after 30 minutes incubation of 10 mM N-benzyl-N-(3-butenyl)benzamide.

Peak	Compound identified
Retention Time: 15.45 minutes	N-benzyl-N-(3-butenyl)benzamide
Retention Time: 9.37 minutes	N-(3-butenyl)benzamide
Retention Time: 15.53 minutes	N-benzylbenzamide

Table 2.21 Products identified from the microsomal metabolism of N-benzyl-N-(butenyl)benzamide.

[Substrate] (mM)	v_i (mM/h/nmol P450)		
	Total metabolism	**N-(3-butenyl) benzamide**	**N-benzyl benzamide**
0.5	1.67 ± 0.07	0.96 ± 0.04	0.36 ± 0.05
1.0	2.30 ± 0.12	1.40 ± 0.06	0.53 ± 0.03
3.0	3.07 ± 0.21	1.97 ± 0.11	0.77 ± 0.05
5.0	3.30 ± 0.16	2.15 ± 0.14	0.85 ± 0.07
10.0	3.49 ± 0.29	2.31 ± 0.21	0.92 ± 0.07
V_{max} (mM/h/nmol P450)	3.70 ± 0.11	2.50 ± 0.11	1.00 ± 0.05
K_m (mM^{-1})	0.61 ± 0.03	0.80 ± 0.02	0.90 ± 0.04
V_{max}/K_m	6.00	3.10	1.11

Table 2.23 Initial rates of metabolism and kinetic parameters for the microsomal oxidation of N-benzyl-N-(3-butenyl)benzamide.

The results indicate that microsomal metabolism of N-benzyl-N-(3-butenyl)benzamide leads to the formation of the two products of N-dealkylation. No cyclic metabolites are observed. Thus, the N-alkenyl system is not able to trap the carbon-centred radical intermediate formed during the microsomal metabolism. These results are quite surprising given that chemical generation of the radical intermediate yields a cyclic product. Moreover, comparison of the rate of metabolism between the substrate that undergoes efficient intramolecular trapping and that which does not undergo radical trapping is not particularly helpful.

2.5 Conclusions

First, attempts to detect iminium ion species failed. It is unlikely that this is due to the ineffectiveness of the systems used, both because of their reported reliability in the detection of such intermediates,[6;25;26;27;28] and also because iminium ion species were successfully detected using N,N-dimethylaniline. Thus, it is clear that formation of iminium ion species can be ruled out in the metabolic dealkylation of amides. By implication, electron transfer from the carbon centred radical **3** in Figure 2.2, and also hydrogen atom abstraction from the cation radical **2** can be ruled out. Moreover, while for amines, formation of an iminium ion is reported to occur from the carbinolamine reaction product,[6-8] such iminium ion formation does not occur for amides. The lower availability of the nitrogen non-bonding electron pair in carbinolamides as compared with carbinolamines probably accounts for this.[29; 30; 31; 32]

In contrast, trapping of the carbon-centred radical intermediate produced during the microsomal P450 oxidation of tertiary amides has been successful. The formation of this intermediate has been demonstrated by the detection of characteristic, rearranged metabolites during the oxidation of the substrate probes. The formation of cyclic metabolites can be explained only by a mechanism that involves formation of a carbon-centred radical intermediate. On the basis of these observations, the pathway of the microsomal oxidation of tertiary amides is shown in Figure 2.30.

The substrate undergoes hydrogen atom abstraction to form a carbon-centred radical intermediate, that undergoes hydroxyl group insertion, from the P450 haem activated oxygen complex, to give the carbinolamide product. In certain instances, this compound can be detected as a product of N-methylamides under physiological conditions,[4] though for N-alkylamides substrate it hydrolyses spontaneously to give the N-dealkylated product.

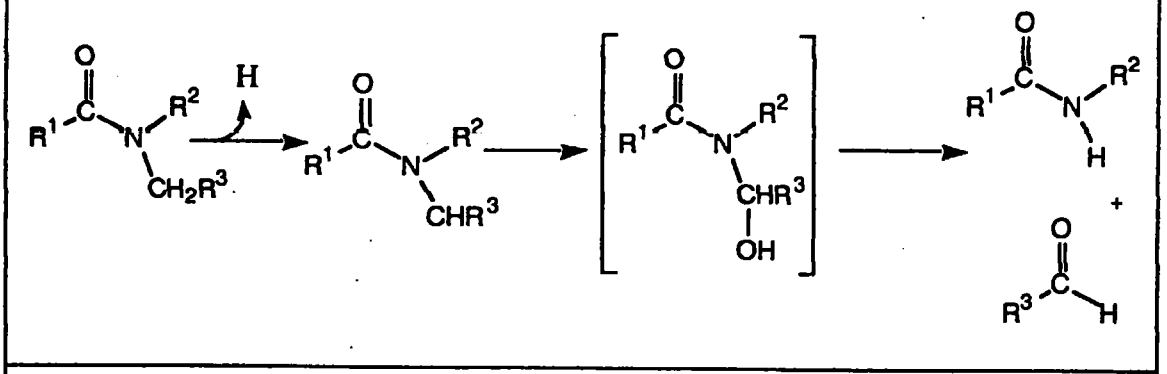

Figure 2.30 Proposed pathway of the microsomal oxidation of tertiary amides.

Analysis of the efficiency of the intermolecular trapping systems adopted in the present study reveals that the C-alkenyl substrates are more efficient than the N-alkenyl substrate in trapping the radical intermediate. Comparison of the kinetic parameters for these reactions does not indicate that the C-alkenyl are significantly more metabolised than the N-alkenyl substrates. Thus, the lower efficiency of the N-alkenyl substrates as trapping systems for carbon centred radicals intermediate is not related to a limitation of their metabolism.

It is possible that, in the active site of the enzyme, these differences may relate to a different position of the radical trapping group with respect to the radical centre. Because of the restricted rotation around the C-N bond in amides, in the C-alkenyl substrates the alkenyl has a relatively fixed conformation with respect to the radical centre. For the N-alkenyl substrates, the trapping group can move relatively freely with respect to the radical centre. Thus, it is possible to argue that capture of the carbon-centred radical by the C-alkenyl substrate is statistically more probable it is by of the N-alkenyl substrate.

The overall conclusion from this part of the study, is that there is direct evidence that the microsomal oxidation of tertiary amides occurs *via* hydrogen atom abstraction from the carbon atom α to nitrogen, resulting in the formation of a carbon-centred radical intermediate.

2.6 References

1 Hall L.R. and Hanzlick R.P., (1990); *J. Biol. Chem.*; **265**: 12349-

2 Hall L.R. and Hanzlick R.P., (1991); *Xenobiotica*; **21**: 1127-

3 Iley J. and Costantino L., (1994); *Biochem. Pharmacol.*; **47**: 275-

4 Constantino L., Rosa E. and Iley J., (1992); *Biochem. Pharmacol.*; **44**: 651-

5 Bowry V.W., Lusztyk J. and Ingold K.V., (1991); *J. Am. Chem. Soc.*; **113**: 5678-

6 Murphy P.J., (1973); *J.Biol. Chem.*; **248**: 2796-

7 Beke D., (1963); *Adv. Heterocyclic Chem.*; **1**: 167-

8 Breck G.D. and Trager W.F., (1971); *Science*; **173**: 544-

9 Overton M., Hickman J.A., Threadgill M.D., Vaughan K. and Gescher A., (1985); *Biochem. Pharmacol.*; **34**, 12; 2055-

10 Bowry VW. and Ingold K.U., (1991); *J. Am. Chem. Soc.*; **113**: 5687-

11 Shannon P. and Bruice T.C., (1981); *J.Am. Chem. Soc.*; **103**: 4580-

12 Logan C.J., Cottee F.H. and Page J.A., (1984); *Biochem. Pharmacol.*; **33**: 2345-

13 Gaudette L.E. and Brodie B.B., (1959); *Biochem. Pharmacol.*; **2**: 89-

14 Martin Y. and Hansch C., (1971); *J. Med. Chem.*; **14**, 9: 777-

15 Hart D.J., (1984); *Science*; **223**: 883-

16 Giese B., (1985); *Angew. Chem. Int. Ed. Engl.*; **24**: 553-

17 Giese B., (1985); *Tetrahedron*; **41**: 3887-

18 Beckwith A.L.J.and Schieser C.H., (1985); *Tetrahedron*; **41**: 3925-

19 Beckwith A.L.J. and Meijs J., (1979); *J.Chem. Soc. Perkin Trans. II*; 1535-

20 Beckwith A.L.J., Phillipou G. and Serelis A.K., (1981); *Tetrahedron Lett.*; **22**: 2811-

21 Bachi M.D., Frolow F. and Hoornoert C., (1983); *J. Org. Chem.*; **48**: 1841-

22 Burnett D.A.; Choi J.K., Hart D.J. and Tsai Y.M., (1981); *J.Am.Chem.Soc.*; **106**: 8201-

23 Julia M., (1971); *Acc. Chem. Res.*; **4**: 386-

24 Julia M., (1974); *Pure Appl. Chem.*; **40**: 553-

25 Peterson A., Trevor A and Castagnoli N. Jr., (1987); *J. Biol. Chem.*; **30**: 249-

26 Nguyen T.L., Gruenke L.D. and Castagnoli N. Jr., (1979);*J.Am.Chem.Soc.* **22**: 259-

27 Ho B. and Castagnoli N Jr., (1980); *J. Med. Chem*; **23**: 133-

28 Ziegler R., Ho B. and Castagnoli N. Jr.; (1981); J. Med. Chem.; 24: 1133-

29 Ross D., Farmer P.B., Ghescher A., Hickman J.A. and Threadgill M.D., (1983); *Biochem. Pharmacol.*; **32**: 1773-

30 Gidley M.J. and Sanders J.K.M., (1982); *Biochem. J.*; **203**: 331-

31 Ross D., Farmer P.B., Gescher A., Hickman J.A. and Threadgill M.D., (1982); *Biochem Pharmacol.*; **31**: 3621-

32 Kolar G.F. and Carubelli R., (1979); *Cancer Lett.*; 7: 209-

CHAPTER 3

ESR studies of the microsomal P450 metabolism of tertiary amides

3.1 Introduction

ESR is considered the least ambiguous method for the detection of free radicals. Unfortunately, it is not always possible to directly observe the free radicals of interest as their concentration may be below the limit of detection (*ca.* 10^{-8} M, a practical limit is probably *ca.* 10^{-6} M).[1] In addition, some radicals, even if present at a concentration greater than 10^{-8} M, are not observable at room or physiological temperature as their spin relaxation times are very short, making their linewidth too broad to be observed by ESR.

The spin trapping technique has been developed to overcome the problems associated with detection of the transient free radicals in chemical and biological systems.[2-7] This technique is characterised by the addition of the free radical of interest to a diamagnetic compound to produce a relatively long-lived nitroxyl free radical product, that can accumulate sufficiently to be studied by ESR.

Nitroxyls are relatively stable because the unpaired electron is stabilised by resonance:

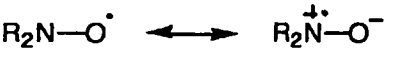

Two kind of spin traps have been developed, nitrones and nitroso compounds. Nitroso compounds can provide considerably more information than nitrones as the radical to be trapped adds directly to the nitroso nitrogen:

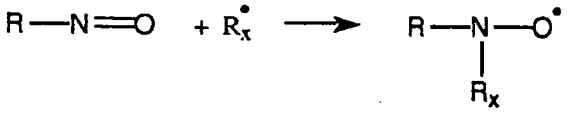

In this case coupling of the unpaired electron with the hydrogen atoms attached to the carbon atom of the $R_x^{\bullet}$ radical occur. With nitrones, some information is lost because the trapped radical adds to the carbon atom adjacent to the nitrogen:

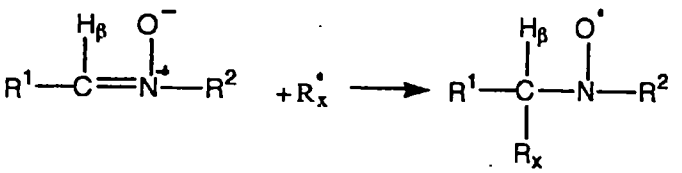

The use of PBN (for the structure of PBN, see Figure 3.1) in the present study was justified in part because it is one of the most effective reported spin trapping agents for biological systems *in vivo* and *in vitro*,[8-11] and because it has both hydrophilic and lipophilic character. This latter property makes it ideal for the analysis of microsomal and similar systems since it has the dual potential of capturing free radicals both in the hydrophobic pocket of the active site of P450 as well as in solution if such radicals are released.[9;10]

The information about the radical trapped is contained in the multiplicity and magnitude of the hyperfine splitting in the spin adduct. The solvent is known to have a major effect on the hyperfine splitting constant. In general, increases in solvent polarity produce an increases in the nitrogen-hyperfine splitting as the spin density on the nitrogen increases. Concomitantly, the β-hydrogen splitting constant usually (but not always) increase.[1] Empirically, it has been demonstrated that for a particular spin adduct in different solvents, a_N and a_β^H can be linearly correlated with the polarity of the solvent.[12;13]

The present study involves attempts to trap the postulated carbon-centred radical by intermolecular trapping with PBN. The expected reaction is that summarised in Figure 3.1, where the short lived carbon-centred radical is "stabilised" by being the bound to the spin trap. The amide substrates used in the present study are illustrated in Figure 3.2.

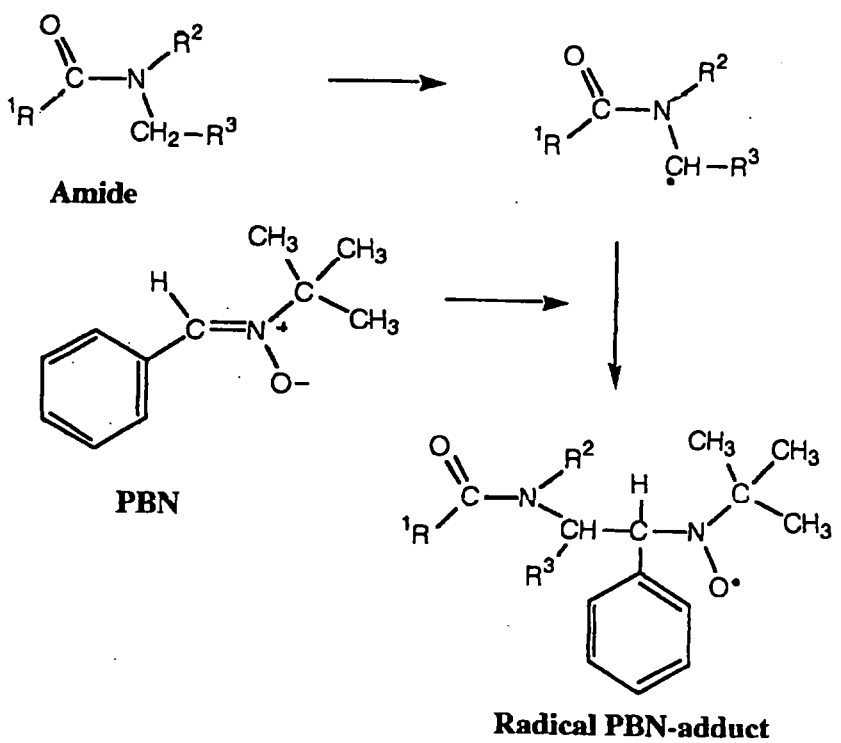

Figure 3.1 Spin trapping of the amide carbon-centred radical by PBN

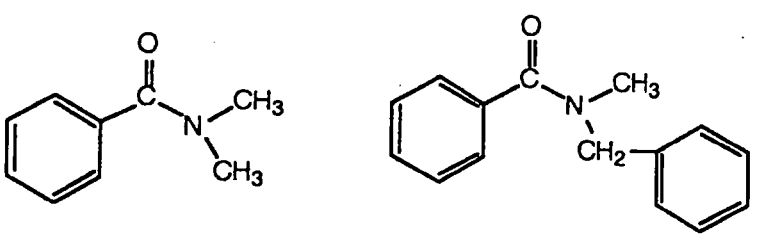

Figure 3.2 Amides used in the study.

3.2 ESR analysis of the microsomal oxidation of N,N-dimethylbenzamide and N-benzyl-N-methylbenzamide

Microsomal incubation of 5 mM N-benzyl-N-methylbenzamide in the presence of a 15 mM solution of the spin trapping agent PBN gave, after extraction into a 2/1

solution of chloroform/ methanol, as used in experiments elsewhere,[9;14] the typical ESR spectrum recorded in Figure 3.3.

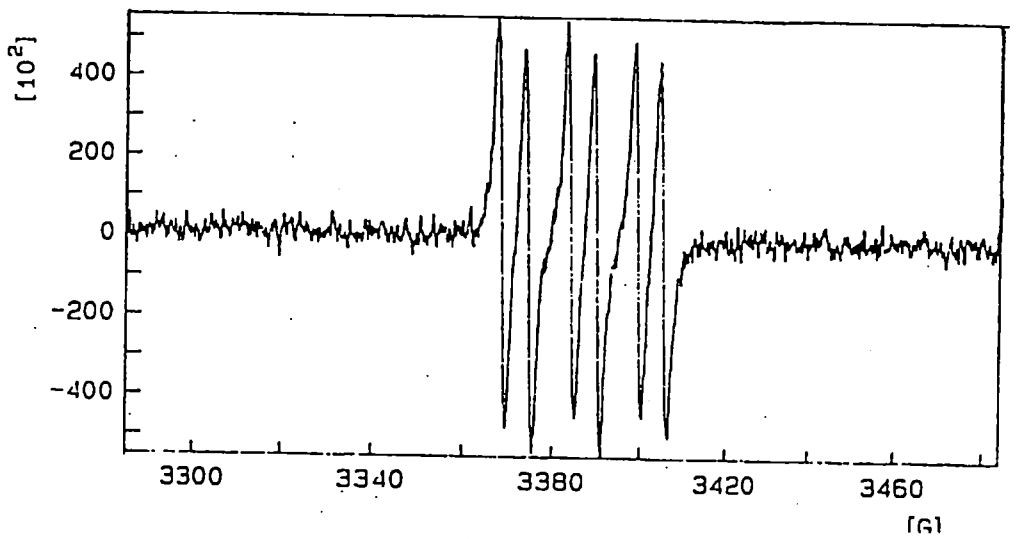

Figure 3.3 ESR spectrum of a chloroform/methanol extract of the microsomal incubation of N-methyl-N-benzyl benzamide 5 mM after 30 minutes.

To avoid false positive signals, the spectrum from a series of control incubations were recorded. The results, Figure 3.4, indicate that the ESR signal is recorded only if the full metabolic system (enzymes and cofactors), substrate and PBN are present. Omission of one of these component results in the absence of a detectable ESR signal.

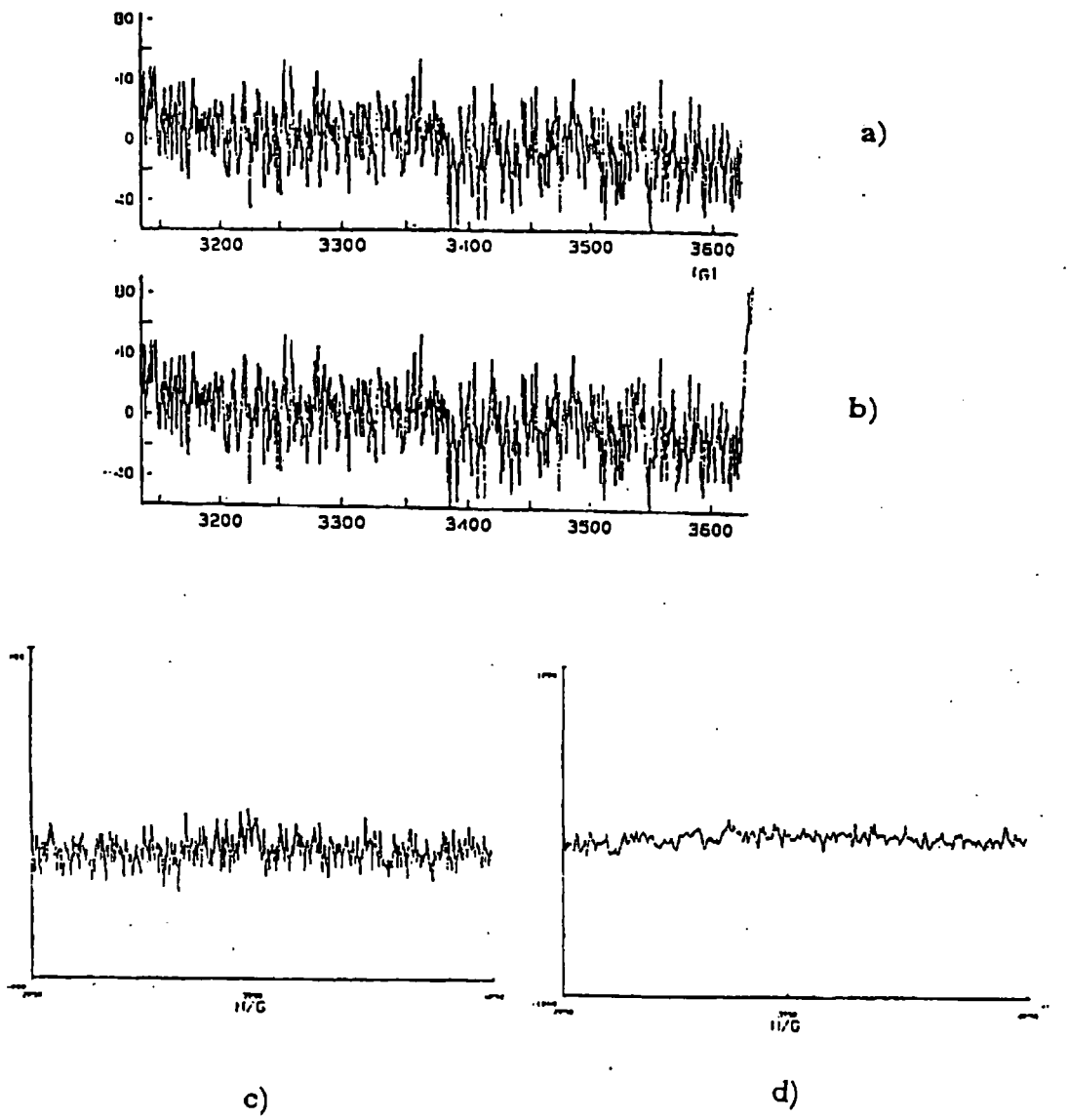

Figure 3.4 ESR spectra of controls incubations: (a) microsomal monooxygense system and PBN 30 mM, (b) microsomes, 5 mM substrate and 15 mM PBN (without NADPH regenerating system), (c) NADPH regenerating system and 15 mM PBN and (d) 5mM substrate, 15 mM PBN and NADPH regenerating system.

Furthermore, because of the reported efficiency of PBN in trapping the hydroxyl radical,[1] control reactions of microsomal metabolism of the substrate in the presence of PBN and varying concentration of superoxide dismutase (SOD) were carried out. The results are shown in Figure 3.5.

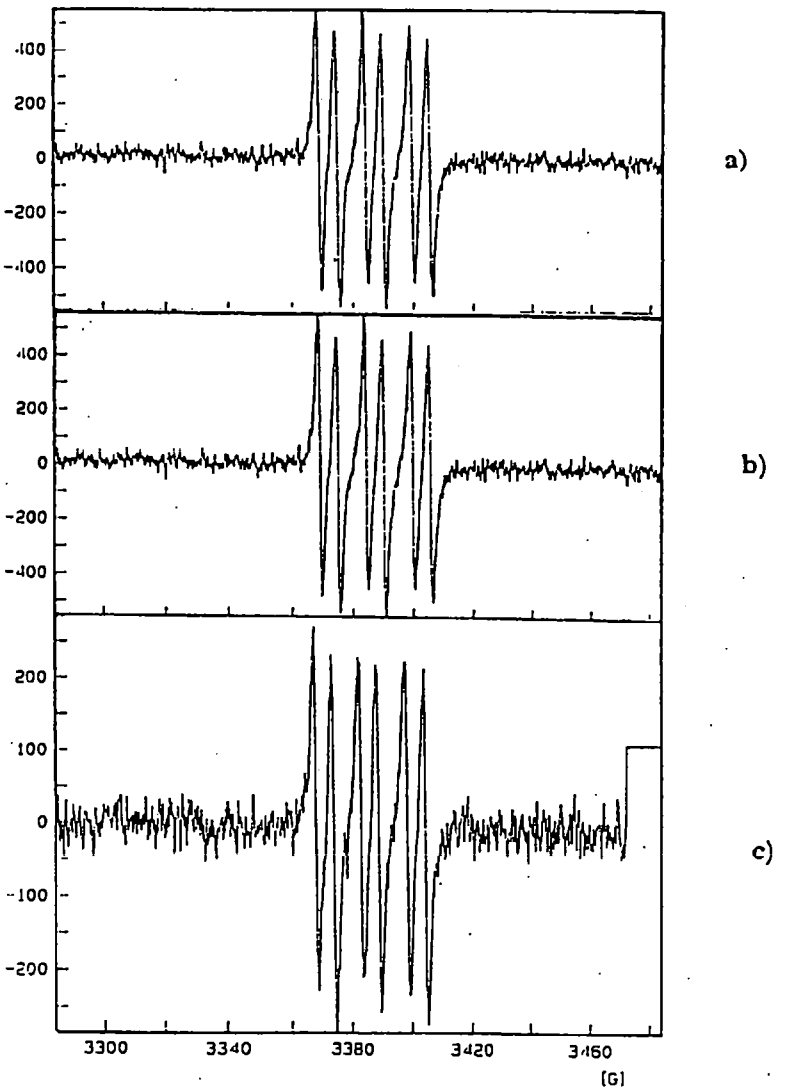

Figure 3.5 ESR spectra of chloroform/methanol extracts from microsomal incubations of 5 mM N-benzyl-N-methylbenzamide carried out in presence of 15 mM PBN and (a) 50, (b) 100 and (c) 300 SOD units.

The presence of SOD does not modify the ESR spectra at any of the concentrations used. This is a good indication that the signal is not due to the trapping of reactive oxygen radicals by PBN.

Particular attention was also paid to the choice of the concentrations of PBN and substrate. High concentrations of both substrate and PBN should lead to high concentrations of radical adduct and thus to a better signal. However, it is possible that

the spin trapping agent interferes with substrate metabolism by competing for the active site. It is known that high concentrations of PBN (> 50 mM *in vitro* and > 100 mM *in vivo*) interact with P450 resulting in inhibition of substrate metabolism.[9;16] In all the microsomal reactions carried out here the PBN concentration was kept below 50 mM. To maximise the probability of trapping of the radical, the relative ratio of PBN to substrate was examined. The best signals are obtained using a PBN/substrate ratio of 3 to 1. Subsequently, all microsomal oxidations of the amides were carried out using a substrate concentration of 5 mM in the presence of 15 mM PBN. These concentrations being the best compromise between intensity of the signal and reciprocal interference of the P450-dependent metabolism.

Figure 3.6 is a typical ESR spectrum obtained from chloroform/methanol extracts of the microsomal incubation of 5 mM N,N-dimethyl benzamide in the presence of 15 mM PBN. This spectrum, like that for N-benzyl-N-methylbenzamide, displays the typical triplet of doublets of the nitroxyl radical from which the hyperfine splitting constants summarised in Table 3.1 are obtained.

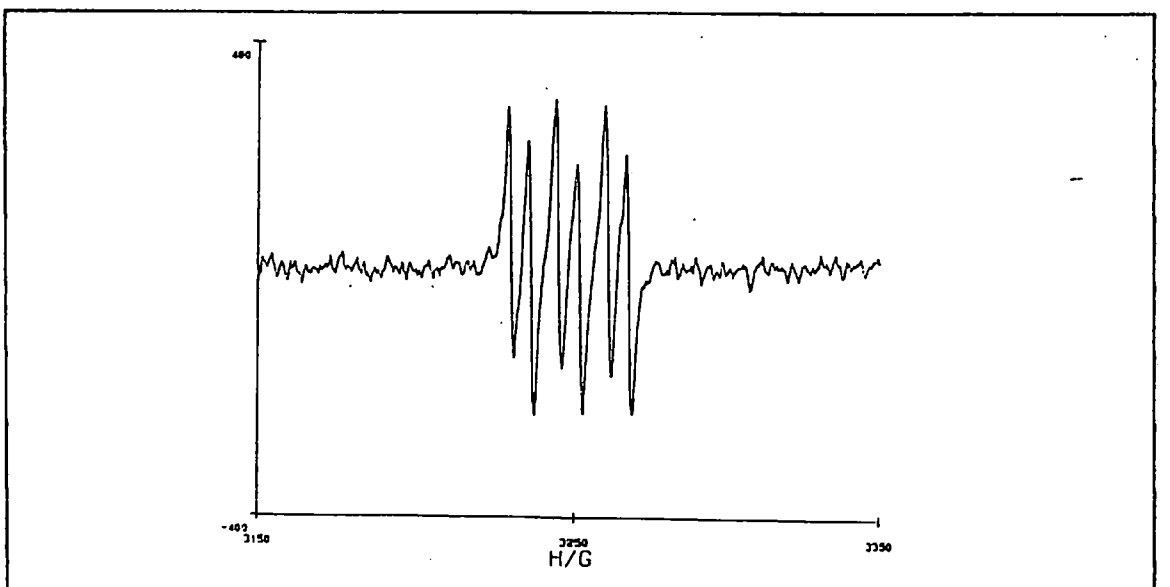

Figure 3.6 ESR spectrum of the chloroform/methanol extracts of the microsomal incubation of 5 mM N,N-dimethylbenzamide in the presence of 15 mM PBN

Substrate	a_N (G)	a_β^H (G)
N,N-dimethyl benzamide	14.8	6.5
N-methyl-N-benzyl benzamide	15.0	4.6

Table 3.1 Hyperfine splitting constants for the radicals spectra obtained from microsomal metabolism of 5 mM N,N-dimethylbenzamide or N-benzyl-N-methylbenzamide in the presence of 15 mM PBN.

The spectral parameters reported in Table 3.1 compare favourably with literature data for the chemically generated, PBN trapped carbon-centred radicals of N,N-dimethyl formamide and N,N-diethyl acetamide (a_N=14.7 and 15.1 G, a_β^H= 2.8 and 1 G, respectively).[15] Agreement of the a_N values is excellent, while the measured a_β^H splitting is slightly higher. This probably reflects the different solvents used in the experiments (chloroform/methanol 2/1) compared to that used in the experiments reported in the literature (benzene).[16;17]

3.2.1 Identification of the PBN-N,N-dimethylbenzamide adduct

Although it is clear that a radical species is trapped by PBN, its structure cannot be determined from spectral parameters alone. Therefore, a different approach was employed to identify the structure of the PBN adduct. Assuming (based on the results in Chapter 2) that the reaction involves hydrogen atom abstraction from the carbon α to nitrogen, then the structure of the PBN-trapped radical will be that shown in Figure 3.7. This PBN-N,N-dimethylbenzamide adduct was then synthesised by reaction of N-chloromethyl-N-methylbenzamide with Bu_3SnH/AIBN and PBN, and its ESR spectrum is shown in Figure 3.8. This spectrum displays the same six line pattern obtained from the extracts of the microsomal oxidation of N,N-dimethylbenzamide and the same nitrogen and hydrogen hyperfine splitting constants: a_N= 14.8 G and $a\beta^H$= 6.4 G.

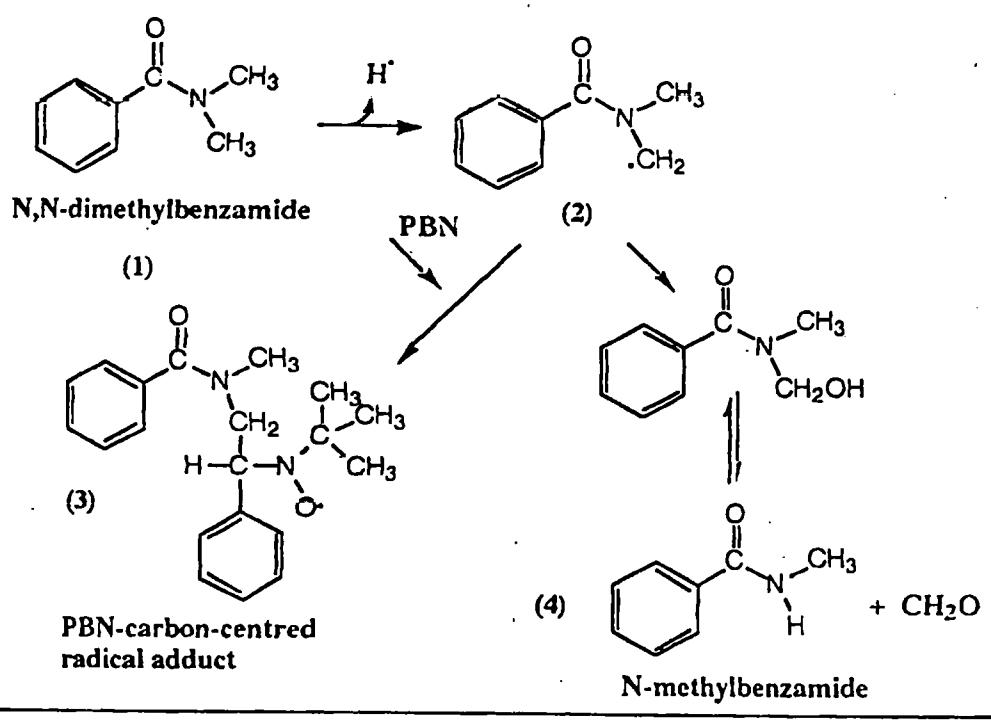

Figure 3.7 Proposed pathway for the formation of the PBN adduct.

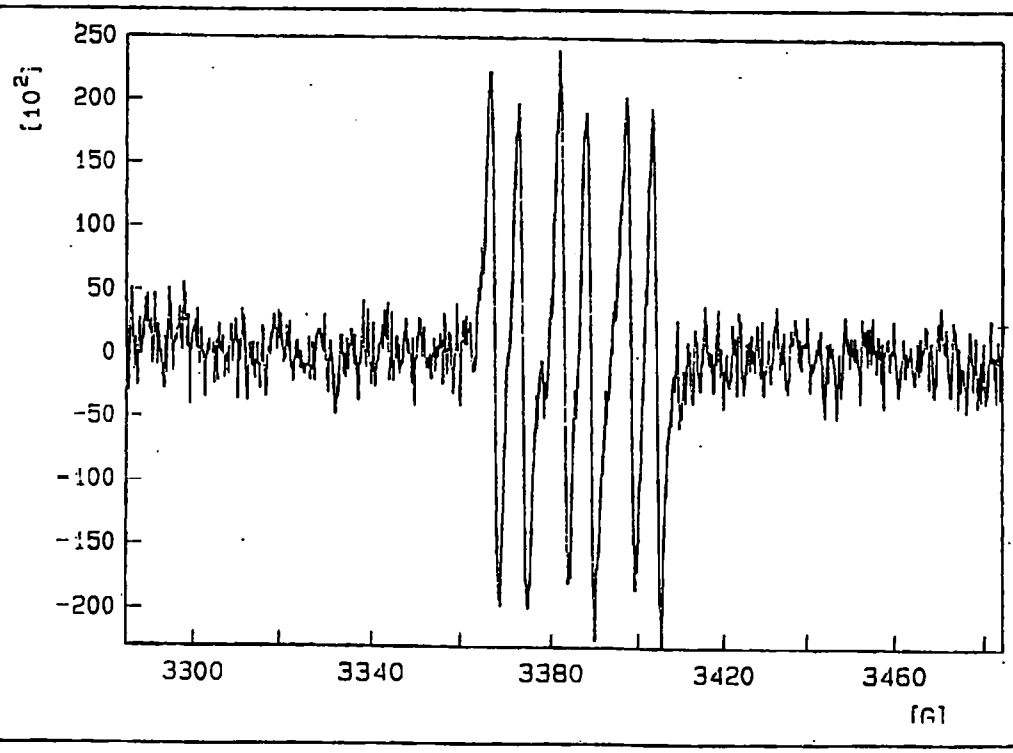

Figure 3.8 ESR spectrum of the PBN adduct derived from N,N-dimethylbenzamide in chloroform/methanol (2/1).

This result seems to strongly indicate that the carbon-centred radical adduct with PBN is the product of the microsomal oxidation of N,N-dimethylbenzamide formed in presence of PBN. However, Table 3.1 reveals that the differences in the hyperfine splitting constants between the different carbon-centred PBN-adducts is small. Thus, more conclusive evidence is needed to confirm the structure of the radical intermediates generated in the P450 oxidation of amides. This was obtained from HPLC analysis of the microsomal reaction mixtures involving N,N-dimethylbenzamide performed in presence of PBN. Comparison of the chromatograms obtained from these reactions with that for the synthetic PBN-adduct standard (Figure 3.10 and 3.11, respectively) reveals that one of the new peaks that appears in the chromatogram of the microsomal reaction has the same retention time as the synthetic adduct (14.1 min). It should be noted that this adduct has the hydroxylamine structure (Figure 3.9) rather than nitroxyl structure seen in the ESR spectrum.

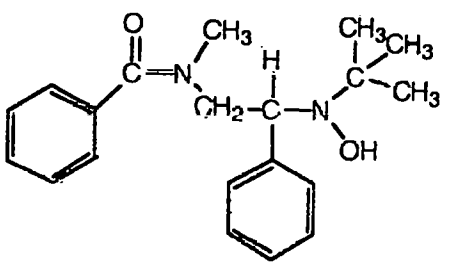

Figure 3.9 Postulted structure of the adduct from the microsomal metabolism of N,N-dimethylbenzamide in presence of PBN.

The other products of the microsomal reaction are reported in Table 3.2. Comparison of the UV spectra (recorded by a diode array detector) of the synthetic PBN-N,N-dimethylbenzamide adduct with that of the peak with retention time 14.1 minutes in the chromatogram obtained for the microsomal reaction, illustrated in Figure 3.12 provides confirmatory evidence that the two structure are identical. Moreover, such a product is formed only in incubations were PBN is present and where metabolism of the substrate occurs (Figure 3.10).

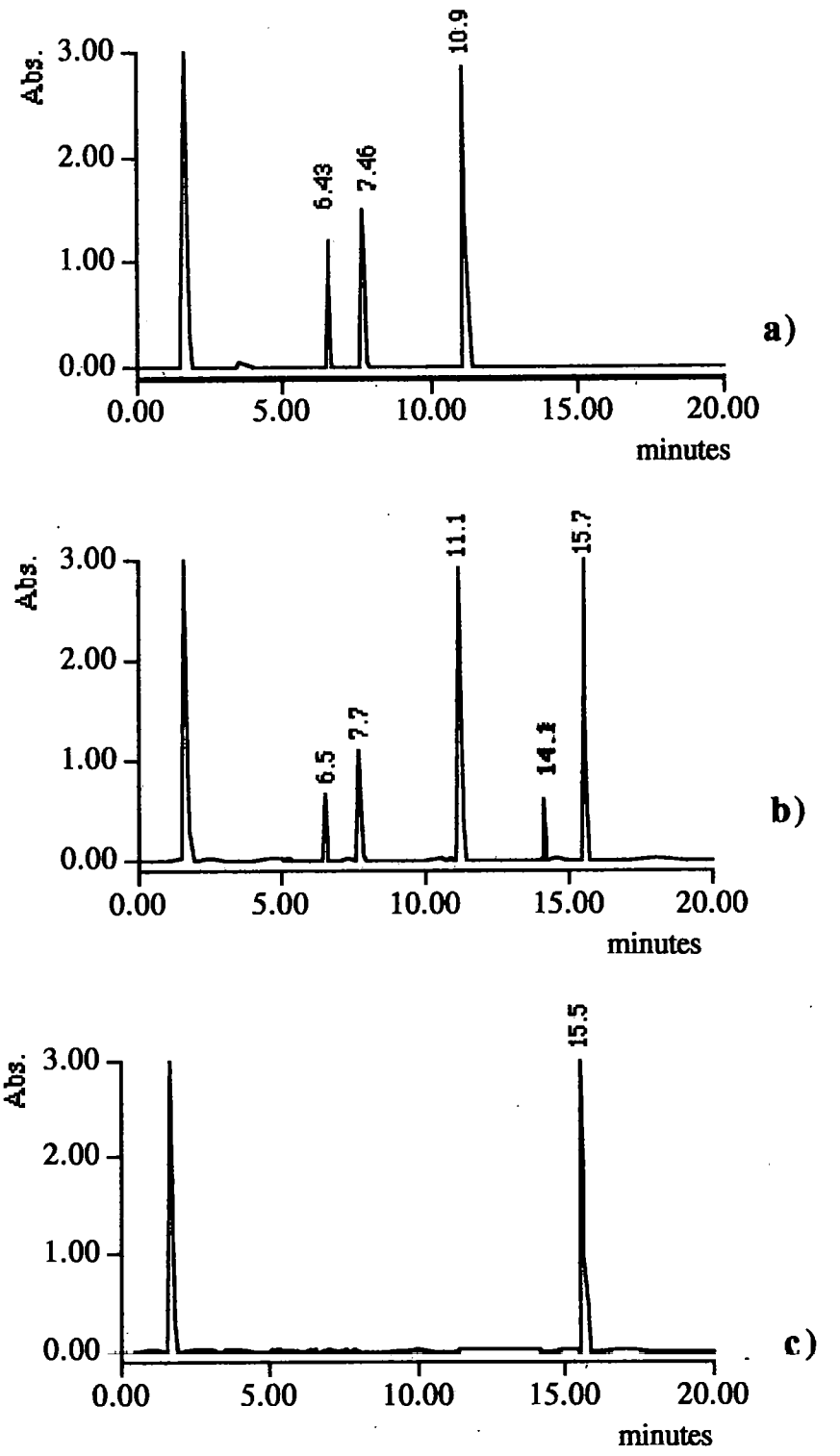

Figure 3.10 HPLC chromatograms of microsomal incubations of 5 mM N,N-dimethylbenzamide carried out (a) without, (b) with 15 mM PBN, and (c) of microsomal incubations of 15 mM PBN carried out without substrate.

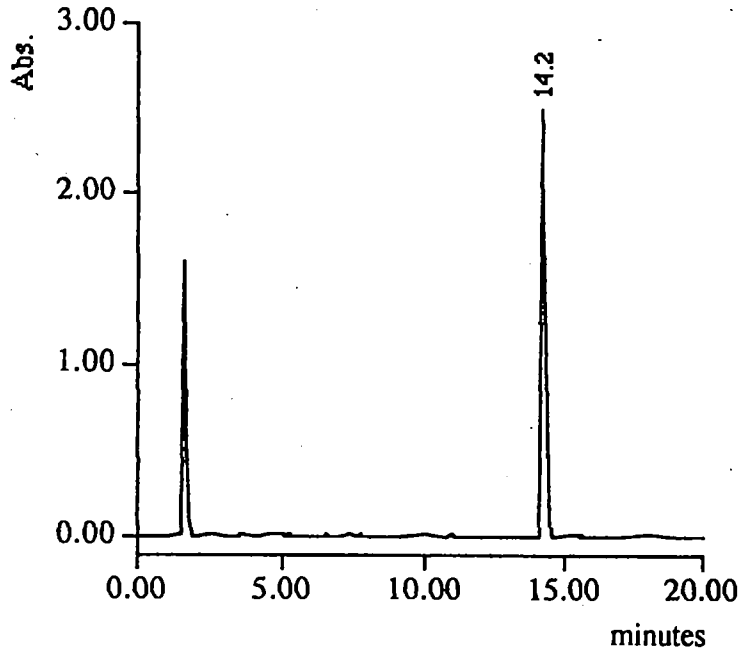

Figure 3.11 HPLC chromatogram of the standard PBN-N,N-dimethylbenzamide adduct.

Peak	Compound identified
Retention time: 6.5 minutes	**N-methyl-N-hydroxymethyl benzamide**
Retention time: 7.7 minutes	**N-methyl benzamide**
Retention time: 11.1 minutes	**N,N-dimethyl benzamide**
Retention time: 14.1 minutes	**PBN-N,N-dimethyl benzamide adduct**
Retention time: 15.5 minutes	**PBN**

Table 3.2 Products identified from the HPLC analysis of a 30 minutes microsomal incubation of 5 mM N,N-dimethyl benzamide carried out in presence of 15 mM PBN.

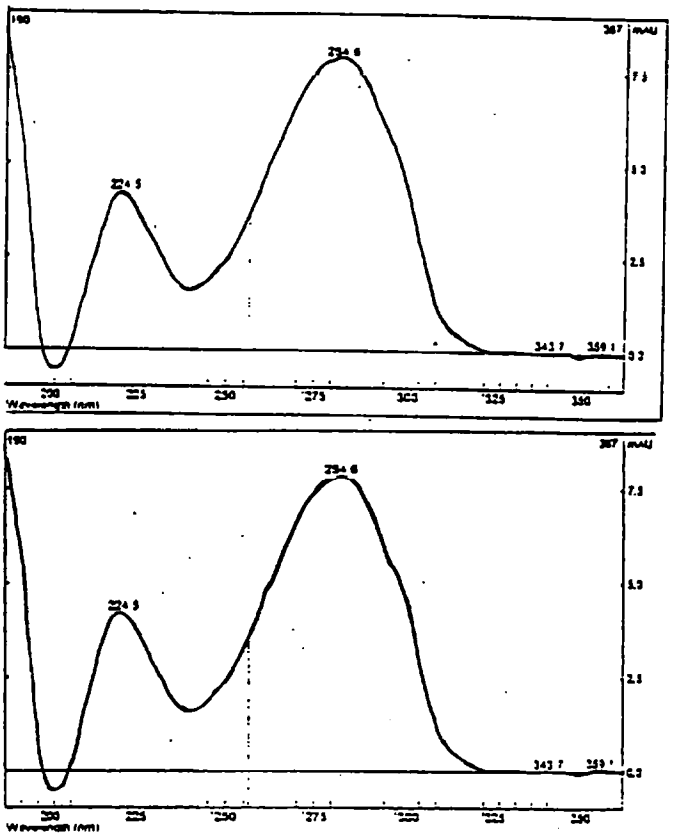

Figure 3.12 Diode array UV spectra of the PBN-adduct produced (a) during microsomal oxidation of 5 mM N,N-dimethyl benzamide in presence of 15 mM PBN and (b) synthetically.

In conclusion, the microsomal metabolism of N,N-dimethylbenzamide involves the abstraction of a hydrogen atom from the carbon atom α to nitrogen to form a carbon-centred radical that is trapped intermolecularly by PBN or undergoes insertion of a hydroxyl group leading to the formation of the carbinolamide product.

3.2.2 Effect of PBN on the microsomal metabolism of N,N-dimethyl benzamide

Inspection of the chromatograms in Figure 3.10 reveals that the presence of PBN lowers the relative amounts of both the usual N-methyl- and N-hydroxymethyl-N-methylbenzamide products formed. Thus, the effect of PBN on the microsomal

metabolism of N,N-dimethylbenzamide was studied in more detail. Microsomal incubations were performed (i) using varying concentrations of PBN at a fixed substrate concentration and (ii) using varying substrate concentrations at a fixed PBN concentration. Table 3.3 reports the rates of N-methylbenzamide and adduct production in the microsomal incubations of N,N-dimethylbenzamide involving a range of PBN concentrations. Table 3.4 reports the corresponding rates of formation from incubation performed in the presence of a fixed concentration of PBN.

The results demonstrate that the formation of N-methylbenzamide decreases with increasing concentration of PBN until 30 mM, whereas the rate of formation of the PBN adduct increases. However, the total rate of metabolism does not change in this range of PBN concentrations. In contrast, at a fixed concentration of PBN, an increase in the substrate concentration leads to a corresponding increase in the rate of formation of both products.

[PBN] (mM)	**Total metabolism** (mM/h/nmol P450)	**N-methyl benzamide** (mM/h/nmol P450)	**PBN-N,N-dimethyl benzamide adduct** (mM/h/nmol P450)
0.0	2.33 ± 0.10	2.33 ± 0.10	0.00
0.5	2.35 ± 0.06	2.20 ± 0.07	0.15 ± 0.01
1.0	2.33 ± 0.06	2.10 ± 0.04	0.23 ± 0.02
5.0	2.30 ± 0.07	1.87 ± 0.05	0.33 ± 0.08
10.0	2.26 ± 0.06	1.60 ± 0.04	0.66 ± 0.03
30.0	2.30 ± 0.11	1.29 ± 0.11	1.00 ± 0.10
100.0	1.60 ± 0.07	1.15 ± 0.16	0.45 ± 0.14

Table 3.3 Rates of the microsomal metabolism of 5 mM N,N-dimethylbenzamide in the presence of varying concentrations of PBN.

[Substrate] (mM)	Total metabolism (mM/h/nmol P450)	N-methyl benzamide (mM/h/nmol P450)	PBN-N,N-dimethyl benzamide adduct (mM/h/nmol P450)
0.5	0.55 ± 0.03	0.39 ± 0.02	0.16 ± 0.01
1.0	0.91 ± 0.07	0.71 ± 0.04	0.20 ± 0.03
5.0	2.00 ± 0.11	1.50 ± 0.08	0.50 ± 0.09
10.0	2.30 ± 0.14	1.60 ± 0.11	0.70 ± 0.04
50.0	2.61 ± 0.14	2.00 ± 0.06	0.61 ± 0.03
100.0	2.66 ± 0.16	2.18 ± 0.11	0.48 ± 0.05

Table 3.4 Rates of microsomal metabolism of varying concentration of N,N-dimethylbenzamide in the presence of 30 mM PBN.

Figure 3.13 shows the time-course of the microsomal metabolism of 10 mM N,N-dimethylbenzamide incubated in the presence and absence of 30 mM PBN. From these results it is quite clear that the presence of PBN does not interfere with the total metabolism of the substrate. The results also indicate that, at the concentrations used in the previous part of the study, PBN does not inhibit the metabolism of N,N-dimethylbenzamide. However, it does change the pattern of the products, as the carbon-centred radical intermediate is partially trapped by PBN (leading to the formation of the PBN-adduct) and partially undergoes hydroxylation (to give the N-demethylated product).

Although the coupling reaction that leads to the formation of the PBN-adduct is reported to be fast,[1] it is logical to argue that the addition of the hydroxyl group to the carbon-centred radical from the P450-haem oxoiron complexes is a more favoured reaction. As an indication the ratio of N-methylbenzamide produced with respect to PBN-adduct is 3 > 1. Formation of the intermediate radical occurs in the hydrophobic environment of the active site of the enzyme where, even if the non-polar characteristics

of PBN enables it to accumulate sufficiently to react with the intermediate, the relative position of the radical with respect to the activated haem group favours the hydroxyl insertion reaction.

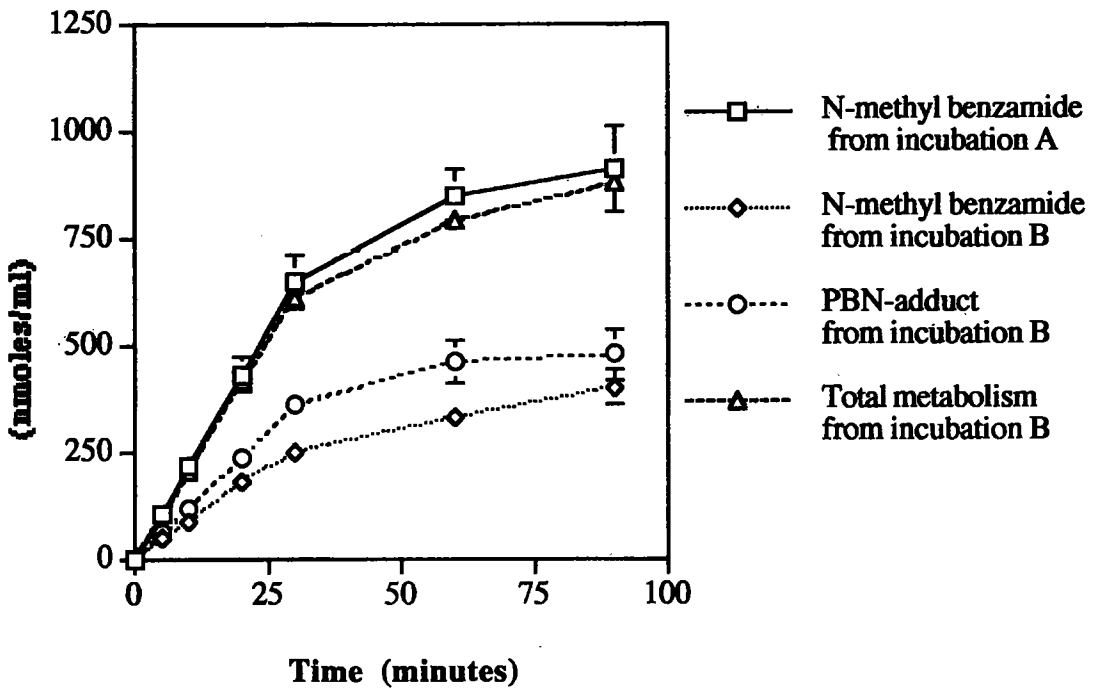

Incubation A: Microsomes + NADPH regenerating system + N,N-dimethyl benzamide 10 mM

Incubation B: Microsomes + NADPH regenerating system + N,N-dimethyl benzamide 10 mM +PBN 30 mM

Figure 3.13 Time-course of the microsomal metabolism of 10 mM N,N-dimethyl benzamide curried out in presence and in absence of 30 mM PBN

3.3 Comparison of spin-trapping and intermolecular trapping

A comparison between intramolecular trapping and intermolecular PBN trapping was made using the substrates illustrated in Figure 3.14.

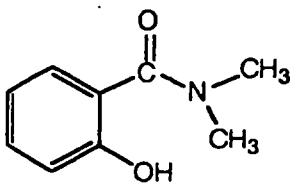

N,N-dimethyl-2-hydroxybenzamide

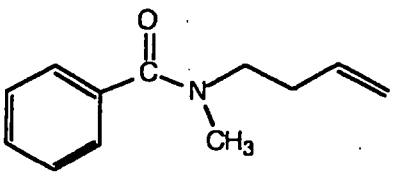

N-(3-butenyl)-N-methylbenzamide

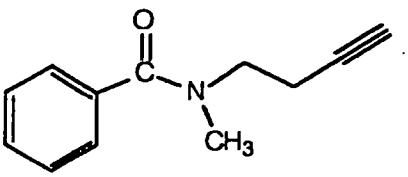

N-(3-butynyl)-N-methylbenzamide

Figure 3.14 Substrates used to compare intermolecular PBN-trapping with intramolecular trapping

Figure 3.15 shows the typical ESR spectra obtained from extracts of the microsomal incubations of 10 mM N,N-dimethyl-2-hydroxybenzamide performed in the presence of 30 mM PBN. Control incubations confirm that the signal is due to a metabolism-dependent PBN radical adduct.

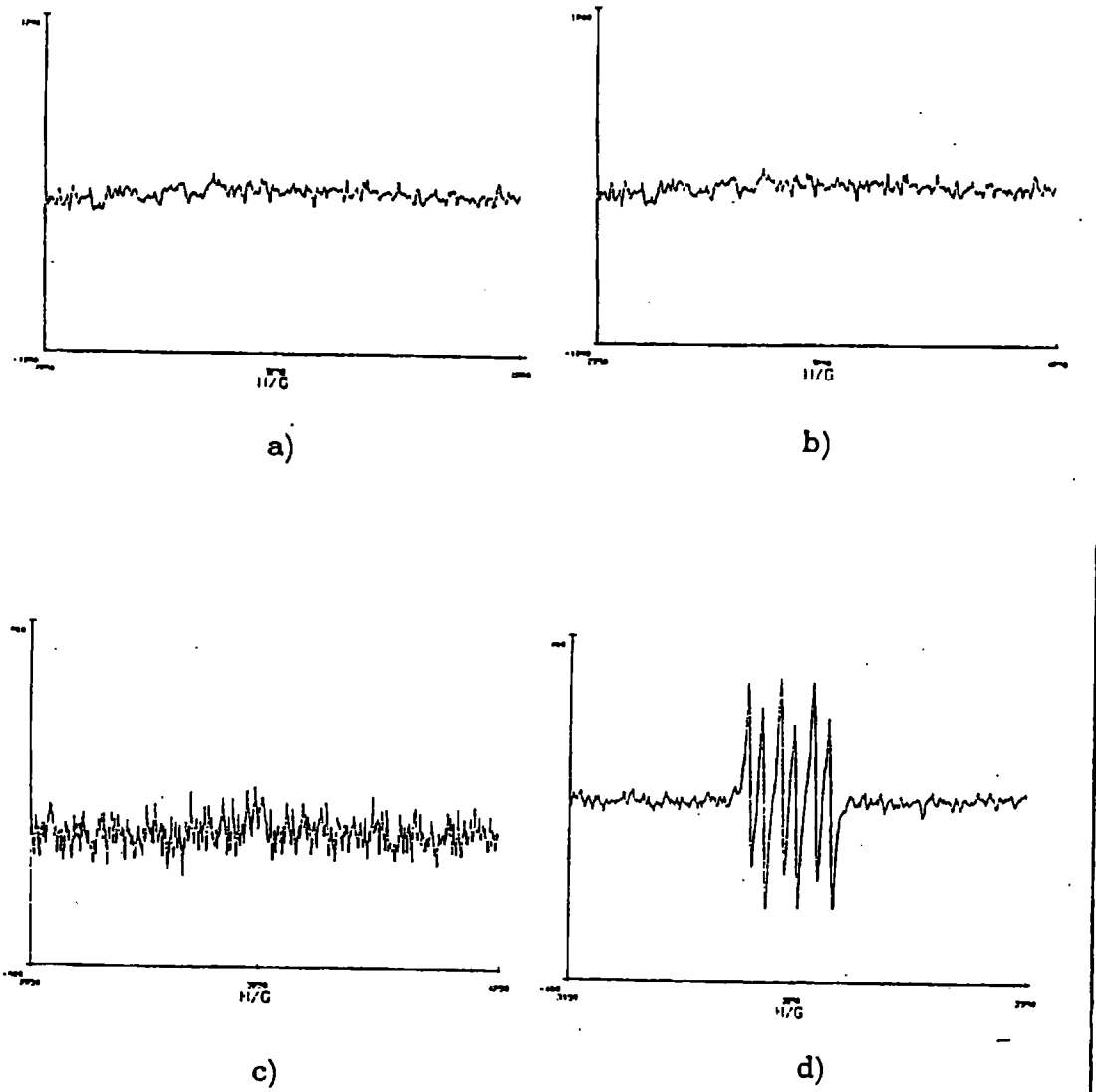

Figure 3.15 ESR spectra of chloroform/methanol extracts from incubation of (a) microsomes, NADPH regenerating system and 30 mM PBN (control), (b) microsomes, 10 mM N,N-dimethyl-2-hydroxybenzamide and 30 mM PBN (control), (c) NADPH regenerating system, 10 mM N,N-dimethyl-2-hydroxybenzamide and 30 mM PBN (control) and (d) microsomes, NADPH regenerating system, 10 mM N,N-dimethyl-2-hydroxybenzamide and 30 mM PBN.

The spectrum is a typical triplet of doublets with hyperfine parameters a_N= 15 G and a_β^H= 6.0 G. Comparison of these data with those obtained from N,N-dimethylbenzamide (Figure 3.6 and Table 3.1), leads to the conclusion that this spectrum is due to a carbon-centred radical-PBN adduct. These results provides a further indication that metabolism of N,N-dimethyl-2-hydroxy benzamide occurs *via* the formation of a carbon-centred radical and not an iminium ion.

Typical ESR spectra obtained from chloroform/methanol extracts of microsomal oxidation of 10 mM N-(3-butenyl)-N-methylbenzamide and N-(3-butynyl)-N-methylbenzamide in the presence of 30 mM PBN are reported in Figures 3.16 and 3.17, respectively.

For both substrates microsomal incubation produces a PBN adduct radical characterised by a triplet of doublets with hyperfine splitting parameters of a_N= 14.8 G and a_β^H= 6.0 G (from N-(3-butenyl)-N-methylbenzamide and a_N= 14.75 G and a_β^H= 6.3 G (from N-(3butynyl)-N-methylbenzamide. These data imply that metabolism of these substrates produced a carbon-centred radical that is trapped by PBN. It is worth emphasising that metabolism of N-(3-butenyl)-N-methylbenzamide yields a carbon-centred radical that is trapped by PBN intermolecularly, but not intramolecularly by the alkene functional group (Chapter 2).

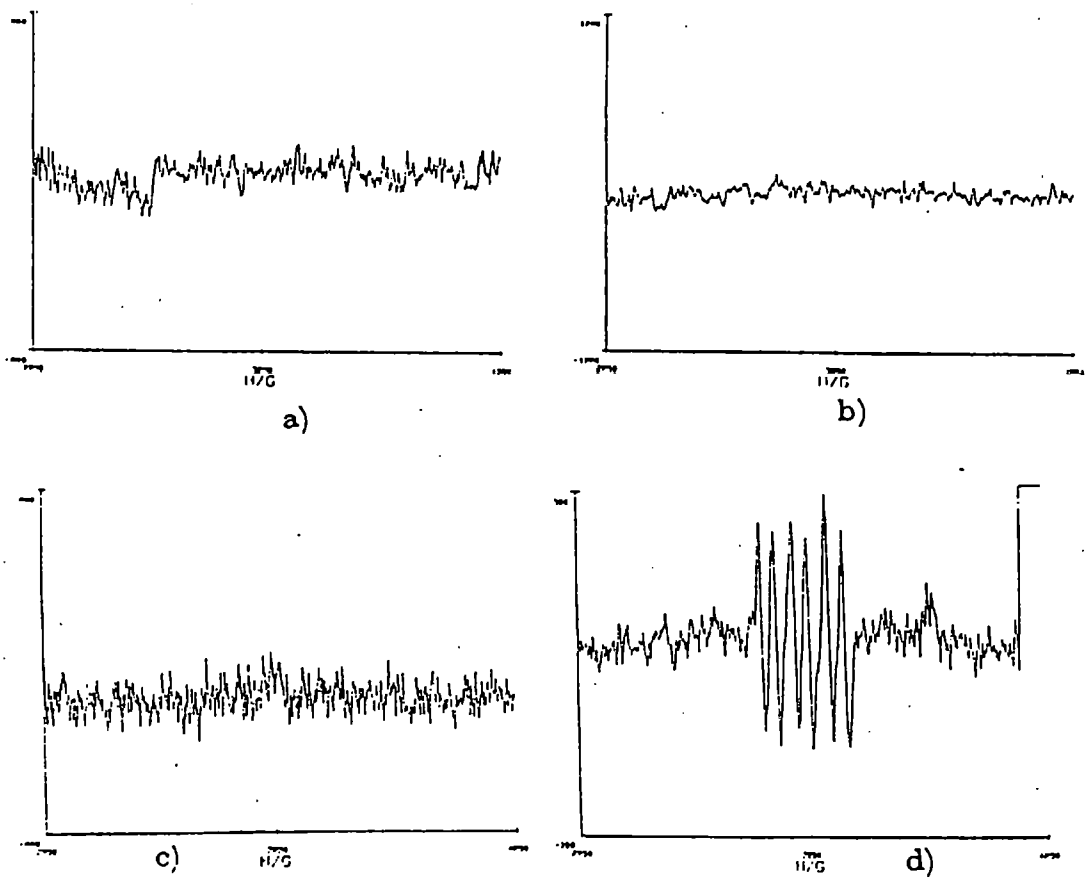

Figure 3.16 ESR spectra of chloroform/methanol extracts from incubation of: (a) microsomes, NADPH regenerating system and 30 mM PBN (control), (b) microsomes, 10 mM N-(3-butenyl)-N-methylbenzamide and 30 mM PBN (control), (c) NADPH regenerating system, 10 mM N-(3-butenyl)-N-methylbenzamide and 30 mM PBN (control), and (d) microsomes, NADPH regenerating system, 10 mM N-(3-butenyl)-N-methylbenzamide and 30 mM PBN.

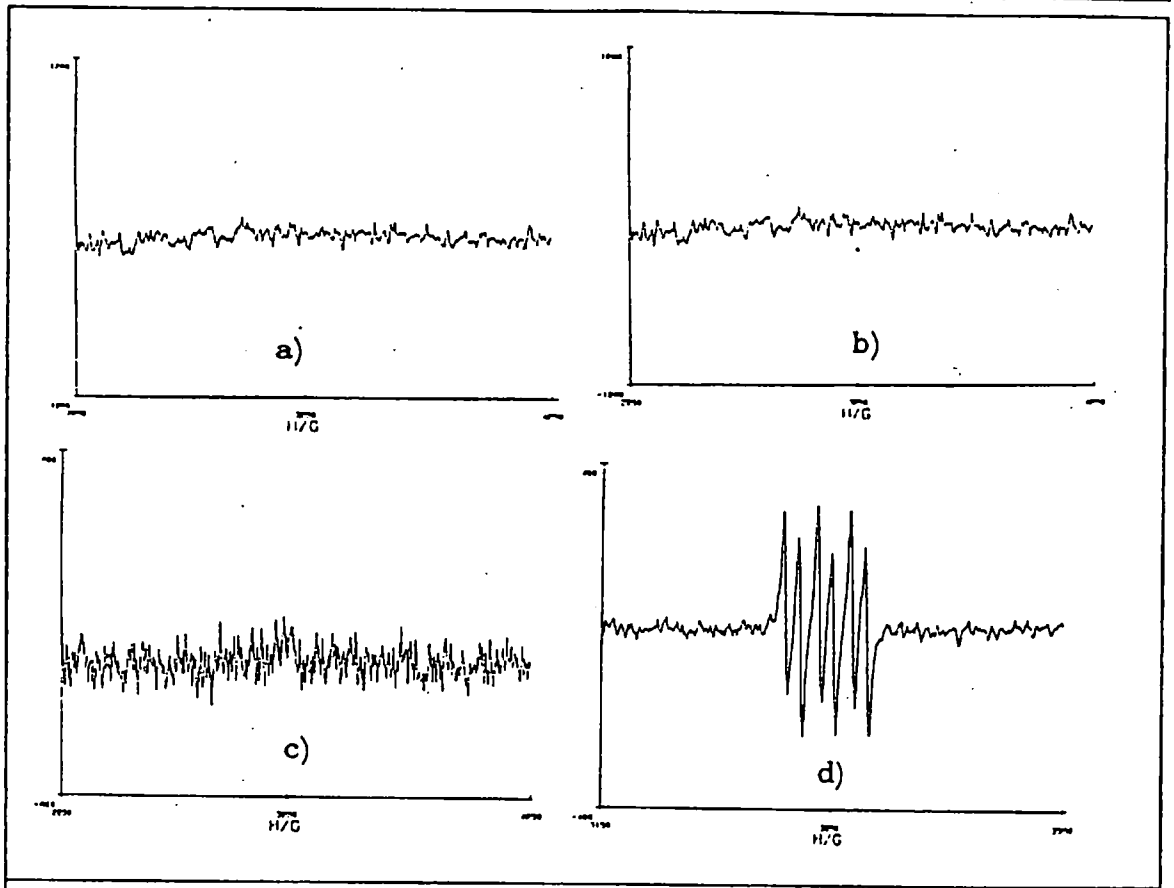

Figure 3.17 ESR spectra of chloroform/methanol extracts from incubation of: (a) microsomes, NADPH regenerating system and 30 mM PBN (control), (b) microsomes, 10 mM N-(3-butynyl)-N-methylbenzamide and 30 mM PBN (control), (c) NADPH regenerating system, 10 mM N-(3-butynyl)-N-methylbenzamide and 30 mM PBN (control), and (d) microsomes, NADPH regenerating system, 10 mM N-(3-butynyl)-N-methylbenzamide and 30 mM PBN.

3.5 Conclusions

The intermolecular spin trapping technique is a successful tool for the detection of the radical intermediates formed during the microsomal P450 metabolism of tertiary amides. These intermediates have been identified as carbon-centred radicals, giving further support to a mechanism involving hydrogen atom abstraction as the first step in the P450-dependent metabolism of tertiary amides.

The spectra of the trapped radicals exhibit a triplet of doublets characteristic of a nitroxyl radical. The triplet splitting is due to interaction with the nitrogen atom, and

reported values of a_N= 14 / 15 G for PBN-trapped carbon radical,[15] are consistent with our interpretation of the present results. The doublet structure is due to the coupling of the β-hydrogen atom, for which a_β^H is reported to be between 2.5 and 4 G for acyl radicals.[20] The values obtained in the present study are somewhat larger, probably due to the different polarities of the solvent used in this study (chloroform/methanol, 2/1) and that used in analogous investigations (benzene).[15]

The PBN adduct of the carbon-centred radical generated during the microsomal metabolism of N,N-dimethylbenzamide was characterised and shown to have the structure illustrated in Figure 3.18.

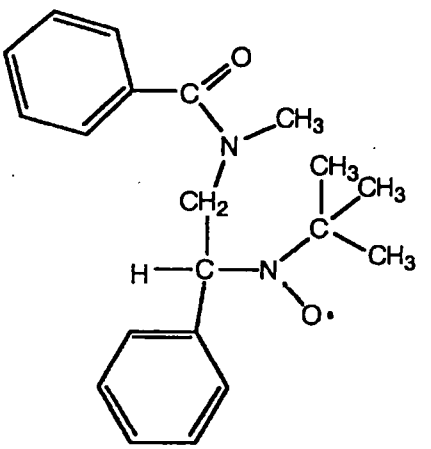

Figure 3.18 Structure of the PBN-adduct formed during microsomal metabolism of N,N-dimethylbenzamide.

It has been reported that PBN interacts with P450 to give a type I binding spectrum with microsomes from phenobarbital-treated rats, and to have an inhibitory effects on the mixed-function oxidation of aminopyrene.[9] However, kinetic investigation revealed that PBN does not inhibit the overall metabolism of N,N-dimethylbenzamide but diverts the reaction to form a new product that is an adduct of PBN and the amide. It follows that PBN traps a reaction intermediates, but does not affect the formation of the intermediate.

3.6 References

1 Buettner G.R., (1987); *Free Rad. Biol. Med.*; **3**: 259-

2 Perkins M.J., Ward P.and Horsfield A., (1970); *J. Chem. Soc.*; **B**: 395-

3 Perkins M.J., (1980); *Adv. Phys. Org. Chem.*; **17**: 1-

4 Janzen E.G., (1971); *Acc. Chem Res.*; **4**: 31-

5 Janzen E.G., (1980); In: Free Radicals in Biology (Pryor, W.A., ed.); vol IV: 115-. Academic Press, New York.

6 Finkelstein E., Rosen G.M. and Ranckman E.J., (1980); *Arch. Biochem. Biophys.*; **200**: 1-

7 Kalyanaraman B., (1982); *Rev. Biochem. Toxicol.*; **4**: 73-

8 Chen G. Janzen E.G. and Bray T.M., (1994); *Free Rad. Biol. Med.*; **17**, 1: 19-

9 Albano E., Lott K.A.K., Slater T.F., Stier A., Symons M.C.R. and Tomasi A., (1982); *Biochem. J.*; **204**: 593-

10 Socci D.J., Crandall B.M. and Arendash G.W., (1995); *Brain Res.*; **693**: 88-

11 Kadkhodaee M., Hanson G.R., Towner R.A. and Endre Z.H., (1996); *Free Rad. Res.*; **25**, 1: 31-

12 Janzen E.G., Wang Y.Y. and Shetty R.V., (1978); *J. Am. Chem. Soc.*; **100**: 2923-

13 Janzen E.G., Coulter G.A., Oehler U.M. and Bergsma L., (1982); *Can. J. Chem.*; **60**: 2725-

14 Iley J and Constantino L., (1992); *Biochem. Pharmacol.*; **44**,4: 651-

15 Janzen E.G., Davis E.R. and Dubose C.M. (1995); *Magn. Res. Chem.*; **33**: S166-

16 Kubow S., Bray T.M. and Janzen E.G.; (1985); *Biochem. Pharmacol.*; **34**: 1117-

17 Britigan B.E.; Rosen G.M., Chai Y. and Cohen M.S., (1986); *J. Biol. Chem.*; **261**: 4426-

CHAPTER 4

The regioselectivity of the microsomal metabolism of tertiary amides

The present chapter describes the studies related to the regioselectivity of the oxidation of three cyclic amides using the following models:

- semi-empirical AM1 molecular orbital calculations,
- P450 biomimetic system,
- rat liver microsomes.

4.1 Introduction

The regioselectivity of biotransformations catalysed by P450 appears to be substrate dependent. For example, no regioselectivity is observed in some P450-dependent carbon oxidation reactions, as, for example, in the metabolism of norbornane[1] or in the 5-exohydroxylation of camphor by bacterial $P450_{cam}$.[2] For these reactions, it is suggested that the species responsible for the hydrogen abstraction step has access to both the *pro* S and the *pro* R protons. In contrast, regioselectivity was found for the hydroxylation of the E- versus Z- methyl groups in the P450 metabolism of olefins such as R(+) pulegone,[3] as well as in the metabolism of testosterone and androsterone by certain P450 isoenzymes.[4] In amines, regioselectivity has also been reported. For example, in (S)-nicotine there is preferred abstraction of the *5'-pro* S hydrogen atom,[5] while for tertiary amines such as N-methyl-N,N-diisopropylamine,[6] the regioselectivity appears to be governed by steric factors.

The N,N-dimethylamides, and the equivalent N,N-dialkylamides, have non-equivalent (alkyl) methyl groups (i.e. E- and Z- isomers) as illustrated in Figure 4.1. Thus, it is conceivable that two P450-substrate interactions are possible; one that is not regioselective, the other where E/Z regioselectivity could occur.

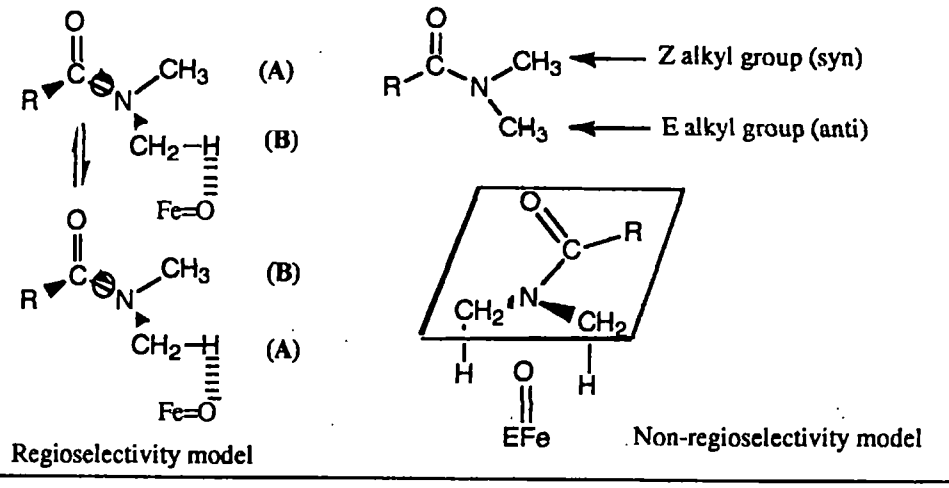

Figure 4.1 Hypothetical active site interactions of the "iron-oxo" intermediate of P450.

It is reported that, on the basis of AM1 self-consistent field molecular orbital calculations, abstraction of a hydrogen atom from the methyl group E- to the carbonyl oxygen atom is energetically favoured by *ca.* 5 kJ/mol^{-1} over similar hydrogen atom abstraction from the Z-methyl group.[7] However, at the product level such regioselectivity might be obscured by amide bond rotation. While amide bond rotation in aqueous solution is faster than P450 turnover,[8] it is not known if amide bond rotation can occur within the enzyme substrate complex. What is known is that, in solution the amide rotation rate increases as solvent polarity decreases [9] and that the active site of the closely related bacterial $P450_{cam}$ is very non-polar.[10] Therefore, purely on polarity considerations, it would seem unlikely that amide bond rotation in the active site would be slow enough to give observable regioselectivity. However, it is quite conceivable that the enzyme would impose steric constrains on amide bond rotation in the enzyme-substrate complex. If P450 is absolutely regiospecific for the E- (or Z-) methyl group, amide rotation in the active site is essentially zero.

On the basis of these considerations we chose to investigate the regioselective aspects of the P450-dependent oxidation of tertiary amides using the series of cyclic substrates illustrated in Figure 4.2. These substrates possess fixed conformations due to almost completely restricted rotation about the C-N bond.

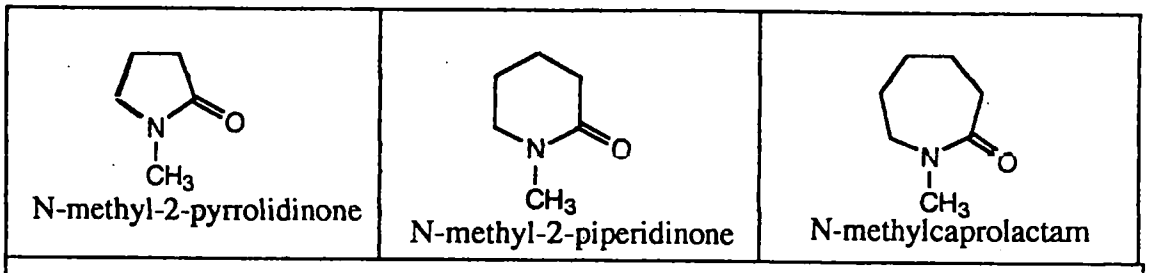

Figure 4.2 Fixed conformation amides used in the study of the regioselectivity of the P450-dependent oxidation of tertiary amides.

These substrates can, theoretically, undergo P450 oxidation in the E- and Z-alkyl groups to form two clearly identifiable products (Figure 4.3). The primary oxidation products **2** and **3** of Figure 4.3 (a), resulting from N-demethylation and ring hydroxylation respectively, potentially can both undergo further metabolism to give the secondary product **4** of figure 4.3 (b). Whether these additional pathways occur, and if they do, which of the two routes also form the subject of the current investigation.

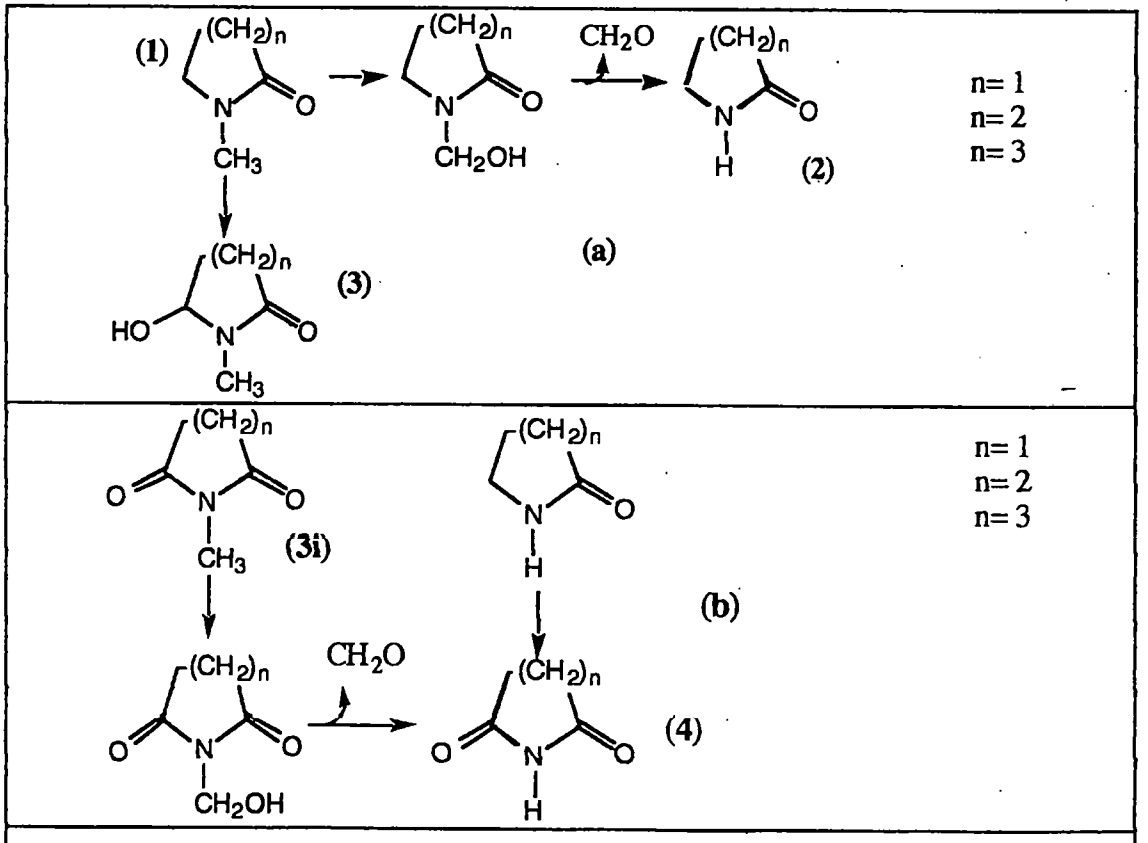

Figure 4.3 Potential metabolic pathways of the P450-dependent oxidation of cyclic amides.

Three lines of investigations were adopted. First semi-empirical AM1 self-consistent field molecular orbital calculations were performed on the potential radical species to identify the most favourable pathway from a thermodynamic point of view. Second oxidation of the compounds catalysed by the $TPPFe^{(III)}$/*tert*-tbutylhydroperoxide P450 biomimetic system was carried out to identify the most oxidisable position from a chemical point of view. Finally, the results of the chemical model and the MO calculations were compared with those obtained for the microsomal oxidation of these substrates.

4.2 AM1 Molecular orbital calculations

Using the semi-empirical AM1 self-consistent field molecular orbital model, the heats of formation (ΔH_f) were calculated for the amides illustrated in Figure 4.2 and for their postulated intermediates. The assumption made for these calculations based on the results of the previous chapter, is that the reaction involves abstraction of a hydrogen atom from α-carbon to form a carbon-centred radical. The values obtained are summarised in Table 4.1.

These heats of formation clearly indicates that the abstraction of the hydrogen atom is much more favoured from the ring carbon (E- position) than that of the N-methyl group (Z- position). Similar results have been reported before for acyclic N,N-dialkylbenzamides, though the differences between the E- and Z- radicals in the present case are somewhat greater (98.2 to 102.8 kJ/mol^{-1}, E- versus Z- for N,N-dimethylbenzamide as opposed to 93.1 to 99.3 kJ/mol^{-1}, E- versus Z- for N-methyl-2-pyrrolidinone). Presumably, this is due to the cyclic nature of the E- radical. Using the differences in the heats of formation between the starting materials and the radicals ($\Delta\Delta H_f$) as an estimate for the differences in the energy barrier to reaction, the ratio of the constants for ring and N-methyl carbon-centred radical formation could be calculated (Chapter 8).

	ΔH_f (kJ/mol^{-1})	
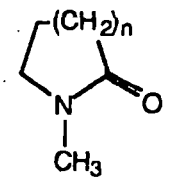	n=1	-168.5
	n=2	-201.9
	n=3	-215.9
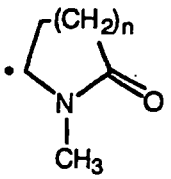	n=1	-75.35
	n=2	-129.30
	n=3	-134.1
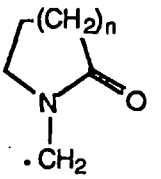	n=1	-69.2
	n=2	-100.8
	n=3	-112.0

Table 4.1 Heats of formation, ΔH_f, for the cyclic amides and their corresponding radicals.

The data are contained in Table 4.2 and indicate that ring hydrogen abstraction is favoured by a large factor over the N-methyl hydrogen abstraction. Moreover, the size of the ring seems to play a significant role in favouring the hydrogen atom abstraction from the E- position, at least on thermodynamic grounds, though there is not a clear relationship between ring size and the calculated ratio.

	Ring radical/N-methyl radical	
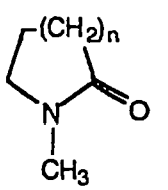	n=1	12
	n=2	100878
	n=3	7376

Table 4.2 Ratio of estimated rate constants for E/Z hydrogen atom abstraction calculated from the difference in the heats of formation, $\Delta\Delta H_f$.

4.3 Biomimetic Oxidation

• Identification of the products

Biomimetic oxidations were analysed by treating the reaction mixtures with 1M sodium hydroxide in methanol to hydrolyse carbinolamides to the corresponding amides.[7; 11] Samples were divided into two fractions. One was analysed directly by gas chromatography (for the N-methyl products) while the second was derivatised using MTBSTFA (N-methyl-N-*tert*-butyldimethylsilyltrifluoroacetamide) before analysis (for the N-dealkylated products). More detailed description of the GC analysis and sample preparation is reported in the Experimental section).

Typical gas chromatograms obtained after 60 minutes of TPPFe(III) catalysed oxidation of 10 mM solutions of the amides are reported in Figure 4.4 (for the direct GC analysis) and Figure 4.5 (for the GC analysis of the derivatised nor-lactams products). The compounds corresponding to the peak found in each chromatogram were identified by comparison of the retention times and mass spectra with those of synthetic standards. The identified products are reported in Tables 4.4 and 4.5.

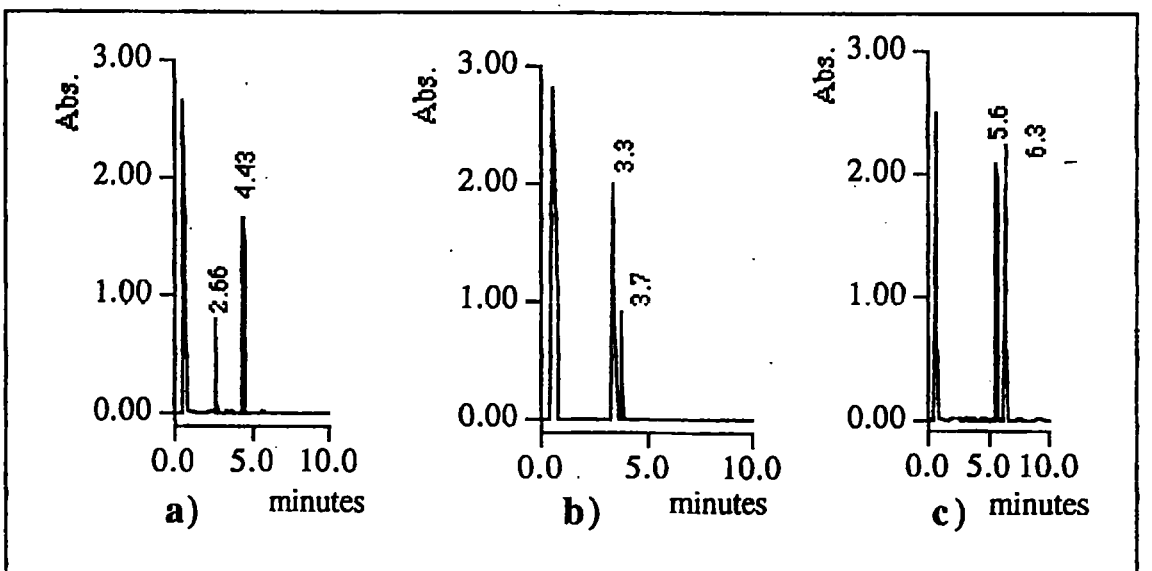

Figure 4.4 Gas chromatograms of underivatised samples from the biomimetic oxidation of (a) N-methyl-2-pyrrolidinone, (b) N-methyl-2-piperidinone and (c) N-methylcaprolactam.

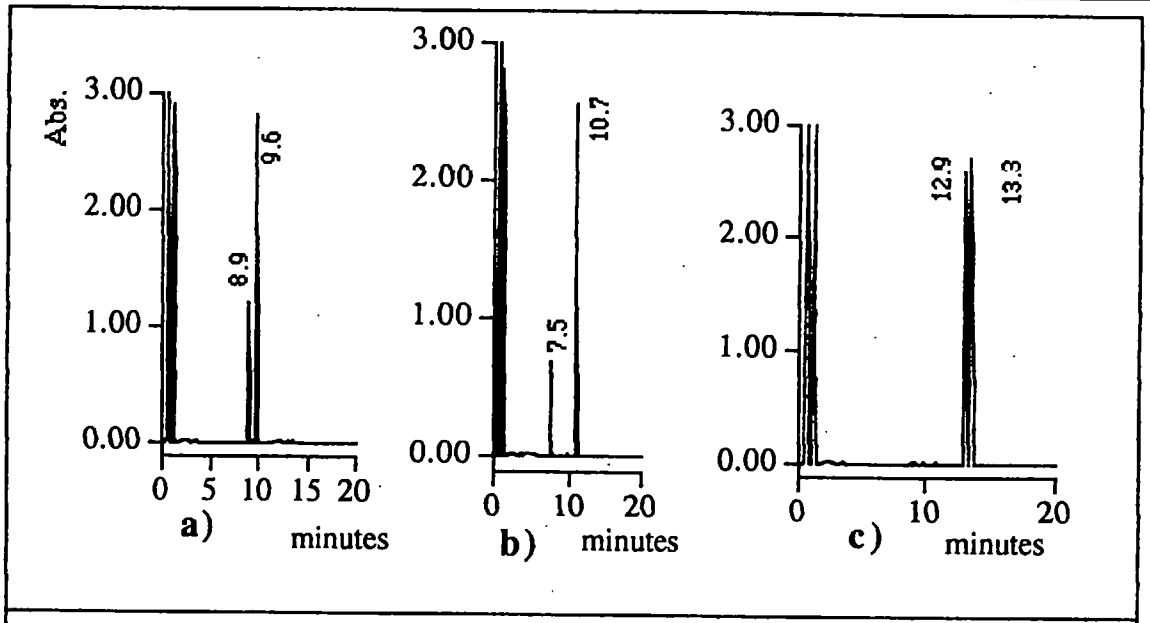

Figure 4.5 Gas chromatograms derivatised samples from the biomimetic oxidation of (a) N-methyl-2-pyrrolidinone, (b) N-methyl-2-piperidinone and (c) N-methylcaprolactam

Peak	Compounds identified	Peak	Compounds identified
Chromatogram a) Retention time: **4.43 minutes**	**N-methyl-2-pyrrolidinone**	Chromatogram a) Retention time: **2.66 minutes**	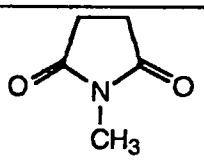 N-methylsuccinimide
Chromatogram b) Retention time: **3.30 minutes**	**N-methyl-2-piperidinone**	Chromatogram b) Retention time: **3.67 minutes**	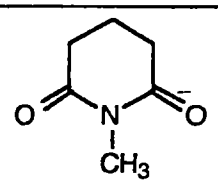 N-methylglutarimide
Chromatogram c) Retention time: **5.57 minutes**	**N-methyl caprolactam**	Chromatogram c) Retention time: **6.29 minutes**	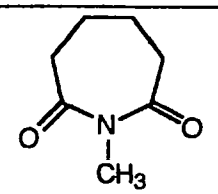 N-methyladipimide

Table 4.3 Products of the biomimetic oxidation of N-methyl-2-pyrrolidinone, N-methyl-2-piperidinone and N-methylcaprolactam identified without derivatisation.

The results can be summarised as follows. Biomimetic oxidation of all three amides gives three products; the imide product of ring oxidation, the N-dealkylated product, and the norimide product of both ring oxidation and dealkylation. Since the formation of the latter product can occur by two routes, i.e. oxidation of both first products **2** and **3** of Figure 4.3, the biomimetic oxidation of such compounds was investigated further.

Peak	**Compounds identified**	**Peak**	**Compounds identified**
Chromatogram a) Retention time: **8.87 minutes**	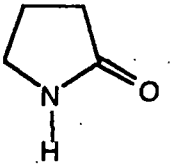 2-pyrrolidinone	Chromatogram a) Retention time: **9.56 minutes**	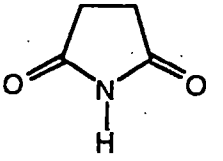 succinimide
Chromatogram b) Retention time: **7.53 minutes**	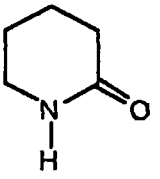 δ-valerolactam	Chromatogram b) Retention time: **10.68 minutes**	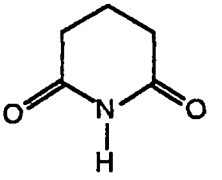 glutarimide
Chromatogram c) Retention time: **12.94 minutes**	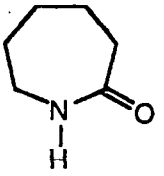 caprolactam	Chromatogram c) Retention time: **13.32 minutes**	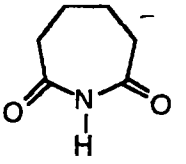 adipimide

Table 4.4 Products of the biomimetic oxidation of N-methyl-2-pyrrolidinone, N-methyl-2-piperidinone and N-methyl caprolactam identified after derivatisation.

Biomimetic oxidations of N-methylsuccinimide, N-methylglutarimide and N-methyladipimide, and of 2-pyrrolidinone, δ-valerolactam, were carried out and analysed by GC after derivatisation since the aim of this investigation was the identification of the

norimine (product **4** of Figure 4.3). Typical gas chromatograms obtained after 60 minutes are reported in Figures 4.6 and 4.7, while Tables 4.5 and 4.6 detail the identified compounds. Product identification relied upon comparison of retention times and mass spectra of the products with that of synthetic standards.

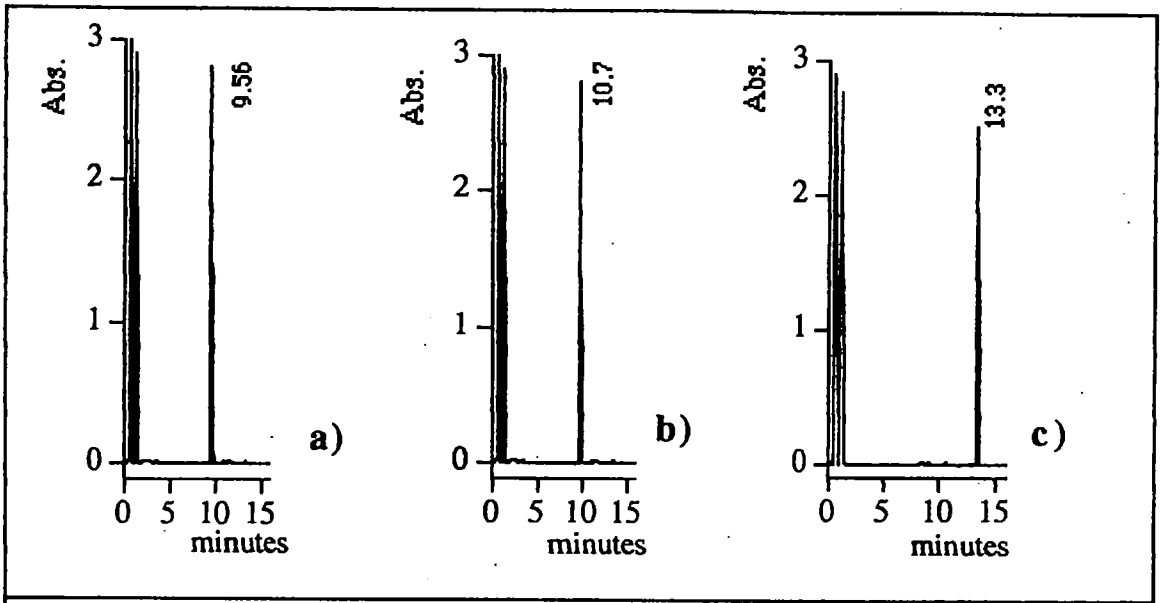

Figure 4.6 Gas chromatograms from the biomimetic oxidation of (**a**) N-methylsuccinimide, (**b**) N-methylglutarimide and (**c**) N-methyladipimide, obtained from MBTSTFA-derivatised samples.

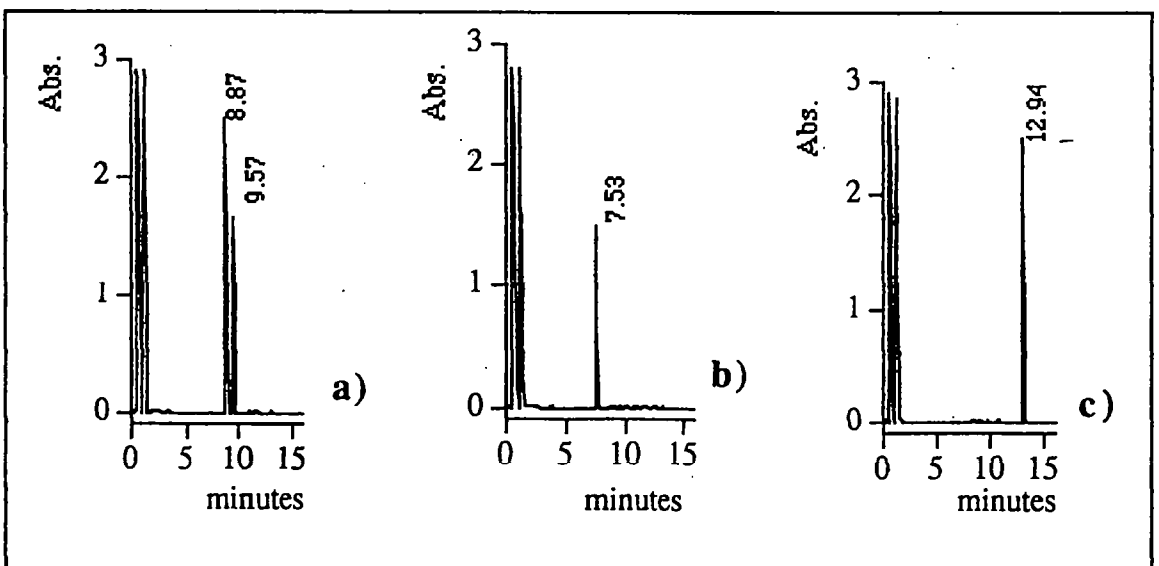

Figure 4.7 Gas chromatograms from biomimetic oxidation of (**a**) 2-pyrrolidinone, (**b**) δ-valerolactam and (**c**) adipimide, obtained from MBTSTFA-derivatised samples.

Peak	Compounds identified
Chromatogram a) Retention time: **9.56 minutes**	**succinimide**
Chromatogram b) Retention time: **10.68 minutes**	**glutarimide**
Chromatogram c) Retention time: **13.32 minutes**	**adipimide**

Table 4.5 Identified products from the biomimetic oxidation of N-methylsuccinimide, N-methylglutarimide and N-methyladipimide.

Peak	Compounds identified
Chromatogram a) Retention time: **8.87 minutes**	**2-pyrrolidinone**
Chromatogram a) Retention time: **9.56 minutes**	**succinimide**
Chromatogram b) Retention time: **7.53 minutes**	**δ-valerolactam**
Chromatogram c) Retention time: **12.94 minutes**	**caprolactam**

Table 4.6 Identified products from the biomimetic oxidation of 2-pyrrolidinone, δ-valerolactam and caprolactam.

It is interesting to note that formation of glutarimide and adipimide is observed from the biomimetic oxidation of N-methylglutarimide and N-methyladipimide respectively whereas these compounds are not observed in the oxidation of the corresponding δ-valerolactam and caprolactam. In contrast, biomimetic oxidation of both N-methyl succinimide and 2-pyrrolidinone lead to the formation of succinimide.

Thus, biomimetic oxidation of N-methyl-2-pyrrolidinone leads to the formation of succinimide can potentially occur *via* both N-demethylation of N-methylsuccinimide or ring oxidation of 2-pyrrolidinone. However, similar biomimetic oxidation of N-methyl-2-piperidinone and N-methylcaprolactam yields glutarimide or adipimide only *via* the initial N-demethylation.

- **Reaction kinetics**

The time-courses of the biomimetic oxidation of 5 mM solutions of the amides were studied over an interval of 2 hours. These are presented in Figure 4.8 and refer to the main metabolite produced, *i.e.* the primary ring oxidation compounds. The reactions present a fairly linear rate of formation of products within the first 30 minutes followed by a gradual decrease over the remaining time of the reaction. This is probably due to the degradation of the catalyst. Indeed, side reactions such as catalyst auto-oxidation (as indicated by catalyst bleaching) and solvent oxidation are reported.[12] These are known to result in the observed emphatic 'tailing-off' in the reaction progress. Thus, the time chosen for the determination of the initial rates of the reaction, v_i, for all these biomimetic oxidations was the first 20 minutes. This reaction time provides a good compromise between the need to determine the products in the initial linear phase and the formation of a measurable quantity of metabolites.

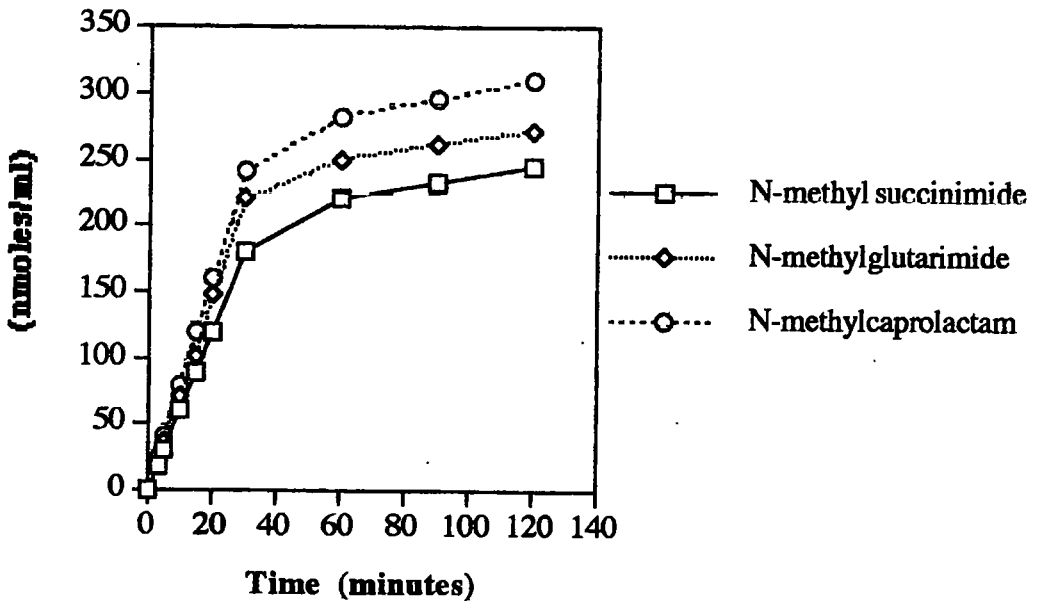

Figure 4.8 Time-course for the formation of the major product in the biomimetic oxidations of 5 mM N-methyl-2-pyrrolidinone, N-methyl-2-piperidinone and N-methylcaprolactam.

The initial rates for the biomimetic oxidation of these substrates were determined at various concentrations of the substrates (ranging between 0.02 and 10.0 mM) and these are reported in Tables 4.7-4.9. The reproducibility of these values was ± 5 %.

[Substrate] (mM)	N-methylsuccinimide (mM/h/mmol cat.)	2-pyrrolidinone (mM/h/mmol cat.)	succinimide (mM/h/mmol cat.)
0.02	0.034 ± 0.002	0.003 ± 0.001	0.014 ± 0.003
0.10	0.170 ± 0.012	0.013 ± 0.003	0.061 ± 0.005
1.00	1.510 ± 0.110	0.116 ± 0.006	0.260 ± 0.021
3.00	3.630 ± 0.210	0.288 ± 0.011	0.342 ± 0.041
5.00	5.020 ± 0.500	0.404 ± 0.021	0.365 ± 0.033
10.0	7.100 ± 0.800	0.565 ± 0.026	0.384 ± 0.018

Table 4.7 Initial rates, v_i, of product formation for the biomimetic oxidation of N-methyl-2-pyrrolidinone.

[Substrate] (mM)	N-methylglutarimide (mM/h/mmol cat.)	δ-valerolactam (mM/h/mmol cat.)	glutarimide (mM/h/mmol cat.)
0.02	0.112 ± 0.004	$1.99 \cdot 10^{-5} \pm 1 \cdot 10^{-6}$	0.074 ± 0.002
0.10	0.544 ± 0.104	$9.86 \cdot 10^{-5} \pm 3 \cdot 10^{-6}$	0.345 ± 0.008
1.0	4.187 ± 0.260	$8.79 \cdot 10^{-4} \pm 1.9 \cdot 10^{-5}$	1.900 ± 0.230
3.00	8.300 ± 0.210	0.0021 ± 0.0005	3.087 ± 0.315
5.00	10.335 ± 0.400	0.0029 ± 0.0003	3.466 ± 0.230
10.0	12.659 ± 0.880	0.0042 ± 0.0006	3.820 ± 0.181

Table 4.8 Initial rates, v_i, of product formation for the biomimetic oxidation of N-methyl-2-piperidinone.

[Substrate] (mM)	N-methyl adipimide (mM/h/mmol cat.)	caprolactam (mM/h/mmol cat.)	adipimide (mM/h/mmol cat.)
0.02	0.054 ± 0.006	0.0015 ± 0.001	0.059 ± 0.008
0.10	0.268 ± 0.012	0.015 ± 0.005	0.289 ± 0.026
1.0	2.451 ± 0.210	0.075 ± 0.004	2.293 ± 0.119
3.00	6.168 ± 0.331	0.216 ± 0.011	4.717 ± 0.176
5.00	8.85 ± 0.521	0.344 ± 0.016	5.981 ± 0.233
10.0	13.15 ± 0.811	0.621 ± 0.033	7.485 ± 0.385

Table 4.9 Initial rates, v_i, of product formation for the biomimetic oxidation of N-methylcaprolactam.

Based on the qualitative results reported earlier, the formation of succinimide in the biomimetic oxidation of N-methyl-2-pyrrolidinone could arise from further oxidation of the primary products. Thus, the evaluate of the total amount of initial ring oxidation with respect to N-demethylation rate of formation of succinimide from N-

methylsuccinimide and from 2-pyrrolidinone was determinated. The results are reported in Table 4.10.

	v_i of succinimide (mM/h/mmol cat.)		
[Substrate] (mM)	**From N-methylsuccinimide**	**From 2-pyrrolidinone**	**Rate ratio**
0.5	0.788 ± 0.090	0.454 ± 0.040	1.74
3.0	3.120 ± 0.096	1.930 ± 0.040	1.62
5.0	4.740 ± 0.250	2.986 ± 0.099	1.59
10.0	5.110 ± 0.066	3.260 ± 0.090	1.57

Table 4.10. Values of the initial ratio, v_i, of the formation of succinimide for the biomimetic oxidation of N-methylsuccinimide and 2-pyrrolidinone

The plot v_i of N-methylglutarimide *versus* N-methyl-2-piperidinone concentrations, illustrated in Figure 4.9, is curved at a substrate concentration of ca 5.0 mM. This apparent limiting of the reaction rate can be rationalised in terms of a saturating "enzyme-type" catalysis. Analysis of the data can be achieved using the Michaelis-Menten method. Kinetic parameters for the oxidation reactions, reported in Table 4.11, were obtained from the data of Tables 4.7, 4.8 and 4.9 by using the Hanes plot. The Hanes plot was chosen because of its better reliability and it does not magnify any errors in the data points at low v_i and low substrate concentrations.

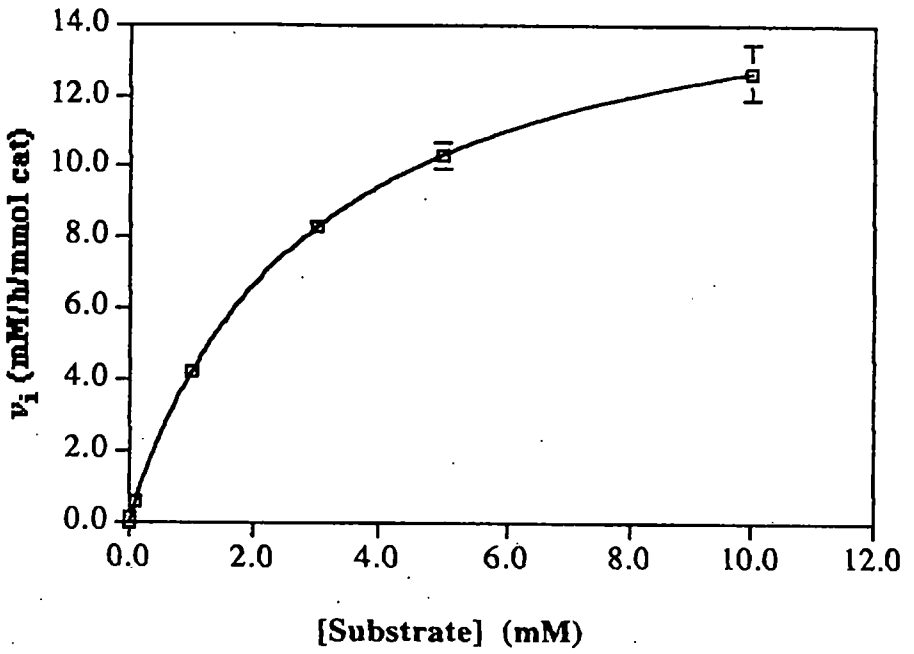

Figure 4.9 Initial rate, v_i, of N-methylglutarimide formation *versus* substrate concentration in the biomimetic oxidation of N-methyl-2-piperidinone.

The kinetic parameters reported in Table 4.11 for ring oxidation include the formation of glutarimide and adipimide since these products almost entirely arise from the N-demethylation of the primary products N-methylglutarimide and N-methyladipimide. The parameters for ring oxidation and N-demethylation include a partitioning of the formation of succinimide in a ratio of 1.62.

Compound	N-demethylation (Z- oxidation)	Ring oxidation (E- oxidation)
N-methyl-2-pyrrolidinone	V_{max}: 1.17 ± 0.07 (mM/h/mmol cat) K_m: 7.31 ± 0.16 (mM^{-1}) V_{max}/K_m: 0.16	V_{max}: 12.33 ± 0.47 (mM/h/mmol cat) K_m: 7.04 ± 0.12 (mM^{-1}) V_{max}/K_m: 1.75
N-methyl-2-piperidinone	V_{max}: 0.007 ± 0.0004 (mM/h/mmol cat) K_m 7.00 ± 0.3 (mM^{-1}) V_{max}/K_m: 0.001	V_{max}: 16.33 ± 0.90 (mM/h/mmol cat) K_m: 2.90 ± 0.15 (mM^{-1}) V_{max}/K_m: 5.62
N-methylcaprolactam	V_{max}: 0.320 ± 0.016 (mM/h/mmol cat) K_m: 4.15 ± 0.18 (mM^{-1}) V_{max}/K_m: 0.077	V_{max}: 29.90 ± 1.89 (mM/h/mmol cat) K_m: 4.82 ± 0.21 (mM^{-1}) V_{max}/K_m: 6.19

Table 4.11 Kinetic parameters V_{max}, K_m and V_{max}/K_m calculated for the biomimetic oxidation of N-methyl-2-pyrrolidinone, N-methyl-2-piperidinone and N-methylcaprolactam.

The kinetic parameters obtained from these reactions indicate that, for all the amides a regioselectivity for the abstraction of the hydrogen atom from the E- carbon is preferred by a large factor. The ratio of the regiopreference in these biomimetic oxidations is summarised in Table 4.12. The data obtained are in excellent agreement with those obtained from the semi-empirical AM1 calculations (Table 4.2).

Substrate	Ring oxidation (E) *vs* N-demethylation (Z)
N-methyl-2-pyrrolidinone	10.9
N-methyl-2-piperidinone	5620
N-methylcaprolactam	80.4

Table 4.12 Ratios of the ring oxidation *versus* N-demethylation for the biomimetic oxidation of N-methyl-2-pyrrolidinone, N-methyl-2-piperidinone and N-methylcaprolactam.

In conclusion, for the chemical catalysed oxidation of the three cyclic amides thermodynamic factors are the main, if not the only, driving force in determining the reaction profile.

4.4 Microsomal oxidation

- **Identification of the products**

The three cyclic substrates were incubated with phenobarbital-induced rat liver microsomes in presence of a NADPH regenerating system. Product identification involved treating samples of the reaction mixture with 1.0 M aqueous sodium hydroxide (to hydrolyse any carbinolamides formed) then splitting the samples in two, one of which was analysed directly by GC while the other was derivatised by MTBSTFA before analysis.

Typical gas chromatograms, obtained after 30 minutes from samples with and without derivatisation, for the microsomal oxidations of 5 mM N-methyl-2-pyrrolidinone, N-methyl-2-piperidinone and N-methylcaprolactam are reported in Figures 4.10, 4.11 and 4.12, respectively. The products corresponding to each peak in the chromatograms were identified by comparison of their retention times and mass spectra with synthetic standards. Table 4.13 summarises the identified metabolites for the three amides analysed.

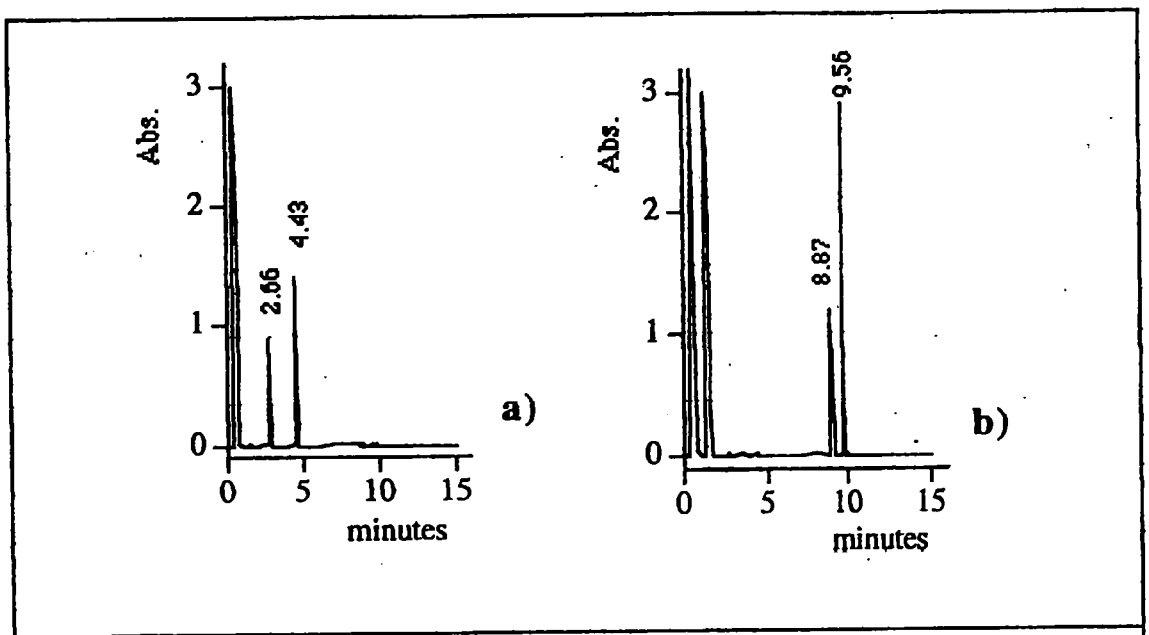

Figure 4.10 GC analysis of the products of microsomal oxidation of 5 mM N-methyl-2-pyrrolidinone obtained from a) underivatised and b) MTBSTFA-derivatised samples.

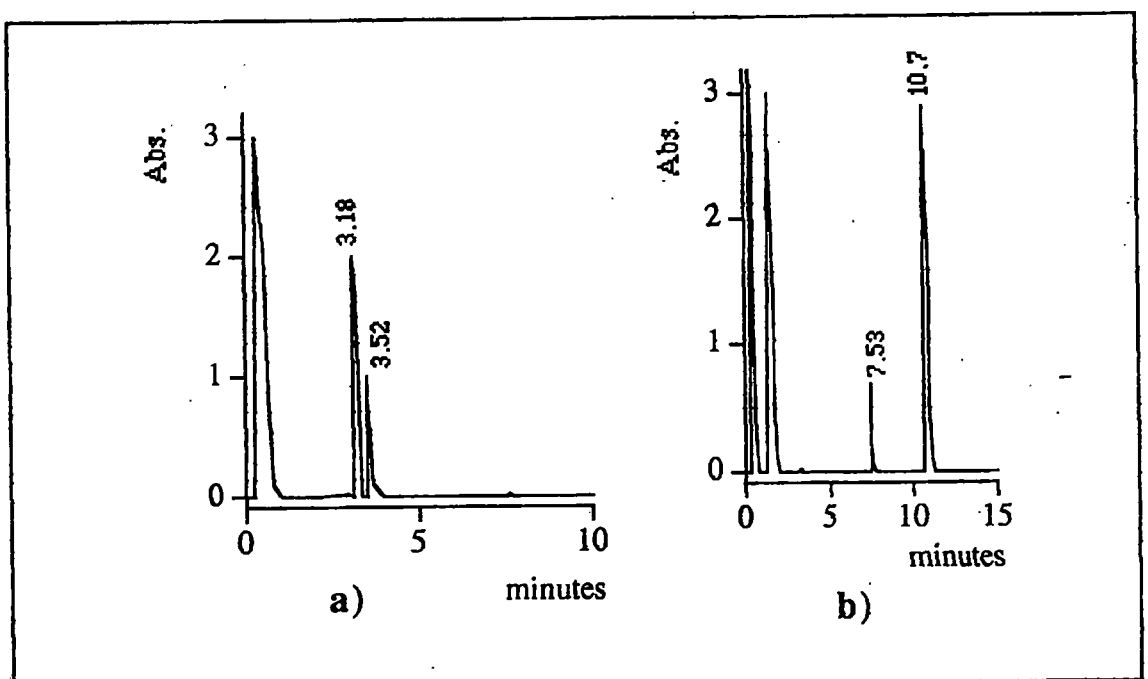

Figure 4.11 GC analysis of the products of microsomal oxidation of 5 mM N-methyl-2-piperidinone obtained from a) underivatised and b) MTBSTFA-derivatised samples.

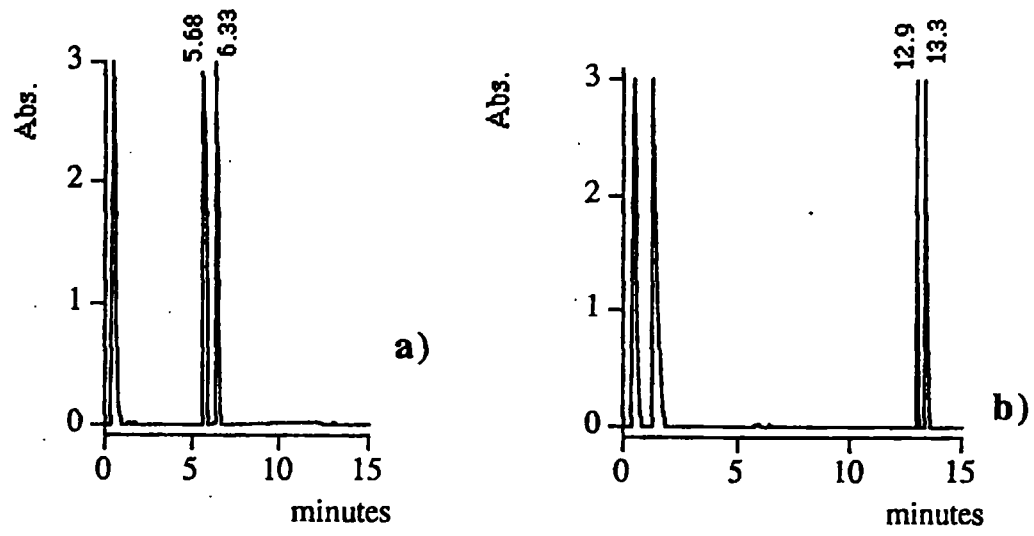

Figure 4.12 GC analysis of the products of microsomal oxidation of 5 mM N-methylcaprolactam obtained from a) underivatised and b) MTBSTFA-derivatised samples.

Substrate	Peak	Compound identified	Peak	Compound identified
N-methyl-2-pyrrolidinone	Chromatogram a) Figure 4.10 **4.43 min.**	**N-methyl-2-pyrrolidinone**	Chromatogram b) Figure 4.10 **8.87 min.**	**2-pyrrolidinone**
N-methyl-2-pyrrolidinone	Chromatogram a) Figure 4.10 **2.66 min.**	**N-methyl succinimide**	Chromatogram b) Figure 4.10 **9.56 min.**	**Succinimide**
N-methyl-2-piperidinone	Chromatogram a) Figure 4.11 **3.16 min.**	**N-methyl-2-piperidinone**	Chromatogram b) Figure 4.11 **7.35 min.**	**δ-Valerolactam**
N-methyl-2-piperidinone	Chromatogram a) Figure 4.11 **3.52 min.**	**N-methyl glutarimide**	Chromatogram b) Figure 4.11 **10.68 min.**	**Glutarimide**
N-methyl caprolactam	Chromatogram a) Figure 4.12 **5.60 min.**	**N-methyl caprolactam**	Chromatogram b) Figure 4.12 **12.94 min.**	**Caprolactam**
N-methyl caprolactam	Chromatogram a) Figure 4.12 **6.31 min.**	**N-methyl adipimide**	Chromatogram b) Figure 4.12 **13.32 min.**	**Adipimide**

Table 4.13 Identified metabolites from the microsomal oxidation of N-methyl-2-pyrrolidinone, N-methyl-2-piperidinone and N-methylcaprolactam.

Control incubations confirmed that the products are metabolism dependent. Figure 4.13 reports the gas chromatograms for 10 mM of a control incubation involving N-methyl-2-piperidinone and microsomes but without the NADPH regenerating system.

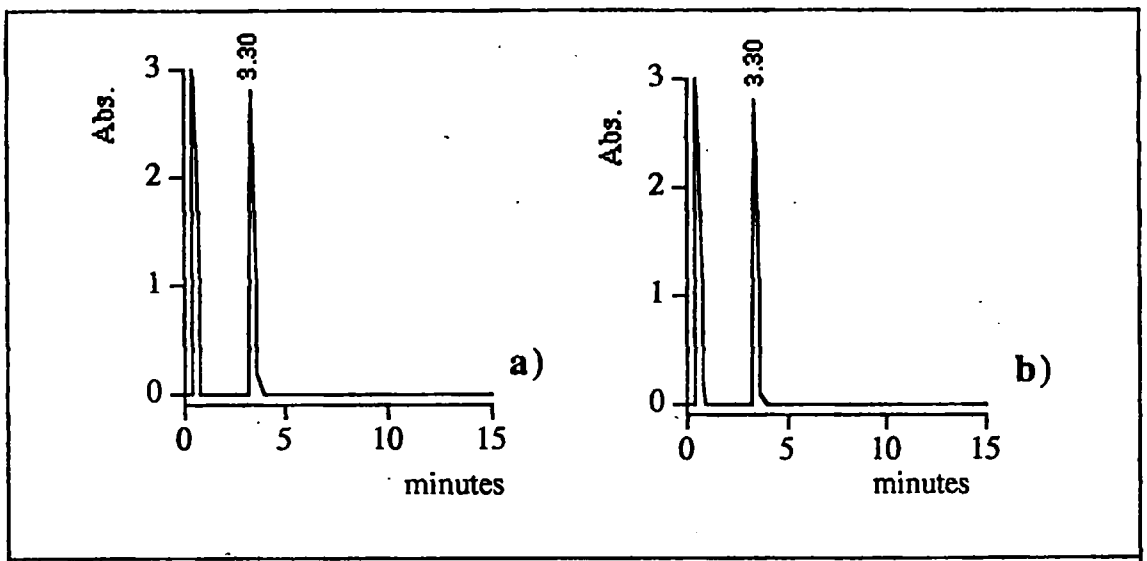

Figure 4.13. GC analysis of a control incubation for the microsomal oxidation of 10 mM N-methyl-2-piperidinone: a) underivatised sample; b) MTBSTFA-derivatised sample.

The results indicate that microsomal metabolism of N-methyl-2-pyrrolidinone, N-methyl-2-piperidinone and N-methylcaprolactam leads to the formation of the same metabolites observed in the biomimetic oxidation of these compounds. No other substrate-derived products were identified under any different incubation condition. It is also worthy to note that ring oxidation of the substrates leads results in the imide formation while hydroxyl ring compounds were not identified in these reactions.

The presence of the secondary product of the metabolism for all these substrates, the norimide, requires an analysis as to which of the two potential metabolic pathways, illustrated in Figure 4.3 leads to these metabolite. Thus, microsomal incubations of the primary metabolites **2** and **3i** of Figure 4.3 were also carried out. Typical gas chromatograms of 5 mM incubations of these substrates are reported in Figures 4.14, 4.15 and 4.16. As the norimide is the product of these reactions, gas chromatographic analysis was carried out only on derivatised samples.

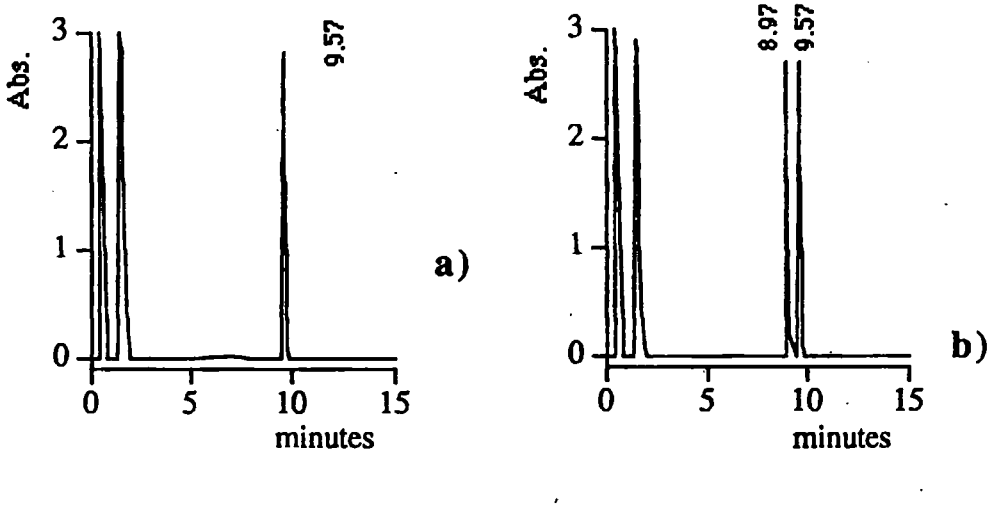

Figure 4.14 GC analysis of the products of microsomal oxidation of 5 mM a) N-methylsuccinimide and b) 2-pyrrolidinone obtained from MTBSTFA-derivatised samples.

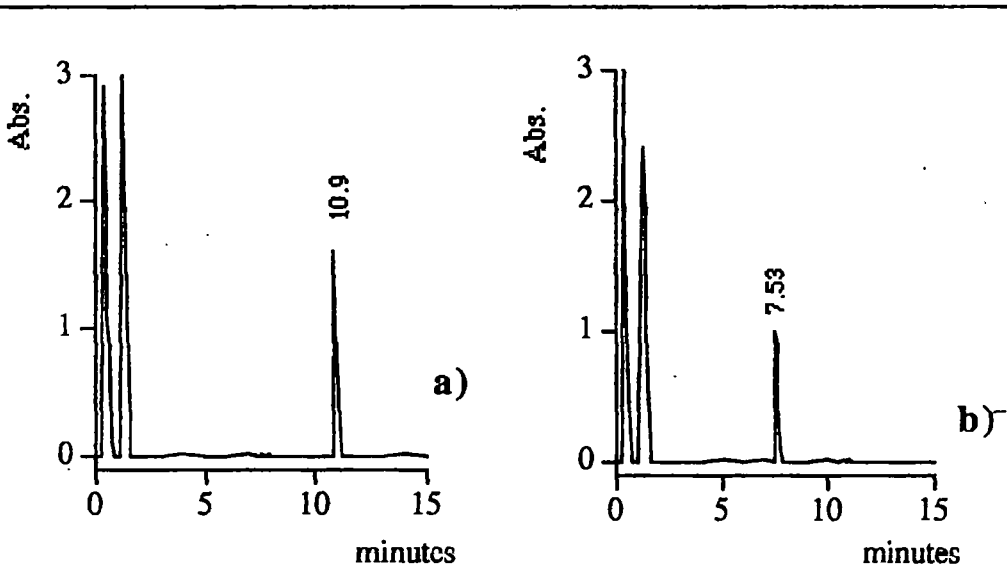

Figure 4.15 GC analysis of the products of microsomal oxidation of 5 mM a) N-methylglutarimide and b) δ-valerolactam obtained from MTBSTFA-derivatised samples.

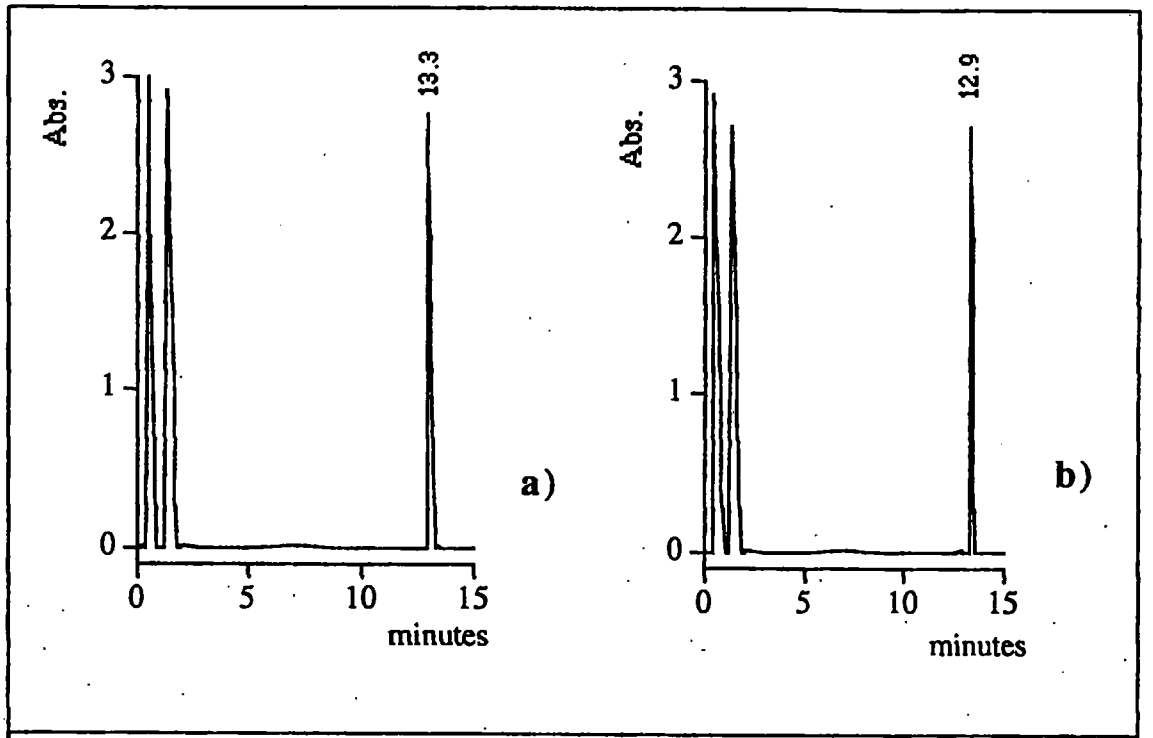

Figure 4.16 GC analysis of the products of microsomal oxidation of 5 mM a) N-methylcaprolactam and b) caprolactam obtained from MTBSTFA-derivatised samples.

As observed for the biomimetic oxidation of these compounds, glutarimide and adipimide are formed only from N-demethylation of N-methylglutarimide and N-methyladipimide respectively, whereas succinimide arises from both N-demethylation of N-methylsuccinimide and ring oxidation of 2-pyrrolidinone.

- **Kinetic parameters**

In a preliminary investigation, the rates of formation of the products of the microsomal oxidations of N-methyl-2-pyrrolidinone, N-methyl-2-piperidinone and N-methylcaprolactam were monitored over a 2 hours reaction period. Figure 4.17 shows the time-dependence of the formation of the main metabolites of the microsomal oxidations of 3 mM solutions of the substrates.

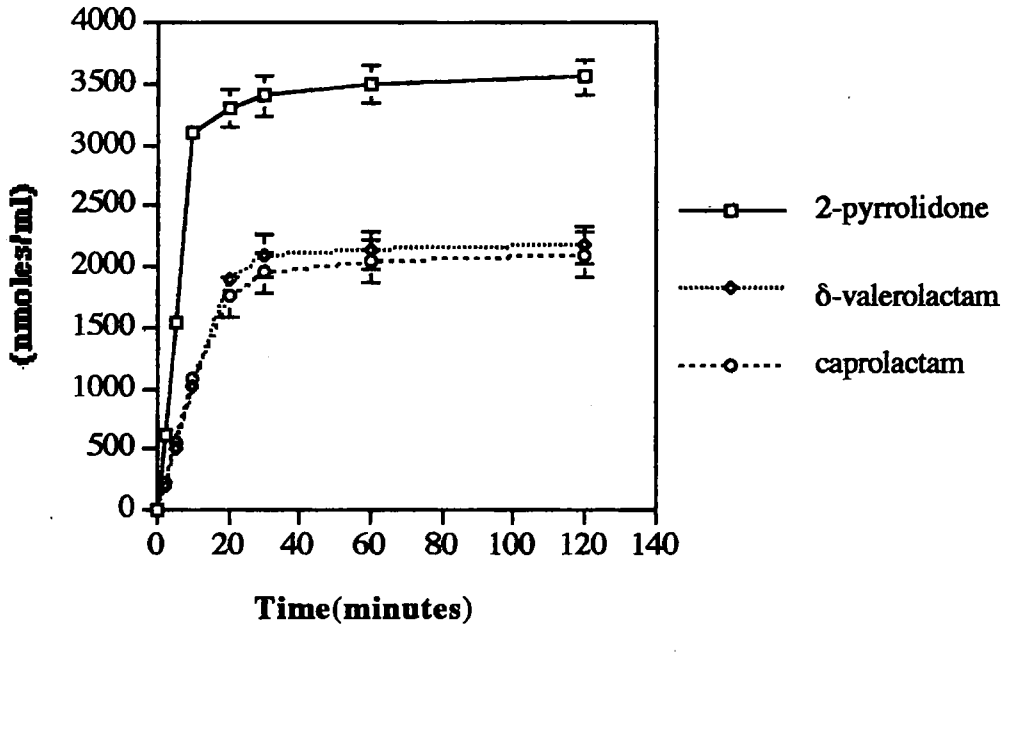

Figures 4.17. Time-course for the formation of 2-pyrrolidinone, δ-valerolactam and caprolactam from the microsomal oxidation of 3 mM N-methyl-2-pyrrolidinone, N-methyl-2-piperidinone and N-methylcaprolactam.

The reactions present a linear phase over the first 20 minutes followed by a significant drop in catalytic activity. Thus, for all the reactions analysed the time chosen for the determination of the initial rates was 10 minutes. The initial rates, v_i, for the formation of the metabolites of the microsomal oxidation of the three substrates at initial concentrations varying between 0.05 and 10 mM, determined by the GC method are given in Tables 4.14, 4.15 and 4.16.

[Substrate] (mM)	N-methyl succinimde (mM/h/nmol P450)	2-pyrrolidinone (mM/h/nmol P450)	succinimide (mM/h/nmol P450)
0.05	0.119 ± 0.008	0.100 ± 0.008	0.025 ± 0.002
0.5	0.927 ± 0.051	0.982 ± 0.021	0.201 ± 0.021
3.0	5.755 ± 0.421	5.429 ± 0.308	1.151 ± 0.090
5.0	9.019 ± 0.816	8.512 ± 0.564	1.971 ± 0.142
10.0	12.970 ± 0.790	14.824 ± 1.090	3.848 ± 0.231

Table 4.14 Initial ratio, v_i, for the microsomal oxidation of N-methyl-2-pyrrolidinone.

[Substrate] (mM)	N-methyl glutarimide (mM/h/nmol P450)	δ-valerolactam (mM/h/nmol P450)	glutarimide (mM/h/nmol P450)
0.05	0.006 ± 0.001	0.121 ± 0.009	0.0003 ± 0.00002
0.5	0.059 ± 0.008	1.060 ± 0.033	0.003 ± 0.0008
3.0	0.312 ± 0.016	6.356 ± 0.219	0.016 ± 0.008
5.0	0.476 ± 0.032	7.398 ± 0.561	0.026 ± 0.006
10.0	0.786 ± 0.012	10.264 ± 0.848	0.041 ± 0.001

Table 4.15 Initial ratio, v_i, for the microsomal oxidation of N-methyl-2-piperidinone.

[Substrate] (mM)	N-methyl adipimide (mM/h/nmol P450)	caprolactam (mM/h/nmol P450)	adipimide (mM/h/nmol P450)
0.05	0.003 ± 0.0004	0.050 ± 0.006	$4 \cdot 10^{-5} \pm 3 \cdot 10^{-6}$
0.5	0.021 ± 0.002	0.506 ± 0.018	0.0004 ± 0.00005
3.0	0.118 ± 0.003	3.401 ± 0.026	0.003 ± 0.0002
5.0	0.190 ± 0.006	5.100 ± 0.019	0.0042 ± 0.0003
10.0	0.389 ± 0.011	11.300 ± 0.056	0.009 ± 0.0006

Table 4.16 Initial ratio, v_i, for the microsomal oxidation of N-methylcaprolactam.

While for N-methyl-2-piperidinone and N-methylcaprolactam the formation of

the norimide metabolite occurs only through one route, namely N-demethylation of the N-methylimide, for N-methyl-2-pyrrolidinone two metabolic routes are possible. Thus, the kinetic parameters for the formation of succinimide from N-methylsuccinimide and 2-pyrrolidinone were also determined. Table 4.17 reports the values so obtained.

	v_i of formation of Succinimide (mM/h/nmol P450)		
[Substrate] (mM)	**From N-methyl succinimide**	**From 2-pyrrolidinone**	**Rate ratio**
0.05	0.35 ± 0.021	0.066 ± 0.008	5.36
0.5	3.41 ± 0.260	0.66 ± 0.03	5.23
1.0	6.70 ± 0.360	1.31 ± 0.23	5.11
3.0	18.02 ± 0.940	3.82 ± 0.56	4.70
5.0	27.21 ± 1.320	6.20 ± 0.85	4.39
10.0	44.06 ± 2.356	11.62 ± 0.94	2.79

Table 4.17 Initial rates, v_i, for succinimide formation in the microsomal oxidation of N-methylsuccinimide and 2-pyrrolidinone.

The v_i values were used to determine the kinetic parameters V_{max}, K_m and V_{max}/K_m for the microsomal oxidations, and these are reported in Table 4.18. As for the corresponding biomimetic reactions, the values are corrected for the known routes of formation of the norimide and expressed as ring oxidation and N-demethylation. Again, the kinetic parameters were calculated using the Hanes plot.

Compound	N-demethylation (Z- oxidation)	Ring oxidation (E- oxidation)	Z-/E-
N-methyl-2-pyrrolidinone	V_{max}: 57.37 ± 3.21 (mM/h/nmol P450) K_m: 0.029 ± 0.005 (mM^{-1}) V_{max}/K_m: 1999	V_{max}: 61.35 ± 2.36 (mM/h/nmol P450) K_m: 0.025 ± 0.003 (mM^{-1}) V_{max}/K_m: 2399	V_{max}: 0.93 V_{max}/K_m: 0.83
N-methyl-2-piperidinone	V_{max}: 18.36 ± 1.56 (mM/h/nmol P450) K_m: 0.0077 ± 0.0005 (mM^{-1}) V_{max}/K_m: 2436	Vmax: 2.36 ± 0.160 (mM/h/nmol P450) Km: 0.0185 ± 0.003 (mM^{-1}) V_{max}/K_m: 127	V_{max}: 7.78 V_{max}/K_m: 19.2
N-methyl caprolactam	V_{max}: 40.05 ± 3.12 (mM/h/nmol P450) K_m: 0.035 ± 0.006 (mM^{-1}) V_{max}/K_m: 1140	V_{max}: 1.71 ± 0.240 (mM/h/nmol P450) K_m: 0.040 ± 0.008 (mM^{-1}) V_{max}/K_m: 42.8	V_{max}: 23.45 V_{max}/K_m: 26.82

Table 4.18 Kinetic parameters calculated for the microsomal oxidation of N-methyl-2-pyrrolidinone, N-methyl-2-piperidinone and N-methylcaprolactam.

The results indicate that a regioselectivity for the Z- *versus* the E- alkyl group is present in the microsomal-dependent metabolism of these cyclic amides. In fact, in contrast to biomimetic oxidation microsomal metabolism of N-methyl 2 pyrrolidinone displays a minor preference for the E- carbon with respect to the Z-. For the other two substrates the Z- carbon atom is the preferred site of P450 metabolism, representing a total reversal of theoretical calculations and the observations from the biomimetic model. There appears to be relationship between the size of the ring and the preference for the Z-carbon, in contrast to the chemical model oxidations or semi-empirical AM1 calculations.

4.5 Conclusions

The results reported here demonstrate that all these substrates undergo biomimetic and microsomal oxidation with the production of two primary metabolites, due to the oxidation of the E- and Z- carbons, and a secondary metabolite formed by the subsequent oxidation of one or both of the primary metabolites. A major difference between the substrate employed is that for the 5-membered ring substrate N-methyl-2-pyrrolidinone, the formation of the norimide secondary metabolite arises from the oxidation of both primary metabolites, whilst the corresponding secondary metabolite from the 6-and 7-membered ring substrates arises only from the oxidation of the N-demethylated primary intermediate.

An interesting difference for the microsomal metabolism of N-methyl-2-pyrrolidinone is also found between the presents results and those reported by Akesson and Jonson.[13] These authors have reported the formation of the 3-hydroxy-N-methylsuccinimide metabolite that was not found in the present study, while the N-demethylation product 2-pyrrolidinone found in this study was not reported.[14; 15] Metabolism of N-methyl-2-pyrrolidinone studied *in vivo* is believed to lead to the formation of the main metabolite, 5-hydroxy-N-methyl-2-pyrrolidinone that is subsequently transformed into N-methylsuccinimide and 3-hydroxy-N-methylsuccinimide.[13] The present results, obtained *in vitro*, suggest a quite different mechanism of oxidation. However, in the *in vivo* study of this compound, not all of the metabolites were identified, and 33 % of the administered dose of ^{13}C N-methyl-2-pyrrolidinone was not recovered.[13] Other reports indicate *in vivo* formation of CO_2 *via* and unidentified metabolic pathway.[14] Thus, it is conceivable that *in vivo,* the N-demethylation of N-methyl-2-pyrrolidinone occurs through the formation of a carbinolamide that can, as is well known,[11] degrade to formaldehyde and subsequently CO_2.

Comparison of the analysis of the results obtained for the oxidation of these

three cyclic amides by the three different systems employed in this study reveals some interesting observations. The energetically favoured hydrogen atom abstraction is from the E- (ring) carbon. This predicted oxidation pattern is followed by the biomimetic system whereas it is completely reversed by the microsomal system (Table 4.19).

	Ring oxidation / N-demethylation			Microsomal Z-selectivity
Compound	**M.O. Calculation**	**Biomimetic System**	**Microsomes**	
N-methyl-2-pyrrolidinone	**11.9**	**10.9**	**1.2**	**9.08**
N-methyl -2-piperidinone	**16416**	**5620**	**5620**	**$1.1 \cdot 10^5$**
N-methyl caprolactam	**86.5**	**80.4**	**0.037**	**$2.17 \cdot 10^3$**

Table 4.19 Ratios of the E- (ring) *versus* Z- (N-methyl) oxidation obtained for the oxidations of N-methyl-2-pyrrolidinone, N-methyl-2-piperidinone and N-methylcaprolactam.

For microsomal system oxidations apparently there is no regioselectivity for the metabolism of the E- or Z- alkyl groups in the five membered ring system, whereas there is a marked increase in regioselectivity for the metabolism on the Z- carbon (N-demethylation) with increasing size of the ring. However, for each compound comparison of the results from the biomimetic and microsomal reactions reveals that for all ring systems the microsomal reaction exhibits a marked preference for the Z- alkyl group.

Regioselectivity in P450-dependent reactions has been reported.[3;4;5] An interesting case is the metabolism of tertiary amines such as N-methyl-N,N-diisopropylamine.[6] The aminium cation radical formed during the metabolism of this

amine loses hydrogen exclusively from the N-methyl group. The regioselectivity of this reaction is postulated to be governed by steric factors, which restrict overlap of the p-orbital on the developing methine carbon radical of the N-isopropyl groups with the half-empty π-orbital of the planar aminium radical. Regioselectivity of the P450-dependent metabolism of nicotine has been ascribed to the effects of the enzyme pockets.[5] Iley and Constantino [16] observed that in the microsomal-dependent metabolism of N-methyl-N-isopropylbenzamide N-demethylation is the preferred reaction despite being less favoured from a thermodynamic point of view.[16]

A possible explanation of the results obtained in the present study could be that, in the microsomal oxidation of the three cyclic amides binding of the substrate to the active site of the enzyme occurs in such a way that the Z- N-methyl group is directed toward the haem plane. This would make the hydrogen atom more available for abstraction in a rate-limiting step of the reaction. The steric bulk of the substrate definitely seems to play an important role. Indeed, N-methylcaprolactam is the substrate with the bigger dimension and also the compound that shows the major Z- regiopreference. Certainly, the marked differences between the biomimetic and microsomal results point to a central role for the protein in the way the substrate is exposed to the haem. It is possible that these substrate-enzyme interactions are due to a hydrophobic pocket in the active site relatively close to the haem plane.

4.6 References

1 Groves J.T., McClusky G.A., White R.E. and Coon M.J., (1978) *Biochem. Biophys. Res. Commun.*; **81**: 154-

2 Gelly M.H., Heinbrook D.C., Malkonen P. and Sligar S.G., (1982), *Biochemistry*, **21**: 370-

3 McClanahan R.H., Huitric A.C., Pearson P.G., Desper J.C. and Nelson S.D., (1988); *J. Am. Chem. Soc.*, **110**: 1979-

4 Wood A., Ryan D.E., Thomas P.E. and Levin W., (1993), *J. Biol. Chem.*, **258**, 14: 8939-

5 Peterson L.A., Trevor A. and Castagnoli N. Jr., (1987), *J. Med. Chem.*, **30**: 249-

6 Lewis F.D. and Ho I., (1980), *J. Am. Chem. Soc.*, **102**: 1751-

7 Constantino L., Rosa E. and Iley J., (1992), *Biochem. Pharmacol.*, **44**, 4: 65-

8 Hall L.R. and Hanzlick R.P., (1990), *J. Biol. Chem.*, **265**, 21: 12349-

9 Bean J.W. and Nelson D.J., (1984), *Biochem. Pharmacol.*, **33**: 2145-

10 Poulos T.L., Finzel B.C., Gunsalus I.C., Wagner G.C. and Kraut J., (1985), *J. Biol. Chem.*, **260**: 16122-

11 Ross D., Farmer P.B., Gescher A., Hickman J.A. and Threadgill M.D., (1983); *Biochem Pharmacol.* **32**: 1773-

12 Mansuy D., Battioni P. and Battioni J.P., (1989); *Eur. J. Biochem.*; **20**: 124-

13 Åkesson B. and Jönsson B.A.G., (1997); *Drug Metabol. Dispos.*; **25**: 267-

14 Wells D.A. and Digenis G.A., (1988); *Drug Metabol. Dispos.*; **16**: 243-

15 Wells D.A., Hawi A.A. and Digenis G.A.; (1992); *Drug Metabol. Dispos.*; **20**: 124-

16 Iley J. and Constantino L., (1994); *Biochem. Pharmacol.*; **47**: 275-.

CHAPTER 5

Stereoselectivity in the oxidation of tertiary amides

The present chapter will describes the studies related to the stereoselectivity of the oxidation of tertiary amides using the following models:

- semi-empirical AM1 molecular orbital calculations,
- P450 biomimetic system,
- rat liver microsomes.

5.1 Introduction

P450 enzymes exhibit stereoselectivity in a wide range of oxidation reactions. The oxidation of π-bonded systems (olefins, acetylene and arenes) presents a marked enantioselectivity on depending of the P450 isoenzymes involved. For example polycyclic aromatic epoxides are produced with high enantioselectivity.[1; 2; 3] P450 is involved in the metabolism of arachidonic acid to a variety of oxygenated metabolites including epoxides and fatty acid alcohols,[4; 5] different isoforms are reported to play a key role in the control of the stereoselectivity of the epoxidation.[6; 7; 8]

The P450-dependent oxidation of sulfur-containing compounds is also a very common asymmetric transformation performed by these enzymes.[9] In the oxidation of cyclic and acyclic sulfides catalysed by phenobarbital-induced rabbit liver P450 both the enantioselectivity and diastereoselectivity were modest.[10; 11] A preference for the R sulfoxidation product was observed in most cases, and in the presence of an electron withdrawing group oxidation at the methylene carbon occurred along with sulfoxidation leading to S-dealkylation.[10; 11]

Analysis of the P450-dependent metabolism of the amine nicotine indicated that phenobarbital-induced rat liver P450 presents a slightly but consistently lower metabolism

The potential metabolic pathway for the oxidation of R(+)- and S(-)- N-methyl-N-(1-phenylethyl)benzamide is shown in Figure 5.3. N-Dealkylation would be expected be the more favoured route of oxidation, as to the presence of the benzylic ring enhances hydrogen atom abstraction by stabilising the carbon-centred radical intermediate through delocalisation.

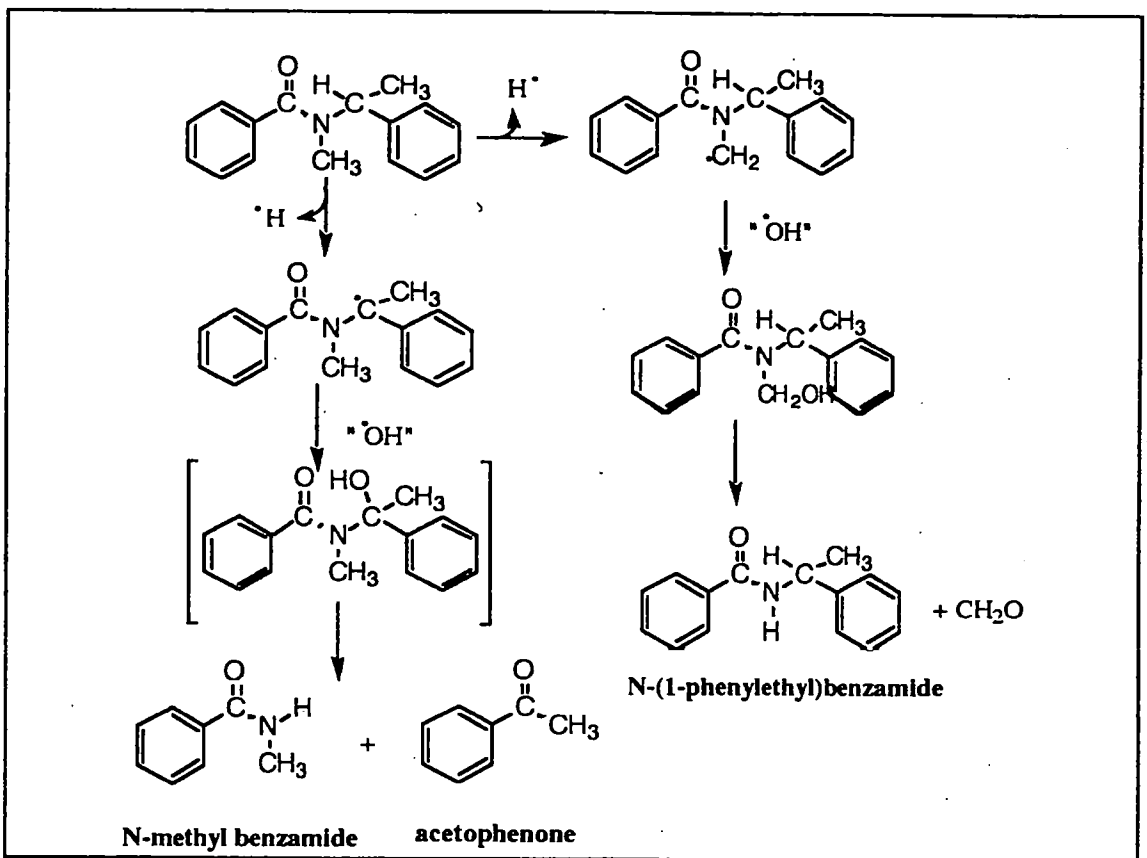

Figure 5.3. Proposed pathway for the oxidation of N-methyl-N-(1-phenylethyl)benzamide

The potential pathway for oxidation of R- and S- N-methyl-5-phenyl-2-pyrrolidinone is presented in Figure 5.4. This substrate is a structural analogue of the main nicotine metabolite, cotinine, the difference being that in cotinine the aryl ring is 3'-pyridyl rather than phenyl. Thus, the proposed pathway is based on the metabolism of cotinine,[19;-22] assuming that the different aryl rings do not elicit major metabolic differences. Thus, oxidation of N-methyl-5-phenyl-2-pyrrolidinone, is expected to involve either N-demethylation or N-dealkylation leading to the formation of products **2**

and 3, respectively. These could undergo further oxidation to give the product 4. From the results obtained for N-methyl-2-pyrrolidinone (Chapter 4) formation of 4 is likely to arise from both oxidation routes.

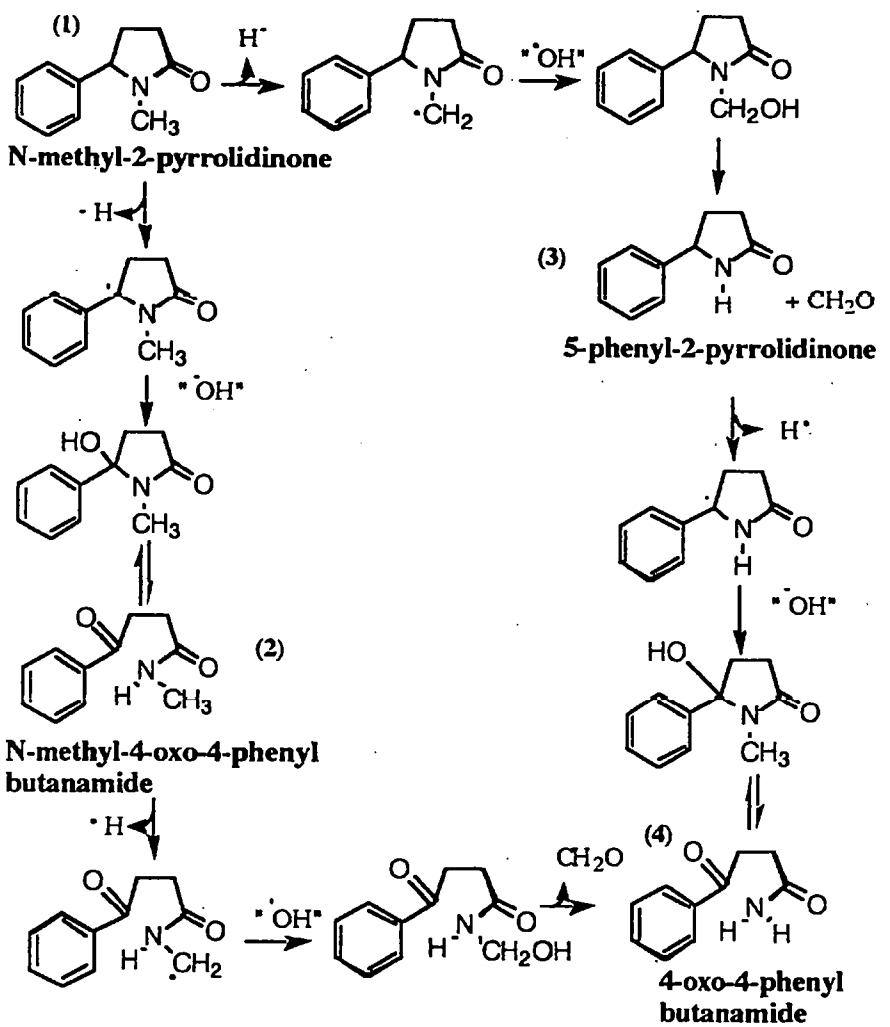

Figure 5.4 Potential pathway for the oxidation of N-methyl-5-phenyl-2-pyrrolidinone.

The strategy adopted in this study followed that employed for the investigation of regioselectivity illustrated in Chapter 4. Namely, three models were used; AM1 semi-empirical self-consistent field calculations, a biomimetic system and phenobarbital-induced rat liver microsomal P450. From the AM1 calculations, a reaction model based on energetic considerations is made. This is subsequently tested using the biomimetic

system. Finally, microsomal metabolism of the substrate probes was analysed. The results from these three models were compared to clarify the main structural features of these reactions.

5.2 AM1 Molecular orbital calculations

Assuming oxidation of the substrates occurs *via* hydrogen atom abstraction from the α-carbon, the reaction involves formation of a carbon-centred radical. Semi-empirical AM1 calculations were then made for the substrates and their carbon-centred radicals intermediates. Tables 5.1 and 5.2 report the results of the AM1 calculations for R(+)- and S(-)-N-methyl-N-(1-phenylethyl)benzamide, R- and S-N-methyl-5-phenyl-2-pyrrolidinone and their carbon centred intermediates, respectively. The enthalpies obtained allow a pathway for the oxidation to be predicted.

Compound	ΔH_f (kJ/mol)
S(-)-N-methyl-N-(1-phenylethyl)benzamide	**85.11**
R(+)-N-methyl-N-(1-phenylethyl)benzamide	**85.08**
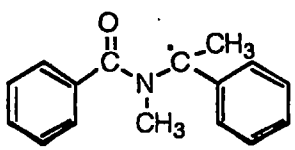	**151.10**
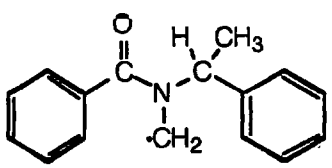	**180.04**

Table 5.1 ΔH_f values calculated by AM1 for R(+)- and S(-)-N-methyl-N-(1-phenylethyl)benzamide and their corresponding radicals.

Compound	ΔH_f (kJ/mol)
R-N-methyl-5-phenyl-2-pyrrolidinone	- 42.76
S-N-methyl-5-phenyl-2-pyrrolidinone	- 42.79
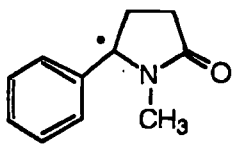	11.71
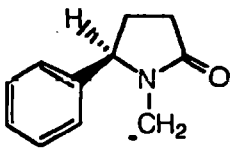	56.93
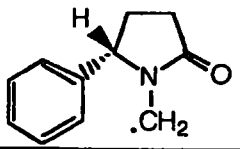	56.95

Table 5.2 ΔH_f values calculated by AM1 for R- and S-N-methyl-5-phenyl-2-pyrrolidinone and their corresponding radicals.

As expected, no energetic differences are observed between the two enantiomers of either compound or their corresponding radicals. Thus implies that from a chemical viewpoint, there is no inherent preference for the oxidation of the R- or S- stereoisomers. However, there is a clear preference for formation of the N-alkyl centred-carbon centred radical compared with the N-methyl carbon centred radical. The ratio of the rate constants of these two potential reaction can be estimated from the differences between the ΔH_f values of the radicals and the amide substrates. These ratios are given in Table 5.3.

Compound	N-dealkylation/N-demethylation
R(+)-	110139
S(-)-	110150

Table 5.3 Ratio of N-dealkylation *versus* N-demethylation estimated from the ΔH_f values for in Table 5.2.

Given that 4-oxo-4-phenylbutanamide can arise from oxidation of either 5-phenyl-2-pyrrolidinone or N-methyl-4-oxo-4-phenylbutanamide, the ΔH_f values of these substrates and their postulated carbon-centred radicals intermediates were also calculated (Table 5.4). Clearly, ring oxidation is the less energy-demanding process.

Compound	ΔH_f (kJ/mol)
5-phenyl-2-pyrrolidinone	**- 65.79**
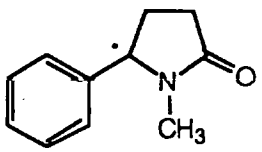	**- 4.91**
N-methyl-4-oxo-4-phenylbutanamide	**- 57.18**
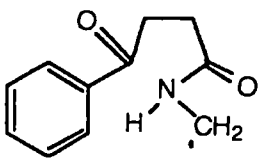	**19.82**

Table 5.4 ΔH_f values calculated by AM1 for 5-phenyl-2-pyrrolidinone, N-methyl-4-oxo-phenylbutanamide and their postulated intermediates.

5.3 Biomimetic oxidation

• Identification of the products from R(+)- and S(-)-N-methyl-N-(1-phenylethyl)benzamide

Model oxidation of the amides by $TPPFe^{(III)}$/ *ter*-butylhydroperoxide was followed by treatment of the samples with 1M sodium hydroxide in methanol (to completely hydrolyse any labile carbinolamide products)[23; 24] and analysis using HPLC.

Figure 5.5 displays a the typical HPLC profile. The compounds corresponding to the new peaks were identified by comparison of their retention time and UV spectra with those of synthetic standards (Table 5.5).

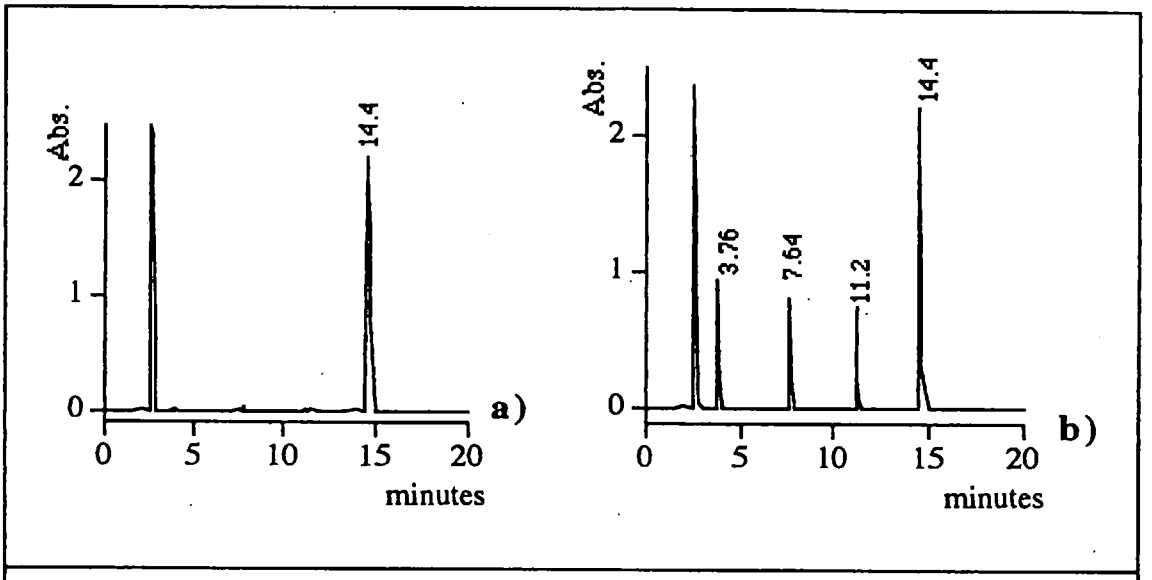

Figure 5.5 HPLC of the reaction mixture from biomimetic system oxidation of a 5 mM solution of R(+)-N-methyl-N-(1-phenylethyl) benzamide after a) 0 and b) 60 minutes.

Peak found	Compound identified
14.4 minutes	**N-methyl-N-(1-phenylethyl)benzamide**
11.3 minutes	**N-(1-phenylethyl)benzamide**
7.6 minutes	**acetophenone**
3.7 minutes	**N-methylbenzamide**

Table 5.5 Products identified from the oxidation of a 5 mM solution of R(+)-N-methyl-N-(1-phenylethyl)benzamide.

These results indicates that, as predicted, the biomimetic oxidation occurs as illustrated in Figure 5.3 both *via* N-dealkylation and N-demethylation. N-Methylbenzamide and acetophenone arise from the N-dealkylation reaction whereas N-(1-phenylethyl)benzamide arises from the N-demethylation route. To assess the presence of stereoselectivity the kinetic characteristics of the reactions were examined.

• Kinetic of the biomimetic oxidation of R(+)- and S(-)-N-methyl-N-(1-phenylethyl)benzamide

The time-course, over a period of 2 hours, for the biomimetic oxidation of 5 mM solution of N-methyl-(1-phenylethyl)benzamide is illustrated in Figure 5.6. The rather emphatic "tailing-off" in the reaction progress is almost certainly due to side reactions such as catalyst auto-oxidation and solvent oxidation.

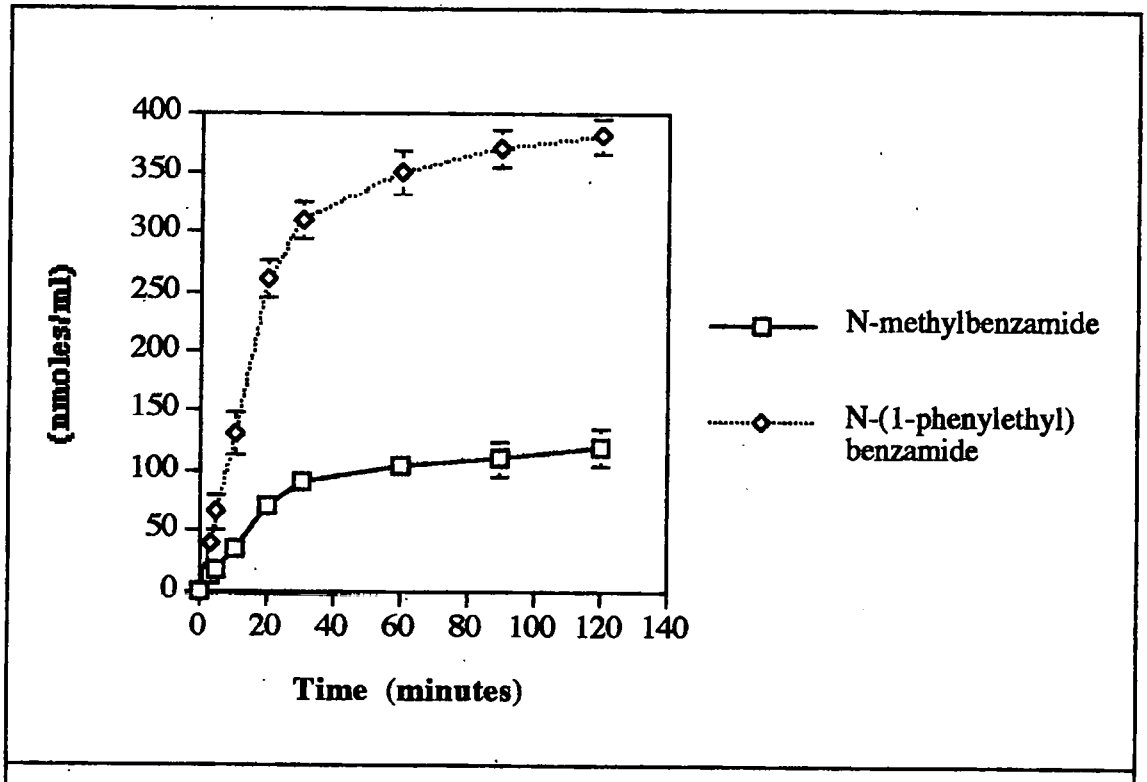

Figure 5.6 Time-course of the biomimetic oxidation of 5 mM R(+)-N-methyl-N-(1-phenylethyl)benzamide.

However, the reaction displays a linear phase within the first 20 minutes. Thus, the time chosen for the determination of the rate of formation of the oxidation products was 15 minutes, which is a convenient reaction time that permits the production of an accurate analytically determinable amount of products.

The initial rates of the biomimetic oxidation of R(+)- and S(-)-N-methyl-N-(1-phenylethyl)benzamide, measured using substrate concentrations between 0.5 and 10.0 mM are contained in Table 5.6.

[Substrate] (mM)	v_i (μM/h/mmol catalyst) N-(1-phenylethyl) benzamide	N-methyl benzamide	acetophenone
R(+)- 0.5	82.10 ± 6.1	220.67 ± 12.9	214.4 ± 10.2
R(+)- 1.0	125.47 ± 9.6	387.25 ± 19.0	390.6 ± 16.3
R(+)- 2.0	170.51 ± 11.8	622.05 ± 33.5	616.5 ± 28.0
R(+)- 3.0	193.68 ± 14.3	779.60 ± 28.1	781.5 ± 33.4
R(+)- 5.0	217.32 ± 15.2	977.72 ± 36.1	974.6 ± 15.5
R(+)- 10.0	237.5 ± 18.1	1207.95 ± 46.8	1215.3 ± 69.8
S(-)- 0.5	79.30 ± 4.1	210.74 ± 13.5	216.6 ± 11.9
S(-)- 1.0	129.03 ± 19.0	396.51 ± 29.3	400.0 ± 18.5
S(-)- 2.0	167.80 ± 26.5	608.12 ± 26.9	610.5 ± 37.1
S(-)- 3.0	199.73 ± 26.9	771.90 ± 15.0	780.4 ± 28.9
S(-)- 5.0	209.90 ± 35.6	984.65 ± 36.1	988.4 ± 35.5
S(-)- 10.0	240.70 ± 15.2	1213.11 ± 51.0	1201.7 ± 80.0

Table 5.6 Initial rates, v_i, of the biomimetic oxidation of R(+)- and S(-)-N-methyl-N-(1-phenylethyl)benzamide.

The plot of v_i *versus* substrate concentration, illustrated in Figure 5.7, obtained using the data in Table 5.6, is curved and can be rationalised in terms of saturating "enzyme-type" catalysis. Analysis of the data using the Michaelis-Menten method yields the kinetic parameters V_{max}, K_m and V_{max}/K_m reported in Table 5.7. The data in Table 5.6 and Table 5.7 reveal that the rates of formation of N-methylbenzamide and acetophenone are equivalent given that they are the products of the same dealkylation reaction.

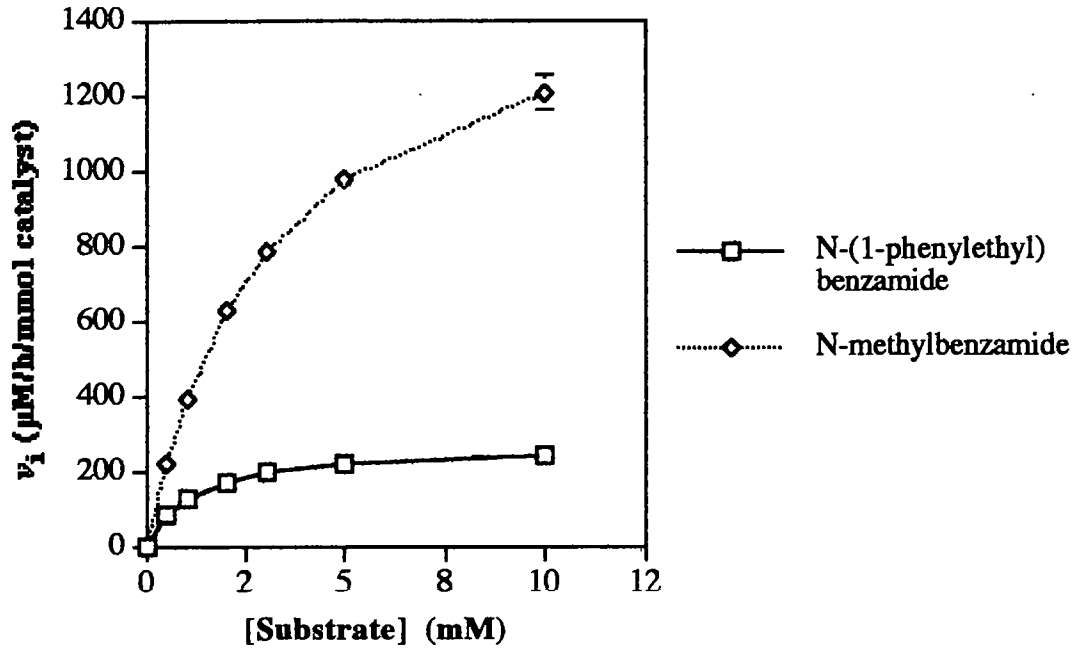

Figure 5.7 Plot of the initial rate, v_i, *versus* [substrate] for the biomimetic oxidation of R(+)-N-methyl-N-(1-phenylethyl)benzamide.

SUBSTRATE	N-demethylation	N-dealkylation
R(+)-	**V_{max}: 266 ± 8** (µM/h/mmol catalyst) **K_m: 1.12 ± 0.14** (mM) **V_{max}/K_m: 237**	**V_{max}: 1580 ± 30** (µM/h/mmol catalyst) **K_m: 3.08 ± 0.45** (mM) **V_{max}/K_m: 512**
S(-)-	**V_{max}: 261 ± 11** (µM/h/mmol catalyst) **K_m: 1.14 ± 0.18** (mM) **V_{max}/K_m: 228**	**Vmax: 1595 ± 46** (µM/h/mmol catalyst) **K_m: 3.14 ± 0.31** (mM) **V_{max}/K_m: 507**

Table 5.7 Kinetic parameters for the biomimetic oxidation of R(+)- and S(-)-N-methyl-N-(1-phenylethyl)benzamide.

The calculate kinetic parameters are essentially identical for both dealkylation and demethylation of the two amides isomers. Though dealkylation is the favoured reaction, the ratios of N-dealkylation /N-demethylation (Table 5.8) markedly differ from

those calculated by AM1. The most likely reason for this is the presence of a bulky N-alkyl group that can protect the hydrogen.

Substrate	N-dealkylation/N-demethylation
R(+)-	2.16
S(-)-	2.22

Table 5.8 Ratio of N-dealkylation to N-demethylation in the biomimetic oxidation of N-methyl-N-(1-phenylethyl)benzamide.

- **Identification of the products from R- and S- N-methyl-5-phenyl-2-pyrrolidinone**

Figure 5.8 is a typical HPLC trace, obtained from the oxidation of S- isomer (the HPLC profile obtained from the oxidation of the R- isomer was essentially identical). The products of the reaction were identified by comparison of their retention time and UV spectra with that of synthetic standard. The products obtained from these biomimetic oxidations are illustrated in Table 5.9.

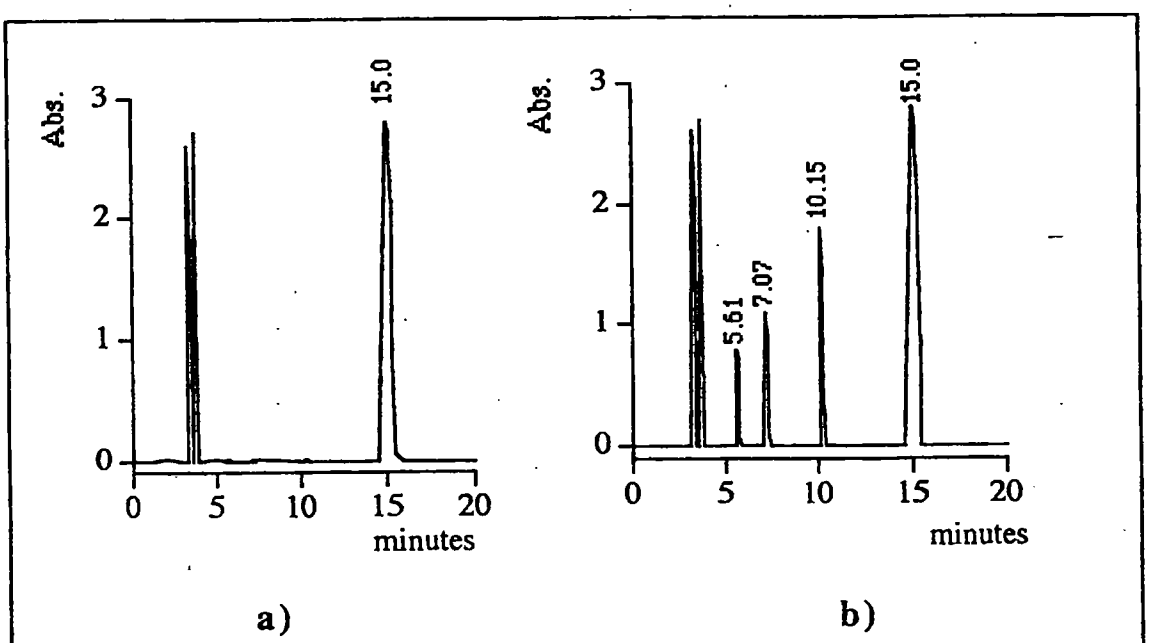

Figure 5.8 HPLC of the products of biomimetic oxidation of 5 mM N-methyl-5-phenyl-2-pyrrolidinone, after a) 0 and b) 1 hour.

Peak	Compound Identified
15.0 minutes	N-methyl-5-phenyl-2-pyrrolidinone
10.1 minutes	5-Phenyl-2-pyrrolidinone
7.1 minutes	N-methyl-4-oxo-4-phenylbutanamide
5.6 minutes	4-oxo-4-phenylbutanamide

Table 5.9 Products identified from the biomimetic oxidation of R- and S- N-methyl-5-phenyl-2-pyrrolidinone.

The products are consistent with the pathway illustrated in Figure 5.4; no other products were identified under any condition. The 4-oxo-4-phenylbutanamide product can arise from two pathways. To clarify which of these is most important, the biomimetic oxidation of 5 mM 5-phenyl-2-pyrrolidinone and N-methyl-4-oxo-4-phenylbutanamide was also studied. Figure 5.9 illustrates typical HPLC chromatograms from biomimetic oxidation of these compounds after 60 minutes. Table 5.10 lists the products identified. It is evident that both primary products undergo further oxidation to 4-oxo-4-phenylbutanamide.

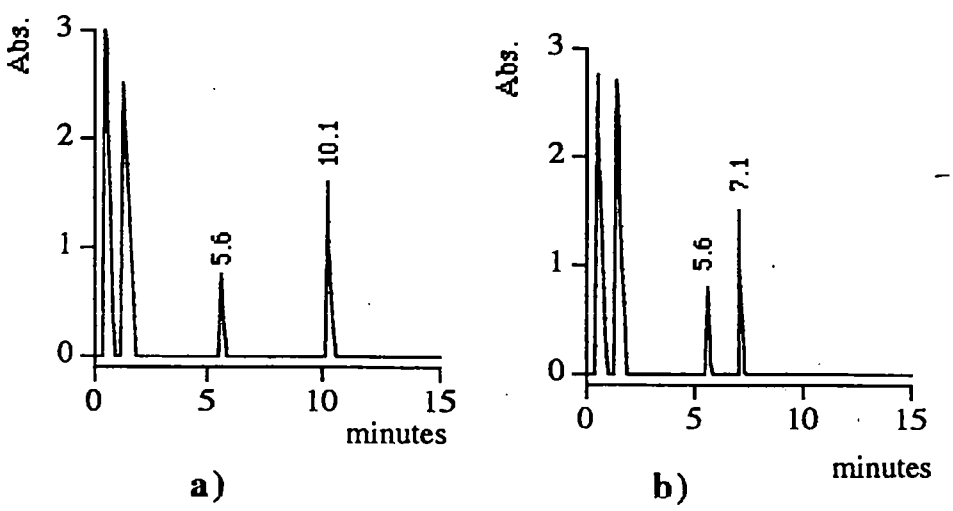

Figure 5.9 HPLC analysis of the biomimetic oxidation of a) 5 mM 5-phenyl-2-pyrrolidinone and b) N-methyl-4-oxo-4-phenylbutanamide, after 60 minutes.

Peak	Compound Identified
Chromatogram a) 10.1 minutes	5-phenyl-2-pyrrolidinone
Chromatogram a) 5.6 minutes	4-oxo-phenylbutanamide
Chromatogram b) 7.1 minutes	N-methyl-4-oxo-4-phenylbutanamide
Chromatogram b) 5.6 minutes	4-oxo-4-phenylbutanamide

Table 5.11 Products identified from the biomimetic oxidation of 5-phenyl-2-pyrrolidinone and N-methyl-4-oxo-4-phenylbutanamide.

- **Kinetic of the biomimetic oxidation of R- and S- N-methyl-5-phenyl-2-pyrrolidinone**

The time-course of the biomimetic oxidation of 5 mM N-methyl-5-phenyl-2-pyrrolidinone was monitored over two hours. The results obtained, Figure 5.10, displays an initial linear phase over the first 20 minutes, follows by a decrease of the reaction rate ascribed to catalyst auto-oxidation. Initial rates were determined after 20 minutes.

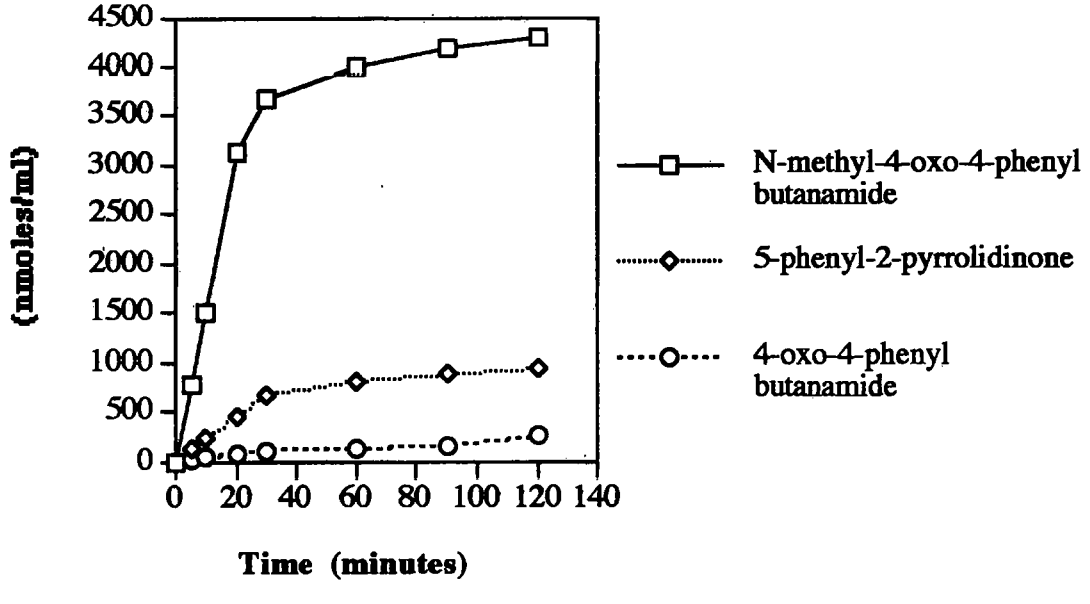

Figure 5.10 Time-course of the biomimetic oxidation of R- 5 mM N-methyl-5-phenyl-2-pyrrolidinone.

The initial rates determined using substrate concentrations between 0.5 and 10.0 mM, are detailed in Table 5.11. Clearly there is no stereoselectivity in the biomimetic oxidation of this substrate.

To evaluate the kinetic parameters for these oxidations, the initial rates for oxidation of N-methyl-4-oxo-4-phenylbutanamide and 5-phenyl-2-pyrrolidinone were determined (Table 5.12. Significantly, formation of 4-oxo-4-phenylbutanamide from 5-phenyl-2-pyrrolidinone is the preferred reaction, consistent with the MO calculations (Table 5.4).

	v_i (mM/h/mmol catalyst)		
[Substrate] (mM)	**5-phenyl-2-pyrrolidinone**	**N-methyl-4-oxo-4-phenylbutanamide**	**4-oxo-4-phenylbutanamide**
R- 0.5	0.98 ± 0.009	2.78± 0.10	0.03 ± 0.001
R- 1.0	1.84 ± 0.09	4.96 ± 0.30	0.05 ± 0.002
R- 2.0	3.28 ± 0.16	8.16 ± 0.35	0.10 ± 0.004
R- 3.0	4.43 ± 0.35	10.40 ± 0.61	0.17 ± 0.004
R- 5.0	6.16 ± 0.70	13.34 ± 1.10	0.23 ± 0.010
R- 10.0	8.70 ± 0.86	16.91 ± 1.18	0.402 ± 0.02
S- 0.5	0.96 ± 0.07	2.74 ± 0.11	0.03 ± 0.001
S- 1.0	1.81 ± 0.11	4.89 ± 0.21	0.05 ± 0.002
S- 2.0	3.23 ± 0.18	8.03 ± 1.05	0.10 ± 0.030
S- 3.0	4.38 ± 0.31	10.23 ± 1.09	0.14 ± 0.020
S- 5.0	6.11 ± 0.51	13.08 ± 1.11	0.23 ± 0.04
S- 10.0	8.68 ± 0.32	16.5 ± 1.23	0.39 ± 0.05

Table 5.11. Initial rates, v_i, of the biomimetic oxidation of R- and S-N-methyl-5-phenyl-2-pyrrolidinone.

[Substrate] (mM)	v_i (mM/h/mmol catalyst) 5-phenyl-2-pyrrolidinone	N-methyl-4-oxo-phenylbutanamide	Ratio
0.5	2.76 ± 0.11	0.06 ± 0.009	46.0
1.0	4.27 ± 0.21	0.12 ± 0.010	35.6
2.0	5.87 ± 0.20	0.22 ± 0.020	26.7
3.0	6.71 ± 0.42	0.31 ± 0.010	21.6
5.0	7.58 ± 0.33	0.47 ± 0.030	16.1
10.0	8.39 ± 0.36	0.76 ± 0.022	11.0

Table 5.12 Initial rates, v_i, for the formation of 4-oxo-4-phenylbutanamide from the biomimetic-dependent oxidation of N-methyl-4-oxo-4-phenylbutanamide and 5-phenyl-2-pyrrolidinone.

The kinetic parameters for the oxidation of R- and S-N-methyl-5-phenyl-2-pyrrolidinone (Table 5.13) were calculated from the data of Table 5.12 by partitioning the formation of 4-oxo-4-phenylbutanamide in a ratio of 26/1 from 5-phenyl-2-pyrrolidinone and N-methyl-4-oxo-4-phenylbutanamide.

Substrate	N-demethylation	Ring oxidation
R-	**V_{max}: 15.2 ± 1.5** (μM/Hr/mmol. cat) **K_m: 6.84 ± 0.52** (μM) **V_{max}/K_m: 2.22**	**V_{max}: 23.1 ± 2.8** (μM/Hr/mmol. cat) **K_m:3.66 ± 0.32** (μM) **V_{max}/K_m: 6.31**
S-	**V_{max}: 15.3 ± 1.2** (μM/Hr/mmol. cat) **K_m: 7.08 ± 0.33** (μM) **V_{max}/K_m: 2.16**	**V_{max}: 22.7 ± 1.12** (μM/Hr/mmol. cat) **K_m: 3.60 ± 0.28** (μM) **V_{max}/K_m: 6.30**

Table 5.13. Kinetic parameters for the biomimetic oxidation of R- and S-N-methyl-5-phenyl-2-pyrrolidinone.

The results show preferential ring oxidation, as predicted from the semi-empirical AM1 calculations. However, 3 to 1 ratio for ring oxidation *versus* N-demethylation (Table 5.14), is significantly smaller of that predicted by the semi-empirical

calculations. As observed for the N-methyl-N-(1-phenylethyl)benzamides the steric bulk of the N-alkyl substituent must mask the large energetic preference for dealkylation.

Substrate	Ring oxidation/N-demethylation
R-	2.82
S-	2.89

Table 5.14 Ratios of N-demethylation to ring oxidation from the biomimetic oxidation of R- and S- N-methyl-5-phenyl-2-pyrrolidinone.

5.4. Microsomal Oxidation

• Identification of the products from R(+)- and S(-)-N-methyl-N-(1-phenylethyl)benzamide

Microsomal incubations of 5 mM substrates were analysed by HPLC after 60 minutes. Product identification was achieved by comparison of the diode array UV spectra with those of synthetic standards. Qualitatively, the HPLC profiles for the two isomers were similar Figure 5.12 is a typical HPLC chromatogram obtained for the microsomal incubation of 5 mM R(+)-N-methyl-N-(1-phenylethyl)benzamide. Table 5.14 details the compound identified.

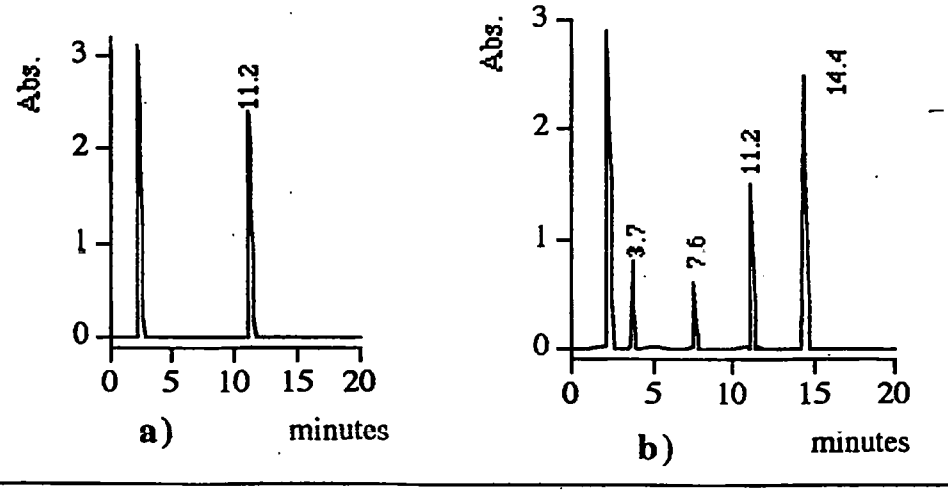

Figure 5.12 HPLC chromatograms of the a) 0 and b) 60, microsomal oxidation of 5 mM R(+)-N-methyl-N-(1-phenylethyl)benzamide after minutes.

Peak	Compound Identified
14.4 minutes	N-methyl-(1-phenylethyl)benzamide
11.2 minutes	N-(1-phenylethyl)benzamide
7.6 minutes	acetophenone
3.7 minutes	N-methylbenzamide

Table 5.14 Compounds identified from the microsomal oxidation of R(+)-N-methyl-N-(1-phenylethyl)benzamide.

The identified products are the only compounds detected in the microsomal metabolism of either isomer under any experimental condition. Microsomal oxidation thus presents a similar pattern of reaction to the biomimetic system.

- **Kinetic of the microsomal oxidation of R(+)- and S(-)-N-methyl-N-(1-phenylethyl)benzamide**

Figure 5.13 illustrates the time-dependent formation of the major metabolite, N-methylbenzamide, from the microsomal oxidation of both isomers. A linear phase is observed over the first 20 minutes. Thus, initial rates were determined after 15 minutes incubation.

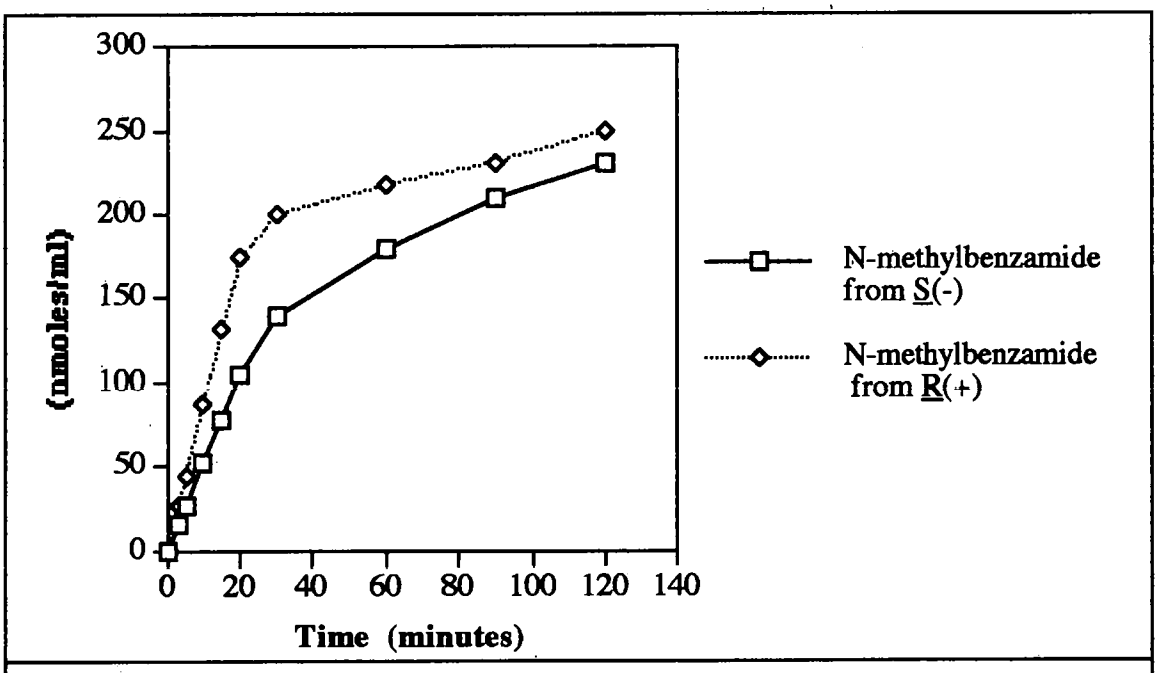

Figure 5.13 Time-course for the formation of N-methylbenzamide during the microsomal oxidation of 5 mM R(+)- and S(-)-N-methyl-N-(1-phenylethyl)benzamide.

The initial rates for the microsomal oxidation of R(+)- and S(-)N-methyl-N-(1-phenylethyl)benzamide were measured using substrate concentrations between 0.5 and 10.0 mM (Table 5.15). The initial rates were used to calculate the kinetic parameters V_{max}, K_m and V_{max}/K_m using the Hanes plot. The results, expressed as N-dealkylation *versus* N-demethylation, are reported in Table 5.16.

	v_i (μM/h/nmol P450)		
[Substrate] (mM)	**N-(1-phenylethyl) benzamide**	**N-methyl benzamide**	**acetophenone**
R(+)- 0.5	51.0 ± 8.5	30.0 ± 1.8	33.0 ± 3.2
R(+)- 1.0	87.5 ± 7.5	52.2 ± 3.2	50.2 ± 3.0
R(+)- 3.0	167.6 ± 8.8	103.8 ± 11.0	105.5 ± 10.0
R(+)- 5.0	205.2 ± 14.0	129.2 ± 11.0	130.6 ± 12.0
R(+)-10.0	246.6 ± 11.0	158.5 ± 21.0	160.0 ± 21.0
S(-)- 0.5	53.2 ± 2.4	15.2 ± 0.8	14.1 ± 0.5
S(-)- 1.0	90.2 ± 3.8	27.5 ± 1.2	29.0 ± 2.0
S(-)- 3.0	168.2 ± 11.0	59.6 ± 3.2	58.0 ± 2.1
S(-)- 5.0	203.3 ± 13.5	77.7 ± 3.5	79.0 ± 5.2
S(-)-10.0	241.0 ± 16.0	100.7 ± 6.5	103.0 ± 8.0

Table 5.15 Initial rates, v_i, for the microsomal oxidation of R(+)- and S(-)-N-methyl-N-(1-phenylethyl)benzamide.

Substrate	**N-demethylation**	**N-dealkylation**
R(+)-	**V_{max}: 309 ± 30** (μM/h/nmol P450) **K_m: 2.53 ± 0.11** (mM) **V_{max}/K_m: 122**	**V_{max}: 205 ± 16** (μM/h/nmol P450) **K_m: 2.93 ± 0.08** (mM) **V_{max}/K_m: 70**
S(-)-	**V_{max}: 296 ± 20** (μM/h/nmol P450) **K_m: 2.28± 0.07** (mM) **V_{max}/K_m: 130**	**V_{max}: 143 ± 21** (μM/h/nmol P450) **K_m: 4.20 ± 0.31** (mM) **V_{max}/K_m: 34**

Table 5.16 Kinetic parameters for the microsomal oxidation of R(+)- and S(-)-N-methyl-N-(1-phenylethyl)benzamide.

The results demonstrate that N-demethylation exhibits no stereoselectivity whereas N-dealkylation displays a slight stereoselective preference (*ca.* 2:1) for R(+)-isomer. Obviously, the ratios of N-demethylation to N-dealkylation for the two isomers (Table 5.17) reflect the observed stereoselectivity.

Substrate	N-demethylation/N-dealkylation
R(+)-	1.74
S(-)-	3.82

Table 5.17 Ratios of N-demethylation to N-dealkylation in the microsomal oxidation of R(+)- and S(-)-N-methyl-(1-phenylethyl)benzamide.

- **Products of the microsomal oxidation of R- and S-N-methyl-5-phenyl-2-pyrrolidinone**

Identification of the products was achieved by comparison of the retention times and UV spectra of each HPLC peak with those obtained from synthetic standards (Table 5.18). A typical HPLC chromatogram obtained from the microsomal oxidation of 5 mM R-N-methyl-5-phenyl-2-pyrrolidinone is shown in Figure 5.14.

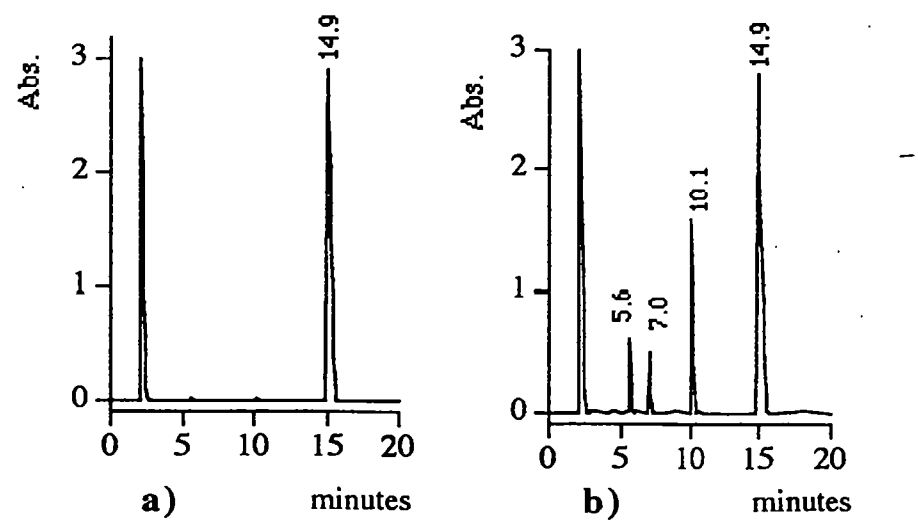

Figure 5.14 HPLC chromatogram of the microsomal oxidation of 5 mM R-N-methyl-5-phenyl-2-pyrrolidinone after a) 0 and b) 60 minutes.

Peak	Compound identified
14.9 minutes	N-methyl-5-phenyl-2-pyrrolidinone
10.1 minutes	5-phenyl-2-pyrrolidinone
7.00 minutes	N-methyl-4-oxo-4-phenylbutanamide
5.6 minutes	4-oxo-4-phenylbutanamide

Table 5.18 Compounds identified from the microsomal oxidation of R-N-methyl-5-phenyl-2-pyrrolidinone.

Since 4-oxo-4-phenylbutanamide is a product of these reactions, the microsomal metabolism of the two primary metabolites 5-phenyl-2-pyrrolidinone and N-methyl-4-oxo-4-phenylbutanamide was studied. Figure 5.15 reports the typical HPLC chromatograms from microsomal oxidation of 5 mM solutions of a) 5-phenyl-2-pyrrolidinone and b) N-methyl-4-oxo-4-phenylbutanamide. The identified products are listed in Table 5.19.

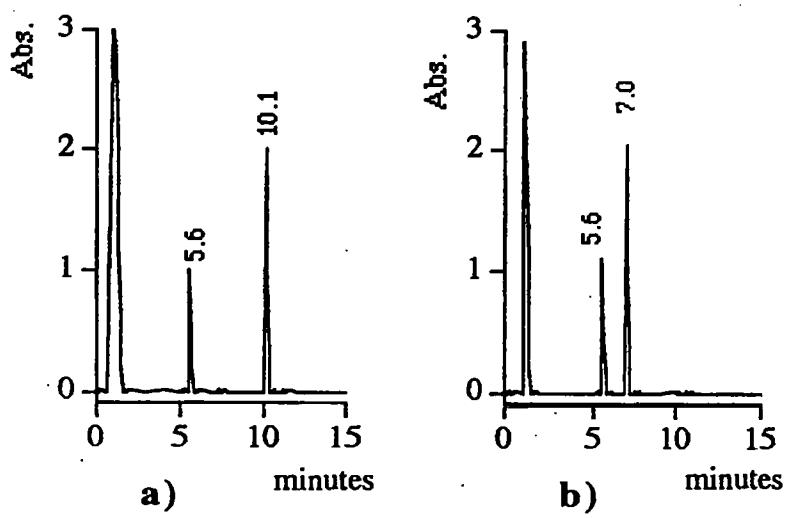

Figure 5.15 HPLC chromatogram of the microsomal oxidation of a) 5-phenyl-2-pyrrolidinone and b) N-methyl-4-oxo-4-phenylbutanamide obtained after 60 minutes.

Peak	Compound identified
Chromatogram a) 10.1 minutes	5-phenyl-2-pyrrolidinone
Chromatogram a) 5.6 minutes	4-oxo-phenylbutanamide
Chromatogram b) 7.0 minutes	N-methyl-4-oxo-4-phenylbutanamide
Chromatogram b) 5.6 minutes	4-oxo-4-phenylbutanamide

Table 5.19 Compounds identified from the microsomal oxidation of 5-phenyl-2-pyrrolidinone and N-methyl-4-oxo-4-phenylbutanamide.

- **Kinetic of the microsomal oxidation of R- and S-N-methyl-5-phenyl-2-pyrrolidinone**

The time-course of the microsomal metabolism of 5 mM solutions of the R- and S- isomers of N-methyl-5-phenyl-2-pyrrolidinone (Figure 5.16) reveals a initial linear phase within the first 15 minutes. Thus, the initial rates of the microsomal oxidation of the two isomers were determined during the first 10 minutes using substrates concentrations between 0.5 and 10.0 mM. The data are contained in Table 5.20.

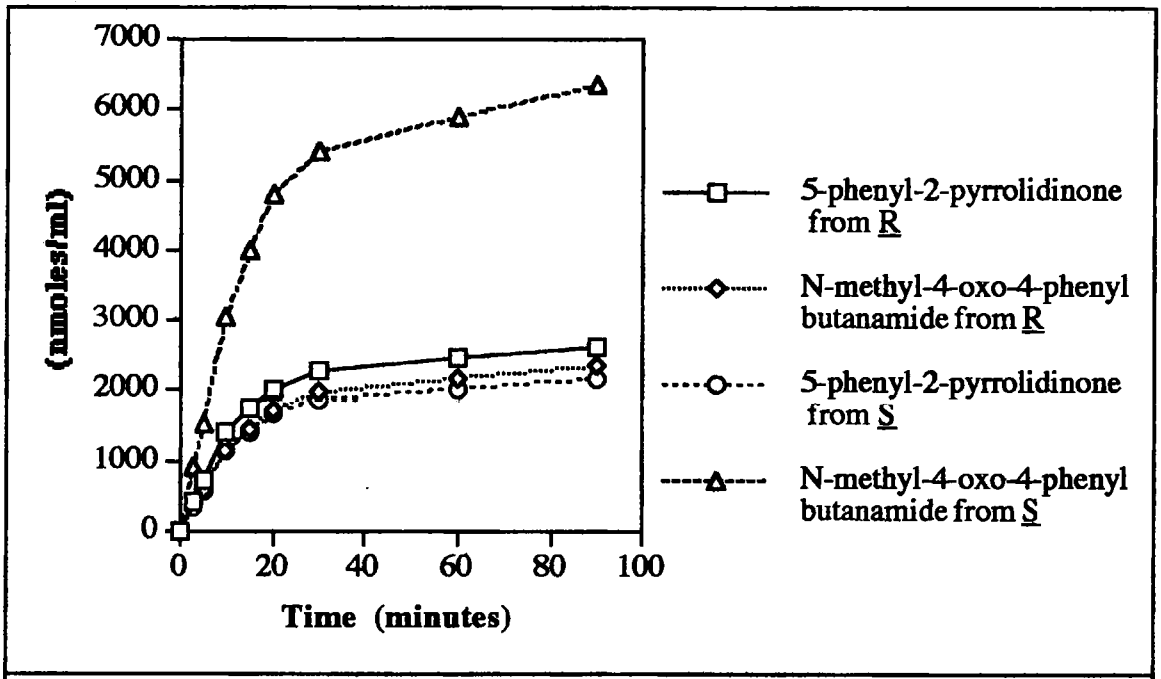

Figure 5.16 Time-course of the microsomal metabolism of R- and S-N-methyl-5-phenyl-2-pyrrolidinone.

Since the formation of the secondary metabolite, 4-oxo-4-phenylbutanamide can arise from both primary products, the initial rates of the microsomal oxidation of N-methyl-4-oxo-4-phenylbutanamide and 5-phenyl-2-pyrrolidinone were also determined (Table 5.21).

	v_i (μM/h/nmol P450)		
[Substrate] (mM)	5-phenyl-2-pyrrolidinone	N-methyl-4-oxo-4-phenylbutanamide	4-oxo-4-phenyl butanamide
R- 0.5	301 ± 12	161 ± 9	97 ± 6
R- 1.0	529 ± 33	313 ± 27	165 ± 11
R- 3.0	1065 ± 23	806 ± 51	300 ± 21
R- 5.0	1334 ± 50	1144 ± 30	357 ± 33
R- 10.0	1648 ± 38	1636 ± 65	414 ± 25
S- 0.5	254 ± 12	598 ± 80	282 ± 12
S- 1.0	541 ± 38	1106 ± 35	426 ± 21
S- 3.0	918 ± 80	2389 ± 55	645 ± 36
S- 5.0	1153 ± 91	3058 ± 65	720 ± 59
S- 10.0	1425 ± 101	3843 ± 85	788 ± 62

Table 5.20 Values of the initial rate of the microsomal oxidation of R- and S-N-methyl-5-phenyl-2-pyrrolidinone.

	v_i (μM/h/nmol P450)		
[Substrate] (mM)	From 5-phenyl-2-pyrrolidinone	From N-methyl-4-oxo-4-phenylbutanamide	Ratio
0.5	15.8 ± 1.2	164 ± 23	10.4
1.0	28.3 ± 1.6	288 ± 31	10.2
5.0	76.6 ± 3.2	736 ± 51	9.6
10.0	97.5 ± 2.6	914 ± 36	9.4

Table 5.21. Initial rates for the of formation of 4-oxo-4-phenylbutanamide from microsomal oxidation of 5-phenyl-2-pyrrolidinone and N-methyl-4-oxo-4-phenylbutanamide.

Clearly 4-oxo-4-phenylbutanamide is formed preferentially from N-methyl-4-oxo-4-phenylbutanamide rather than 5-phenyl-2-pyrrolidinone in a ratio 9.9/1. This is a complete reversal of the selectivity predicted from the M.O. calculations and observed with the biomimetic system. Thus, the rates for initial ring oxidation and N-demethylation were corrected on the basis of these results, allowing calculation of the kinetic parameters of the reaction (Table 5.22). The extent of ring oxidation and N-demethylation is reported in Table 5.23.

The kinetic parameters reveals that there is no stereochemical preference present in the N-demethylation reaction. In contrast, the S-isomer is oxidised in position 5'- approximately 4 times more efficiently. Given that the alkyl group has no effect on demethylation, but that the stereochemistry of the alkyl group affects its own dealkylation, there must be a substrate-enzyme interaction in very close proximity to the haem active site. It is probable that an interaction between the bulky phenyl substituent of the substrate and a hydrophobic pocket of the enzyme active site can account for these observations.

Substrate	N-demethylation	Ring oxidation
R-	**Vmax: 2201 ± 300** (μM/Hr/nmol. P450) **Km: 3.03 ± 0.4** (mM) **Vmax/Km: 726**	**Vmax: 3194 ± 188** (μM/Hr/nmol. P450) **Km: 5.90 ± 0.2** (mM) **Vmax/Km: 540**
S-	**Vmax: 1948 ± 231** (μM/Hr/nmol. P450) **Km: 2.95 ± 0.6** (mM) **Vmax/Km: 662**	**Vmax: 5900 ± 250** (μM/Hr/nmol. P450) **Km: 2.96 ± 0.3** (mM) **Vmax/Km: 1990**

Table 5.21. Kinetic parameters for the microsomal oxidation of R- and S- N-methyl-5-phenyl-2-pyrrolidinone.

Substrate	N-demethylation/Ring oxidation
R-	1.34
S-	0.33

Table 5.23 Ratios of N-demethylation to ring oxidation for the microsomal oxidation of R- and S- N-methyl-5-phenyl-2-pyrrolidinone.

5.5 Conclusion

Qualitatively both molecular orbital calculations and the catalytic by biomimetic system are revealed to be useful tools in predicting the metabolic fate of the substrates used in this study. Not surprisingly however, some features of the P450-mediated oxidations were quite different from those predicted. Thermodynamically, and indeed chemically, N-dealkylation and ring oxidations are more favoured, whereas in microsomal metabolism N-demethylation competes effectively with N-dealkylation. As observed in Chapter 4, kinetic factors seem to be the main driving force of these microsomal reactions. It is also plausible that the steric bulk of the N-alkyl substituents somehow hinders the N-alkyl hydrogen atom in a such a way as to make it less available to the haem plane of the P450. Furthermore, a stereoselectivity, not predicted from energetic considerations and not observed in the biomimetic oxidations, is noted for these microsomal reactions. This stereopreference in the P450 reactions is most likely to be due to interactions between the protein in the active site of the enzyme and the bulky substituent of the substrates. The small, but significant, preference for N-dealkylation of R(+)- N-methyl-(1-phenylethyl)benzamide becomes more pronounced for ring oxidation of the conformationally rigid S-N-methyl-5-phenyl-2-pyrrolidinone. The difference of the extent of stereoselectivity between the two substrates may be due to the fact that N-methyl-(1-phenylethyl)benzamide possess relatively free rotation along the C-N bond which may result in only a small difference in the spatial conformations of the substrates with regard to their relative orientations to the haem plane of the enzyme. The active site of P450 is believed to be very non-polar, based on structural analogy with the well-

known $P450_{cam}$.[23] Moreover, the rate of rotation in amides increases with a decrease in the polarity of the solvent.[26] Therefore, it seems unlikely that amide rotation in the active site is a process slow enough to present any stereoselectivity. Thus, an explanation for the observed stereoselectivity for N-dealkylation may lie with a hydrophobic interaction between the non-polar substituent of the substrate and a hydrophobic moiety of the protein in the enzyme active site. These would slow down rotation about the amide C-N bond resulting in a stabilisation of two different conformational orientations toward the haem plane. However, given the results obtained, these interactions appear to be very small. With the fixed conformation, cyclic substrates, the stereoselectivity for N-dealkylation (ring oxidation) is more evident. A model to explain the stereopreference for the metabolism of the structurally similar substrate nicotine by P450 proposed that interaction between the pyridyl ring and a protein residue is responsible of the stereochemical course of the reaction.[18] It is curious, therefore, that no evidence has been reported of stereoselectivity in the metabolism of nicotine metabolite cotinine,[26; 27] a compound with almost identical molecular structure to the cyclic substrate used in this study (cotinine possess a 3'- pyridyl ring instead of the phenyl group).

The conclusions that can be drawn from the experimental data are that interactions between the non-polar moiety of the substrate and a hydrophobic pocket of the enzyme active site impose a steric constraint on the substrate in such a way as to determine a preferential orientation of the hydrogen atom with respect the haem plane. The S- isomer of N-methyl-5-phenyl-2-pyrrolidinone presents a relative position of the ring that maximises this steric effect. Steric effects are unimportant for N-demethylation, presumably because access to the N-methyl hydrogen atoms is not significantly different between two isomers.

5.6 References

1 Yang S.K., (1988); *Biochem. Pharmacol.*; **37**: 61-

2 Yang S.K., Muslitaq H.B., Weems D.W., Miller D.W and Fu P.P., (1987); *Biochem. J.*; **245**: 191-

3 Prasad G.K.D. and Thakker D.R., (1991); *Biochem. Biophys. Res. Commun.*; **181**: 1516-

4 Capdevila J.H., Karara A., Waxman D.J., Martin M.V., Falck J.R. and Guengerich F.P., (1990); *J. Biol. Chem.*; **265**: 10865-

5 Capdevila J.H. and Falck J.R., (1992); *FASEB J.*; **6**: 731-

6 Fitzpatrick F.A. and Murphy R.C., (1989); *Pharmacol. Rev.* **40**: 229-

7 Karara A., Dishman H., Jacobson H., Falck J.R. and Capdevila H.H. (1990); *FEBS Lett.*; **268**: 227-

8 Laethem R.M., Laethem C.L. and Koop D.R., (1992); *J. Biol. Chem..*; **267**: 5552-

9 Boyd D.R., Walsh C.T. and Chen Y.C.J., (1989); In: Sulfur Containing Drugs and Related Compounds. (ed. L.A.. Damani); p.67; Ellis Horwood Ltd., Chichester, U.K.).

10 Tanaka T., Yamasaki M., Fujimori Y.H., Mim Y.H. and Oae S., (1983); *Bull. Chem. Soc. Jpn.*; **56**: 2300-

11 Oae S., Mikami A., Matsuura T., Ogawa-Asada K., Watanabe Y., Fujimori K. and Iyanagi T., (1985); *Biochem. Biophys. Res. Commun.*; **131**: 567-

12 Jenner P., Gorrod J. W. and Beckett A. H., (1973); *Xenobiotica*; **3**: 573-

13 Booth J and Boyland E., (1970); *Biochem. Pharmacol.*; **19**: 733-

14 Papadopoulus N.M., (1964); *Can. J. Biochem.*; **42**: 435-

15 McKennis H.Jr., Turnbull L.B. and Bowman E.R., (1957); *J. Am Chem. Soc.*; **79**: 6342-

16 Beckett A.H., Gorrod J.W. and Jenner P., (1971); *J. Pharm. Pharmac.*; **23**: Suppl. 55S

17 Park S.B., Jacob P. III, Benowitz N.L. and Cashman J.R., (1993); *Chem. Res. Toxicol.*; **6**: 880-

18 Peterson L.A., Trevor A. and Castagnoli N. Jr., (1987); *J. Med. Chem.*; **30**: 249-

19 Jacob P. III; Benowitz N.L. and Shulgin A.T., (1988); *Pharmacol. Biochemical. Behav.*; **30**: 249-

20 Benowitz N.L., Kuyt F. Jacob P. III, Jones R.T. and Osman A.L., (1983); *Clin. Pharmacol. Ther.*; **34**: 604-

21 De Schepper P.J., Van Hecker A., Daeness P. and Van Rosseem J.M., (1987); *Eur. J. Clin. Pharmacol.*; **31**: 583-

22 Li Y and Gorrod J.W., (1994); *Xenobiotica*; **24**: 409-

23 Bundgaard H. and Johansen M., (1984); *Int. J. Pharmacol.*; **22**: 45-

24 Ross D., Farmer P.B., Gescher A., Hickman J.A. and Threadgill M.D., (1983); *Biochem. Pharmacol.*; **32**: 1773-

25 Bean J.W. and Nelson D.J., (1984); *Biochem. Pharmacol.*; **33**: 2145-

26 Morselli P.L., Ong H.H., Bowman E.R. and McKennis H.Jr., (1967); *J.Med. Chem.*; **10**: 1033-

27 Bjercke R.J., Hammond D.K., Strobel H.W. and Langone J.J., (1990); *Drug Metab. Dispos.*; **18**, 5:759-

CHAPTER 6

Microsomal metabolism of N,N-dimethylformamide (DMF) and N,N-dimethylacetamide (DMAC)

The present chapter will describes the following studies on the interactions between microsomal cytochrome P450 and DMF and DMAC:

- attempts to trap intermolecularly and intramolecularly the carbon-centred radical intermediates
- effects of the oxidation of DMF and DMAC on the metabolising enzyme
- attempts of identification the reactive species produced during the oxidation of DMF and DMAC

6.1 Introduction

N,N-Dimethylformamide (DMF) and N,N-dimethylacetamide (DMAC), are organic solvents widely used in a large variety of industrial process, among them the manufacture of synthetic fibres, leather, films and surface coatings. Consequently, a significant quantity of metabolic and toxicological data for these compounds are available.

Two reported major effects in workers exposed to DMF are gastric irritation and hepatotoxicity.[1] The toxicity of DMF in animals has been cogently reviewed.[2] DMF has been implicated as the cause of alcohol incompatibly reactions in exposed workers [3-6] and is suspected of being carcinogenic.[7;8] However, the results of extensive studies of workers exposed to DMF over many years suggest that the carcinogenic risk associated with occupational exposure is very low.[9;10]

DMAC is reported to present low acute toxicity [2] and animal exposure to high concentrations of the solvent presents liver damage as the first indication of toxicological

change.[2; 11;12] In humans, alteration of liver function has been observed at relatively low chronic exposure.[13]

For both chemicals it is believed that hepatotoxicity is related to their P450-mediated metabolism, a process that involves the formation of reactive species responsible for the toxic effects.[14;15;16] The main route of P450 mediated metabolism is reported to be the oxidation of the carbon α- to nitrogen to give the corresponding N-hydroxylmethyl-N-methylamide.[14-18] On the basis of kinetic isotope effects [16;19;20] it is thought that P450 oxidation of these compound occurs *via* hydrogen atom abstraction leading to the formation of a carbon centred-radical intermediate.

The metabolic fate *in vivo* and *in vitro* of DMF has been reviewed by Gescher.[14] The proposed metabolic pathway leading from DMF to toxic intermediates is illustrated in Figure 6.1.

Oxidation can occur either at the α-carbon or at the carbonyl moiety. Oxidation of the carbonyl moiety is believed to be responsible for the formation, *in vivo*, of glutathione derived products, which are considered the main factors responsible for the toxicity of DMF (as reported for N-methyl formamide (NMF)).[21-26] Oxidation of the α-carbon leads to N-demethylation of DMF resulting in the formation of NMF, which can undergo further metabolism to toxic species. However, the formation of the thiol derivatives of DMF is not reported during the *in vitro* metabolism.[14] Indeed, the α-carbon oxidation reaction has a higher affinity for the enzyme, which results in an inhibition in the formation of the thiol derivatives in the *in vitro* metabolism of NMF.[14;16] Moreover, high concentrations of DMF seem to inhibit its bioconversion into a reactive thiol intermediate.[16,27] Despite the efforts to clarify the full metabolic features responsible for the toxicological response of DMF many aspects of this metabolic bioconversion are still unknown.

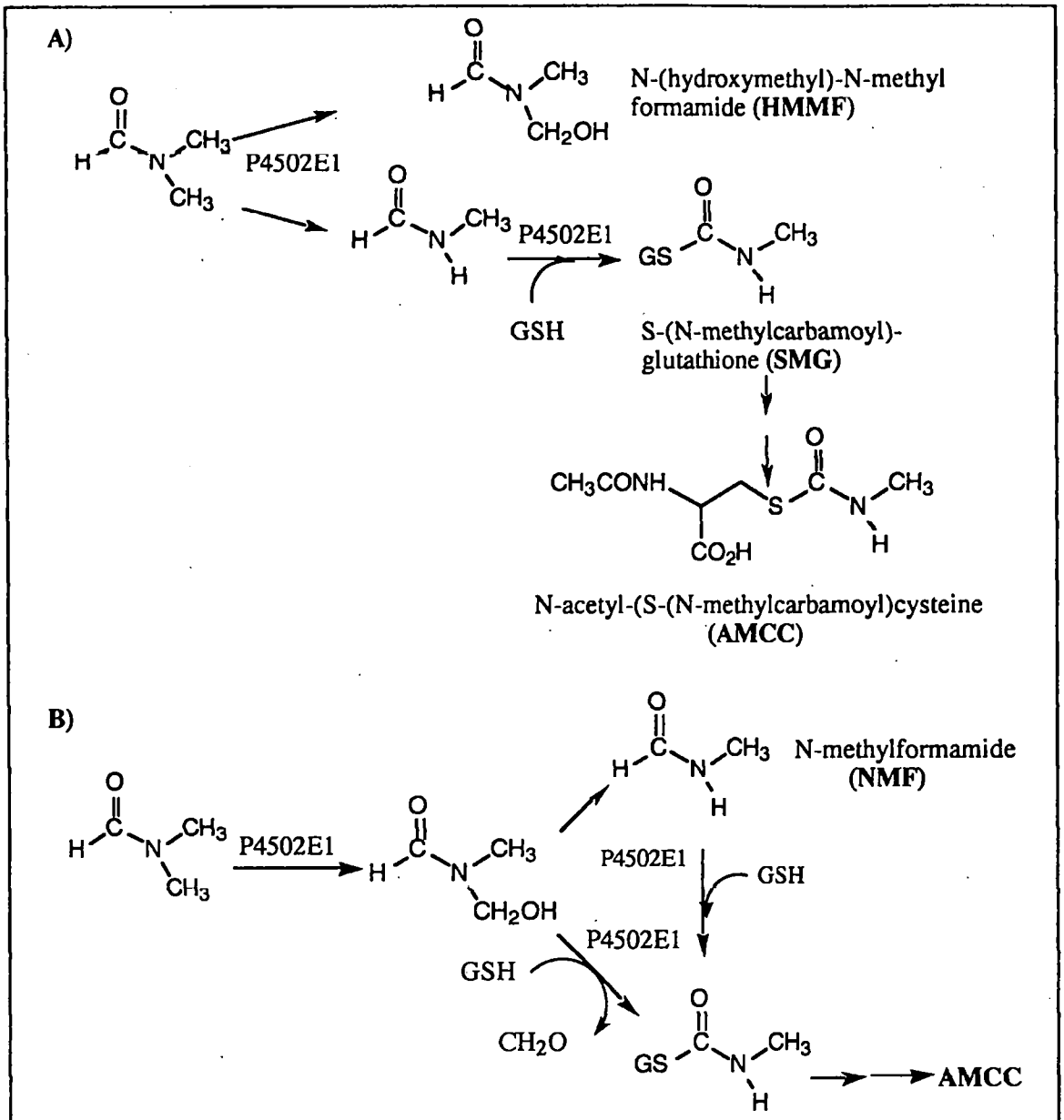

Figure 6.1 Proposed metabolic pathways leading toxic intermediates from DMF.

It is reported that the P450 isoform primarily responsible for the metabolism of DMF is ethanol-induced P450 2E1,[16;26] and that the affinity of DMF for the enzyme is 10 fold higher than that of HMMF and 20 fold higher than that of NMF.[16] Moreover, in rats DMF is more toxic than NMF or HMMF, and the precise diagnosis of DMF toxicity is more accurate when analysed over a prolonged period.[27] In rats DMF is metabolised to HMMF and subsequently to NMF. The time-course of NMF formation fits with a possible role for such a chemical as a precursor to the reactive intermediates responsible

of the DMF toxicity.[27] However, there are differences in the degree of hepatotoxicity after administration of DMF and NMF.

DMAC is reported to be metabolised by P450 to N-hydroxymethyl-N-methylacetamide *in vitro* and in rats, while in humans only the N-demethylated product was identified.[2;15]

A comparative study on the *in vitro* metabolism of DMAC and DMF, using phenobarbital-induced rat liver microsomes reports the production of N-demethylated metabolites from both substrates and that DMAC seems to be more readily metabolised than DMF.[17;28]

Despite extensive investigation into the metabolic fate of DMF, and to a lesser extent DMAC, few studies have reported the effects that the metabolism of these substrates have on the metabolising enzymes. The only indication so far reported in the literature is the study of Imazu and collaborators,[29;30] where in an *in vivo* study using a high concentration of DMF (0.5 ml/kg body weight) for prolonged period (1 week), a decrease in the content of P450 and microsomal haem was observed. The authors suggested three hypotheses to explain these observations:

- enzyme destruction,
- inhibition of the synthesis of protohaem and/or apoprotein, and
- massive cellular damage or damages of the membranes.

The third possibility seems unlikely because membrane bound cytochrome b_5 and NADPH cytochrome *c* reductase are unaffected by the DMF administration.

Inactivation of P450 during the metabolism of tertiary amides has not been reported so far. An indirect indication of P450 inactivation comes from the kinetic analysis of the microsomal metabolism of N,N-dimethylbenzamide, where an initial high rate metabolism is followed by a second phase of slower activity.[19] This bilinear trend,

can be explained either by enzyme inactivation or by the presence of two P450 isoforms of which one exhibits an high metabolic rate and saturation at low substrate concentrations. The authors favoured this second possibility because it was felt there was no rational explanation for the formation of reactive species in the metabolism of this substrate.[14;19;20]

Given the observations reported in Chapters 2 and 3 regarding the formation of free radicals during the oxidation of tertiary amides together with the reported *in vivo* effects of the metabolism of DMF on P450, an investigation into the *in vitro* effects of DMF and DMAC on P450 was therefore undertaken. The rationale underpinning this approach is that carbon-centred radical intermediates are reactive species able to attack any available biological target. Due to the low half-life of these radicals it is possible that the metabolising enzyme becomes the more relevant target of these reactive intermediates. Given that the synthesis of protohaem and of P450 is not present in microsomes, if loss of P450 and microsomal haem is found then the only available hypothesis left to explain the *in vivo* observation [29;30] is the destruction of the enzyme. Further, the choice DMAC as substrate is due to its close structural analogy with DMF and because it can block any potential metabolism at the carbonyl moiety of the amide. Thus, if loss of P450 is also observed for this substrate, then it provides additional structural information as to the reactive species responsible for its biological action.

The initial part of the study involves semi-empirical AM1 calculations of the heats of formation of the substrates and of their postulated radical intermediates, to predict, from a thermodynamic point of view, the most likely metabolic pathway of these substrates. Subsequently, identification of the reactive intermediate was undertaken using inter-and intra-molecular trapping techniques on the assumption that carbon-centred radicals are formed during the reaction. Finally, the effects of the metabolism of the substrates on ethanol-induced rat liver P450 were analysed.

6.2 AM1 Molecular orbital calculations

The heats of formation of DMF, DMAC, their corresponding radical cations and carbon-centred radical intermediates, calculated by AM1 method, are contained in Table 6.1.

The data obtained identify formation of the carbon-centred radical intermediate obtained by abstraction of the hydrogen atom from the α-carbon to be favoured over the abstraction of the formyl hydrogen atom. On the assumption that ΔH_f approximates to E_a then abstraction of the α-carbon hydrogen atom is favoured by a factor of 1260.

Comparison of the ΔH_f values for the formation of the carbon-centred radical intermediates from DMF and DMAC indicates that there are no significant differences; the oxidation of DMF is slightly favoured, by a factors of 1.3.

Compound	ΔH_f (kJ/mol)
DMF	**- 128.82**
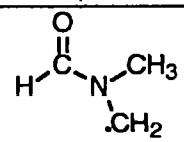	**38.07**
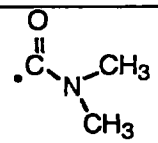	**55.85**
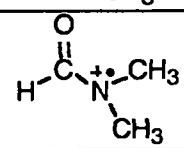	**729.48**
DMAC	**- 147.61**
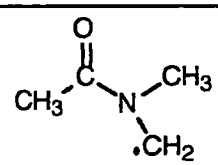	**20.33**
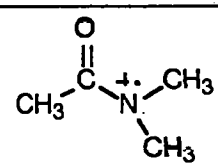	**672.9**

Table 6.1 Heats of formation (ΔH_f) of DMF, DMAC and their postulated radical intermediates.

6.3 Microsomal metabolism of DMF and DMAC

• Identification of the products

Ethanol-induced rat hepatic microsomes were incubated in the presence of 10 mM substrate for 30 minutes. Figures 6.2 and 6.3 display typical gas chromatograms from the incubations of DMF and DMAC after 30 minutes, respectively. The products of the reaction were identified by comparison of their mass spectra with that recorded for pure standards (Table 6.2)

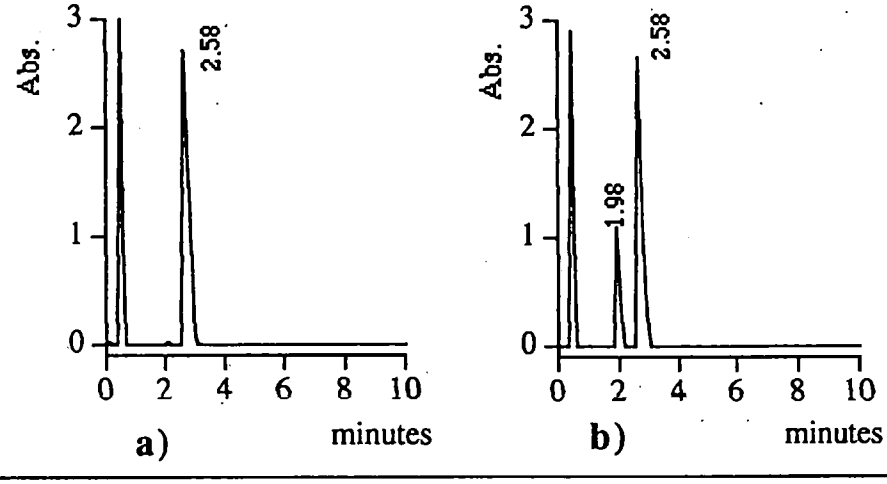

Figure 6.2 Typical gas chromatogram of a sample obtained from microsomal incubation of 10 mM DMF, at reaction time a) 0 and b) 30 minutes.

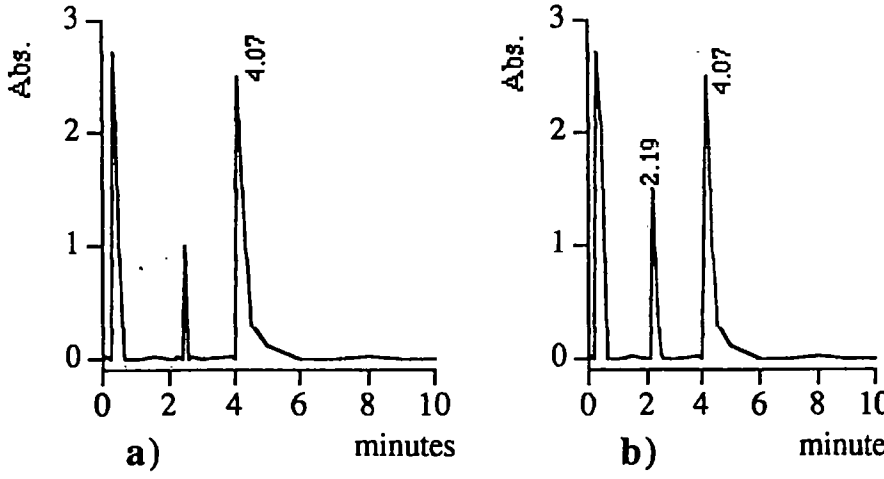

Figure 6.3 Typical gas chromatogram of a sample obtained from microsomal incubation of 10 mM DMAC, at reaction time a) 0 and b) 30 minutes.

Peak	Compound identified
Retention Time: 2.58 minutes Figure 6.2 chromatogram b)	**N,N-dimethylformamide**
Retention Time: 1.98 minutes Figure 6.2 chromatogram b)	**N-methylformamide**
Retention Time: 4.07 minutes Figure 6.3 chromatogram b)	**N,N-dimethylacetamide**
Retention Time: 2.19 minutes Figure 6.3 chromatogram b)	**N-methylacetamide**

Table 6.2 Products identified from microsomal incubations of DMF and DMAC.

No other products were observed under any reaction condition, in agreement with the literature [14] that the only detected metabolite of these substrates *in vitro* is the N-demethylated amide.

- **Quantitative analysis of the microsomal metabolism of DMF and DMAC**

Initial rates for the microsomal oxidation of DMF and DMAC, measured after 5 minutes reaction, are reported in Tables 6.3 and 6.4 respectively, while Table 6.5 summarises the derived kinetic parameters calculated for these reactions.

[Substrate] (mM)	v_i N-methylformamide (μM/min/nmol P450)
0.5	0.89 ± 0.06
1.0	1.21 ± 0.07
3.0	1.62 ± 0.03
5.0	1.74 ± 0.06
10.0	1.84 ± 0.10

Table 6.3 Initial rates v_i, for the microsomal oxidation of DMF.

[Substrate] (mM)	v_i N-methylacetamide (μM/min/nmol P450)
0.5	2.42 ± 0.12
1.0	3.04 ± 0.21
3.0	3.66 ± 0.25
5.0	3.82 ± 0.16
10.0	3.94 ± 0.24

Table 6.4 Initial rates v_i, for the microsomal oxidation of DMAC.

	DMF	DMAC
V_{max} (μM/nmol P450)	1.95 ± 0.12	4.08 ± 0.21
Km (mM^{-1})	0.60 ± 0.03	0.34 ± 0.04
V_{max}/K_m	3.25	12.00

Table 6.5 Kinetic parameters for the microsomal oxidation of DMF and DMAC.

DMAC is more readily metabolised than DMF; comparison of the V_{max}/K_m values reveals a difference in reactivity of *ca.* 3.5.

6.4 Trapping of the reactive intermediates in the metabolism of DMF and DMAC

6.4.1 Intramolecular trapping using an N-alkynyl probe substrate

To identify the nature of the carbon-centred radical intermediate formed during the metabolism of these substrates, a probe substrate with a structure able to trap the radical intramolecularly was synthesised. Based on the results in Chapter 2, the chosen probe substrate is N-(3-butynyl)-N-methylformamide (Figure 6.4).

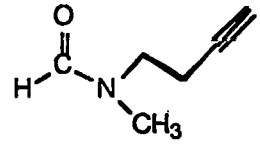

N-(3-butynyl)-N-methylformamide

Figure 6.4 NMF analogue for intramolecular trapping of the carbon-centred radical produced during P450-dependent metabolism.

Three potential carbon-centred radical intermediates can be formed during the metabolism of this substrate (Figure 6.5). Hydrogen atom abstraction from the two carbon atoms α- to nitrogen leads to the formation of radicals **2** and **3** whereas abstraction of the formyl atom leads to the formyl radical **4**. Intermediate **3** will undergo hydroxylation to form the N-dealkylated product N-methylformamide. The intermediates **2** and **4** can undergo intramolecular rearrangement *via* endo and exo pathways to yield the cyclic compounds **5**, **6**, **7** and **8**. Moreover, radical intermediate **2** can also undergo hydroxylation and dealkylation to form N-(3-butynyl)formamide.

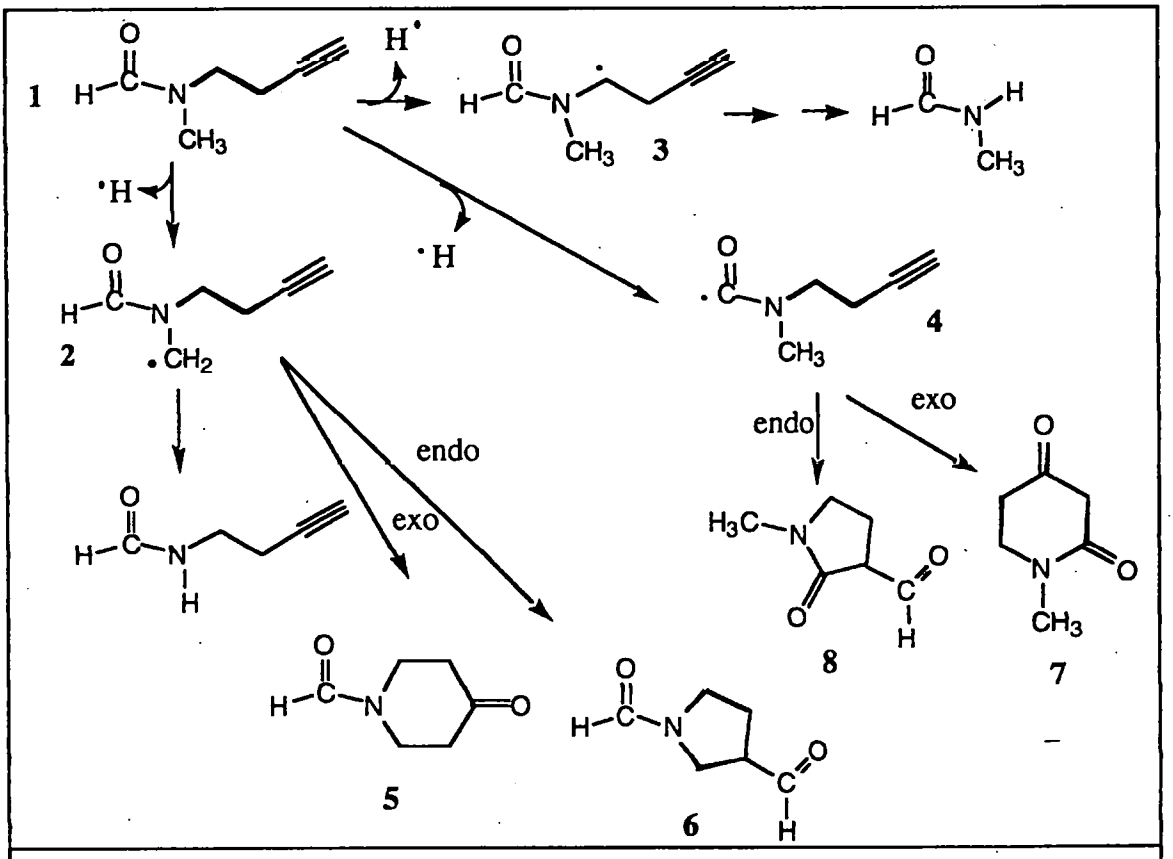

Figure 6.5 Potential pathway for the microsomal oxidation of N-(3-butynyl)-N-methylformamide.

Microsomal incubation of a 10 mM solution of N-(3-butynyl)-N-methylformamide, followed by treatment of the reaction mixture with 1 M sodium hydroxide (to completely hydrolyse the base labile carbinolamide), extraction with ethyl acetate and analysis by gas chromatography, resulted in the typical gas chromatogram illustrated in Figure 6.6. The reaction products were identified by comparison of their

retention times and mass spectra with those obtained for the equivalent synthetic standards; the results are summarised in Table 6.6.

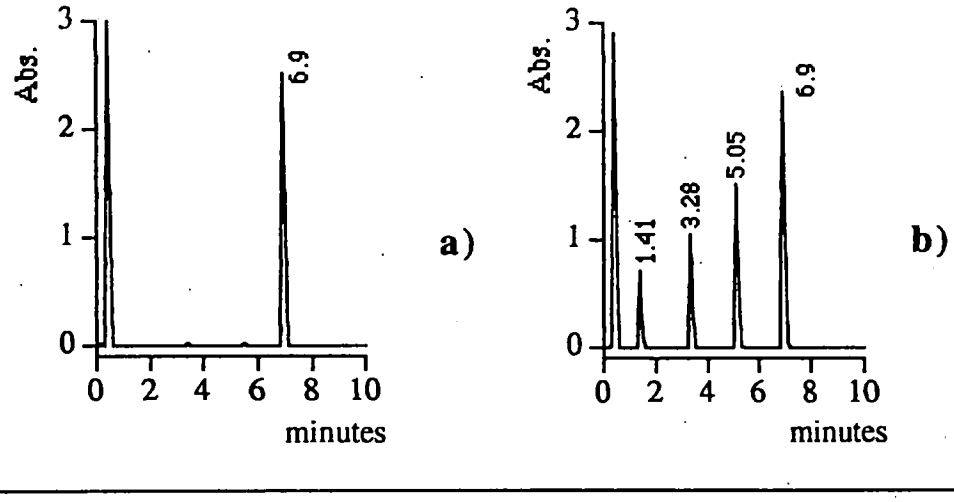

Figure 6.6 Typical gas chromatogram of ethyl acetate extracts obtained from microsomal incubation of 10 mM N-(3-butynyl)-N-methylformamide, at reaction time a) 0 and b) 30 minutes, b).

Peak	Compound identified
Retention time: 1.41 minutes	**N-methyl formamide**
Retention time: 3.28 minutes	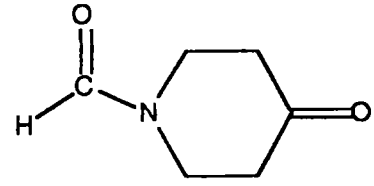
Retention time: 5.05 minutes	**N-(3-butynyl) formamide**
Retention time: 6.92 minutes	**N-methyl-N-(3-butynyl) formamide**

Table 6.6 Metabolites identified from the microsomal oxidation of N-(3-butynyl)-N-methylformamide.

These results are consistent with the formation of the carbon-centred radical intermediates **2** and **3** of Figure 6.5 *via* hydrogen atom abstraction from the two α-carbon atoms. Thus, the mechanism of the microsomal oxidation of N-(3-butynyl)-N-methylformamide is that proposed in Figure 6.7. As well as hydroxyl group insertion, the radical intermediate **2** undergoes intramolecular cyclisation resulting in the formation of the six-membered product. Despite the reported preference for the formation of five-membered ring systems in radicals cyclization reactions, [31-39] only the exo cyclization product was observed. It is worthy to note that no cyclic products were found that could

be ascribed to the formation of the formyl radical **4** of Figure 6.5. Thus, in these *in vitro* conditions, the abstraction of the carbonyl hydrogen does not occur. Nevertheless, structural differences between the N-alkenyl formamide and DMF and DMAC may play a relevant role in the mechanism of the P450 oxidations.

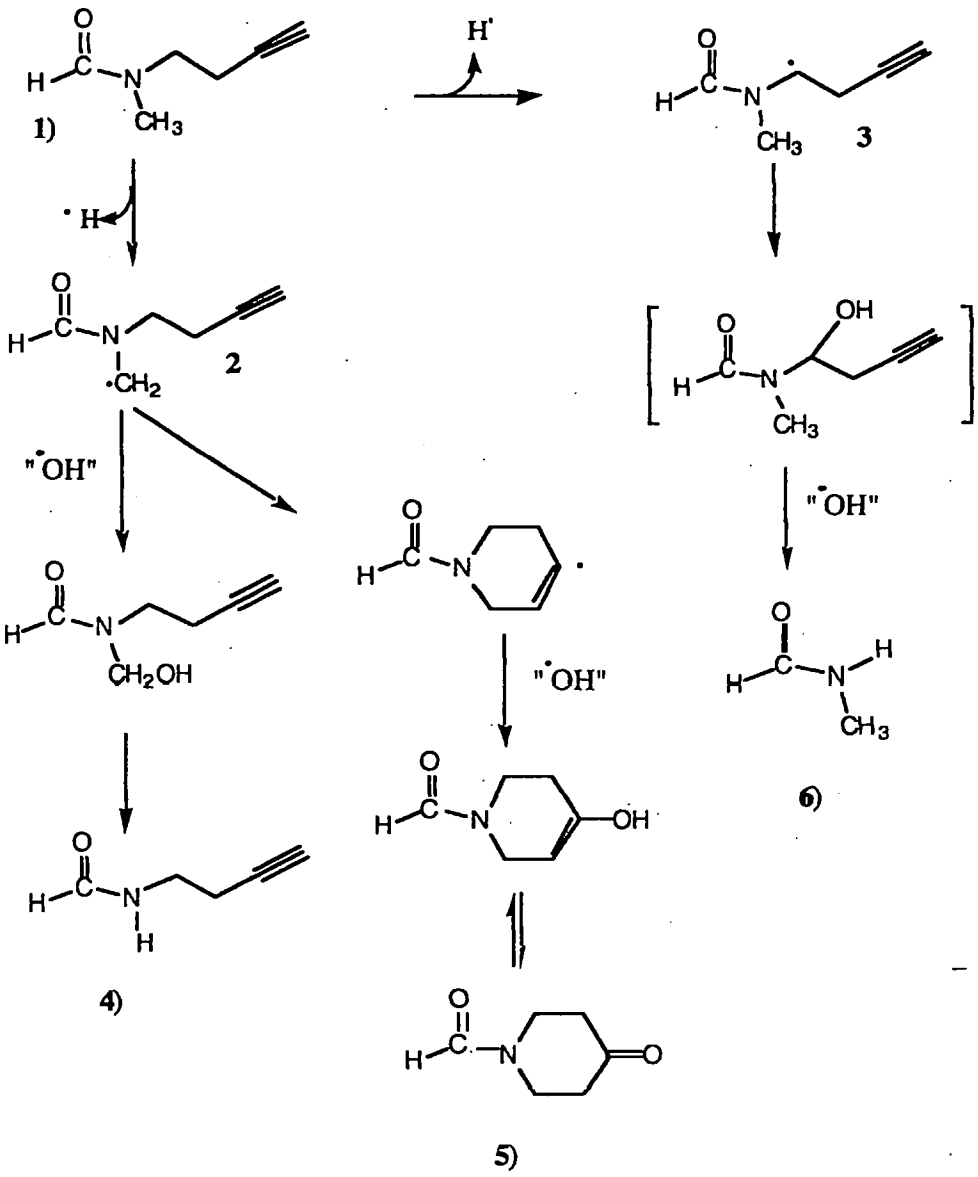

Figure 6.7 Pathway of the microsomal oxidation of N-(3-butynyl)-N-methylformamide.

- **Kinetic of the P450-dependent oxidation of N-(3-butynyl)-N-methylformamide**

Initial rates for the formation of products from N-(3-butynyl)-N-methylformamide were determined using substrate concentrations between 0.5 and 10

mM (Table 6.8). The kinetic parameters (Table 6.8) were calculated as described previously.

	v_i (μM/h/nmol P450)				
[substrate] (mM)	Total metabolism	N-dealk.	N-demeth.	Cyclization	Demeth./ cyclizat.
0.5	0.17 ± 0.008	0.07 ± 0.003	0.07 ± 0.002	0.014 ± 0.002	4.11
1.0	0.34 ± 0.010	0.14 ± 0.010	0.13 ± 0.010	0.03 ± 0.003	4.33
3.0	1.0 ± 0.020	0.41 ± 0.010	0.38 ± 0.014	0.08 ± 0.009	4.75
5.0	1.62 ± 0.090	0.68 ± 0.020	0.63 ± 0.020	0.13 ± 0.010	4.84
10.0	3.08 ± 0.10	1.30 ± 0.090	1.22 ± 0.140	0.25 ± 0.060	4.88
V_{max} (μM/nmol P450)	38.61 ± 0.91	19.5 ± 0.60	18.5 ± 0.83	2.31 ± 0.11	
K_m(μM^{-1})	114.3 ± 3.1	136.0 ± 8.0	141.0 ± 5.0	83.0 ± 3.5	
V_{max}/K_m	0.34	0.140	0.131	0.028	

Table 6.8 Initial rates v_i and kinetic parameters for the microsomal oxidation of N-(3-butynyl)-N-methylformamide.

The kinetic parameters calculated for the total metabolism of microsomal oxidation were then compared with those for the microsomal oxidation of DMF and DMAC (Table 6.9).

	DMF	DMAC	N-(3-butynyl)-N-methylformamide
V_{max} (μM/nmol. P450)	1.95 ± 0.12	4.08 ± 0.21	38.61 ± 0.91
K_m (mM^{-1})	0.60 ± 0.03	0.34 ± 0.04	114.3± 3.1
V_{max}/K_m	3.25	12.00	0.34

Table 6.9 Comparison of the kinetic parameters for the total microsomal metabolism of DMF, DMAC and N-(3-butynyl)-N-methylformamide.

The results obtained indicate that the microsomal metabolism of N-methyl-N-(3-butynyl) formamide occurs less efficiently than that of DMF and DMAC. Despite these quantitative differences it is rational to argue that not major qualitative difference are presents in the metabolism of these three substrates.

6.4.2 ESR spin trapping study of the microsomal oxidation of DMF and DMAC

Since the spin trapping agent PBN was found to be very efficient in the stabilisation of the radicals formed during the microsomal oxidation of benzamides, the metabolism of DMF and DMAC were carried out in the presence of PBN.

The ESR. spectra obtained from chloroform/methanol extracts of microsomal incubations of solutions of 10 mM DMF or DMF after 30 minutes are illustrated in Figure 6.8 and 6.9. The metabolism-dependent signal is a triplet of doublets, for which the hyperfine splitting constants are summarised in Table 6.10.

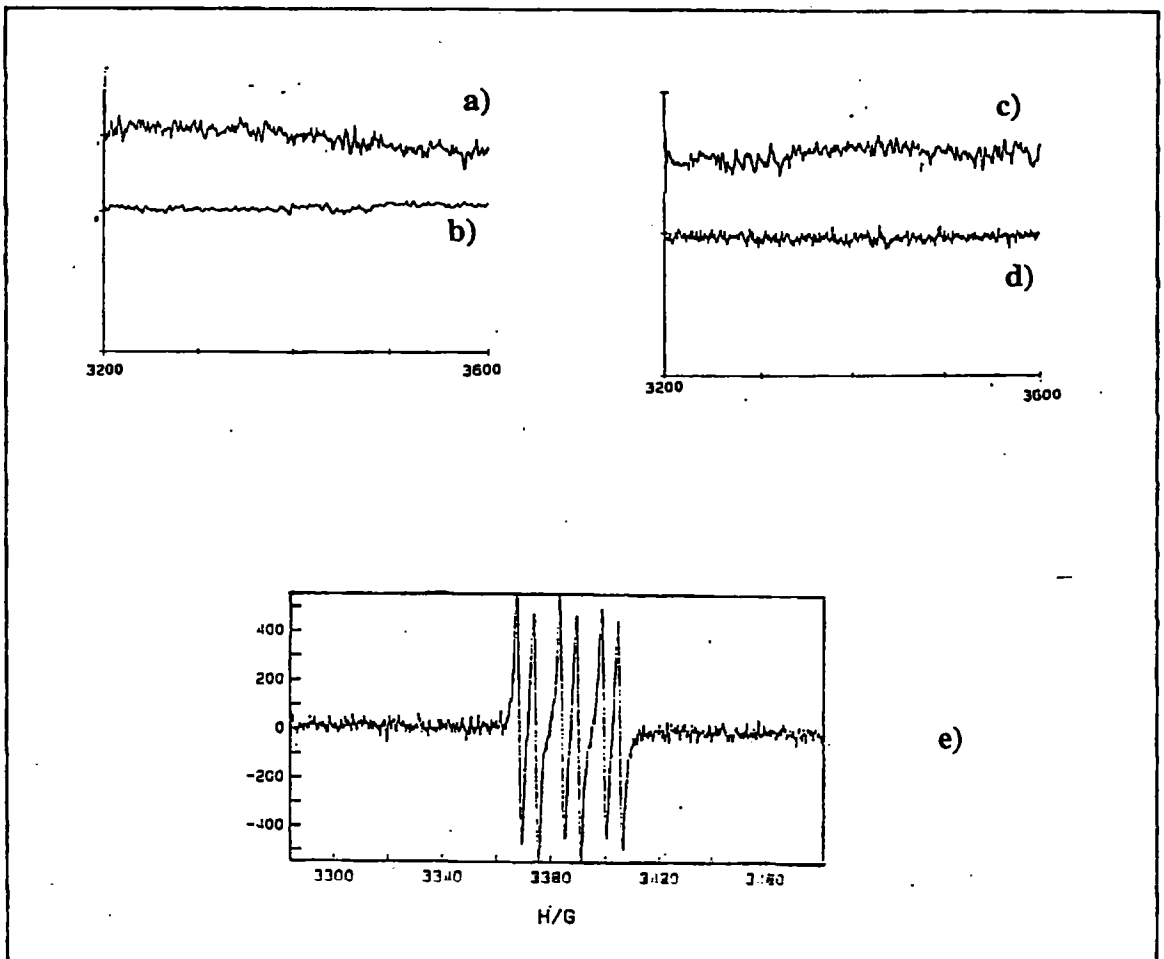

Figure 6.8 ESR spectra of extracts from microsomal oxidation of 10 mM DMF carried out in the presence of 3 mM PBN: a) complete microsomal monooxygenase system and 3 mM PBN, b) microsomes, 10 mM DMF and 3 mM PBN (without NADPH regenerating system) c) NADPH regenerating system and 3 mM PBN d) 10 mM DMF, 3 mM PBN and NADPH regenerating system e) and full system incubation.

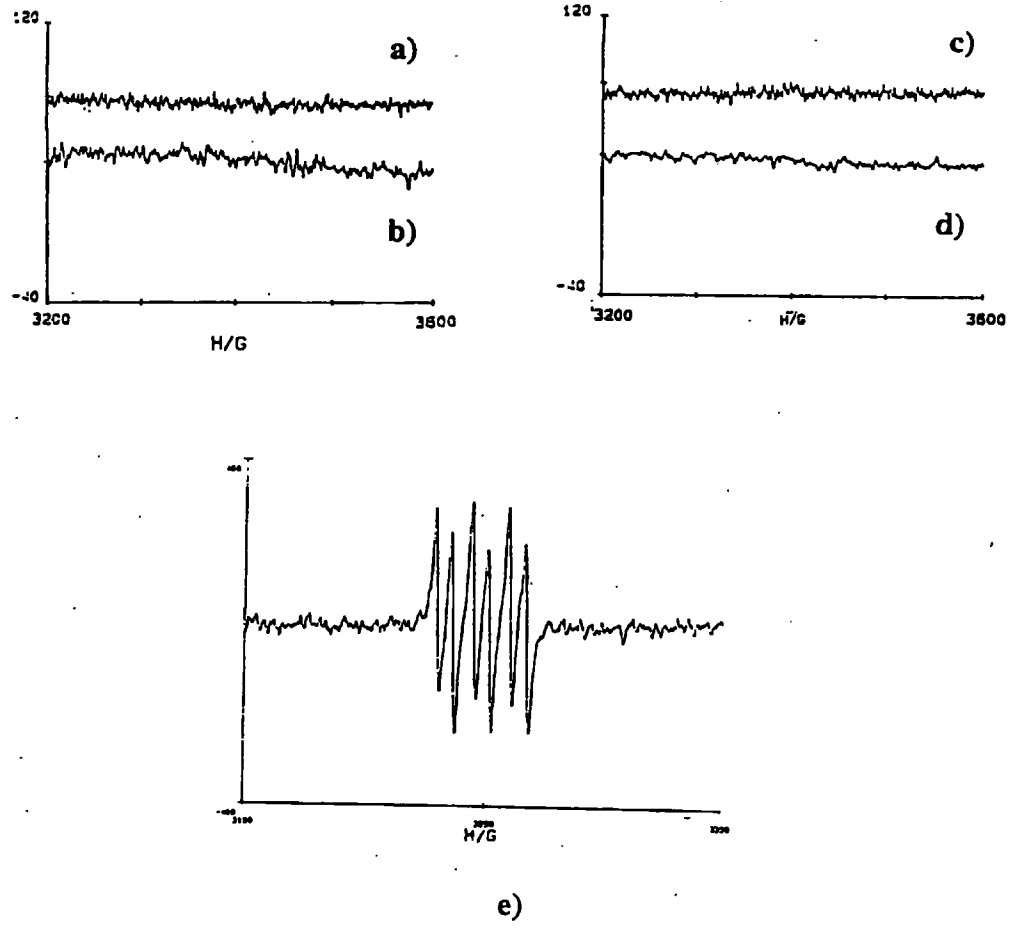

Figure 6.9 ESR spectra of extracts from microsomal oxidation of 10 mM DMAC carried out in the presence of 3 mM PBN: a) complete microsomal monooxygenase system and 3 mM PBN, b) microsomes, 10 mM DMAC and 3 mM PBN (without NADPH regenerating system) c) NADPH regenerating system and 3 mM PBN d) 10 mM DMAC, 3 mM PBN and NADPH regenerating system e) and full system incubation.

Substrate	a_N (G)	a_β^H (G)
DMF	6.85	14.70
DMAC	7.35	15.68

Table 6.10 Hyperfine splitting constants from the ESR. spectra obtained from microsomal oxidation of DMF and DMAC.

The results demonstrate that during the microsomal oxidation a trappable radical intermediate is formed. The formation of these radicals is metabolism dependent. The postulated carbon-centred radicals formed during these reactions are illustrated in Figure 6.10.

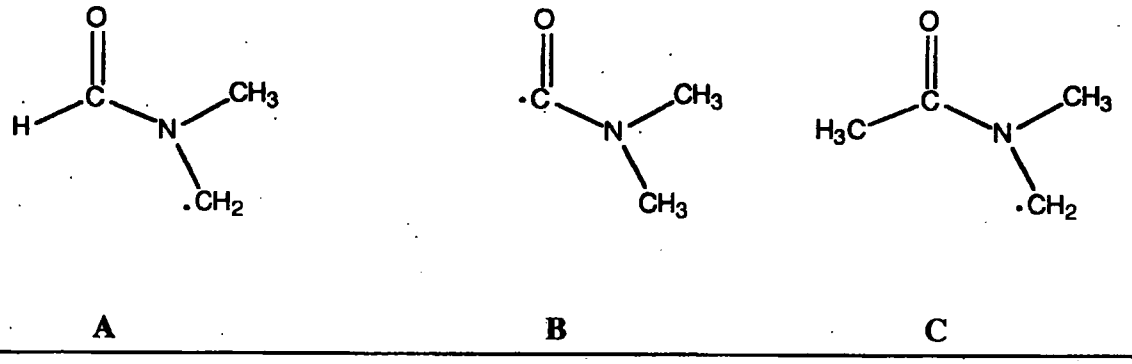

Figure 6.10 Postulated radicals formed during the microsomal oxidation of DMF and DMAC.

To characterise these radicals more fully, they were synthesised by the methods shown in equation 6.A and 6.B.

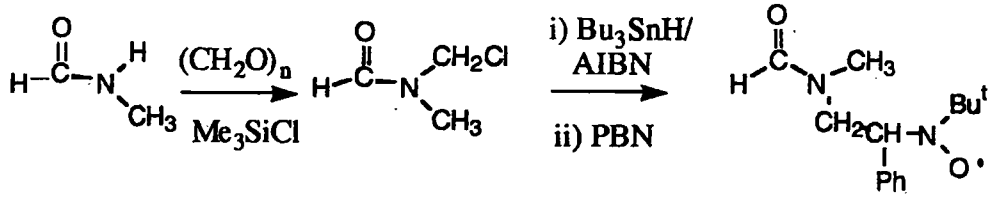

6.A

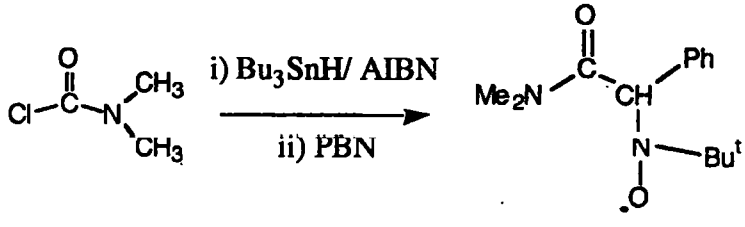

6.B

The ESR. spectra recorded for these radicals in chloroform/methanol are illustrated in Figure 6.11, while their measured hyperfine splitting constants are summarised in Table 6.11.

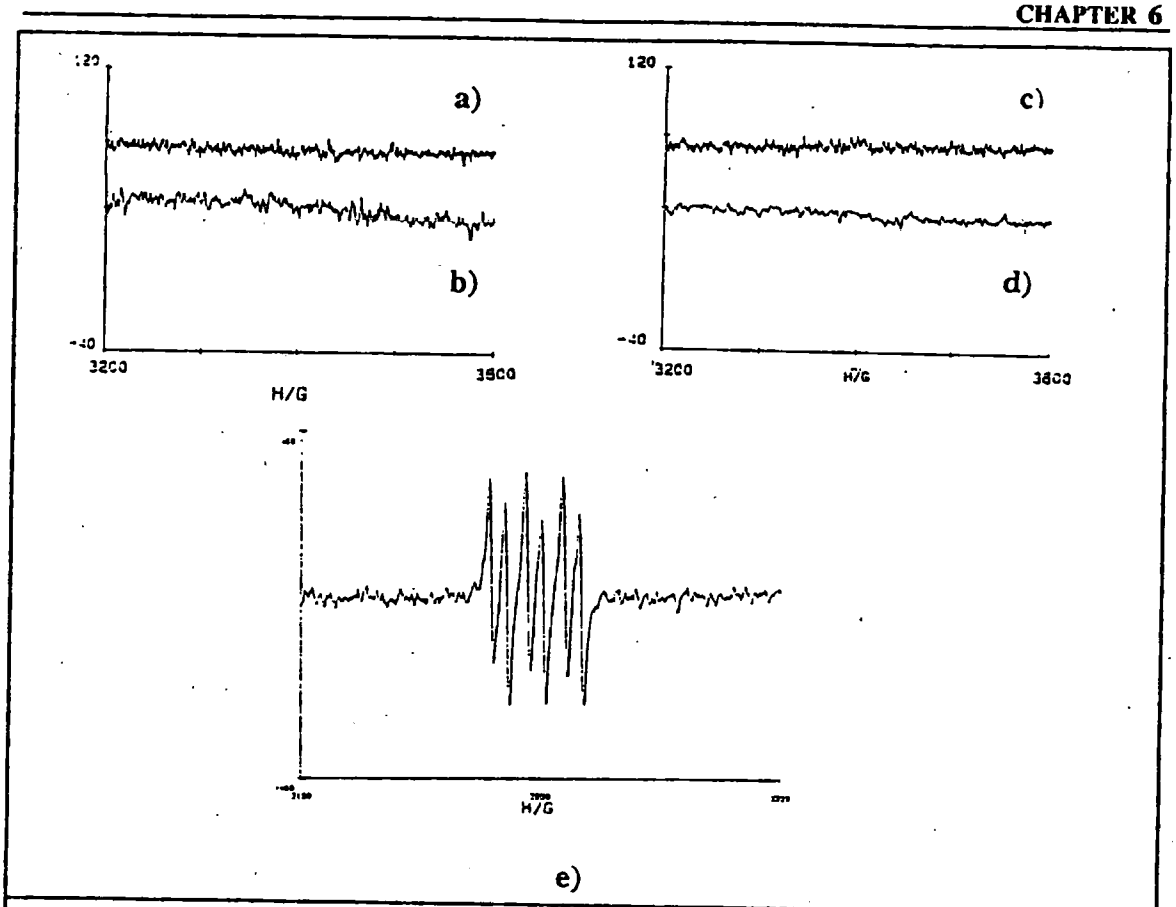

Figure 6.11 ESR. spectra of the PBN adducts of the radicals of Figure 6.10: spectrum 1, from radical A; spectrum 2, from radical B and spectrum 3, from radical C.

	a_β^H (G)	a_N (G)
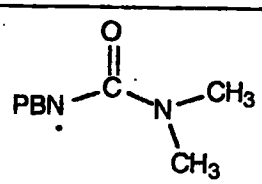		13.60
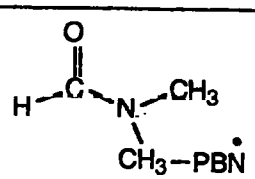	6.80	14.80
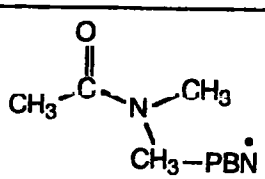	7.40	15.75

Table 6.11 Hyperfine splitting constants of the ESR. spectra obtained from the PBN adducts of the radicals shown in Figure 6.10.

The results indicates that the radical intermediate formed during the microsomal metabolism of DMF and DMAC is the carbon-centred radical generated by hydrogen atom abstraction from the α-carbon. Indeed, the ESR spectrum of the PBN adduct of the carbonyl-centred radical is clearly different from that recorded from the microsomal incubation of DMF, lacking the doublet hyperfine splitting normally observed because of coupling to the hydrogen atom. Presumably, this is because the presence of the carbonyl group allows the radical to enolise:

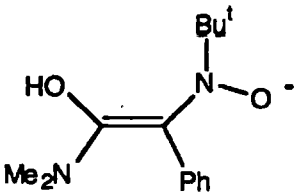

On the base of the *in vivo* effects of the metabolism of DMF on the metabolising enzymes,[29;30] it is arguable that a reactive intermediate is formed that destroy the enzyme system. The following part of the present study is intended to clarify the *in vitro* effect of metabolism of DMF and DMAC on microsomal P450.

6.5 The effect of *in vitro* metabolism of DMF and DMAC on P450

6.5.1 Inactivation of P450

The P450 content was measured at the end of the microsomal incubations of DMF and DMAC by the reduced differential spectra of the P450-CO complex as described by Omura and Sato.[40]

Figure 6.11 reports the time-dependence of the inactivation of microsomal P450 after incubations with 5 mM DMF and DMAC.

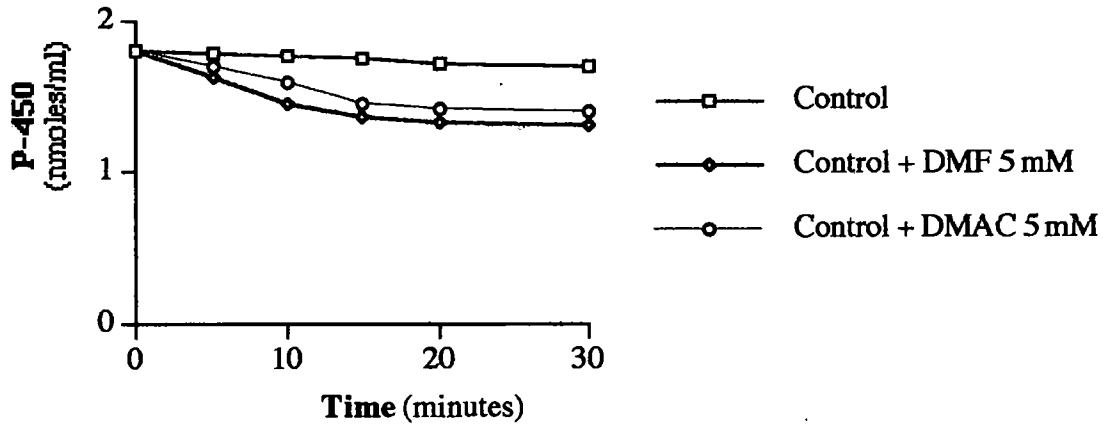

Figure 6.12 Time-course of P450 inactivation during the microsomal oxidation of 5 mM DMF and DMAC. Control incubations are constituted by microsomes and NADPH regenerating systems.

The results clearly demonstrate time-dependent loss of P450 during the microsomal metabolism of DMF and DMAC. Moreover, DMF is more efficient in this enzyme inactivation reaction. To quantify differences between the two substrates on the loss of P450, dose-dependent study of this reaction was performed. Table 6.12 reports the dose-dependent loss of P450 after 15 minute incubations with either DMF or DMAC.

	[P450] (nmoles/ml)		**Loss %**	
Incubation	**DMF**	**DMAC**	**DMF**	**DMAC**
Control	1.80 ± 0.03	1.80 ± 0.03	0.00	0.00
+ Sub. 0.5 mM	1.60 ± 0.03	1.66 ± 0.03	11.2 *	7.8 *
+ Sub. 1.0 mM	1.46 ± 0.02	1.53 ± 0.04	18.9 **	15.0 *
+ Sub. 5.0 mM	1.35 ± 0.03	1.44 ± 0.03	25.0 **	20.0 **
+ Sub.10.0 mM	1.32 ± 0.04	1.40 ± 0.02	26.7 **	22.3 **
+ Sub.20.0 mM	1.30 ± 0.05	1.38 ± 0.04	27.8 **	24.4 **

* $P < 0.01$, ** $P < 0.001$ Student's *t* test.

Table 6.12 Dose-dependent loss of P450 after 15 minute incubations of DMF and DMAC. The control incubations omitted substrate.

Dose-dependent inactivation of P450 during the oxidation of the substrates is present; at low concentration of amides the relationship between substrate concentration and enzyme inactivation is roughly linear.

The results indicate that during the microsomal oxidation of DMF and DMAC a reactive species is form that is able to attack the enzyme.

6.5.2 Loss of microsomal haem

From the point of view of the enzyme, there are two potential targets for the reactive species generated during the reactions: one is the apoprotein, the other is the prosthetic haem group. The latter target seems to be the more likely as it is more readily available being in close proximity to the generated reactive species. A large number of reports indicate that covalent modification of the P450 haem group is one of the mechanisms of metabolism-based suicide inactivation of the enzyme.[41-46] Thus the effect of DMF and DMAC metabolism on the content of the microsomal haem was analysed. Microsomal haem content was measured by the pyridine/haemochromogen methods.[47] The time- and dose-dependent loss of microsomal haem determined during the oxidation of 5 mM solutions of DMF and DMAC are reported in Figure 6.13 and Table 6.13, respectively.

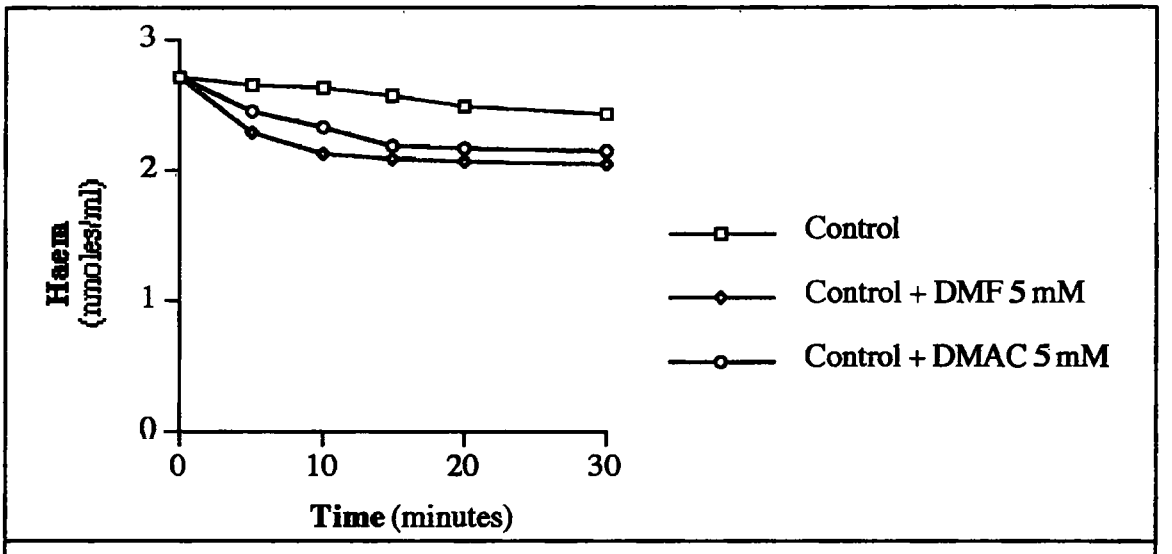

Figure 6.13 Time-course of the loss of microsomal haem during the oxidation of 5 mM DMF and DMAC. Control incubations are constituted by microsomes and NADPH regenerating systems.

	[Haem] (nmoles/ml)		Loss %	
Incubations	**DMF**	**DMAC**	**DMF**	**DMAC**
Control	2.64 ± 0.05	2.64 ± 0.05	0.00	0.00
+Sub. 0.5 mM	2.40 ± 0.03	2.52 ± 0.03	9.10 *	4.6 NS
+Sub. 1.0 mM	2.26 ± 0.02	2.38 ± 0.02	14.4 **	9.9 *
+Sub. 5.0 mM	2.11 ± 0.03	2.26 ± 0.01	20.1 **	14.4 **
+Sub. 10 mM	2.03 ± 0.02	2.14 ±0.03	23.1 **	18.9 **
+Sub. 20 mM	2.01 ± 0.03	2.10 ± 0.02	23.9 **	20.5 **

NS not significant, * $P < 0.01$, ** $P < 0.001$, Student's *t* test.

Table 6.13 Dose-dependent loss of microsomal haem after 15 minutes incubation of DMF and DMAC. The control incubations were constituted by microsomes and NADPH regenerating system.

A clear time- and dose-dependent loss of microsomal haem is present; as for the inactivation of P450, the full metabolic system is required indicating that such loss is metabolism-dependent. Comparison of these data with those for the inactivation of P450 reveals that the amount of haem lost corresponds to the amount of P450 inactivated during these oxidations. The discrepancy between the percentage values for the loss of haem and the inactivation of P450 can be ascribed to the analytical method used for the determination of the haem, which measures total microsomal haem. Given the presence in the microsomes of heamoproteins other than P450, and of the presence of P450 isoforms not involved in the metabolism of the substrates, the content of haem determined is higher than that which is "enzymatically active" in these reactions.

Thus, it is possible to conclude that the prosthetic haem group of the P450 is the target of the reactive species generated during the oxidation of the substrates; modification of the haem results in the inactivation of the enzyme.

The nature of the modification of the P450 haem occurring during the microsomal metabolism of DMF and DMAC was further investigated. The content of the microsomal haem at the end of the reactions was quantified by two different analytical methods: fluorimetric measurement of protoporphyrin IX, and HPLC analysis.

After 15 minutes microsomal incubations of DMF and DMAC the content of protoporphyrin IX was measured by the method of Morrison.[48] Using the same incubation, the haem was also quantified by the pyridine/haemochromogen method. The results are reported in Tables 6.14 and 6.15.

	Protoporphyrin IX		Haem	
Incubation	**[Proto. IX]** (nmoles/ml)	**Loss %**	**[Haem]** (nmoles/ml)	**Loss %**
Control	2.55 ± 0.11	0.00	2.64 ± 0.05	0.00
+ DMF 0.5 mM	2.51 ± 0.09	1.60 NS	2.40 ± 0.03	9.10 *
+ DMF 1.0 mM	2.48 ± 0.12	2.80 NS	2.26 ± 0.02	14.4 **
+ DMF 5.0 mM	2.50 ± 0.13	2.00 NS	2.11 ± 0.03	20.1 **
+ DMF 10.0 mM	2.49 ± 0.20	2.40 NS	2.03 ± 0.02	23.1 **
+ DMF 20.0 mM	2.47 ± 0.14	3.20 NS	2.01 ± 0.03	23.9 **

NS not significant, * $P < 0.01$, ** $P < 0.001$, Student's *t* test.

Table 6.14 Determination of the content of microsomal protoporphyrin IX and haem after 15 minute incubations using DMF. The control incubations were constituted by microsomes and NADPH regenerating system.

Incubation	Protoporphyrin IX		Haem	
	[Proto. IX] (nmoles/ml)	Loss %	[Haem] (nmoles/ml)	Loss %
Control	2.55 ± 0.11	0.00	2.64 ± 0.05	0.00
+ DMAC 0.5 mM	2.53 ± 0.10	0.80 S	2.52 ± 0.03	4.6 NS
+ DMAC 1.0 mM	2.50 ± 0.09	2.00 NS	2.38 ± 0.02	9.9 *
+ DMAC 5.0 mM	2.46 ± 0.21	3.60 NS	2.26 ± 0.01	14.4 **
+ DMAC 10.0 mM	2.44 ± 0.23	4.40 NS	2.14 ±0.03	18.9 **
+ DMAC 20.0 mM	2.48 ± 0.18	2.80 NS	2.10 ± 0.02	20.5 **

NS not significant, * $P < 0.01$, ** $P < 0.001$, Student's *t* test.

Table 6.15. Determination of the content of microsomal protoporphyrin IX and haem after 15 minute incubations using DMAC. The control incubations were constituted by microsomes and NADPH regenerating system.

It is interesting to note that the metabolism-dependent loss of microsomal haem does not correspond to a loss of protoporphyrin IX. This observation can be rationalised by the two analytical methods used. It is probable that the modification occurring in the haem group does not permit the formation of the pyridine-haemochromogen complex resulting in an measurable loss of the haem. In contrast, the failure to determine a loss of protoporphyrin IX is probably due to the fact that the haem modification does not result in the loss of the tetrapyrrolic structure.

6.5.2.1 Analysis of the modified microsomal haem

Ethanol-induced rat liver microsomes were incubated in presence of DMF or DMAC. After 30 minutes the content of microsomal haem was analysed by HPLC. Typical HPLC chromatograms obtained with 10 mM DMF and DMAC are illustrated in Figure 6.14.

The peak with retention time 3.10 minutes, present in each chromatogram, was identified as unmodified haem by comparison of its UV/VIS spectra with that of a pure standard. The peaks with retention time 4.48 minutes of chromatogram b) and 6.12 minutes of chromatogram d) correspond to a modified haem occurring during the metabolism of the substrate, as indicated by their absence at time 0 minutes. The UV/VIS spectra, recorded by a diode array detector, of these metabolism-dependent modified haems are similar of that of pure haem, as illustrated in Figure 6. 15, indicating the haem nature of these compounds.

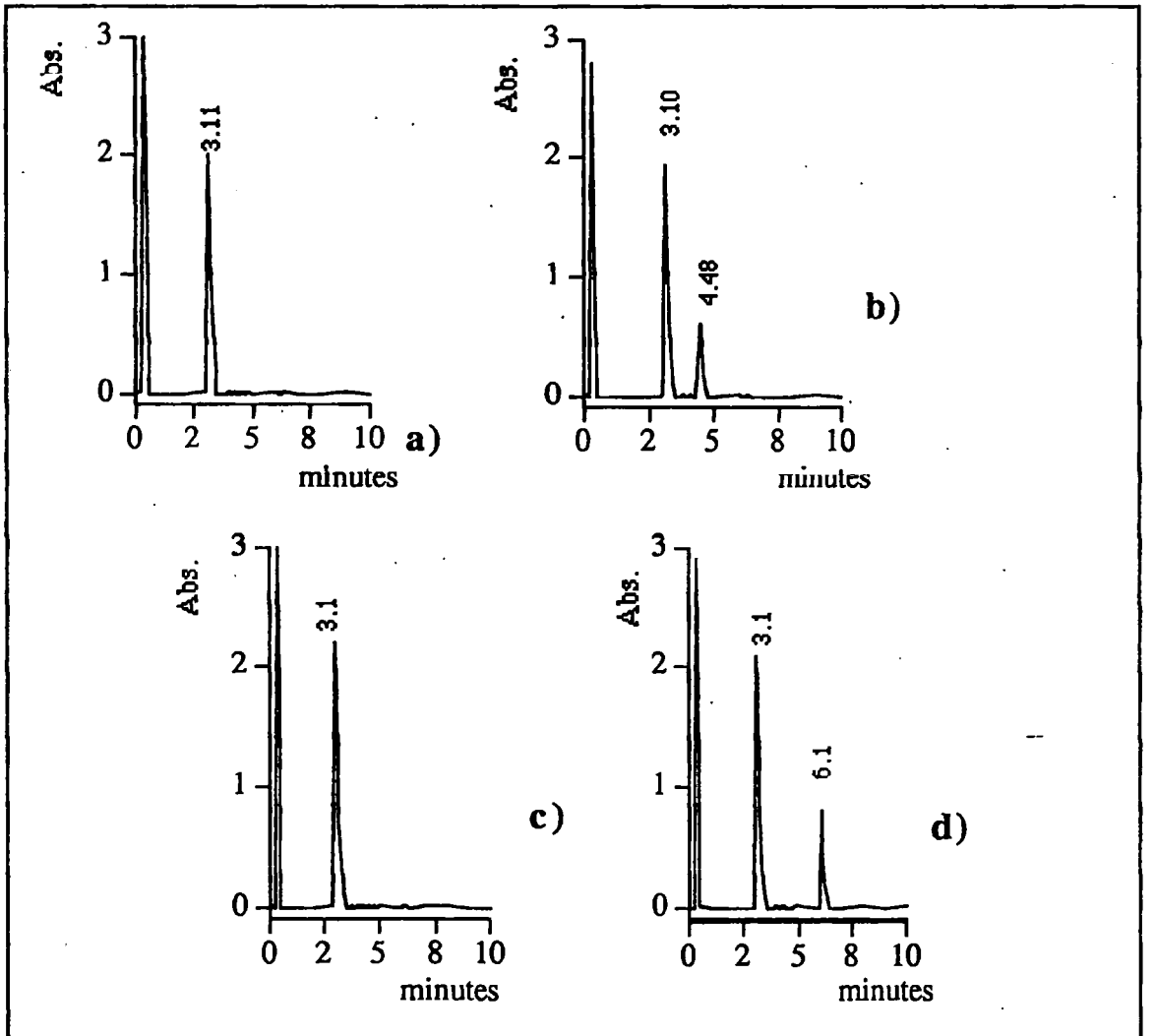

Figure 6.14 HPLC chromatograms of samples obtained from 30 minute microsomal incubations of 10 mM DMF and DMAC: a): microsomal oxidation system and 10 mM DMF at reaction time 0 minutes, b) microsomal oxidation system and 10 mM DMF at reaction time 30 minutes, c) microsomal oxidation system and 10 mM DMAC at reaction time 0 minutes, and d) microsomal oxidation system and 10 mM DMAC at reaction time 30 minutes

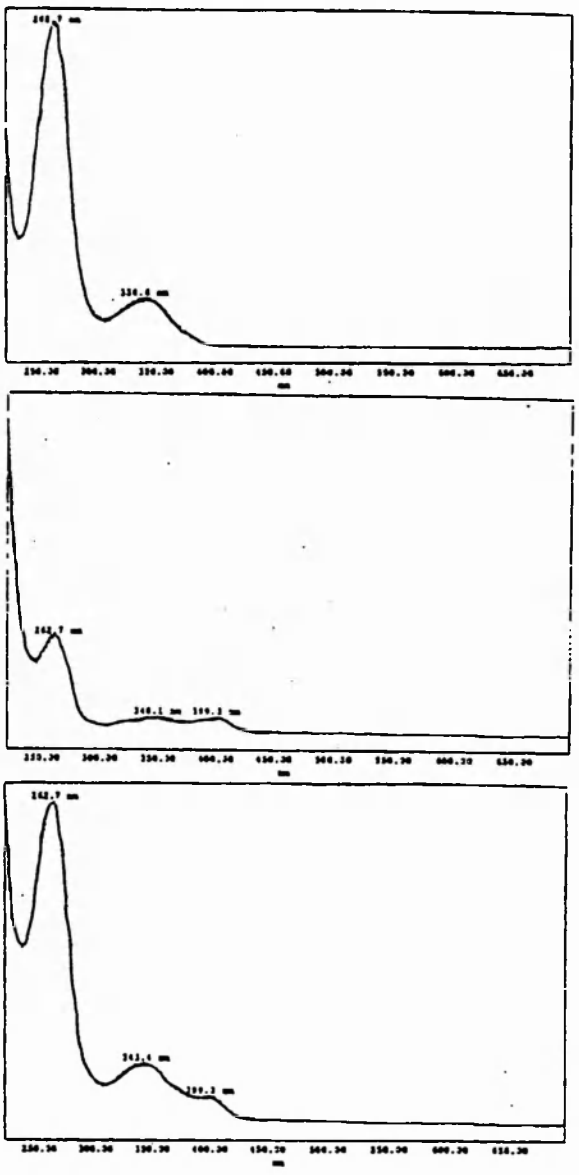

a)

b)

c)

Figure 6.15 UV/VIS spectra of the DMF and DMAC metabolism-dependent haem modified products and of pure haem standard: a) compound with retention time 4.48 minutes of chromatogram b) of Figure 6.14, b) compound with retention time 6.12 minutes of chromatogram d) of Figure 6.14, and c) pure haem.

Attempts to purify and characterise the modified haem products proved unsuccessful. However, a series of indirect observation into the nature of these compounds were obtained.

It seems plausible to assume that the α- carbon-centred radical species are responsible of the observed inactivation of the metabolising enzyme. So, these radicals

were chemically generated, by the methods outlined in reaction 6.A and 6.B (but omitting PBN), in the presence of haem. The products of these reactions were analysed by HPLC. The results obtained are illustrated in Figure 6.16.

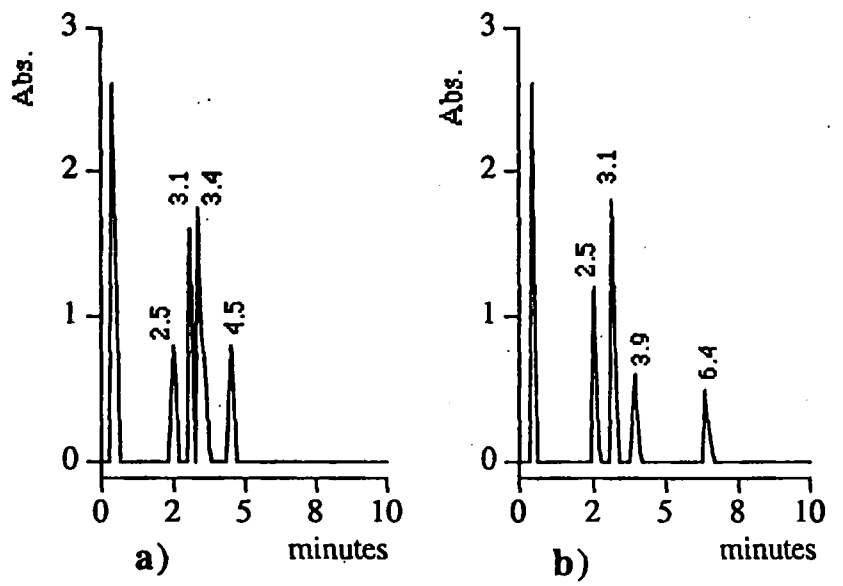

Figure 6.16 HPLC chromatograms of the reaction between the chemically generated carbon-centred radicals and haem: a) from DMF, b) from DMAC.

The peak with a retention time of 3.10 minutes, present in both chromatograms, corresponds to the unchanged haem. The reaction of the DMF and DMAC derived carbon-centred radicals with haem gives rise to three modified haem products for each reaction. The product from the DMF reaction with a retention time of 4.48 minutes, and that from the DMAC reaction with a reaction time of 6.43 minutes, present identical UV/VIS spectra (Figure 6.17) to those produced in the microsomal incubation of DMF and DMAC.

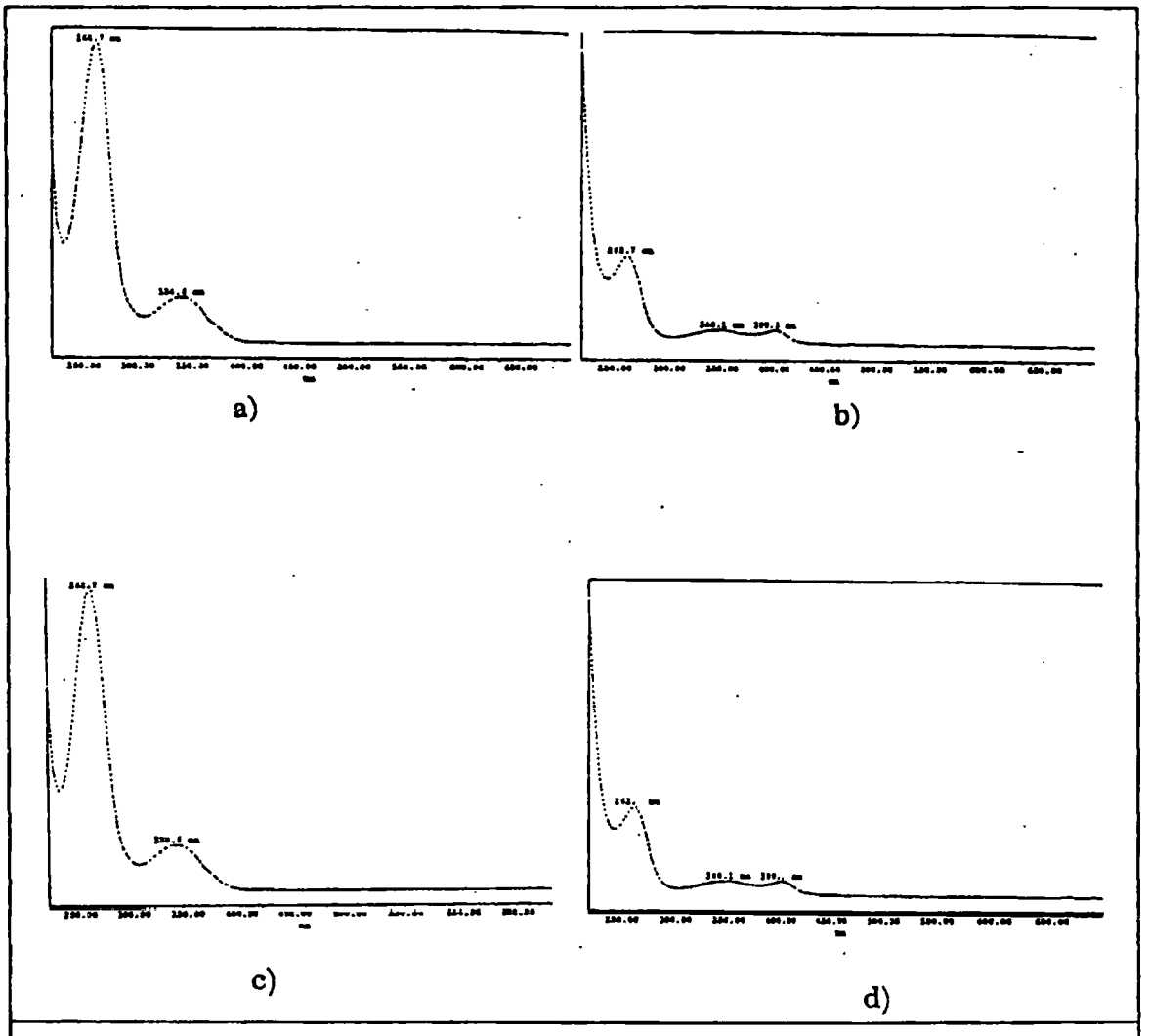

Figure 6.17 Comparison of the UV/VIS spectra of the modified haem compounds obtained from the reaction between the DMF and DMAC chemically generated carbon-centred radicals and haem (spectra a) and b)), with the corresponding haem modified products formed in the microsomal oxidations of DMF and DMAC (spectra c) and d)).

That reaction of the chemically generated radicals with haem produces three modified haem products, whereas the microsomal reactions produces only one modified haem product, is probably due to the availability, in the chemical reaction all the potentially attachable sites for the radical in the haem. In microsomal reactions, the apoprotein "protects" some of the haem sites from attack. In fact, a regioselectivity is reported for the modification of haem in many metabolism-based inactivations of P450.[41;46] Covalent modification of the haem can arise by the attack of radical species at three different point of the haem molecule (Figure 6.18).[41;44;46]

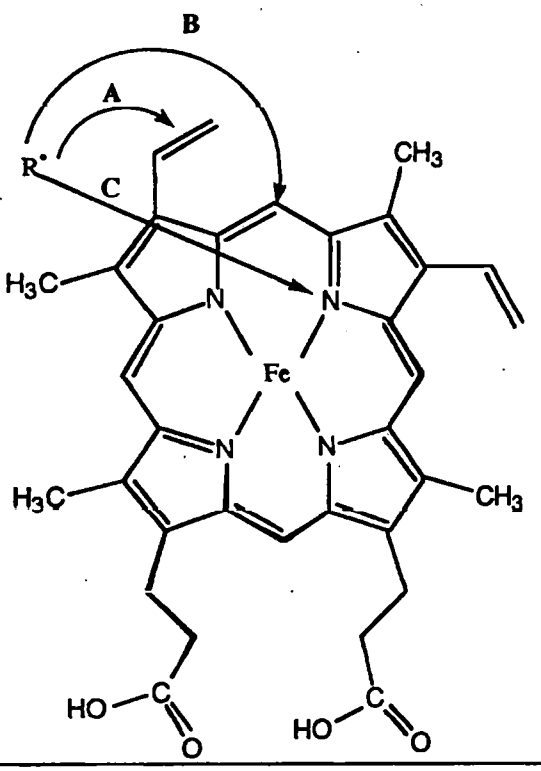

Figure 6.18 Potential sites for covalent modification of haem by radical species.

The addition to the nitrogen atom of the haem of the carbon-centred radical generated from DMF and DMAC (route C) generates an aminal functionality:

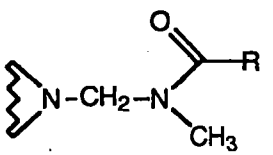

Addition to the haem by routes A and B, involving C-C bond formation, should generate relatively stable compounds. Thus, the samples obtained from microsomal incubation of DMF and DMAC were then analysed by HPLC both before and after treatment with 1M hydrochloric acid. The samples obtained from the reactions between the chemically generated radicals of DMF or DMAC and haem were similarly analysed. The results are illustrated in Figures 6.19 and 6.20, respectively.

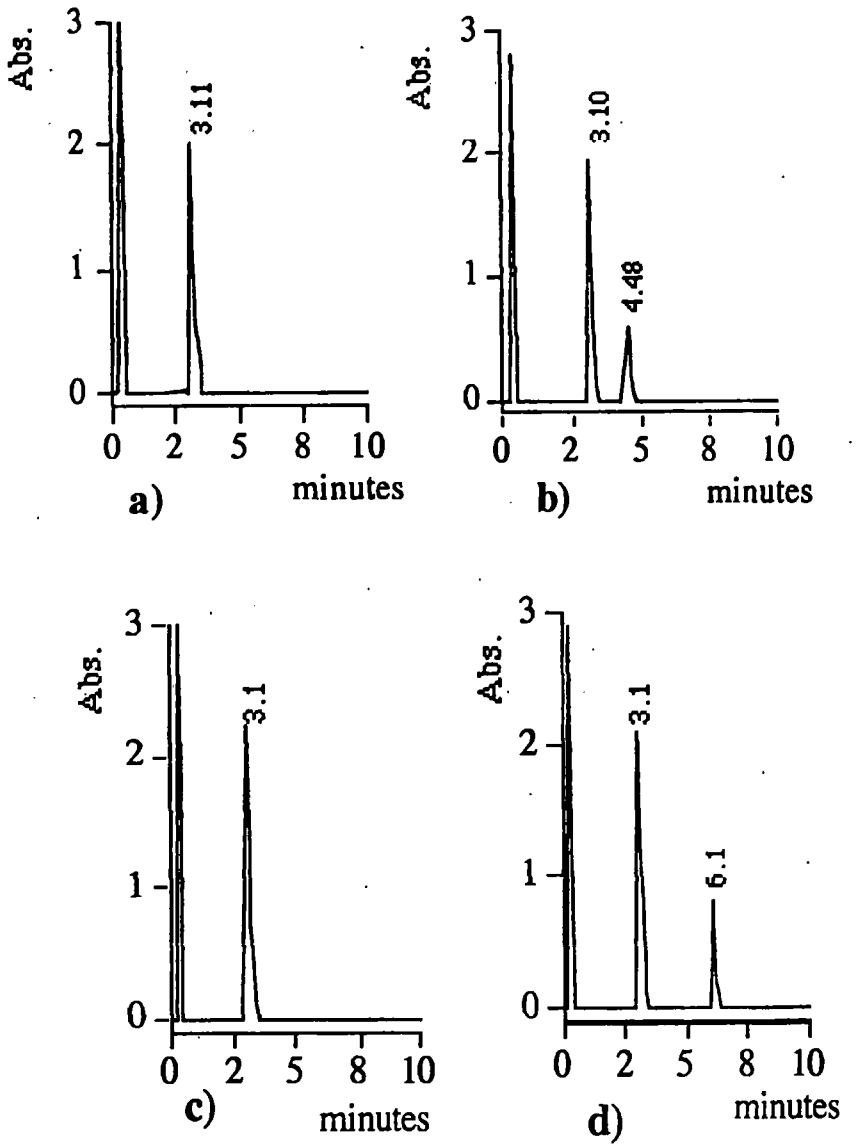

Figure 6.19. HPLC analysis of the samples obtained from microsomal incubations of DMF and DMAC, before and after 1M hydrochloric acid treatment: a) microsomes and DMF without acid treatment, b) microsomes and DMF after acid treatment, c) microsomes and DMAC without acid treatment, d) microsomes and DMAC after acid treatment.

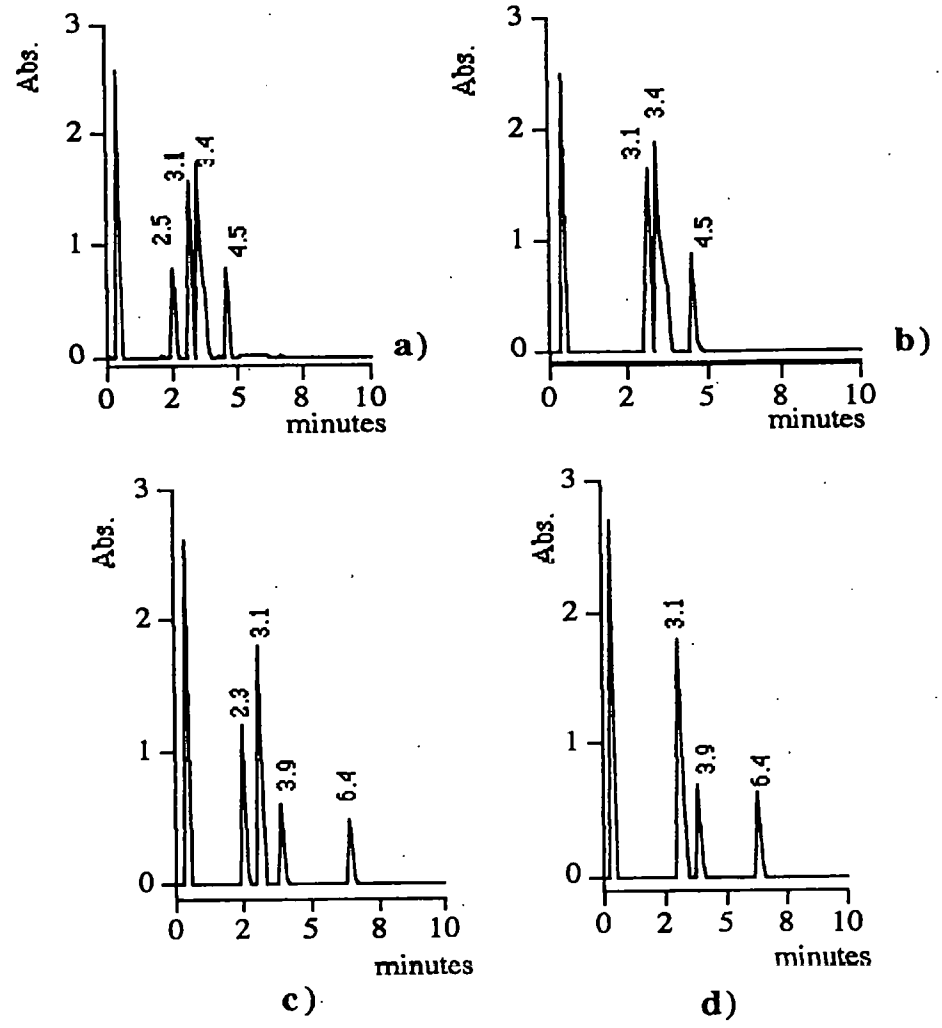

Figure 6.20 HPLC analysis of the samples obtained from the reaction between the DMF and DMAC chemically generated carbon centred radical and haem, before and after 1M hydrochloric acid treatment: a) DMF radical and haem without acid treatment, b) DMF radical and haem after acid treatment, c) DMAC radical and haem without acid treatment, d) DMAC radical and haem after acid treatment.

The acid treatment of the modified haem obtained from the reaction of the chemically generated DMF and DMAC radicals with haem results in the disappearance of the peak with retention time *ca.* 2.5 minutes for both DMF and DMAC radical. Similar acid treatment of the sample obtained from microsomal incubations does not result in any modification of the HPLC chromatograms. These results suggest that the 2.5 minutes peaks correspond to haem modified at one or more nitrogen atom of the tetrapyrrolic ring. Thus, the modified haem originating from the microsomal oxidation of DMF and DMAC is probably the result of radical addition at the vinyl or *meso* positions.

6.5.3 Effect of PBN, glutathione (GSH), CO and vitamin C on the inactivation of P450 and loss of haem

The final part of this study of the metabolism-based inactivation of P450 during the microsomal oxidation of DMF and DMAC involved the effects of the enzyme inhibitor CO and of various radical trapping agents.

Microsomal oxidations of DMF and DMAC were performed in the presence and absence of saturating concentrations of CO. The P450 content was quantified at the end of the reaction period by the method of Omura and Sato.[40] Table 6.16 summarises the results obtained after 15 minutes incubation of 10 mM DMF and DMAC.

Incubation	[P450] (nmoles/ml)	Loss %
Control	1.85 ± 0.03	0.00
+ DMF	1.29 ± 0.04	30.3 *
+ DMF + CO	1.81 ± 0.08	2.2 NS
+ DMAC	1.40 ± 0.02	24.4 *
+ DMAC + CO	1.86 ± 0.05	0.00

NS not significant, * $P < 0.001$, Student's t test.

Table 6.16 Effect of a saturating concentration of CO on the metabolism-dependent inactivation of P450 incubations of 10 mM DMF and DMAC for 15 minutes. Control incubations are constituted by microsomes and NADPH regenerating system.

Not surprisely, the presence of a saturating concentration of CO completely inhibits the inactivation of the enzyme, due the well known inhibitory effect of CO on the P450 metabolism. The results confirm that the metabolic transformation of the substrates is required for the inactivation of the enzyme.

The effects of radical trapping agents on the loss of microsomal haem during substrate oxidation was then investigated. Microsomal incubations of 10 mM DMF and DMAC were performed for 15 minutes in the presence and absence of 5 mM PBN, 10 mM GSH and 10 mM vitamin C. The results are summarised in Table 6.17.

Incubation	[Haem] (nmoles/ml)	Loss %
Control	2.67 ± 0.03	0.00
+ DMF	2.10 ± 0.05	21.4 **
+ DMF + PBN	2.44 ± 0.04	8.6 *
+ DMF + GSH	2.11 ± 0.06	21.0 **
+ DMF + Vitamin C	2.09 ± 0.03	21.7 **
+ DMAC	2.28 ± 0.02	14.6 **
+ DMAC + PBN	2.50 ± 0.03	6.4 *
+ DMAC + GSH	2.26 ± 0.04	15.4 *
+ DMAC + Vitamin C	2.29 ± 0.04	14.2 *

* $P < 0.01$, ** $P < 0.001$, Student's *t* test.

Table 6.17 Effects of 5 mM PBN, 10 mM GSH and 10 mM vitamin C on the loss of microsomal haem after 15 minute incubations of 10 mM DMF and DMAC. Control is constituted by microsomes and NADPH regenerating system. Incubation in presence of PBN, GSH and vitamin C but in absence of substrate does not result in any change of the microsomal haem content.

Neither GSH nor vitamin C are effective in preventing the loss of microsomal haem. Incubations involving different concentrations of GSH and vitamin C do not result in any protection of haem loss occurring. However, the presence of PBN results in a protection of the loss of haem by about 50 %. Since it is reported that PBN interacts with P450,[50] it is possible that inhibition of the substrate metabolism is responsible for the decrease in inactivation of the haem. This possibility can be ruled out on the basis of the data in Chapter 3 on the effect of PBN on the metabolism of N,N-dimethyl benzamide. The inability of GSH and vitamin C to prevent haem loss is probably due to their increased hydrophilicity compared with PBN and consequent reduced access to the active site of the enzyme.

6.6 Conclusions

It has been widely reported that the *in vivo* and *in vitro* metabolism of DMF and DMAC occurs *via* P450-mediated hydroxylation of the carbon α- to nitrogen leading to the formation of an N-hydroxylmethyl-N-methylamide.[14;16] The *in vivo* metabolism of DMF also occurs *via* oxidation of the carbonyl moiety of the substrate, resulting in the

formation of thiocarbamates that are believed to be major species responsible of the metabolism-dependent toxicity of this compound.[14] However, such a metabolic route has not been reported *in vitro*.[14] The P450 isoenzyme involved in the oxidation of DMF and DMAC is reported to be the ethanol-induced P4502E1.[16;26] From the data obtained in the present study, it appears that the metabolism of DMAC is approximately 4 times greater than that of DMF. No oxidation of the carbonyl moiety of DMF was observed under any of the experimental conditions used during this study. This result is not too surprising, as it has been reported that N-methyl oxidation of DMF is 20 times more efficient than oxidation of the carbonyl group.[14;16;27]

By using a substrate probe, structurally related to DMF, capable of trapping intramolecularly a carbon-centred radical, and by using PBN as a spin trap, the formation of a carbon-centred radical intermediate during the oxidation of DMF and DMAC has been demonstrated. The intermediates were identified as the radicals centred on the α-carbon (Figure 6.21).

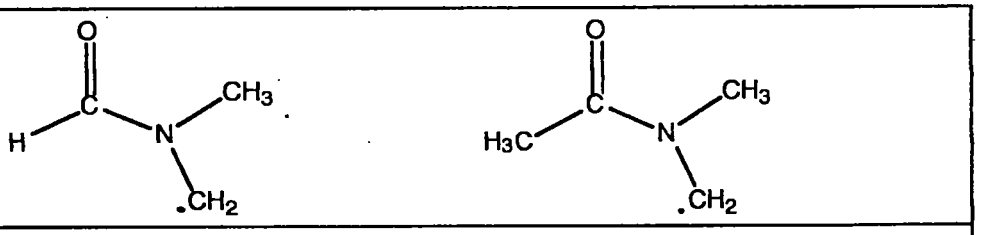

Figure 6.21 Carbon-centred radical intermediates identified during the microsomal oxidation of DMF and DMAC.

It is concluded that microsomal oxidation of DMF and DMAC occurs *via* hydrogen atom abstraction from the α-carbon leading to the formation of a carbon-centred radical intermediate. This intermediate can undergo either hydroxyl group insertion from the P450 haem-activated oxygen complex to give an N-hydroxylmethyl-N-methylamide product, or it can attack the haem leading to inactivation of the enzyme. Indeed, microsomal oxidations of DMF and DMAC results in metabolism-dependent inactivation of P450, that is completely inhibited by the presence of a saturating concentration of CO. The target of the radical species is the haem prosthetic group of the enzyme. P450

inactivation is due to a modification of the haem moiety without destruction of its protoporphyrin IX tetrapyrrolic structure. Reactions of chemically generated carbon-centred radicals with haem results in the formation of identical haem modified products. The presence of the spin trapping agent, PBN, in the microsomal incubation of the substrates significantly protects against the loss of haem. The hydrophilic radical trapping agents, GSH and ascorbic acid, completely fail to prevent the haem modification during these microsomal oxidations. The structure of the modified haem products formed during the microsomal oxidations of DMF and DMAC remains to be investigated. The evidence available from the current study implies a compound that retains its tetrapyrrolic structure and which is modified at the vinyl or *meso* positions rather than at a pyrrole N-atom. Further investigation is needed to isolate and characterise these P450-derived DMF- and DMAC-dependent haem products.

On the basis of these results a scheme for the metabolism of DMF and DMAC is proposed in Figure 6.22.

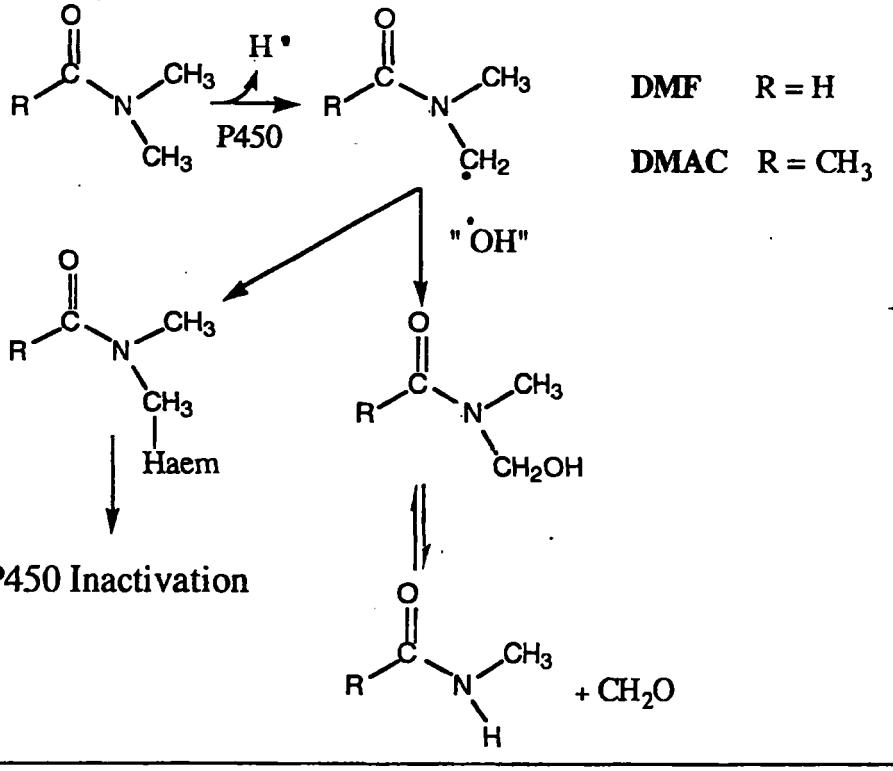

Figure 6.22 Proposed mechanism for the P450-dependent metabolism of DMF and DMAC.

6.7 References

1 Gescher A., (1990); In: *Ethel Browing's Toxicity and Metabolism of Industrial Solvents*; (Buhler D.R. and Reed D.J. Eds.); Vol.**2**: 149-; Elsevier, Amsterdam.

2 Kennedy G.L., (1986); *Crit. Rev. Toxicol.*; **17**: 129-

3 Chivers, C.P., (1978); *Lancet*;; **8059**: 331

4 Lyle W.H., Spence T.W.M., McKinneley W.M. and Duckers K., (1979); *Br. J. Ind. Med.*; **36**: 63-

5 Tomasini M., Todaro A., Piazzoni M. and Peruzzo G.F., (1983); *Med. Lav.*; **74**: 217-

6 Cox N.H. and Mustchin C.P., (1991); *Contact Dermatitis*; **24**: 69-

7 Ducatman A.M., Conwill D.E. and Crawl J., (1986); *J. Urol.*; **136**: 834-

8 Levin S.M., Baker D.B., Landrigan P.J., Monaghan S.V., Frumin E., Braithwaite M. and Towne W., (1987); *Lancet* ; **8568**: 1153-

9 Chen J.L.,Fayerwezther W.E. and Pell S., (1988); *J. Occup. Med.*; **30**: 813-

10 Walrath J., (1989); *J. Occup. Med.*; **31**: 432-

11 Horn H.J., (1963); *Toxicol. Appl. Pharmacol.*; **3**: 12-

12 Kennedy G.L. and Sherman H., (1984); *Drug Chem. Toxicol.*; **9**: 147-

13 Corsi G.C., (1971); *Med. Lav.*; **62**: 28-

14 Gescher A., (1993); *Chem. Res. Toxicol.*; **6**: 245-

15 Barnes J.R. and Ranta K.E., (1972); *Toxicol. Appl. Pharmacol.*; **23**: 271-

16 Mraz J., Jheeta P., Gescher A., Hyland R., Thummel K. and Threadgill M.D., (1993); *Chem. Res. Toxicol.*; **6**: 197-

17 Menicagli S., Longo V., Mazzacaro A. and Gervasi P.G., (1994); *Biochem. Pharmacol.*; **48**, 4: 717-

18 Kestell P., Gill M.H., Threadgill M.D., Gescher A., Howarth O.W. and Curzon E.H., (1986); *Life Sci.*; **38**: 719-

19 Hall L.R. and Hanzlick R.P., (1991); *Xenobiotica* ; **21**, 9: 1127-

20 Hall L.R. and Hanzlick R.P., (1990); *J. Biol. Chem.* ; **265**, 21: 12349-

21 Mraz J. and Turecek F., (1987); *J. Chromatogr. Biomed. Appl.*; **414**: 399-

22 Kestell P., Gledhill A.P., Threadgill M.D. and Gescher A., (1986); *Biochem. Pharmacol.*; **35**: 2283-

23 Threadgill M.D., Axworthy D.B., Baillie T.A., Farmer P.B., Farrow K.C., Gescher A., Kestell P., Pearson P.G. and Shaw A.J., (1987); *J. Pharmacol. Exp. Ther.*; **242**: 312-

24 Cross H., Dayal R., Hyland R. and Gescher A., (1990); *Chem. Res. Toxicol.*; **3**: 357-

25 Shaw A.J., Gescher A. and Mraz J., (1988); *Toxicol. Appl. Pharmacol.*; **95**: 162-

26 Hyland R., Gescher A., Thummel K., Schiller C., Jheeta P., Mynett K., Smith A.W. and Mraz J., (1992); *Mol. Pharmacol.*; **41**: 259-

27 Van de Bulke M., Rosseel M.T., Buylaert W and Belpaire F.M., (1994); *Arch. Toxicol.*; **68**: 291-

28 Chieli E., Saviozzi M., Menicagli S., Branca T. and Gervasi P.G., (1995); *Arch. Toxicol.*; **69**: 165-

29 Imazu K., Fujishiro K. and Inoue N., (1992); *Toxicology*; **72**: 41-

30 Imazu K., Fujishiro K. and Inoue N., (1992); *Fukuoka Acta Med.*; **85**: 147-

31 Giese B., (1985); *Angew. Chem. Int. Ed. Engl.*; **24**: 553-

32 Giese B., (1985); *Tetrahedron*; **41**: 3887-

33 Beckwith A.L.J.and Schieser C.H., (1985); *Tetrahedron*; **41**: 3925-

34 Beckwith A.L.J. and Meijs J., (1979); *J.Chem. Soc. Perkin Trans. 2*; 1535-

35 Beckwith A.L.J., Phillipou G. and Serelis A.K. (1981); *Tetrahedron Lett.*; **22**: 2811-

36 Bachi M.D., Frolow F. and Hoornoert C., (1983); *J. Org. Chem.*; **48**: 1841-

37 Burnett D.A.; Choi J.K., Hart D.J. and Tsai Y.M., (1981); *J. Am. Chem. Soc.*; **106**: 8201-

38 Julia M., (1971); *Acc. Chem. Res.*; **4**: 386-

39 Julia M., (1974); *Pure Appl. Chem.*; **40**: 553-

40 Omura T. and Sato R., (1964); *J. Biol. Chem.*; **239**: 2370-

41 Ortiz de Montellano P.R., (1990); *Pharmac. Ter.* 48: 95-

42 Ortiz de Montellano P.R. and Mico B.A., (1980); *Mol. Pharmacol.* **18**: 128-

43 Ortiz de Montellano P.R. and Mico B.A. (1981); *Arch. Biochem. Biophys.*; **206**: 43-

44 De Matteis F. and Gibbs A.H., (1980); *Biochem. J.*; **187**: 285-

45 De Matteis F., Gibbs A.H., Jackson A.H. and Weerasinghe S., (1980); *FEBS Letters;* **119**: 109-

46 Osawa Y. and Pohl L.R., (1989); *Chem. Res. Toxicol.* ; **2**: 131-

47 Paul K.G., Theorell H. and Akeson A., (1953); *Acta. Chem. Scand.*; **7**: 1284-

48 Morrison G.R., (1965); *Anal. Chem.*; **37**: 1124-

CHAPTER 7

Metabolism-dependent inactivation of microsomal P450 by tertiary amides

The present chapter will describe the studies related to the effects of the P450-dependent metabolism of tertiary amides on the enzyme itself.

7.1 Introduction

It has been reported that the time-course of the microsomal metabolism of tertiary amides presents a bilinear progress characterised by an initial short-lived (< 5 minutes) burst followed by a longer linear phase with lower rate of oxidation.[1] Similar bilinear progress curves have been observed also for the oxidation of halobenzenes by phenobarbital-induced rat liver microsomes.[2;3] The origin of this effect can be attributed to two mechanisms

- enzyme inactivation, or
- the presence of a minor but kinetically significant isoenzyme of the P450.

The latter hypothesis was proposed to occur during the microsomal metabolism of N,N-dimethylbenzamide.[1] This hypothesis was based on the supposition that there is no obvious way to generate a particularly reactive metabolite from N,N-dialkylamides.[3] However, the data reported in Chapter 6 indicate that, during the microsomal oxidation of N,N-dimethylformamide and N,N-dimethylacetamide, P450 undergoes inactivation. The results imply that the metabolism-based inactivation of the enzyme is due to the covalent modification of its prosthetic haem group by the carbon-centred radical intermediates formed during the reaction.

Here the effects of the microsomal metabolism of other N,N-dialkylamides on P450 are examined. The substrates used were N,N-dimethylbenzamide (DMB) and N-benzyl-N-methylbenzamide (BMB) (Figure 7.1). Given that the N-benzyl group is much

more reactive than N-methyl,[1] and that the benzylic- carbon-centred radical intermediate should be more stable due to resonance stabilisation, it might be expected that the inactivation of P450 by this substrate should be more marked.

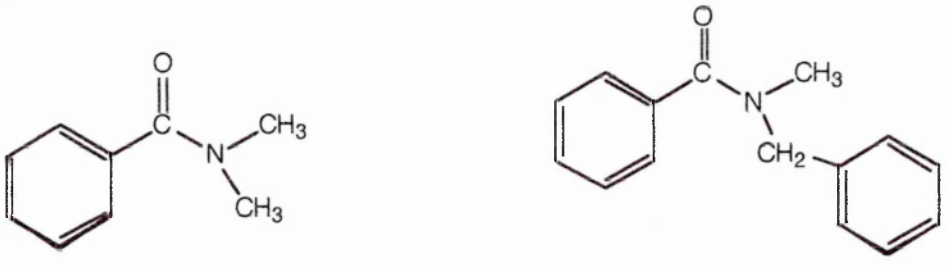

N,N-dimethylbenzamide (DMB) **N-benzyl-N-methylbenzamide (BMB)**

Figure 7.1 Substrates used in the present study.

7.2 Inactivation of P450

Following incubation of phenobarbital-induced rat liver microsomes with the appropiate substrate, the P450 content was measured from the reduced spectrum of the P450-CO complex, as described by Omura and Sato.[4] Initially, the concentration of the enzyme was monitored over 2 hour microsomal incubations of 5 mM DMB and BMB (Figure 7.2).

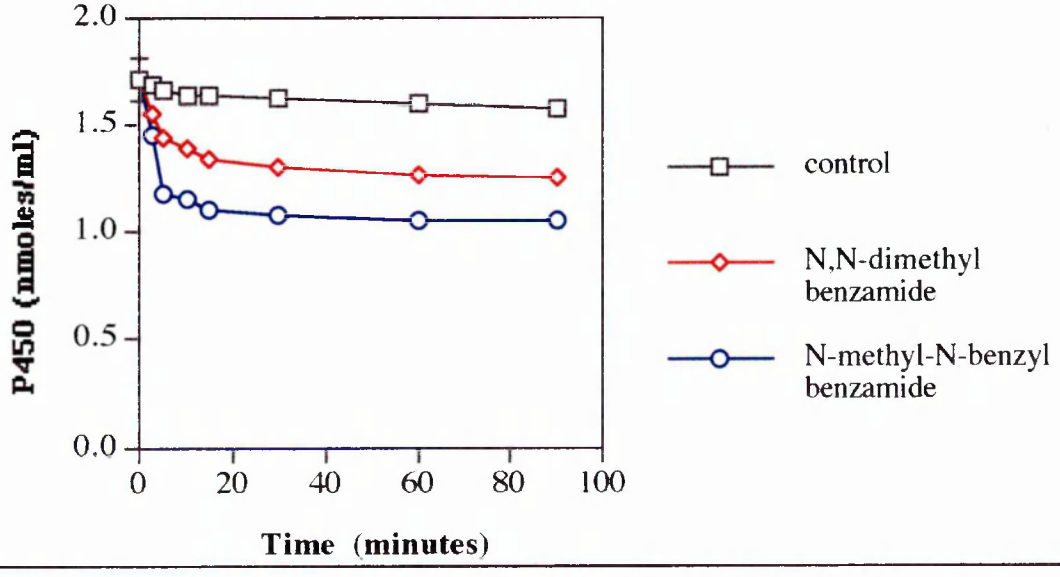

Figure 7.2 Time-course for the inactivation of P450 during the microsomal oxidation of 5 mM N,N-dimethylbenzamide and N-benzyl-N-methylbenzamide.

more reactive than N-methyl,[1] and that the benzylic- carbon-centred radical intermediate should be more stable due to resonance stabilisation, it might be expected that the inactivation of P450 by this substrate should be more marked.

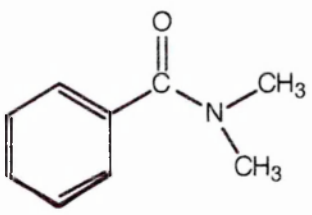

N,N-dimethylbenzamide (DMB)

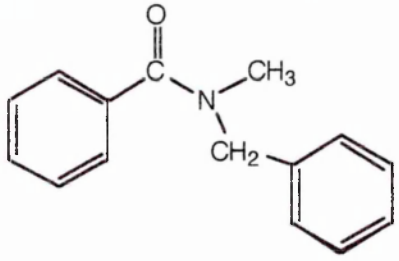

N-benzyl-N-methylbenzamide (BMB)

Figure 7.1 Substrates used in the present study.

7.2 Inactivation of P450

Following incubation of phenobarbital-induced rat liver microsomes with the appropiate substrate, the P450 content was measured from the reduced spectrum of the P450-CO complex, as described by Omura and Sato.[4] Initially, the concentration of the enzyme was monitored over 2 hour microsomal incubations of 5 mM DMB and BMB (Figure 7.2).

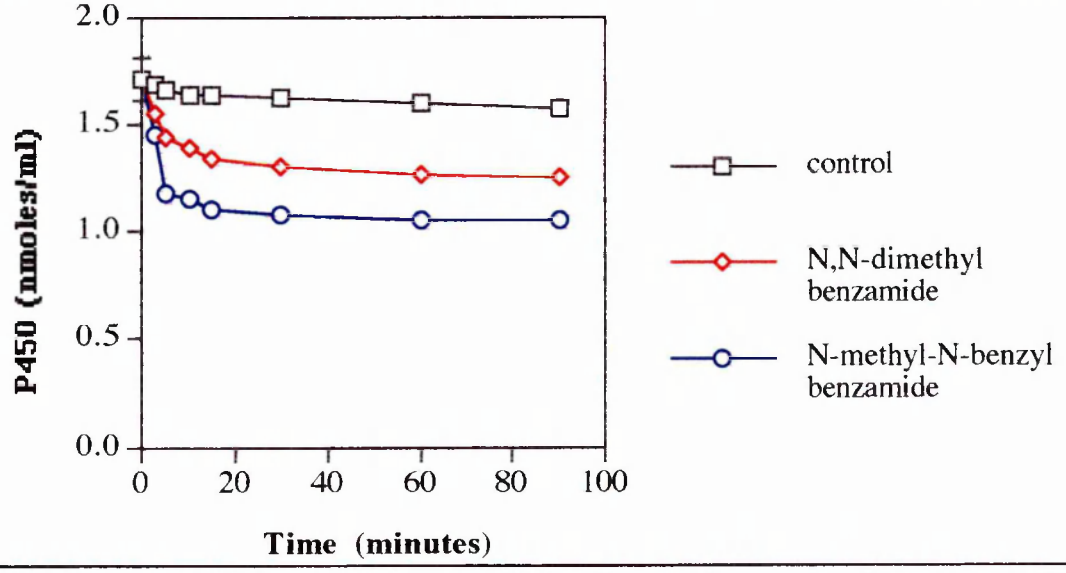

Figure 7.2 Time-course for the inactivation of P450 during the microsomal oxidation of 5 mM N,N-dimethylbenzamide and N-benzyl-N-methylbenzamide.

more reactive than N-methyl,[1] and that the benzylic- carbon-centred radical intermediate should be more stable due to resonance stabilisation, it might be expected that the inactivation of P450 by this substrate should be more marked.

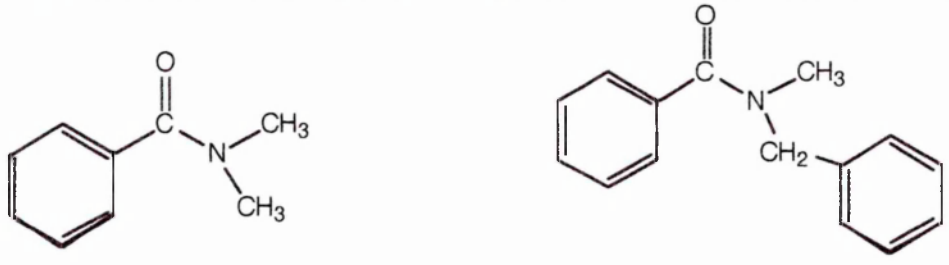

N,N-dimethylbenzamide (DMB) **N-benzyl-N-methylbenzamide (BMB)**

Figure 7.1 Substrates used in the present study.

7.2 Inactivation of P450

Following incubation of phenobarbital-induced rat liver microsomes with the appropiate substrate, the P450 content was measured from the reduced spectrum of the P450-CO complex, as described by Omura and Sato.[4] Initially, the concentration of the enzyme was monitored over 2 hour microsomal incubations of 5 mM DMB and BMB (Figure 7.2).

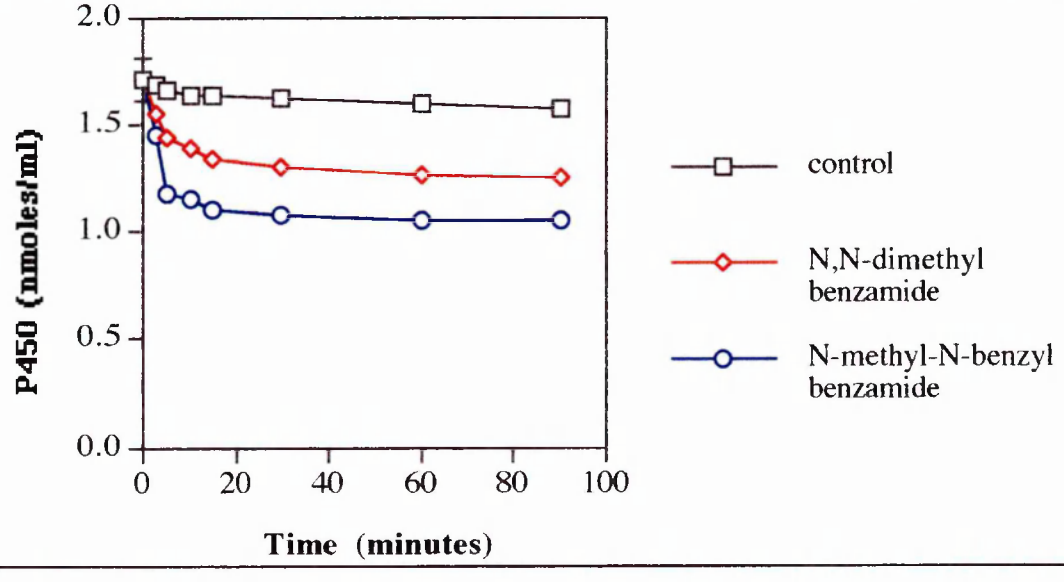

Figure 7.2 Time-course for the inactivation of P450 during the microsomal oxidation of 5 mM N,N-dimethylbenzamide and N-benzyl-N-methylbenzamide.

more reactive than N-methyl,[1] and that the benzylic- carbon-centred radical intermediate should be more stable due to resonance stabilisation, it might be expected that the inactivation of P450 by this substrate should be more marked.

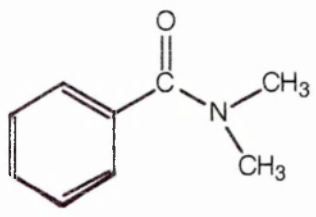

N,N-dimethylbenzamide (DMB)

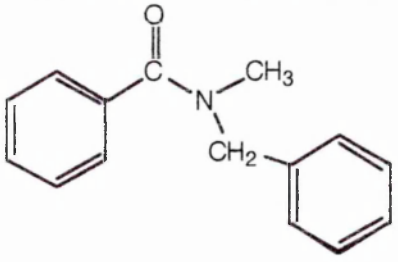

N-benzyl-N-methylbenzamide (BMB)

Figure 7.1 Substrates used in the present study.

7.2 Inactivation of P450

Following incubation of phenobarbital-induced rat liver microsomes with the appropiate substrate, the P450 content was measured from the reduced spectrum of the P450-CO complex, as described by Omura and Sato.[4] Initially, the concentration of the enzyme was monitored over 2 hour microsomal incubations of 5 mM DMB and BMB (Figure 7.2).

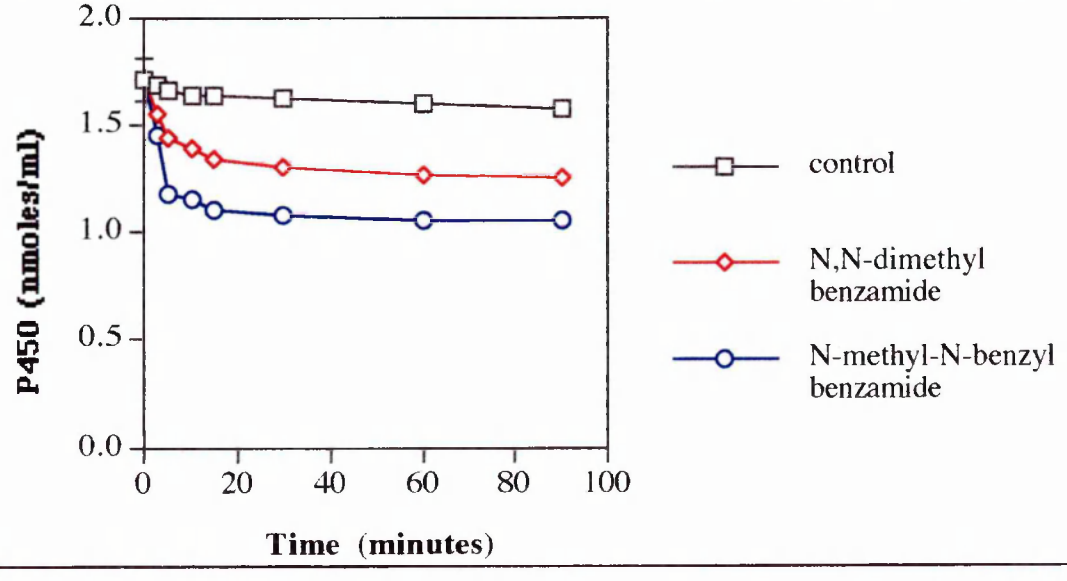

Figure 7.2 Time-course for the inactivation of P450 during the microsomal oxidation of 5 mM N,N-dimethylbenzamide and N-benzyl-N-methylbenzamide.

more reactive than N-methyl,[1] and that the benzylic- carbon-centred radical intermediate should be more stable due to resonance stabilisation, it might be expected that the inactivation of P450 by this substrate should be more marked.

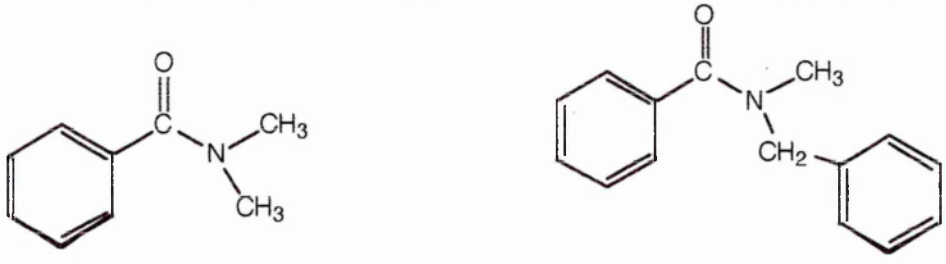

N,N-dimethylbenzamide (DMB) **N-benzyl-N-methylbenzamide (BMB)**

Figure 7.1 Substrates used in the present study.

7.2 Inactivation of P450

Following incubation of phenobarbital-induced rat liver microsomes with the appropiate substrate, the P450 content was measured from the reduced spectrum of the P450-CO complex, as described by Omura and Sato.[4] Initially, the concentration of the enzyme was monitored over 2 hour microsomal incubations of 5 mM DMB and BMB (Figure 7.2).

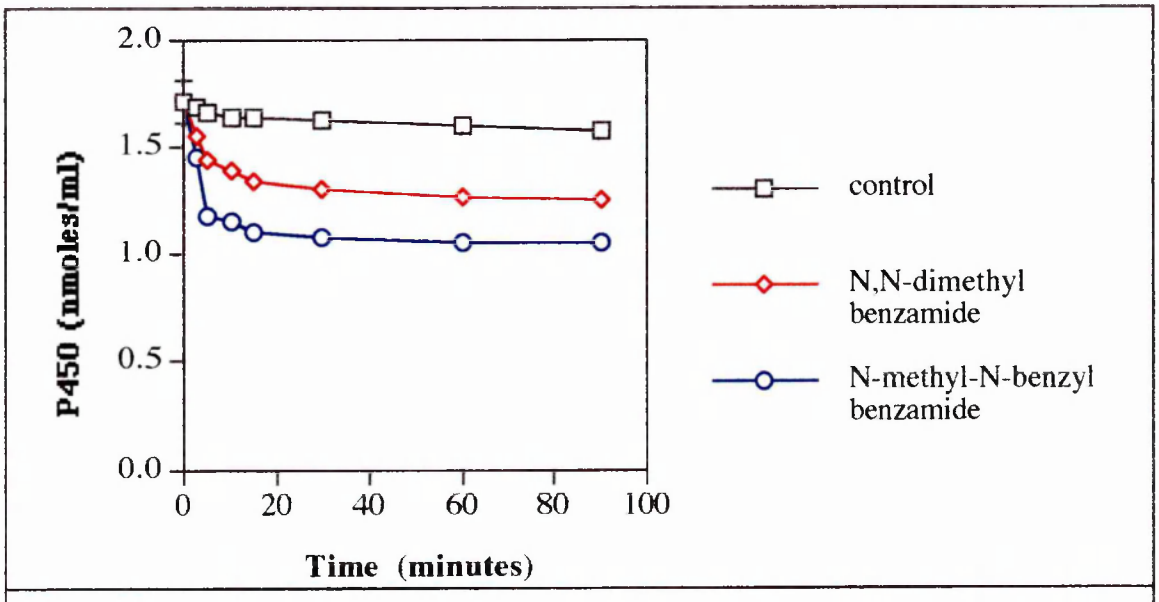

Figure 7.2 Time-course for the inactivation of P450 during the microsomal oxidation of 5 mM N,N-dimethylbenzamide and N-benzyl-N-methylbenzamide.

more reactive than N-methyl,[1] and that the benzylic- carbon-centred radical intermediate should be more stable due to resonance stabilisation, it might be expected that the inactivation of P450 by this substrate should be more marked.

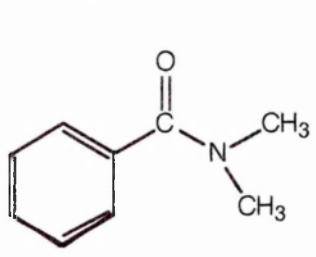

N,N-dimethylbenzamide (DMB)

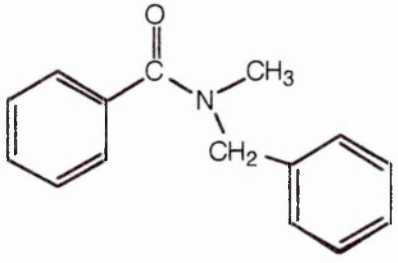

N-benzyl-N-methylbenzamide (BMB)

Figure 7.1 Substrates used in the present study.

7.2 Inactivation of P450

Following incubation of phenobarbital-induced rat liver microsomes with the appropiate substrate, the P450 content was measured from the reduced spectrum of the P450-CO complex, as described by Omura and Sato.[4] Initially, the concentration of the enzyme was monitored over 2 hour microsomal incubations of 5 mM DMB and BMB (Figure 7.2).

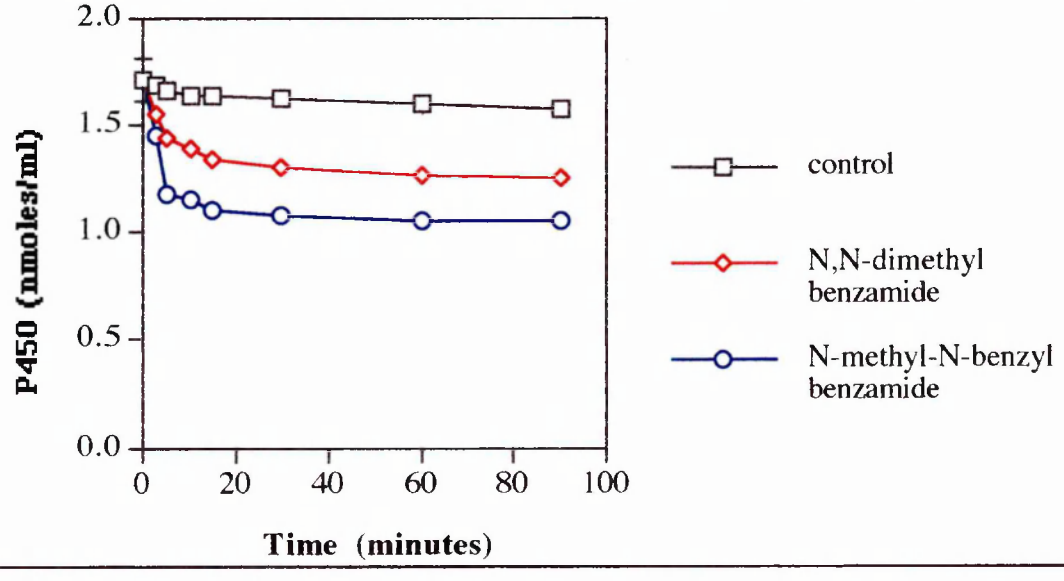

Figure 7.2 Time-course for the inactivation of P450 during the microsomal oxidation of 5 mM N,N-dimethylbenzamide and N-benzyl-N-methylbenzamide.

Microsomal metabolism of DMB and BMB results in time-dependent inactivation of P450. The inactivation of the enzyme occurs within the first 5 minutes of the reaction, subsequently reaching a plateau where not significant further loss is observed.

Subsequently, to quantify the metabolism-dependent inactivation of P450, a dose-dependence analysis was performed by incubating phenobarbital-induced rat liver microsomes for 15 minutes in presence of a range of substrate concentrations between 0.5 and 20 mM. The results (Table 7.1) show a dose-dependent inactivation of P450 that progresses linearly up to a substrate concentration of 10 mM; thereafter, an increase in the concentration of the amides beyond 10 mM produces smaller increase in the extent of enzyme inactivation. More especially, enzyme inactivation by BMB is greater by a factor of *ca.* 2.

	[P450] (nmoles/ml)		Loss %	
Incubations	**DMB**	**BMB**	**DMB**	**BMB**
Control	1.67 ± 0.08	1.67 ± 0.08	0.00	0.00
+ Sub. 0.5 mM	1.60 ± 0.06	1.49 ± 0.05	4.2 *	10.8 **
+ Sub. 1.0 mM	1.50 ± 0.04	1.30 ± 0.03	10.2 **	22.2 ***
+ Sub. 5.0 mM	1.39 ± 0.03	1.10 ± 0.04	16.8 ***	34.2 ***
+ Sub. 10 mM	1.36 ± 0.05	1.07 ± 0.06	18.6 ***	36.0 ***
+ Sub. 20 mM	1.35 ± 0.06	1.08 ± 0.04	19.2 ***	35.4 ***

* $P < 0.05$, ** $P < 0.01$, *** $P < 0.001$, Student's *t* test.

Table 7.1 Dose-dependent inactivation of P450 during 15 minute microsomal incubations of DMB and BMB.

The greater extent of inactivation of P450 by BMB, compared to that by DMB, can be ascribed to a higher degree of metabolism of BMB. Indeed, for the *para*-chloro analogue of BMB, N-dealkylation is preferred to N-demethylation.[3] To examine whether

the higher production of carbon-centred radical intermediates, is related to the different extent of P450 inactivation, the rate and the time-course of the microsomal metabolism of the substrates was then analysed. The results obtained are reported in Table 7.2 and Figure 7.3.

	v_i (μmoles/min/nmoles P450)		
Substrate	**Total metabolism**	**N-demethylation**	**N-dealkylation**
DMB	51.6± 2.5	25.8 ± 1.9	----
BMB	70.0 ± 3.6	15 ± 1.2	55 ± 2.3

Table 7.2 Rate of microsomal metabolism of DMB and BMB.

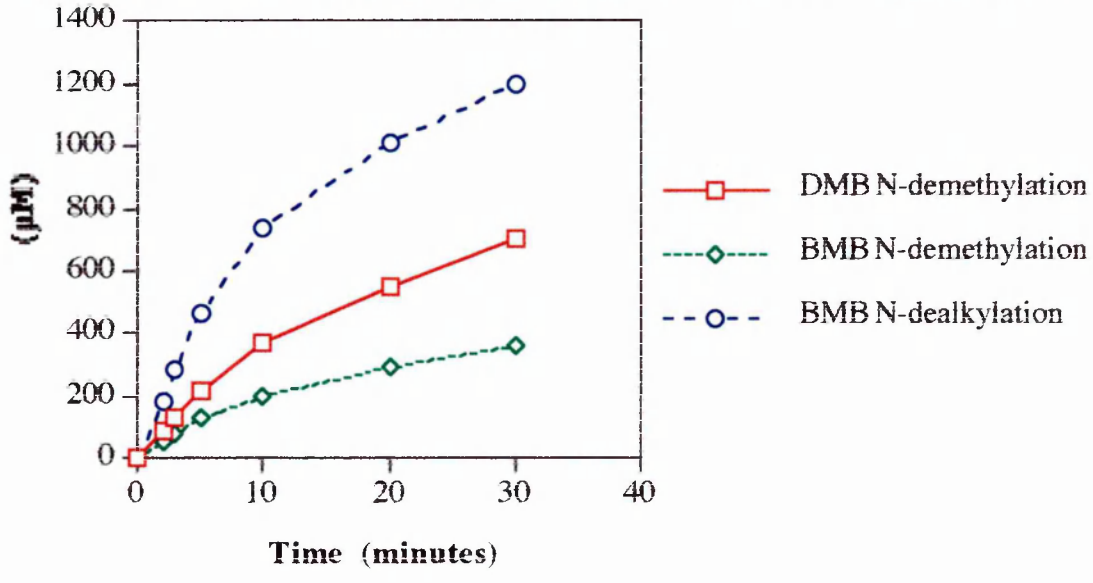

Figure 7.3 Time-course for the microsomal metabolism of 5 mM DMB and BMB.

Both inactivation of enzyme and rate of substrate metabolism exhibit an initial burst in the first five minutes of the reactions. Possibly, the initial high rate of metabolism results in an inactivation of the enzyme which effects the overall rate of metabolism of the substrate. Alternatively, the substrate may have high affinity for an isoform of P450 that is particularly sensitive of metabolism-based inactivation.

7.3 Loss of microsomal haem

Following, microsomal incubations of DMB and BMB, the haem content was measured by the pyridine/haemochromogen method[5] and by the fluorimetric determination of the protoporphyrin IX,[6] as described in the experimental section. The concentration of haem was monitored for microsomal incubations of 5 mM DMB or MBB over two hours. Subsequently, the effect of different concentrations of substrate on the microsomal haem content was analysed after incubation for 15 minutes. The results are illustrated in Figure 7.4 and summarised in Tables 7.3 and 7.4, respectively.

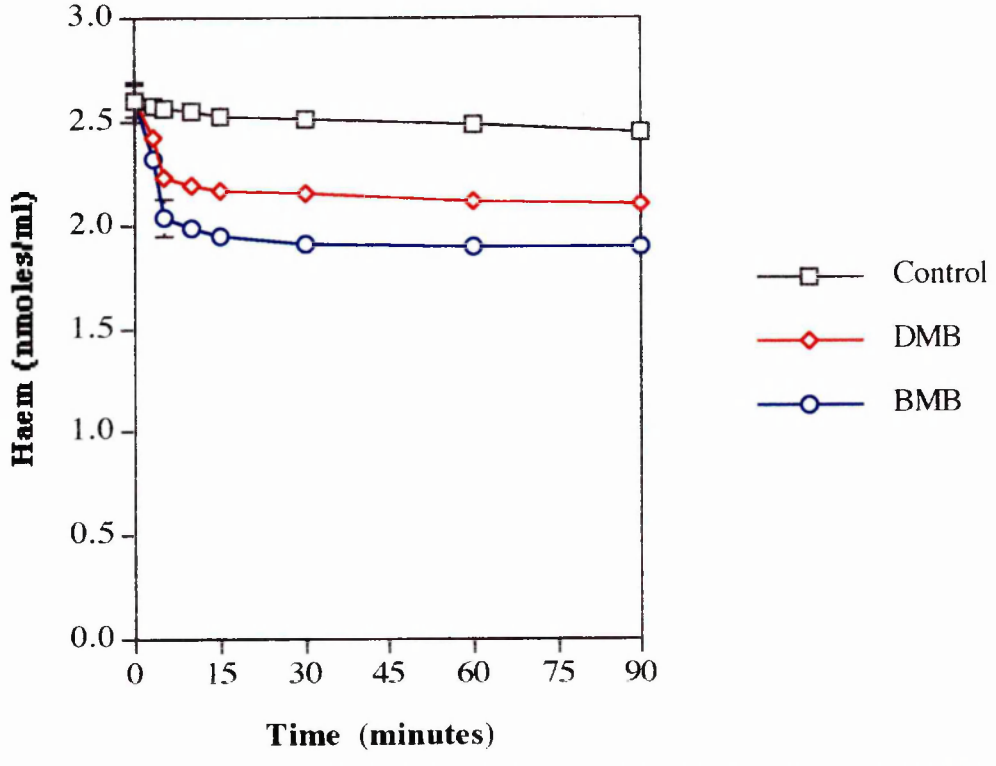

Figure 7.4 Time-course for the loss of microsomal haem during the oxidation of 5 mM N,N-dimethylbenzamide and N-benzyl-N-methylbenzamide.

	[Haem] (nmoles/ml)		[Protoporphyrin IX]	
Incubations	**(nmoles/ml)**	**Loss %**	**(nmoles/ml)**	**Loss %**
Control	2.00 ± 0.05	0.00	1.95 ± 0.06	0.00
+ Sub. 0.5 mM	1.90 ± 0.03	5.00 *	1.91 ± 0.10	2.10 NS
+ Sub. 1.0 mM	1.81 ± 0.05	9.5 *	1.90 ± 0.09	2.6 NS
+ Sub. 5.0 mM	1.72 ± 0.03	14.0 **	1.98 ± 0.08	
+ Sub. 10 mM	1.70 ± 0.06	15.0 **	1.88 ± 0.11	3.6 NS
+ Sub. 20 mM	1.68 ± 0.04	16.0 **	2.00 ± 0.06	

NS = not significant, * $P < 0.01$, ** $P < 0.001$, Student's *t* test.

Table 7.3 Dose-dependent loss of microsomal haem during a 15 minute microsomal incubation of DMB.

	[Haem] (nmoles/ml)		**[Protoporphyrin IX]** (nmoles/ml)	
Incubations	**(nmoles/ml)**	**Loss %**	**(nmoles/ml)**	**Loss %**
Control	2.00 ± 0.05	0.00	1.95 ± 0.06	0.00
+ Sub. 0.5 mM	1.74 ± 0.04	13.0 *	1.90 ± 0.12	2.60 NS
+ Sub. 1.0 mM	1.66 ± 0.03	17.0 *	1.88 ± 0.11	3.6 NS
+ Sub. 5.0 mM	1.50 ± 0.06	25.0 *	1.90 ± 0.09	2.60 NS
+ Sub. 10 mM	1.48 ± 0.07	26.0 *	2.01 ± 0.13	-------
+ Sub. 20 mM	1.47 ± 0.05	26.5 *	1.87 ± 0.12	4.2 NS

NS = not significant, * $P < 0.001$, Student's *t* test.

Table. **7.4**. Dose-dependent loss of microsomal haem during a 15 minute microsomal incubation of BMB.

The loss of microsomal haem is time-and dose-dependent and presents an equimolar equivalence with the inactivation of P450. Moreover, as observed for the

inactivation of P450, the effects of the BMB-dependent loss of haem is approximately twice that due to the metabolism of DMB. This is probably due to the major rate of the microsomal metabolism of this substrate which results in a higher formation of reactive species. Moreover, as observed for the inactivation of P450 by DMF and DMAC (Chapter 6), the loss of microsomal haem is observed when the haemochromogen pyridine method is used, while no significant loss was observed when measuring the content of microsomal protoporphyrin IX fluorimetrically. These results can be interpreted as indicating a modification of haem, during substrate metabolism, that does not result in the loss of its tetrapyrrolic structure.

7.4. Effects of CO, PBN, GSH and ascorbic acid on the inactivation of P450 and microsomal haem loss by DMB and MBB

The content of P450 was measured after 15 minute microsomal incubations of 5 mM DMB and BMB carried out both in presence and absence of a saturating concentration of CO. The results obtained (Table 7.5) indicate that inactivation of P450 does not occur if microsomal incubation is performed in the presence of CO.

	[P450] (nmoles/ml)		Loss %	
Incubation	**DMB**	**BMB**	**DMB**	**BMB**
Control	1.70 ± 0.08	1.70 ± 0.08	0.00	0.00
+ CO	1.67 ± 0.07	1.65 ± 0.07	1.8 NS	0.00
+ Substrate	1.47 ± 0.03	1.25 ± 0.04	13.6 *	22.5 *
+ Substrate + CO	1.67 ± 0.05	1.68 ± 0.06	1.8 NS	1.2 NS

* $P < 0.001$, NS = not significant Student's *t* test.

Table 7.5 Effect of a saturating concentration of CO on the inactivation of P450 during 15 minute microsomal incubations of 5 mM DMB and BMB.

Microsomal incubations of 5 mM substrate carried out in presence of PBN, GSH and ascorbic acid and analysed after 15 minutes, give rise to the results in Table 7.6.

	[Haem] (nmoles/ml)		Loss %	
Incubation	**DMB**	**BMB**	**DMB**	**BMB**
Control	2.00 ± 0.05	2.00 ± 0.05	0.00	0.00
+ Substrate	1.75 ± 0.02	1.57 ± 0.03	12.5 **	21.5 **
+ Substrate + 1 mM PBN	1.83 ± 0.03	1.79 ± 0.04	8.5 *	10.5 *
+ Substrate + 10 mM GSH	1.72 ± 0.04	1.55 ± 0.04	14.0 **	22.5 **
+ Substrate + Ascorbic acid 10 mM	1.73 ± 0.06	1.56 ± 0.08	13.5 **	22.0 **

NS = not significant, * $P < 0.01$, ** $P < 0.001$, Student's *t* test.

Table 7.6 Effect of the presence of PBN, GSH and ascorbic acid on the loss of microsomal haem during 15 minute microsomal incubations of 5 mM DMB and BMB.

The results demonstrate that the presence of the spin trapping agent PBN results in a significant protection of the loss of microsomal haem during the DMB and BMB oxidations. That prevention by PBN is not complete probably can be rationalised by competitive reaction of the carbon-centred radical with PBN and haem itself.

In conclusion, the reactive species responsible for the observed loss of microsomal haem during the metabolism of DMB and BMB are the carbon-centred radical intermediates generated by the P450-dependent hydrogen atom abstraction from the carbon α– to nitrogen.

7.5 Conclusions

The results obtained in the present study show significant metabolism-based time-and dose-dependent inactivation of P450 during the microsomal oxidation of DMB and BMB. The time-dependence of the enzyme inactivation displays a bilinear progress with 90% occurring within the first 10 minutes of the reaction. Microsomal metabolism of DMB and MBB present a bilinear progress, with a burst in the first five minutes of the reaction. Comparison of the progress of substrate metabolism with that for P450 inactivation indicates a common initial burst. These results are in agreement with the proposal suggested by Hall and Hanzlik[1] of the inactivation of a minor but kinetically significant isoenzyme of P450. Inactivation of the enzyme is due to covalent modification of its prosthetic haem group by the carbon-centred radicals generated during the oxidation. Carbon-centred radical intermediates have been identified during the microsomal metabolism of DMB and BMB by PBN spin trapping (Chapter 3). Moreover, the presence of PBN in the microsomal incubations of the substrates results in a significant reduction in the loss of haem, consistent with radical intermediates being responsible for the modification of the prosthetic group of the enzyme.

7.6 References

1 Hall L.R. and Hanzlick R.P., (1991); *Xenobiotica* ; **21**, 9: 1127-

2 Narasiman N., Weller P.E., Buben J.A., Wiley R.A. and Hanzlik R.P., (1988); *Xenobiotica*; **18**: 491-

3 Burka L.T., Plucinski T.M. and MacDonald T.L., (1983); *Proc. Natl. Acad. Sci. U.S.A.*; **80**: 6680-

4 Omura T. and Sato R., (1964); *J. Biol.Chem.*; **239**: 2370-

5 Paul K.G., Theorell H. and Akeson A., (1953); *Acta. Chem. Scand.*; **7**: 1284-

6 Morrison G.R., (1965); *Anal. Chem.*; **37**: 1124-

CHAPTER 8

Experimental

8.1 Instrumentation

NMR spectra were recorded using Perkin Elmer R12B (^1H), and Jeol FX 90Q Fourier and Jeol 400 FT spectrometers (^1H and ^{13}C). UV-VIS spectra were recorded using a Kontron Uvikon 810P spectrophotometer, and infra-red spectra were recorded using a Nicolet 205 FTIR spectrophotometer. Gas chromatography was performed using a Perkin Elmer chromatograph equipped with a BP5 20 m x 0.5 mm ID column and FID detector. GC/MS were performed using a Hewlett-Packard 5809-A chromatograph equipped with a BP5 20m x 0.5 mm column connected to a mass Lab 25-250 mass spectrometer. HPLC was carried out using a Varian 5000 chromatograph equipped with a 25 cm X 5 mm C_{18} Jones chromatography analytical column, with a Cecil 2112 variable wavelength detector and a Waters integrator. Diode array HPLC was performed using a Varian 9060 polychrom diode array detector. ESR spectra were recorded using a Varian I 109 X band spectrometer. Melting points were recorded using a Pye model 290 melting point apparatus. Elemental analysis were carried out by Medac Ltd., Brunel University, Uxbridge, England using a Perkin Elmer 240 C elemental analyser model 3400 data station.

8.2. Solvents and reagents

8.2.1 Substrates and reagents

N,N-Dimethylbenzamide, N-methylbenzamide, N-benzylbenzamide, N,N-dimethylaniline, N-methylaniline, N-benzoylpiperidine, N-*tert*-butyl-α-phenylnitrone, N-methylpyrrolidinone, N-methylpiperidinone, N-methylcaprolactam, N-methylsuccinimide, glutarimide, δ-valerolactam, 2-pyrrolidinone, ε-caprolactam, succinimide, N,N-dimethylformamide, N,N-dimethylacetamide, N-methylformamide, N-

methylacetamide, haemin, pyridine, diisopropylamine, acetylsalicilic acid, ethyl chloroformate, dimethylamine, monomethylamine, triethylamine, chloroacetonitrile, paraformaldehyde, chlorotrimethylsilane, acryloyl chloride, 3-hydroxydihydrofuran, 3-(aminomethyl)pyridine, lithium diisopropylamide, molybdenum trioxide, 25% (w/v) hydrogen peroxide, hexamethylphosphorictriamide, *n*-butyllithium, S-cotinine, 4-bromo-1-butene, potassium phthalimide, hydrazine monohydrate, benzoyl chloride, N-benzoylpiperidinone, benzyl bromide, N,N-dimethylcarbamyl chloride, 4-toluenesulfonyl chloride, methyltriphenylphosphorium iodide, 2-carboxybenzaldehyde, azobis(cyclohexane-carbonitrile) (AIBN), tributyltin hydride, glutaric anhydride, adipamide, adipoyl chloride, pyroglutamic acid, benzene, phosphorus pentoxide, methanesulfonic acid, S-(-)-1-phenylethylisociante, acetophenone, 3-benzoylpropionic acid, S(-)-α-methylbenzylamine, R(+)-α-methylbenzylamine, iodomethane, pyridine, (S)-2,2,2-trifluoro-1-(9-anthryl)ethanol and 4-piperidinone hydrochloride were purchased from Aldrich. $NADP^+$, glucose-6-phosphate, glucose-6-phosphate dehydrogenase, haemin, tetraphenylporphirinatoiron (III) chloride, and *tert*-butylhydroperoxide were purchased from Sigma.

8.2.2 Solvents

Benzene BDH Analar grade dried by sodium and distilled onto molecular sieves. Ethanol was 97%, dried by a 12 hour reflux over magnesium and distilled when required. Ether and hexane used for microcolumn chromatography were BDH sodium dried and Rathburn glass distilled respectively. Both were sodium dried and distilled when required. Acetonitrile was BDH Analar and was dried by calcium hydride and distilled accordingly. Dichloromethane used for the biomimetic studies, was distilled onto molecular sieves and stored at 5° C in the dark. Tetrahydrofuran was distilled from calcium hydride prior used. All solvents used for HPLC were Rathburn HPLC grade and were used without further purification.

8.3 Synthesis

N-Cyanomethyl-N-methylaniline: N-methylaniline (0.05 mol, 5.36 g) and potassium carbonate (0.05 mol, 6.0 g) were dissolved in dry acetonitrile (50 cm^3). To this solution was added chloroacetonitrile (0.055 mol, 3.82 g). The mixture was refluxed for 2 h, then left at room temperature, under stirring, for a further 24 h. At the end of the reaction, the solution was filtered and the solvent removed under reduced pressure. The solid residue was resuspended in diethyl ether (50 cm^3), the organic phase washed with water (2 x 15 cm^3) and dried ($MgSO_4$). The solvent was removed *in vacuo* to give the desired product. $\upsilon_{max/cm^{-1}}$: 3080, 3040, 2200, 1600, 1580, 1500, 1400, 1300, 1220. δ_H ($CDCl_3$): 2.75 (3H, s), 3.9 (2H, s), 7.1 (5H, m). m/z (%): 146 (30) (M^+), 120 (15), 106 (100), 91 (35), 77 (25). $C_9H_{10}N_2$ requires: C: 73.97 %; H: 6.85 %; N: 19.18 % Found: C: 74.14 %; H: 7.00 %; N: 19.34 %.

N-Cyanomethyl-N-methylbenzamide: N-methylbenzamide (0.01 mol, 1.34 g) and paraformaldehyde (0.5 g) were dissolved in chlorotrimethylsilane (30 cm^3); the solution was refluxed for 2 h, the solid filtered off, and the solvent removed under reduced pressure. The solid residue was dissolved in dry tetrahydrofuran (50 cm^3) and to this solution was added sodium cyanide (0.01 mol, 0.5 g). The mixture was refluxed for 3 h, then left at room temperature for further 24 h. The mixture was filtered and the solvent removed under reduced pressure. The solid residue was resuspended in diethyl ether (50 cm^3), the organic phase was washed with water (2 x 15 cm^3) and dried ($MgSO_4$). The solvent was removed *in vacuo* to give the desired product. $\upsilon_{max/cm^{-1}}$: 1680, 1500, 1300. δ_H ($CDCl_3$): 3.14 (3H, s), 4.1 (2H, s), 7.35 (5H, m). m/z (%): 174 (20), 148 (10), 135 (90), 105 (100), 77 (100). $C_{10}H_{10}N_2O$ requires: C: 68.96 %; H: 5.75 %; N: 16.09 %. Found: C: 69.15 %; H: 5.81 %; N: 16.25 %.

N,N-Dimethyl-2-hydroxybenzamide: Acetylsalicylic acid (0.1 mol, 18.0 g), triethylamine (0.1 mol, 10.1 g) and ethyl chloroformate (0.1 mol, 10.85 g), were dissolved in dry tetrahydrofuran (50 cm^3). The solution was cooled to -10 °C, and a large

excess of dimethylamine was added. The reaction mixture was brought at room temperature and left, under stirring, for 1 h. The solid was filtered off, the solvent removed under reduced pressure and the solid residue resuspended in 2.0 M sodium hydroxide solution (50 cm^3). The solution was refluxed for 1 h and after cooling the pH was brought to 7 by addition of concentrated hydrochloric acid. The solution was extracted with dichloromethane (50 cm^3), washed with 1 M hydrochloric acid (1 x 20 cm^3), saturated sodium bicarbonate (2 x 10 cm^3), water (2 x 10 cm^3) and dried ($MgSO_4$). The solvent was removed to give the desired product. m.p.: 112-116 °C. $\upsilon_{max/cm^{-1}}$: 3450, 1680, 1600, 1520, 1500, 1400. δ_H ($CDCl_3$): 3.12 (6H, s), 7.1 (4 H, m), 8.1 (1H, br). m/z (%): 165 (55), 151 (15), 121 (100), 93 (25), 44 (60). $C_9H_{11}NO_2$ requires: C: 65.45 %; H: 6.66%; N: 8.48 % Found: C: 65.73 %; H: 6.21 %; N: 8.21 %.

N-Methyl-2-hydroxybenzamide: A similar procedure to the synthesis of N,N-dimethyl-2-hydroxybenzamide was adopted, substituting methylamine for dimethylamine. m.p.: 130-133 °C. $\upsilon_{max/cm^{-1}}$: 3450, 3300, 1650, 1600, 1500, 1480, 1380. δ_H ($CDCl_3$): 2.9 (3H, d, J=5 Hz), 6.4 (1H, br.), 7.0 (4 H, m), 9.3 (1H, br.). m/z (%): 152 (50), 137 (10), 121 (100), 93 (25). $C_8H_9NO_2$ requires: C: 63.16 %; H: 5.92 %; N: 9.21 %. Found: C: 63.52 %; H: 6.10 %; N: 9.40 %.

3-Methyl-4-oxobenz-1,3-oxazinane: N-Methyl-2-hydroxybenzamide (2.0 mmol, 0.3 g), concentrated hydrochloric acid (0.05 cm^3) and paraformaldehyde (20 mg) were dissolved in dry acetonitrile (30 cm^3). The solution was refluxed for 2 h, cooled, filtered and the solvent removed under reduced pressure. The solid residue was resuspended in dichloromethane (20 cm^3), washed with water (2 x 10 cm^3) dried ($MgSO_4$), and the solvent was removed *in vacuo* to give the desired product. $\upsilon_{max/cm^{-1}}$: 3080, 1680, 1600, 1520, 1500, 1400, 1350. δ_H ($CDCl_3$): 3.00 (3H, s), 5.1 (2H, s), 7.30 (4H, m). m/z (%): 163 (30), 148 (10), 120 (40), 93 (100). $C_{10}H_9NO_2$ requires: C: 68.57 %; H: 5.14 %; N: 8.00 %. Found: C: 68.72 %; H: 5.31 %; N: 8.11 %.

N-Methylacrylamide: To an ice cold solution of acryloyl chloride (0.1 mol, 9.05 g) in dry diethyl ether (100 cm^3) was added, under stirring, dry methylamine in large excess. The solution was maintained at room temperature for 30 minutes, the solid filtered off, and the solvent removed under reduced pressure to give a solid residue that was resuspended in dichloromethane (50 cm^3), washed with brine (2 x 10 cm^3), water (2 x 10 cm^3) and dried ($MgSO_4$). The solvent was removed to give the desired product as pale yellow liquid. $\upsilon_{max/cm^{-1}}$: 3380, 1700, 1620, 1580. δ_H ($CDCl_3$): 3.14 (3H, s), 4.2 (1H, br.), 5.42-5.72 (1H, m), 6.14-6.65 (2H, m). m/z (%): 85 (40) ($M^{+\bullet}$), 58 (60) ($M^{+\bullet}$- CH_2=CH), 55 (100) ($M^{+\bullet}$ - NHMe). C_4H_7NO requires: C: 56.47 %; H: 8.23 %; N: 16.47 %. Found: C: 56.20 %; H: 8.00 %; N: 16.70 %.

N-Pyridylmethylacrylamide: The procedure for N-methylacrylamide was adopted using 3-(aminomethyl)pyridine in place of methylamine. $\upsilon_{max/cm^{-1}}$: 3400, 1690, 1600. δ_H ($CDCl_3$): 3.4 (2H, d) 4.4 (1H, d), 5.6 (1H, m), 6.0 (2H, m), 6.7 (1H, br), 7.2 (1H, m), 7.6 (1H, m), 8.4 (2H, m). m/z (%): 162 (30) ($M^{+\bullet}$), 135 (45) ($M^{+\bullet}$ -CH_2=CH), 107 (80) ($NHCH_2Pyr$), 55 (100) ($M^{+\bullet}$ - $NHCH_2Pyr$). $C_9H_{10}N_2O$ requires: C: 66.67%; H: 6.17 %; N: 17.28 %. Found: C: 66.90 %; H: 5.98 %; N: 16.96 %.

N-Methyl-N-3-pyridylmethylacrylamide: N-(3-pyridylmethyl)acrylamide (0.05 mol, 8.1 g) was dissolved in dry tetrahydrofuran (50 cm^3). Under a N_2 atmosphere and at -10 °C, a lithium diisopropylamide (0.045 mol, 22.5 cm^3) 2.0 M solution in hepthane/tetrahydrofuran was added. The mixture was left under stirring at room temperature for 15 minutes, then iodomethane (0.06 mol, 8.5 g) was added dropwise. The mixture was kept at room temperature under stirring for 1 h, then the solvent removed and the solid residue was resuspended in dichloromethane (50 cm^3). The solution was washed with water (2 x 10 cm^3) and dried ($MgSO_4$). After concentration the crude product was purified by silica gel chromatography using 9:1 dichloromethane/methanol eluent. $\upsilon_{max/cm^{-1}}$: 3010, 1690, 1600. δ_H ($CDCl_3$): 3.0 (3H, s), 4.66 (2H, s), 5.7-5.77 (1H, m), 6.4-6.71 (2H, m), 7.2-7.8 (4H, m). m/z (%): 176 (25) ($M^{+\bullet}$), 148 (60) ($M^{+\bullet}$ - CH_2=CH), 121 (50) ($M^{+\bullet}$ - CH_2=CHCO), 79 (15) (Pyr),

55 (100) (CH_2=CHCH). $C_{10}H_{12}N_2O$ requires: C: 68.18 %; H: 6.82 %; N: 15.90 %. Found: C: 68.40 %; H: 7.04 %; N: 16.21 %.

N,N-Dimethyl acrylamide: The method for synthesising N-methylacrylamide was followed substituting dimethylamine for methylamine. $\upsilon_{max/cm^{-1}}$: 1710, 1640, 1580. δ_H ($CDCl_3$): 3.10 (6 H, s), 5.52-5.8 (1H, m), 6.04-6.52 (2H, m). m/z (%): 99 (30) ($M^{+\bullet}$), 72 (60) ($M^{+\bullet}$ - CH_2=CH), 55 (100) ($M^{+\bullet}$ - MeNMe). C_5H_9NO requires: C: 60.61 %; H: 9.1 %; N: 14.14 %. Found: C: 61.0 %; H: 9.3 %; N: 14.62 %.

5-S-3'-Hydroxycotinine[1,2]: Molybdenum trioxide (33 mmol, 5.0 g) and a 25 % (w/v) hydrogen peroxide of hydrogen peroxide (25 cm^3) were stirred and maintained at a temperature of 40 °C for 3.5 h. After cooling the reaction mixture was filtered, and the yellow solution was cooled down to 10° C. Hexamethylphosphorictriamide (0.035 mol, 6.2 g) was added and the crystalline precipitate collected. Recrystallization from hot methanol (40° C maximum temperature) gave $MoO_5 \cdot H_2O \cdot$ HMPA as yellow needles. This (8.65 mmol, 3 g) was dissolved in dry tetrahydrofuran (40 cm^3), cooled to 20° C, and pyridine (8.65 mmol, 0.68 g) was added dropwise. The yellow crystalline precipitate was collected, washed with water (10 cm^3), diethyl ether (100 cm^3) and dried under vacuum to give $MoO_5 \cdot$ (Pyridine)$\cdot$ HMPA, that was stored in the dark at 0° C until used.

Diisopropylamine (11.36 mmol, 1.15 g) was dissolved in dry tetrahydrofuran (35 cm^3) and cooled to -78° C. A 2.0 M solution of *n*-butyllithium in *n*-hexane was added (11.36 mmol, 5.68 cm^3), the temperature was brought up to 0° C for 10 minutes, then recooled to -78° C. A solution of (S)-cotinine (5.6 mmol, 1.0 g) in dry tetrahydrofuran (20 cm^3) was added. After 10 minutes, under a strong flow of N_2, $MoO_5 \cdot$ (Pyridine)$\cdot$ HMPA (11.36 mmol, 4.93 g), dissolved in dry tetrahydrofuran (10 cm^3), was added. The solution was brought to 0° C for 10 minutes, then to 10° C for an additional 15 minutes, after which the reaction was quenched by addition of saturated sodium sulfite (80 cm^3). The organic phase was separated and the remaining aqueous

phase extracted with 1:1 dichloromethane/ 2-propanol (3 x 75 cm^3). The extracts were pooled the solvent removed to give a deep blue solid. This was dried by azeotropic distillation, first with dichloromethane (400 cm^3) followed by chloroform (400 cm^3). m.p.: 74-78° C. $\upsilon_{max/cm^{-1}}$: 3420, 3100, 1698, 1150, 1190, 1050, 1030. δ_H ($CDCl_3$): 2.0 (2H, m, J= 2.5 Hz), 2.78 (3H, s), 2.98 (1H, m, J= 2.5 Hz), 4.5 (1H, m, J= 2.5), 5.5 (1H, br.), 7.4 (2H, m, J= 2.5 Hz), 8.0 (2H, m, J= 2.5 Hz). m/z (%): 192 (10), 174 (30), 135 (30), 114 (25), 106 (100). $C_{10}H_{12}N_2O_2$ requires: C: 62.5 %; H: 6.25%; N: 14.58 %. Found: C: 62.70 %; H: 6.40 %; N: 14.80 %.

(±) **N-Methyl-3-hydroxy-2-pyrrolidinone**[1,2]: A similar procedure to that used to synthesise 3'-hydroxycotinine was used, substituting N-methyl-2-Pyrrolidinone (11.3 mmol, 1.12 g) in place of cotinine b.p.: 106-110° C. $\upsilon_{max/cm^{-1}}$: 3400, 1700, 1640, 1520. δ_H ($CDCl_3$): 2.0 (2H, m, J= 2.5 Hz), 2.85 (3H, s), 3.1 (2H, q, J= 2.5), 4.3 (1H, t, J= 2.5), 4.85 (1H, br.). m/z (%): 115 (20), 100 (25), 98 (100), 47 (60). $C_5H_9NO_2$ requires: C: 52.17 %; H: 7.82 %; N: 12.17 %. Found: C: 52.30 %; H: 7.99 %; N: 12.33 %.

N-Chloromethyl-N-methylacrylamide: N-Methyl acrylamide (0.02 mol, 1.7 g), was dissolved in trimethylsylilchloride (50 cm^3). To this solution was added paraformaldehyde (2.0 g) before refluxing for 2 h. After cooling the solvent was removed and the solid residue purified by chromatography using 9:1 dichloromethane/methanol as the mobile phase. $\upsilon_{max/cm^{-1}}$: 1670, 1590, 1410, 1280, 1260. δ_H ($CDCl_3$): 3.00 (3H, s), 5.3 (2H, s), 5.6-5.80 (1H, m), 6.00-6.25 (2H, m). m/z (%): 135 (5) 133 (18) ($M^{+\bullet}$), 84 (40) ($M^{+\bullet}$ - CH_2Cl), 55 (100), 27 (10).

N,N-Dimethyl-2-vinylbenzamide: Methyltriphenylphosphonium iodide (50 mmol, 17.8 g) and diisopropylamine (100 mmol, 10.1 g) were dissolved in dry tetrahydrofuran (100 cm^3) in a N_2 atmosphere and cooled to -10° C. A solution 2.5 M of butyllithium in *n*-hexane (100 mmol, 6.4 g) was added dropwise when a deep orange coloured solution was observed. The mixture was left stirring under a N_2 atmosphere at

0° C for 15 minutes. To this solution was added 2-carboxybenzaldehyde (50 mmol, 7.5 g). The mixture was left at room temperature for 1 h. The solvent was removed and the solid residue was resuspended in dichloromethane (100 cm^3), and extracted with saturated sodium bicarbonate (2 x 50 cm^3). The aqueous extracts were acidified with concentrated hydrochloric acid and extracted with dichloromethane (100 cm^3). The organic phase was dried ($MgSO_4$) and the solvent removed to give the crude vinyl carboxylic acid (20 mmol, 2.98 g). The crude product and triethylamine (20 mmol, 2.8 cm^3) were dissolved in dry tetrahydrofuran (50 cm^3), cooled to -10° C for 20 minutes, then ethylchloroformate (20 mmol, 1.73 cm^3) dissolved in dry tetrahydrofuran (10 cm^3) was added dropwise. The solution was maintained under stirring at -10 °C for 30 minutes, then excess dry dimethylamine was added. The reaction was brought to room temperature and left stirring for 1 h. The solid was filtered off and the solvent removed to give a solid residue which was resuspended in dichloromethane (50 cm^3), washed with 0.1 N hydrochloric acid (2 x 10 cm^3), aqueous saturated sodium bicarbonate (2 x 10 cm^3) and dried ($MgSO_4$). Evaporation of the solvent gave the desired product. $\upsilon_{max/cm^{-1}}$: 3100, 1720, 1650. δ_H ($CDCl_3$): 2.85 (3H, s), 3.12 (3H, s), 5.2-5.6 (2H, m), 5.84 (1H, d, J=2.5 Hz), 6.44-6.88 (2H, m), 7.16-7.56 (2H, m). m/z (%): 175 (50) ($M^{+\bullet}$), 160 (25) ($M^{+\bullet}$ -Me), 148 (10) (M^+ -$CH{=}CH_2$), 131 (100) (M^+ - MeNMe), 103 (80) (M^+ - MeNMeCO), 77 (75). $C_{11}H_{13}NO$ requires: C: 75.42 %; H: 7.43 %; N: 8.00 %. Found: C: 75.21 %; H: 7.60 %; N: 7.81 %.

N-(3-Butenyl)phthalimide: 4-Bromo-1-butene (0.133 mol, 17.0 g), potassium phthalimide (0.141 mol, 26.17 g) and potassium iodide (4.8 mmol, 0.8 g) were dissolved in dry dimethylformamide (200 cm^3). The solution was heated at 130° C for 2 hours under a N_2 atmosphere then poured onto crushed ice (200 g). Extraction with diethyl ether (4 x 200 cm^3) was followed by washing with 1 M sodium hydroxide (200 cm^3),water (2 x 100 cm^3), and 0.5 M hydrochloric acid (200 cm^3). The organic layer was dried ($MgSO_4$) and the solvent removed to leave the product as a yellow oil which solidified on standing and was recrystallized from diethyl ether/hexane to give the pure

product as a white crystalline solid. m.p.: 50-51° C. $\upsilon_{max/cm^{-1}}$: 1700, 1680 1620, 1480, 1460. δ_H ($CDCl_3$): 2.45 (2H, m, J =5.0 Hz), 3.77 (2H, t, J= 5.0 Hz), 5.05 (2H, m, J= 5.0 Hz), 5.70 (1H, m, J= 5.0 Hz), 7.70-7.85 (4H, m, J= 5.0 Hz). m/z (%): 210 (15), 174 (10), 146 (30), 132 (100), 105 (30), 97 (20). $C_{12}H_{11}NO_2$ requires: C: 71.64 %; H: 5.47 %; N: 6.96 %. Found: C: 71.80 %; H: 5.63 %; N: 7.09 %.

3-Butenylamine hydrochloride: N-(3-Butenyl)phthalimide (0.05 mmol, 10.05 g) was dissolved in ethanol (200 cm^3) and refluxed in the presence of hydrazine monohydrate (0.05 mol, 2.5 g) for 3 h. After cooling, water (100 cm^3) and 1 M hydrochloric acid (to pH 4.0) were added. Filtration of the white precipitate gave a clear yellow solution which was concentrated to leave the product as a yellow hygroscopic solid. $\upsilon_{max/cm^{-1}}$: 3350, 1400, 1000. δ_H ($CDCl_3$): 2.39 (2H, m, J =5.0 Hz), 2.84 (2H, t, J= 5.0 Hz), 5.12 (2H, m, J= 5.0 Hz), 5.82 (1H, m, J= 5.0 Hz), 8.3 (3H, br.). m/z (%): 72 (80), 55 (55), 30 (100).

N-(3-Butenyl)benzamide: 3-Butenylamine hydrochloride (0.10 mol, 11.8 g) was dissolved in dry tetrahydrofuran (200 cm^3) in the presence of a large excess of triethylamine. To this solution tetrahydrofuran (50 cm^3) containing benzoyl chloride (0.11 mol, 12.7 g) was added dropwise, the mixture was maintained basic by adding further triethylamine. The reaction mixture was refluxed overnight, after cooling the white precipitate was filtered off, the solvent removed and the solid residue purified by silica gel chromatography, using diethyl ether as eluent. $\upsilon_{max/cm^{-1}}$: 3320, 3050, 1650, 1580, 1500, 1480, 1350. δ_H ($CDCl_3$): 2.1 (2H, m, J= 3.5 Hz), 3.3 (2H, q, J= 3.55), 5,0 (2H, q, J= 3.5 Hz), 5.6 (1H, m, J= 3.5 Hz), 6.8 (1H, br.), 7.5 (5H, m, J= 3.5 Hz). m/z (%): 175 (10), 134 (50), 105 (100), 77 (55), 39 (25). $C_{11}H_{13}NO$ requires: C: 75.42 %; H: 7.43 %; N: 8.00 %. Found: C: 75.60 %; H: 7.58 %; N: 8.10 %.

N-(3-Butenyl)-N-methylbenzamide: N-(3-butenyl)benzamide (0.02 mol, 3.5 g) was dissolved in dry tetrahydrofuran (50 cm^3) under a N_2 atmosphere. To this solution, at 0° C, lithium diisopropylamide was added (0.022 mol, 11 cm^3 of a 2.0 M

solution in tetrahydrofuran), after 15 minutes at room temperature, iodomethane (0.022 mol, 3.12 g) was added dropwise and the mixture left for a further 1 h. The solvent was removed, the solid residue resuspended in dichloromethane (50 cm^3), washed with water (2 x 20 cm^3), dried ($MgSO_4$) and concentrated. The crude product was purified by column chromatography using 8:2 dichloromethane/methanol as mobile phase. $\upsilon_{max/cm^{-1}}$: 3010, 1650, 1510, 1500, 1480, 1380. δ_H ($CDCl_3$): 2.1 (2H, m, J= 3.5 Hz), 3.1 (3H, s), 3.3 (2H, m, J= 3.5), 5,0 (2H, m, J= 3.5 Hz), 5.6 (1H, m, J= 3.5 Hz), 7.5 (5H, m). m/z (%): 189 (8), 148 (60) 135 (10), 105 (100), 77 (60), 39 (10). $C_{12}H_{15}NO$ requires: C: 76.19 %; H: 7.94 %; N: 7.41 %. Found: C: 76.34 %; H: 8.01 %; N: 7.33 %.

N-Benzyl-N-(3-butenyl)benzamide: N-(3-butenyl)benzamide (0.02 mol, 3.5 g) was dissolved in of dry tetrahydrofuran (50 cm^3) under a N_2 atmosphere; to this solution , at 0° C, lithium diisopropylamide was added (0.022 mol, 11 cm^3 of a 2.0 M solution in tetrahydrofuran). After 15 minutes at room temperature, dry tetrahydrofuran (10 cm^3) containing benzyl bromide (0.022 mol, 3.76 g) and potassium iodide (2.4 mmol, 0.4 g) was added dropwise and the mixture left under stirring for a further 1 h. The solvent was removed, the solid residue resuspended in dichloromethane (50 cm^3), washed with water (2 x 20 cm^3), dried ($MgSO_4$) and concentrated. The product was purified by column chromatography using 8:2 dichloromethane/methanol as mobile phase. $\upsilon_{max/cm^{-1}}$: 3010, 1700, 1660, 1600, 1500, 1480, 1440, 1370, 1300, 1240. δ_H ($CDCl_3$): 2.1 (2H, m, J= 5 Hz), 3.3 (2H, m, J= 5), 3.6 (2H, s), 5,0 (2H, m, J= 5 Hz), 5.6 (1H, m, J= 5 Hz), 7.5 (10H, m). m/z (%): 265 (10), 224 (45) 210 (8), 174 (5), 105 (100), 91 (45), 77 (50). $C_{18}H_{19}NO$ requires: C: 81.50 %; H: 7.17 %; N: 5.28 %. Found: C: 81.78 %; H: 7.21 %; N: 5.33 %.

3'-Butynyl-(4'-toluene) sulfonate: 3-Butyn-1-ol (0.1 mol, 7.01 g) and triethylamine (0.11 mol, 11.1 g) were dissolved in dry tetrahydrofuran (100 cm^3). To this, a solution of dry tetrahydrofuran (50 cm^3) containing 4-toluensulfonyl chloride (0.1 mol, 19.1 g) was added dropwise and the reaction mixture refluxed for 2 h. After cooling, a white precipitate was filtered off and the solvent removed to give a dark oil

which was resuspended in diethyl ether (50 cm^3), washed with 1 M hydrochloric acid (2 x 20 cm^3), saturated sodium bicarbonate (2 x 20 cm^3), water (2 x 20 cm^3) and dried ($MgSO_4$). The solvent was removed to give the desired product. $\upsilon_{max/cm^{-1}}$: 3400, 3000, 2920, 1580, 1380, 1180. δ_H ($CDCl_3$): 2.1 (1H, t, J= 2.0 Hz), 2.4 (3H, s), 2.7 (2H, m, J= 7 Hz), 4.12 (2H, t, J= 7.0), 7.4 (2H, d, J_1= 7, J_2= 9), 7.8 (2H, d, J_1= 9, J_2= 9). m/z (%): 224 (25), 209 (5), 185 (15), 171 (10), 155 (100), 91 (100), 69 (40), 39 (15). $C_{11}H_{12}SO_3$ requires: C: 58.89 %; H: 5.37 %. Found: C: 59.05 %; H: 5.45.

N-(3-Butynyl)phthalimide: 3-Butynyl-4-toluensulfonate (0.067 mol, 14.2 g), potassium iodide (3.6 mmol, 0.6 g) and potassium phthalimide (0.074 mol, 13.65 g) were dissolved in dry dimethylformamide (200 cm^3) and refluxed for 24 h under a N_2 atmosphere. After cooling, the solution was poured onto crushed ice (200 g). Extraction with diethyl ether (4 x 200 cm^3) was followed by washing with 1 M sodium hydroxide (200 cm^3), water (2 X 100 cm^3), and 0.5 M hydrochloric acid (200 cm^3). The organic layer was dried ($MgSO_4$) and the solvent was removed to leave the product which was recrystallized from diethyl ether/hexane as a white crystalline solid. $\upsilon_{max/cm^{-1}}$: 3300, 3050, 1780, 1700, 1500, 1450, 1400. δ_H ($CDCl_3$): 2.1 (1H, t, J= 5.0), 2.6 (2H, t d, J_1= 7.0, J_2= 7.0), 4.0 (2H, t, J= 7.0), 7.7 (4H, m). m/z (%): 199 (35), 160 (100), 132 (35), 105 (30), 77 (35), 39 (10). $C_{12}H_9NO_2$ requires: C: 72.36 %; H: 4.52 %; N: 7.03 %. Found: C: 72.51 %; H: 4.62 %; N: 7.20 %

3-Butynylamine hydrochloride: N-(3-Butynyl)phthalimide (0.05 mmol, 9.95 g) was dissolved in ethanol (200 cm^3) and refluxed in the presence of hydrazine monohydrate (0.05 mol, 2.5 g) for 3 h. After cooling, water (100 cm^3) and 1 M hydrochloric acid (to pH 4.0) were added. Filtration of the white precipitate gave a clear yellow solution which was concentrated to leave the product as a yellow hygroscopic solid $\upsilon_{max/cm^{-1}}$: 3350, 1700, 1500, 1380. δ_H ($CDCl_3$): 2.0 (1H, m), 2.6 (2H, q, J =5 Hz), 3.04 (2H, t, J= 5 Hz), 7.5 (3H, br.). m/z (%): 70 (80), 53 (45), 39 (100).

N-(3-Butynyl)benzamide: N-(3-Butynyl)aminehydrochloride (0.10 mol, 10.55 g) was dissolved in dry tetrahydrofuran (200 cm^3) in the presence of a large excess of triethylamine. To this solution tetrahydrofuran (50 cm^3) containing benzoyl chloride (0.11 mol, 12.7 g) was added dropwise. The pH of the mixture was monitored and maintained at 10 throughout by adding further triethylamine. The reaction mixture was refluxed overnight, cooled the white precipitate filtered off, the solvent removed and the solid residue purified by chromatography using diethyl ether as mobile phase. $\upsilon_{max/cm^{-1}}$: 3350, 3300, 3150, 1710, 1650, 1550, 1500, 1480. δ_H ($CDCl_3$): 1.9 (1H, t, J= 2.0 Hz), 2.3 (2H, m, J_1=5 Hz, J_2= 5 Hz), 3.2 (2H, m, J= 5 Hz), 6.8 (1H, br.), 7.6 (5H, m). m/z (%): 173 (20), 149 (15), 134 (50), 105 (100), 77 (90), 68 (50), 39 (25). $C_{11}H_{11}NO$ requires: C: 76.30 %; H: 6.36 %; N: 8.09 %. Found:C: 76.58 %; H: 6.41 %; N: 8.00 %.

N-(3-Butynyl)-N-methylbenzamide: N-(3-Butynyl)benzamide (0.02 mol, 3.46 g) was dissolved in of dry tetrahydrofuran (50 cm^3) under a N_2 atmosphere. To this solution , at 0° C, lithium diisopropylamide was added (0.022 mol, 11 cm^3 of a 2.0 M solution in tetrahydrofuran) After 15 minutes at room temperature iodomethane (0.022 mol, 3.12 g) was added dropwise, the mixture stirred for further 1 h, the solvent removed and, the solid residue resuspended in dichloromethane (50 cm^3), washed with water (2 x 20 cm^3), dried ($MgSO_4$) and concentrated. The crude product was purified by column chromatography using 8:2 dichloromethane/methanol as mobile phase. $\upsilon_{max/cm^{-1}}$: 3050, 1650, 1580, 1550, 1520, 1500, 1480, 1400, 1350, 1300, 1280. δ_H ($CDCl_3$): 1.9 (1H, t, J= 2.0 Hz), 2.3 (2H, m, J_1=2 Hz, J_2= 5 Hz), 2.92 (3H, s), 3.2 (2H, q, J= 5 Hz), 7.6 (5H, m). m/z (%): 187 (10), 148 (55), 134 (20), 105 (100), 77 (70), 39 (12). $C_{12}H_{13}NO$ requires: C: 77.00 %; H: 6.95 %; N: 7.49 %. Found: C: 77.22 %; H: 7.01 %; N: 7.38 %.

N-Butenyl-N-chloromethylbenzamide: N-(3-Butenyl)benzamide (0.02 mol, 3.5 g), was dissolved in trimethylsylil chloride (50 cm^3). To this solution was added paraformaldehyde (2.0 g). the solution was refluxed for 2 h. After cooling the

solvent was removed and the solid residue purified by silica gel chromatography using dichloromethane as mobile phase. $\upsilon_{max/cm^{-1}}$: 3010, 1650, 1510, 1500, 1480, 1380. δ_H ($CDCl_3$): 2.1 (2H, m, J= 5 Hz), 3.3 (2H, m, J= 5), 5,0 (2H, m, J= 5 Hz), 5.30 (2H, s), 5.6 (1H, m, J= 5 Hz), 7.28 (5H, s). m/z (%): 225 (15) ($M^{+\bullet}$), 173 (40) ($M^{+\bullet}$ - CH_2Cl), 105 (44), 77 (100).

N-(3-Butynyl)-N-chloromethylbenzamide: N-(3-Butynyl)benzamide (0.02 mol, 3.45 g), was dissolved in trimethylsylilchloride (50 cm^3), to this solution was then added paraformaldehyde (2.0 g). The solution was refluxed for 2 h. After cooling the solvent was removed and the solid residue was purified by silica gel using dichloromethane as mobile phase. m.p. 88-91 °C. $\upsilon_{max/cm^{-1}}$: 3050, 1650, 1580, 1550, 1520, 1500, 1480, 1400, 1350, 1300, 1280. δ_H ($CDCl_3$): 1.9 (1H, t, J= 2 Hz), 2.3 (2H, m, J_1=2 Hz, J_2= 5 Hz), 3.2 (2H, m, J= 5 Hz), 5.30 (2H, s), 7.28 (5H, s). m/z (%): 223 (10) ($M^{+\bullet}$), 171 (55) ($M^{+\bullet}$ - CH_2Cl), 105 (35), 77 (100).

N-Benzoyl-1,2,5,6-tetrahydropyridine: Benzoyl chloride (0.05 mol; 7.0 g) was dissolved in 10% aqueous NaOH (30 cm^3). To this solution was added 1,2,5,6-tetrahydropyridine (0.045 mol, 3.73 g). The reaction mixture was stirred vigorously for 30 minutes. The products were extracted using dichloromethane (2 x 30 cm^3), the organic phase was, washed with water (2 x 20 cm^3), dried ($MgSO_4$) and concentrated. The resulting oil was then purified by silica gel chromatography using diethyl ether as eluent. $\upsilon_{max/cm^{-1}}$: 3010, 2450, 2400, 1650, 1500, 1480. δ_H ($CDCl_3$): 2.1 (2H, m), 3.2 (2H, m), 3.4 (2H, m), 5.8 (2H, m), 7.0 (5H, m). m/z (%): 187 (15), 105 (100), 79 (40), 77 (70). $C_{12}H_{13}NO$ requires: C: 77.00 %; H: 6.95 %; N: 7.49 %. Found: C: 77.40 %; H: 6.80 %; N: 7.55 %.

N-Benzoyl-3-methylpyrrolidine: 3-Methyl-2-pyrrolidinone (125 mol; 1.26 g) was dissolved in dry tetrahydrofuran (25 cm^3). The solution was cooled to 0° C and borane methylsulphide (125 mmol) was added dropwise. After vigorous reaction ceased, the resulting mixture was brought to gentle reflux and maintained at that temperature for 3

h. The reaction mixture was cooled to 0° C, methanol (20 cm^3) was added and the solution was stirred well for further 1 h. Anhydrous hydrogen chloride was added to the mixture to obtain a pH < 2, and the resulting mixture was gently refluxed for 1 h. After cooling, methanol (100 cm^3) was added and the solvents removed by reduced pressure. The residue obtained was made basic (H_2O; NaOH pellets, pH > 12) and extracted with diethyl ether (3 x 100 cm^3), dried ($MgSO_4$) and the solvent was removed to give pure 3-methyl pyrrolidine.

3-Methylpyrrolidinone (0.045 mol; 3.82 g) was added to a 10% NaOH solution (30 cm^3) containing benzoyl chloride (0.05 mol; 7.0 g). The reaction mixture was stirred vigorously for 30 minutes, extracted by dichloromethane (2 x 50 cm^3), the organic phase was washed with water (2 x 20 cm^3), dried ($MgSO_4$) and the solvent was removed to give N-benzoyl-3-methylpyrrolidine. $\upsilon_{max/cm^{-1}}$: 3000, 1630, 1580,1400. δ_H ($CDCl_3$): 1.2 (3H, d, J=5 Hz), 1.3 (1H, m), 2.0 (2H, m), 3.0 (2H, m), 3.2 (2H, m), 7.0 (5H, m). m/z (%): 189 (20), 174 (30), 105 (100), 84 (50), 77 (80). $C_{12}H_{15}NO$ requires: C: 76.16 %; H: 6.95 %; N: 7.48 %. Found: C: 76.5 %; H: 6.70 %; N: 7.75 %.

N-Benzoyl-3-methylenepyrrolidine: N-Benzylpyrrolidin-3-one (0.02 mol; 3.5 g) was dissolved in dry dichloromethane (30 cm^3). To this solution, was added with stirring a dichloromethane (10 cm^3) solution containing 5,10,15,20-tetraphenylporphine iron(III)chloride (TPP) (3.0 mmol, 2.1 g) and *tert*-butylhydroperoxide (0.2 mol; 18 g). The reaction mixture was maintained at room temperature for 48 hours, every 4 hours a dichloromethane solution (10 cm^3) containing *tert*-butylhydroperoxide (0.2 mol) was added. The solvent was removed and the solid residue subjected to chromatography on silica gel using diethyl ether/ hexane 8:2 as the mobile phase to obtain N-benzoyl-pyrrolidin-3-one.

Methyltriphenylphosphonium bromide (4.07 mmol; 1.45 g) was dissolved in dry tetrahydrofuran (30 cm^3). The solution was cooled to -15° C and, under N_2, a 2.5 M butyllithium solution in hexane was added dropwise (4.07 mmol; 1.53 cm^3). The mixture

was maintained at -15° C under stirring until the colour changed to orange, then a dry tetrahydrofuran solution (20 cm^3) containing N-benzoylpyrrolidin-3-one (3.9 mmol; 0.70 g) was added. The reaction mixture was maintained at -15° C for 30 minutes, brought to room temperature and left for a further 2 h. Upon completion of the reaction, ammonium chloride was added (0.1 mol; 5.2 g), the solvent removed, the solid residue resuspended in dichloromethane (100 cm^3) and the organic phase washed with water (2 x 20 cm^3), dried ($MgSO_4$) and, after concentration subjected to cromatography on silica gel using diethyl ether/ hexane 7:3 as eluent. $\upsilon_{max/cm^{-1}}$: 3000, 1680, 1520, 1470. δ_H ($CDCl_3$): 2.0 (2H, t, J= 5 Hz), 3.2 (2H, m), 3.4 (2H, m), 5.0 (2H, d, J= 5 Hz), 7.1 (5H, m). m/z (%): 187 (25), 173 (35), 105 (100), 82 (40), 77 (70). $C_{12}H_{13}NO$ requires: C: 77.00 %; H: 6.95 %; N: 7.49 %. Found: C: 77.60 %; H: 7.05 %; N: 7.61 %.

N-Benzoyl-3-formylpyrrolidine: in dry tetrahydrofuran (30 cm^3), Methoxymethyltriphenylphosphonium bromide (5.23 mmol; 2.23 g) was dissolved. The solution was cooled to -15° C and, under N_2, a 2.5 M butyllithiun solution in hexane (5.23 mmol; 2.1 cm^3) was added dropwise. The mixture was maintained at -15° C until the colour changed to orange, then a dry tetrahydrofuran solution (20 cm^3) containing N-benzoylpyrrolidin-3-one (5.0 mmol; 0.90 g) was added. The reaction mixture was maintained at -15° C for 30 minutes, brought to room temperature and left for a further 2 h. Ammonium chloride was added (0.1 mol; 5.2 g), and the solution extracted with chloroform (2 x 50 cm^3), the organic phase evaporated, the solid residue resuspended in 0.1 N hydrochloric acid (50 cm^3) and refluxed for 30 minutes. After cooling, the acid solution was extracted with chloroform (2 x 50 cm^3), the organic phase washed with water (2 x 20 cm^3), dried ($MgSO_4$) and, after concentration, subjected to cromatography on silica gel using diethyl ether/ hexane 8:2 as eluent. $\upsilon_{max/cm^{-1}}$: 3020, 1725, 1700, 1610, 1500. δ_H ($CDCl_3$): 2.1 (2H, t, J= 5 Hz), 2.4 (1H, m), 3.0 (2H, m), 3.2 (2H, t, J= 5 Hz), 7.1 (5H, m), 9.1 (1H, s). M/z (%): 203 (20), 174 (30), 105 (100), 98 (40), 77 (70). $C_{12}H_{13}NO_2$ requires: C: 70.93 %; H: 6.40 %; N: 6.89 %. Found: C: 70.20 %; H: 6.15 %; N: 7.01 %.

N-Hydroxymethyl-N-methylbenzamide: was synthesised following the method reported by Constantino *et al.*[3]

N-Chloromethyl-N-methylbenzamide: was synthesised following the method reported by Moreira *et al.*[4]

N-Benzoyl-N-*tert*-butyl-N-hydroxy-N-methyl-1-phenyl-1,2-diaminoethane (PBN-DMB adduct): N-Chloromethyl-N-methyl benzamide (0.01 mol, 1.83 g) and PBN (0.01 mol, 1.77 g), were dissolved in dry acetonitrile (20 cm^3) and refluxed. An acetonitrile solution (5 cm^3) containing 1,1-azobis(cyclohexanecarbonitrile) (0.001 mol, 0.24 g) and tributyltin hydride (0.001 mol, 0.29 g) was added dropwise within 30 minutes. The mixture was refluxed for a further 30 minutes. After cooling, the solvent was removed and the residue purified by silica gel chromatography using diethyl ether as mobile phase. $\upsilon_{max/cm^{-1}}$: 3450, 1630, 1580, 1540, 1500, 1460, 1400, 1380. $\delta_H (CDCl_3)$: 1.91 (9H, s), 3.0 (3H, s), 3.6 (2H, d, J= 5 Hz), 4.8 (1H, t, J=5 Hz), 7.4 (10H, m), 8.1 (1H, br). m/z (%): 325 (10), 310 (10), 268 (20), 238 (40), 205 (20), 191 (10), 105 (100), 77 (80).

N-Methylglutarimide: Glutaric anhydride (0.175 mol, 20 g) was added to an aqueous solution of methylamine (40 %, 0.967 mol). The solution was stirred and refluxed for 4 hours, cooled, the water removed under reduced pressure and the organic residue distilled under vacuum (15 mmHg). The fraction containing the product was subsequently purified by chromatography on silica gel using ethyl acetate/*n*-hexane 5:2 as eluent. B.p.: 224° C. $\upsilon_{max/cm^{-1}}$: 1705, 1670. $\delta_H (CDCl_3)$: 2.04 (2H, q, J= 7. Hz), 2.76 (4H, t, J= 7 Hz), 3.14 (3H, s). m/z (%): 127 (75) ($M^{+\bullet}$), 98 (25) ($M^{+\bullet}$- Me-N), 70 (35) ($M^{+\bullet}$- Me-NCO), 42 (100). $C_6H_9NO_2$ requires C: 56.69 %; H: 7.08 %; N: 11.02 % found: C: 56.58 %; H: 7.14 %; N: 10.9 %.

Adipimide: Adipamide (0.14 mol; 20 g) was heated to 250-260° C, resulting in a copious evolution of ammonia. When gas evolution subsided the pressure was reduced to 60-100 mm Hg and about 1 g of water was removed. Further reduction of pressure to

12-17 mm Hg resulted in distillation of 10.4 g of a clear syrup boiling at 160-170° C. A third fraction, b.p. 180° C solidified in the receiver. Redistillation of the middle fraction though a 25 cm packed column gave three liquid fractions after removed: 1° b.p. 145-150° C (7.5 mmHg); 2°, b.p. 154-160° C (7.5 mmHg) and 3, b.p. 156-168° C (4 mmHg). Cooling fraction 2 gave a crystalline deposit which was filtered and recrystallized from benzene-petroleum ether to give 0.25 g of adipimide. m.p. 98°C. $\upsilon_{max/cm^{-1}}$:3400, 1690, 1640. δ_H ($CDCl_3$): 2.3 (4H, q, J= 7. Hz), 2.76 (4H, t, J= 7 Hz), 6.5 (H, br.). m/z (%): 127 (20) ($M^{+\bullet}$), 84 (25) ($M^{+\bullet}$- HNCO), 68 (80), 54 (80), 42 (100) $C_6H_9NO_2$ requires C: 56.69 %; H: 7.08 %; N: 11.02 %. Found: C: 57.0 %; H: 7.21 %; N: 11.2 %.

N-Methyladipimide: To a solution of adipoyl chloride (0.16 mol; 30 g) in dry ether at -78° C was added, under stirring, a large excess of methylamine. The solution was left at - 78° C for 10 minutes, and the temperature then raised to 25° C for 30 minutes. The solid was filtered off and the solvent was removed. The solid residue was heated at 250-260° C, resulting in a copious evolution of methylamine. When gas evolution subside the pressure was reduced to 60-100 mmHg and about 2 g of water were removed. Further reduction of pressure to 12-17 mmHg resulted in distillation of 15.0 g of a clear yellow syrup boiling at 150-165° C. A third fraction, b.p. 195 °C solidified in the receiver. Fraction 2 was redistilled though a 25 cm packed column to give a fraction : 1° b.p. 130-135 °C (7.5 mm); 2°, b.p. 140-150 °C (7.5 mm) and 3°, b.p. 155-160 °C (4 mm) that solidified on cooling. m.p 88° C. $\upsilon_{max/cm^{-1}}$: 1705, 1670. δ_H ($CDCl_3$): 2.04 (4H, q, J= 7. Hz), 2.76 (4H, t, J= 7 Hz), 3.14 (3H, s). m/z (%): 141 (65) ($M^{+\bullet}$), 112 (25) ($M^{+\bullet}$- Me-N), 84 (25) ($M^{+\bullet}$- Me-NCO), 55 (100) $C_7H_{11}NO_2$ requires: C: 59.57 %; H: 7.80 %; N: 9.93 %. Found: C: 59.8 %; H: 7.90 %; N: 10.1 %.

R(+)- or S(-)-N-(1-Phenylethyl)benzamide: To an aqueous solution of 10 % w/w sodium hydroxide (45 cm^3) were added benzoyl chloride (0.06 mol; 8.5 g) and R(+)- or S(-)-α-methyl benzylamine (0.05 mol; 6.6 g). The solution was maintained at pH 10, stirred vigorously, diluted with water (100 cm^3), and the product filtered, washed with water and finally recrystallized from hot methanol. $\upsilon_{max/cm^{-1}}$: 3375, 1640.

δH($CDCl_3$): 1.52 (3H, d, J= 7.2 Hz), 5.4 (1H, br.), 6.4 (1H, br.) 7.05 (5H, s), 7.15 (5H, s). m/z (%): 225 (30) ($M^{+\bullet}$), 210 (10) ($M^{+\bullet}$ - Me), 120 (10), 105 (100), 77 (40). $C_{15}H_{15}NO$ requires C: 80.0 %; H: 6.67 %; N: 6.22 %. Found for R(+)-: C: 80.05 %; H: 6.72 %; N: 6.37 %. and for S(-)-: C:80.2 %; H: 6.60 %; N: 6.40 %.

R(+)- or S(-)-N-Methyl-(1-phenylethyl)benzamide: N(+)- or S(-)-N-(1-Phenylethyl)benzamide (0.013 mol; 2.92 g) was dissolved in tetrahydrofuran (30 cm^3) and to this was added, under a N_2 atmosphere and with stirring, a solution of butyllithium in *n*-hexane (0.06 mol; 5 cm^3). After 10 minutes, a solution of iodomethane (0.11 mol) in tetrahydrofuran (5 cm^3) was added, and stirring continued for 45 minutes. Ethanol (5 cm^3) was added to terminate the reaction. The solvents were removed and the suspended in ethyl acetate (30 cm^3). The organic phase was washed with water (2 x 10 cm^3) dried ($MgSO_4$) and concentrated to give the crude product which was purified by column chromatography on silica gel (eluent: ethyl acetate/*n*-hexane 3:1). m.p 56° C. $\upsilon_{max/cm^{-1}}$ 3090, 3060, 1640. δH($CDCl_3$): 1.52 (3H, d, J= 7.2 Hz), 2.64 (3H, s), 5.4 (1H, q, J=7 Hz), 7.05 (5H, s), 7.15 (5H, s). m/z (%): 239 (30) ($M^{+\bullet}$), 224 (10) ($M^{+\bullet}$ - Me), 105 (100), 77 (45). $C_{16}H_{17}NO$ requires C: 80.30 %; H: 7.16 %; N: 5.85 %. Found for R(+)-: C: 80.1 %; H: 7.2 %; N: 5.7 %. and for S(-)-: C:80.3 %; H7.2 %; N: 5.8 %.

5-Phenyl-2-pyrrolidinone (racemic mixture):[5] A well stirred mixture of pyroglutamic acid (0.039 mol; 5 g), benzene (0.040 mol, 3.12 g) and P_2O_5/CH_3SO_3H (1/10 w/w, 35 g) was heated at 100 °C for 60 minutes. After cooling the solution was added to water (200 cm^3), then extracted with dichloromethane (3 x 30 cm^3) and dried ($MgSO_4$). After evaporation of the solvent, the solid was recrystallized from ether/ethanol 1:1. m.p. 107 °C. $\upsilon_{max/cm^{-1}}$: 3450, 1710, 1670, 1580. δ_H($CDCl_3$): 2.76 (4H, m), 4.6 (1H, t, J= 7 Hz), 6.7 (1H, br.), 7.05 (5H, s). m/z (%): 161 (100) ($M^{+\bullet}$), 107 (60) ($M^{+\bullet}$ - NCO), 84 (45) ($M^{+\bullet}$ -Ph), 77 (45) (Ph^+). $C_{10}H_{11}NO$ requires: C: 74.53 %; H: 6.83 %; N: 8.69 %. Found: C: 74.80 %; H: 6.95 %; N: 9.00 %

N-[(S)-N'-(1-Phenyl)ethyl)carbamoyl]-5-phenyl-2-pyrrolidinone: A solution of racemic 5-phenyl-2-pyrrolidinone (10.1 mmol; 1.70 g) and (S)-1-phenylethyl isocyanate (11.0 mmol; 1.62 g) in toluene (10 cm^3) was refluxed for 24 h. After cooling to room temperature the reaction mixture was washed quickly with water, dried ($MgSO_4$) and concentrated. The solid residue was dissolved in dichloromethane (5 cm^3) and filtered. The mixture of diasteroisomers was subsequently resolved using chromatography (silica gel, 97:3 dichloromethane/ acetonitrile as eluent).

High-r_f (rf. 0.8) diasteromer: colourless solid. m.p.: 100 °C. $\upsilon_{max/cm^{-1}}$: 3230, 1705, 1680, 1510, 1230. δ_H ($CDCl_3$): 1.52 (3H, d, J=5 Hz), 1.87-1.96 (1 H, m), 2.44-2.79 (3H, m), 4.90-5.0 (1H, m), 5.3-5.35 (1H, m), 7.0-7.21 (10H, m), 8.90 (1H, d, J= 5 Hz). m/z (%): 308 (15) ($M^{+\cdot}$), 293 (10) ($M^{+\cdot}$ - Me), 188 (10) ($M^{+\cdot}$ - $PhCHCH_2NH$), 160 (20) (M^+ -$PhCHCH_2NHCO$), 120 (100).

Low-r_f (rf. 0.5) diasteromer: colourless oil: $\upsilon_{max/cm^{-1}}$: 3240, 1700, 1670, 1520, 1220. δ_H ($CDCl_3$): 1.52 (3H, d, J=5 Hz), 1.85-2.00 (1 H, m), 2.40-2.70 (3H, m), 4.90-5.05 (1H, m), 5.35-5.45 (1H, m), 7.10-7.30 (10H, m), 8.91 (1H, d, J=5Hz). m/z (%): 308 (15) ($M^{+\cdot}$), 293 (10) ($M^{+\cdot}$ - Me), 188 (10) ($M^{+\cdot}$ - $PhCHCH_2NH$), 160 (20) ($M^{+\cdot}$ -$PhCHCH_2NHCO$), 120 (100).

R- and S-5-Phenyl-2-pyrrolidinone (enantiomerically pure)[6;7;8]: A solution of diasterometically pure N-[(S)-N'-(1-phenylethyl)carbamoyl]-5-phenyl-2-pyrrolidinone (5.0 mmol; 1.54 g) and sodium methoxide (17.6 mmol; 0.95 g) in tetrahydrofuran (150 cm^3) was refluxed for 48 h. After cooling to room temperature, saturated ammonium chloride (100 cm^3) and 3M hydrochloric acid (100 cm^3) were added successively, and the organic phase was separated, washed with brine and dried ($MgSO_4$). After filtration and concentration, the residue was chromatographed on silica gel with ethyl acetate as the mobile phase. The desired lactam was collected and, after recrystallization pure 5-phenyl-2-pyrrolidinone was obtained. The absolute configuration of the lactams was confirmed by using the NMR chiral resolving agent (S)-2,2,2-

trifluoro-1-(9-anthryl)ethanol as reported.[6;7;8] m.p. 107 °C. $\upsilon_{max/cm^{-1}}$: 3450, 1710, 1670, 1580. δ_H ($CDCl_3$): 2.76 (4H, m), 4.6 (1H, t, J=7 Hz), 6.7 (1H, br.), 7.05 (5H, s). m/z (%): 161 (100) ($M^{+\bullet}$), 107 (60) ($M^{+\bullet}$ - NCO), 84 (45) ($M^{+\bullet}$ -Ph), 77 (45) (Ph^+). $C_{10}H_{11}NO$ requires: C: 74.53 %; H: 6.83 %; N: 8.69 %. Found: for R: C: 74.50 %; H: 7.00 %; N: 8.55 % For S: C: 74.45 %; H: 6.88 %; N: 8.40 %

R- and S-N-Methyl-5-phenyl-2-pyrrolidinone: R- or S-5-Phenyl-2-pyrrolidinone (3 mmol, 483 mg) is dissolved in dry tetrahydrofuran (50 cm^3) and maintained under a N_2 atmosphere. With continuos stirring sodium hydride (3.3 mmol; 79.2 mg) followed by iodomethane (15 mmol, 2.13 g) was added and left at room temperature for 48 h. After removal the solvent the solid residue was resuspended in ethyl acetate (20 cm^3), washed with water (2 x 10 cm^3) and dried ($MgSO_4$). After concentration, the product was purified by silica gel chromatography using 3:1 ethyl acetate/hexane as the mobile phase. $\upsilon_{max/cm^{-1}}$: 1720, 1660, 1580. δ_H ($CDCl_3$): 2.76 (4H, m), 3.2 (3H, s), 4.6 (1H, t, J= 7 Hz), 7.05 (5H, s). m/z (%): 175 (70) ($M^{+\bullet}$), 145 (50) ($M^{+\bullet}$ - MeN), 117 (60) ($M^{+\bullet}$ - MeNCO), 98 (40) ($M^{+\bullet}$ -Ph), 77 (40) (Ph^+). $C_{11}H_{13}NO$ requires: C: 75.43 %; H: 7.43 %; N: 8.00 % Found: for R: C: 75.80 %; H: 7.65 %; N: 8.30 %. For S: C: 75.60 %; H: 7.78 %; N: 8.20 %

N-Methyl-4-oxo-4-phenylbutanamide: A solution of 3-benzoylpropionic acid (15 mmol, 2.67 g) and triethylamine (15 mmol, 2.1 cm^3) in dry tetrahydrofuran (25 cm^3) was cooled at -10° C. A solution of ethyl chloroformate (15 mmol, 1.6 g) in tetrahydrofuran (25 cm^3) was added dropwise with stirring. After 30 minutes a large excess of dry methylamine was added and the solution was left at room temperature for 1 h. The solution was filtered and the oil obtained after solvent evaporation was dissolved in dichloromethane (50 cm^3), washed with 0.1 M hydrochloric acid (2 x 10 cm^3), aqueous saturated sodium bicarbonate (2 x 10 cm^3) and dried ($MgSO_4$). Evaporation of the solvent gave the desired product. $\upsilon_{max/cm^{-1}}$: 3300, 1680, 1640, 1580. δ_H ($CDCl_3$): 2.3-2.72 (4H, m), 3.28 (3H, d), 6.1 (1H, br.), 7.2-7.48 (5H, m). m/z (%): 191 (20) ($M^{+\bullet}$), 174 (10) ($M^{+\bullet}$ -OH), 161 (15) ($M^{+\bullet}$ -$NHCH_3$), 133 (20) ($M^{+\bullet}$ -MeNCO), 114

(30) ($M^{+\cdot}$ -Ph), 105 (100), 77 (60). $C_{11}H_{13}NO_2$ requires: C: 69.09 %; H: 6.85 %; N: 7.32 %. Found: C: 68.87 %; H: 7.02 %; N: 7.22 %.

4-Oxo-4-phenylbutanamide: The procedure used for N-methyl-4-oxo-4-phenylbutanamide was followed using ammonia in place of methylamine. $\upsilon_{max/cm^{-1}}$: 3410, 3250, 1700, 1650, 1580. δ_H ($CDCl_3$): 2.6 (2H, t, J= 5Hz), 3.2 (2H, t, J= 5 Hz), 5.7 (1H, br.), 5.8 (1H, br), 7.2-7.52 (5H, m). m/z (%): 177 (20) ($M^{+\cdot}$), 160 (10) ($M^{+\cdot}$ -OH), 133 (10) ($M^{+\cdot}$ -NH_2CO), 105 (100), 77 (60). $C_{10}H_{11}NO_2$ requires: C: 67.78 %; H: 6.26 %; N: 7.90 %. Found: C: 67.41 %; H: 6.20 %; N: 7.80 %.

N-Chloromethyl-N-methylformamide: N-Methylformamide (0.02 mol, 1.18 g), was dissolved in trimethylsilylchloride (50 cm^3). Paraformaldehyde (2.0 g) was added and the solution refluxed for 2 h. After cooling the solvent was removed to give the desired product. $\upsilon_{max/cm^{-1}}$: 1680, 1610, 1280, 1260. δ_H ($CDCl_3$): 3.00 (3H, s), 5.56 (2H, s), 8.28 (1H, s). m/z (%): 107 (15) ($M^{+\cdot}$), 58 (40) ($M^{+\cdot}$ - CH_2Cl), 43 (100), 29 (10).

N-Chloromethyl-N-methylacetamide: was synthesised following the method reported by Moreira *et al.*[4]

N-*tert*-Butyl-N-formyl-N-hydroxy-N-methyl-1-phenyl-1,2-diaminoethane (PBN-DMF adduct): N-Chloromethyl-N-methylformamide (0.01 mol, 1.07 g) and PBN (0.01 mol, 1.77 g), were dissolved in dry acetonitrile (20 cm^3) and refluxed. A solution of acetonitrile (5 cm^3) containing 1,1-azobis(cyclohexanecarbonitrile) (0.001 mol, 0.24 g) and tributyltin hydride (0.001 mol, 0.29 g) was added dropwise within 30 minutes. The mixture was refluxed for a further 30 minutes. After cooling, the solvent was removed and the solid residue purified by silica gel chromatography using diethyl ether as eluent. $\upsilon_{max/cm^{-1}}$: 3460, 1700, 1610, 1508, 1460, 1380, 1200, 1100. δ_H ($CDCl_3$): 2.0 (9H, s), 3.05 (3H, s), 3.7 (2H, d, J=5 Hz), 4.7 (1H, t , J=5 Hz), 7.28 (5H, m), 8.15 (1H, m). m/z (%): 250 (10), 234 (10), 192 (15), 162 (30), 77 (100).

N,N-Dimethyl-2-(N'-*tert*-butylhydroxylamino)phenylacetamide (PBN-DMF adduct II): N,N-dimethylcarbamyl chloride (0.01 mol, 1.07 g) and PBN (0.01 mol, 1.77 g), were dissolved in dry acetonitrile (20 cm3) and refluxed. A solution of acetonitrile (5 cm3) containing 1,1-azobis(cyclohexanecarbonitrile) (0.001 mol, 0.24 g) and tributyltin hydride (0.001 mol, 0.29 g) was added dropwise within 30 minutes. The mixture was refluxed for a further 30 minutes. After cooling, the solvent was removed and the solid residue purified by silica gel chromatography using diethyl ether as eluent. $\upsilon_{max/cm}$-1: 3440 1700, 1600, 1525, 1420. δ_H (CDCl3): 2.05 (9H, s), 3.10 (3H, s), 5.3 (1H, t , J=5 Hz), 7.40 (5H, m), 8.6 (1H, br). m/z (%): 250 (8), 233 (20), 206 (25), 190 (30), 77 (100).

N-Acetyl-N-*tert*-butyl-N-hydroxy-N'-methyl-1-phenyl-1,2-diaminoethane (PBN-DMAC adduct): N-Chloromethyl-N-methyl acetamide (0.01 mol, 1.21 g) and PBN (0.01 mol, 1.77 g), were dissolved in dry acetonitrile (20 cm^3) and refluxed. A solution of acetonitrile (5 cm^3) containing 1,1-azobis(cyclohexanecarbonitrile) (0.001 mol, 0.24 g) and tributyltin hydride (0.001 mol, 0.29 g) was added dropwise within 30 minutes. The mixture was refluxed for a further 30 minutes. After cooling, the solvent was removed and the solid residue purified by silica gel chromatography using diethyl ether as eluent. $\upsilon_{max/cm^{-1}}$: 3500, 1705, 1600, 1520, 1440, 1380, 1210, 1110. δ_H ($CDCl_3$): 1.90 (9H, s), 2.34 (3H, s) 3.12 (3H, s), 3.6 (2H, d J=4.5Hz), 4.5 (1H, t, J=5 Hz), 7.12 (5H, m). m/z (%): 263 (15), 248 (10), 206 (15), 176 (40), 77 (100).

N-(3-Butynyl)formamide: Formamide (0.02 mol; 0.6 g) was dissolved dry tetrahydrofuran (20 cm^3). To this solution, under N_2 and at -10 °C, lithium diisopropylacetamide (0.018 mol) was added dropwise. After 15 minutes dry tetrahydrofuran (10 cm^3) containing 3-butynyl-4-toluenesulfonate (0.02 mol; 2.66 g) was added dropwise; the solution was left at room temperature for 1 h then refluxed for further 3 h. The solvent was removed and the solid residue was resuspended in dichloromethane (50 cm^3), washed with water (2 x 30 cm^3) and dried ($MgSO_4$). After

concentration, the crude mixture was purified by silica gel chromatography using 7/3 dichloromethane/methanol as eluent. $\upsilon_{max/cm^{-1}}$: 3350, 3300, 3150, 1710, 1650, 1550, 1500, 1480. δ_H ($CDCl_3$): 1.9 (1H, t, J= 2.0 Hz), 2.3 (2H, m, J_1=2 Hz, J_2= 5 Hz), 3.2 (2H, m, J= 5 Hz), 6.8 (1H, br.), 8.28 (1H, m). m/z (%): 97 (30), 73 (15), 53 (50), 43 (100). C_5H_7NO requires: C: 61.85 %; H: 7.21 %; N: 14.43 %. Found: C: 62.00 %; H: 7.31 %; N: 14.00 %.

N-(3-Butynyl)-N-methylformamide: The method employed for N-(3-butynyl)formamide was followed substituting N-methylformamide for formamide. $\upsilon_{max/cm^{-1}}$: 3050, 1650, 1580, 1550, 1520, 1500, 1480, 1400, 1350, 1300, 1280. δ_H ($CDCl_3$): 1.9 (1H, t, J= 2.0 Hz), 2.3 (2H, m, J_1=2 Hz, J_2= 5 Hz), 2.92 (3H, s), 3.2 (2H, m, J= 5 Hz), 8.31 (1H, m). m/z (%): 111 (18), 96 (70), 87 (10), 58 (100). C_6H_9NO requires: C: 64.86 %; H: 8.11 %; N: 12.61 %. Found: C: 64.60 %; H: 8.26 %; N: 12.75 %.

N-(3-Butynyl)-N-chloromethylformamide: N-(3-butynyl)formamide (0.02 mol, 1.94 g), was dissolved in of trimethylsilyl chloride (50 cm^3). Paraformaldehyde (2.0 g) was added and the solution refluxed for 2 h. After cooling the solvent was removed to give the desired product $\upsilon_{max/cm^{-1}}$: 3050, 1650, 1580, 1550, 1520, 1500, 1480, 1400, 1350, 1300, 1280. δ_H ($CDCl_3$): 1.9 (1H, t, J= 2.0 Hz), 2.3 (2H, m, J_1=2 Hz, J_2= 5 Hz), 3.2 (2H, m, J= 5 Hz), 5.30 (2H, s), 8.40 (1H, m). m/z (%): 147 (5) ($M^{+\bullet}$), 110 (25), 96 (55) ($M^{+\bullet}$ - CH_2Cl), 56 (100).

N-Methyl-2,4-piperidinedione: Methyl acrylate (0.5 mol; 56 g) was dissolved in methanol (200 cm^3) and this solution 6M methylamine in methanol was added (92 cm^3, 0.55 mol). The solution was left under stirring at room temperature for 2 days, after which time the solvent was removed and the oily residue distilled, at 56-60° C, 17 mmHg. The pure methyl-3-methylaminopropionate obtained from distillation (0.05 mol, 5.61 g) was dissolved in dry diethyl ether (100 cm^3). Triethylamine (0.055 mol; 5.61 g) was added the mixture cooled to 0° C, and a dry diethyl ether solution (20 cm^3)

containing methyl malonylchloride (0.05 mol; 6.1 g) was added. The temperature was brought to 18-20° C and the mixture left under vigorous stirring for 1 hour. At the end of the reaction, solid triethylaminehydrochloride was filtered off, the organic phase washed with water (2 x 50 cm^3), dried ($MgSO_4$) and the solvent was removed under reduced pressure to give a yellow oil. This oil (0.02 mol; 4.34 g) was dissolved in methanol (50 cm^3), to which sodium methoxide (0.022 mol, 1.2g) was added, and mixture was refluxed for 3 hours. After cooling, the solvent was removed and the solid residue dissolved in 10 % (w/v) aqueous HCl and extracted with ethyl acetate (3 X 30 cm^3). The organic phase was washed with water (2 x 20 cm^3), dried ($MgSO_4$) and the solvent was removed under reduced pressure to give a pale yellow oil. The oily residue was suspended in 0.5 M NaOH (50 cm^3) and the mixture refluxed for 30 minutes. After cooling to 0° C, concentrated hydrochloric acid was added to obtain a pH 4 ~ 5, the solution extracted with dichloromethane (3 x 30 cm^3). the organic phase was collected, washed with water (2 X 20 cm^3), dried ($MgSO_4$) and the solvent was removed under reduced pressure to give the desired product. $\upsilon_{max/cm^{-1}}$: 1750, 1670, 1550, 1520, 1500, 1480, 1400, 1350, 1300, 1280. δ_H ($CDCl_3$): 2.5 (2H, m), 3.0 (2H, s), 3.2 (2H, m), 3.4 (3H, s). m/z (%): 127 (15), 112 (100), 71 (25). $C_6H_9NO_2$ requires: C: 56.70 %; H: 7.08 %; N: 11.02 %. Found: C: 56.60 %; H: 7.28 %; N: 11.25 %.

N-Formyl-4-piperidinone: Acetic formic anhydride was generated by dropwise addition of 98% formic acid (160 mmol; 7.5 g) to acetic anhydride (130 mmol; 13.5 g) maintained at 0° C under a N_2 atmosphere followed by gentle heating (50- 60° C). The mixture was cooled to room temperature and dry tetrahydrofuran (20 cm^3) was added. To this solution was added a tetrahydrofuran (20 cm^3) solution containing 4-piperidinone hydrochloride (50 mmol; 6.7 g). The mixture was maintained at room temperature with vigorous stirring for 3 h. The volatile components were removed under reduced pressure to give the product. $\upsilon_{max/cm^{-1}}$: 1710, 1670, 1550, 1520. δ_H ($CDCl_3$): 2.0 (4H, m), 3.3 (4H, m), 9.1 (1H, s). m/z (%): 127 (35),110 (35), 98 (100).

$C_6H_9NO_2$ requires: C: 56.70 %; H: 7.08 %; N: 11.02 %. Found: C: 56.95 %; H: 7.50 %; N: 11.40 %.

N,N-Dimethylformamide-haem adducts: N-Chloromethyl-N-methylform- amide (0.01 mol, 1.07 g) and hemin (1.5 mmol, 1.0 g), were dissolved in dry acetonitrile (20 cm^3) and refluxed. A solution of acetonitrile (5 cm^3) containing 1,1-azobis(cyclohexanecarbonitrile) (0.001 mol, 0.24 g) and tributyltin hydride (0.01 mol, 0.29 g) was added dropwise over 30 minutes. The mixture was refluxed for 30 minutes and after cooling, the solvent was removed. The solid residue was resuspended in diisopropylamine/methanol (25:975 v/v) (1 cm^3) and analysed by HPLC as indicated.

8.4 Microsomes

Phenobarbital-induced rat liver microsomes were obtained from Institute of Cancer Research, Cancer Research Campaign Laboratory, Sutton, Surrey, U.K. Pyridine-induced microsomes were from Institute of Occupational Medicine, University of Padua, Italy.

P450-specific contents were 0.70 and 1.95 nmol/mg microsomal protein for pyridine- and phenobarbital-induced microsomes respectively.

8.5 Microsomal incubations

These were performed in 0.1M pH 7.4 phosphate buffer, using microsomal concentrations of 2.0 and 1.5 mg protein/cm^3 for pyridine- and phenobarbital-induced microsomes respectively, in the presence of an NADPH regenerating system constituted by: 6.25 nmol/cm^3 of glucose-6-phosphate, 1.25 mmol/cm^3 of NADP, 6 mmol/cm^3 of $MgCl_2$ and 2.5 U/cm^3 of glucose-6-phosphate dehydrogenase. The incubations were stabilised at 36° C in a shaking bath for 10 minutes, and the reaction started by addition of the substrate dissolved in 0.1 M pH 7.4 phosphate buffer or in methanol. Substrates concentrations used for the kinetic studies were between 0.5 and 10 mM. Aliquots of incubation mixture were collected for the preparation of the analytical sample.

8.6 Biomimetic system incubations

A 2 mM solution of TPP in dry dichloromethane (2.5 cm^3) in the presence of *tert*-butylhydroperoxide 0.8 M was used. This solution was stabilised at 30° C for 10 minutes in a shaking bath, and the reaction started by addition of the substrate dissolved in dichloromethane. Substrate concentrations used were 0.5-10 mM. Aiquots of incubation mixture were collected for the preparation of the analytical sample.

8.7 Analytical procedure

8.7.1 Sample preparation from microsomal incubations

Aliquots (100 µl) of microsomal incubation mixtures were withdrawn at time intervals and added to a 10% (w/v) solution of trichloroacetic acid (200 µl) to precipitate protein. After centrifugation (5 minutes, 4500 rpm) the supernatant (200 µl) was treated with 1 M NaOH (200 µl) for 10 minutes, then acidified with 1M HCl (200 µl). Samples were then analysed using the appropriate analytical method.

8.7.2 Sample preparation from biomimetic system incubations

Aliquots (100 µl) of biomimetic incubation mixtures were withdrawn at time intervals, added to ethanol (200 µl) to terminate the reaction, subjected to 1M methanolic KOH (200 µl), left for 10 minutes then acidified with 1M methanolic HCl (200 µl). The samples were dried and resuspended in 1:1 methanol/water (1 cm^3) for HPLC analysis or in dry acetonitrile (1 cm^3) for gas chromatographic analysis.

8.7.3 Gas chromatographic analysis

For all methods a Perkin Elmer 8410 Gas Chromatograph was used with direct on column injection. Column: aluminium 12 m, 0.5 mm i.d. BP1 0.1µm thickness. Carrier gas He. Detector FID at 250° C. Injection temperature 210° C.

For the analysis of the products from the reactions of N-methyl-2-piperidione, N-methyl-2-pyrrolidinone and N-methylcaprolactam, two gas chromatographic methods were developed. The first, for the analysis of N-methyl-2-piperidinone, N-methyl-2-pyrrolidinone, N-methylcaprolactam, N-methylglutarimide, N-methylsuccinimide and N-methyladipimide, was isothermal at 90° for 10 minutes. For the analysis of glutarimide, δ-valerolactam, succinimide, 2-pyrrolidinone, adipimide and caprolactam a derivatization method was employed. The sample was dried under N_2 flow and resuspended in 100 μl of dry acetonitrile; 50 μl of this solution were added to N-methyl-N-*tert*-butyldimethylsilyltrifluoroacetamide (MTBSFA) (50 μl), sonicated for 5 minutes and heated at 100° C for 2h. After cooling the sample was analysed using thermal gradient system: 2 minutes isothermal at 90° C, thermal gradient from 90° C to 140° C with a ramp rate of 5° C/min, isothermal at 140° C for 1 minute.

For the determination of the products from the microsomal oxidation of DMF and DMAC an isothermal system at 70° C for 10 minutes was used.

8.7.4 HPLC analysis

Separation of the amides was achieved using a 5 μm C18 25 cm Jones Chromatography column and an eluent consisting of by: solvent A): 5% acetonitrile in phosphate buffer 0.05 M pH 2; solvent B): 60% acetonitrile in phosphate buffer 0.05 M pH 2. A gradient method was used as follows: T= 0 min to T= 15 min from 40% to 0% solvent A, T= 15 min to T= 18 min 100% solvent B, T=18 min to T= 19 min from 0% to 40% solvent A. Flow :1 cm^3/min. The wavelength used for detection was 254 nm. The identification of the products of the reactions was achieved by comparison of their diode array UV-VIS spectra with those of synthetic standards. Injection loop: 20 μl . Separate injections were reproducible to ± 1.5 % and the concentrations of products determined by this technique were accurate to ± 2%.

8.7.5 Gas Chromatographic/Mass spectra (GC/MS) analysis of the products of the microsomal oxidations of amides

For all methods a Hewlett Packard 5890 Gas Chromatograph was used with direct on column injection. Column: SGE 25Q C3 BP5 0.5 12 m, 0.22 mm i.d. BP5 0.25 μm thickness. Carrier gas He. Mass spectrometer VG Mass Lab, VG 20-250, Micromass UK Ltd. Interface at 280° C, source 200 EI.

Samples for the GC/MS analysis from the metabolites of the microsomal oxidations of the amides, were prepared *via* direct extraction of the reaction mixture (previously sutured by addition of ammonium acetate) using ethyl acetate (2 cm^3). The organic phase was collected, dried ($MgSO_4$) and directly injected (0.5 μl) into the gas chromatograph without dilution. The following thermal gradient systems were used:

N,N-dimethylaniline, N,N-dimethylbenzamide and N-cyanomethyl-N-methylaniline: 2 minutes isothermal at 110° C, thermal gradient from 110° C to 190 ° C with a ramp rate of 10° C/min, isothermal at 190° C for 10 minutes.

N,N-dimethyl-2-vinyl benzamide and N,N-dimethyl-2-hydroxy benzamide: 1 minute isothermal at 85° C, thermal gradient from 85° C to 270 ° C with a ramp rate of 10° C/min, isothermal at 270° C for 20 minutes.

N-butynyl and N-butenyl substrates: 1 minute isothermal at 110° C, thermal gradient from 85° C to 270 ° C with a ramp rate of 10° C/min, isothermal at 270° C for 10 minutes.

8.7.6 ESR analysis of PBN spin-trapped radicals

Typical microsomal incubations containing the amide and the PBN spin trap, were performed for 30 minutes at 37° C. The reaction mixture was extracted using chloroform/methanol 2:1 (2 cm^3 of extraction solvent for each 1 cm^3 of incubation mixture). The organic phase was separated and the volume reduced to 0.5 cm^3 by a flow

of N_2. The solution from the reaction between the chemical generated radical and PBN were dried by a N_2 flow and dissolved in chlorofom/methanol 2:1 (1 cm^3).

The sample was placed in an ESR tube and analysed using the following conditions: scan range ± 200 G, time constant 0.5s, modulation amplitude 1 G, modulation frequency 100 KHz, receiver gain 6 X 10^4, microwave power 10 mW, temperature 25° C, microwave frequency 9.155074 GHz.

8.7.7 Determination of microsomal protein

The concentration of the microsomal proteins content was determined by the method of Lowry [9] using bovine serum albumin as standard.

8.7.9 Determination of cytochrome P450

Cytochrome P450 content was determined following the method of Omura and Sato[10; 11] from the difference of absorbance between 490 and 450 nm in the spectrum of the P450-CO complex

8.7.10 Determination of microsomal haem

Microsomal haem was determined by two different assays, the pyridine/haemochromogen method [12] and the measurement of the fluorescence of protoporphyrin IX by the method of Morrison.[13] Briefly, in the haemochomogen/pyridine method, 300 µl of incubation mixture were added to of a pyridine/ 0.3 M NaOH solution (9:5, v/v) (700 µl). To this mixture a few crystals of sodium dithionite were added and the absolute spectrum was recorded in a wavelength range of 500-560 nm. Determination of the haem was achieved using $\varepsilon_{mM(557-541)}$= 20.7 $mM^{-1} \cdot cm^{-1}$ suggested by Falk.[14] The determination of the haem by the porphyrin fluorescence technique was performed by converting the haem into protoporphyrin IX in saturated oxalic acid at 100° C for 30 minutes. The fluorescence using an excitation wavelength of 408 nm and an emission wavelength of 604 nm was recorded.

Quantification of the content of protoporphyrin IX in the sample was obtained by comparison with the fluorescence of a standard of protoporphyrin IX dimethyl ester.

8.7.11. HPLC analysis of microsomal haem

For the HPLC analysis of microsomal haem, 200 µl of reaction mixture were added to diisopropylamine/methanol (25/975 v/v) (9800 µl) solution. The mixture was centrifuged for 20 minutes at 1600 g., then 50 µl of supernatant were directly injected into the HPLC. Separation was achieved using a PLR PS column (5 µm, 100 Å, 25 cm, 4.6 mm i.d.) and an elution system of diisopropylamine/ water/ methanol (25/75/900) isocratically at a flow of 1.0 cm^3/min for 20 minutes. Haem was detected at a wavelength of 400 nm.

8.8.Determination of the kinetic parameters of the P450-mediated oxidations

The microsomal oxidations of the indicated substrates were carried out at 37° C as previously described. The rate of the of the reactions was monitored over two hours. The plot of the formation of the metabolites *versus* time showed, in all the oxidations analysed, the presence of an initial linear phase subsequently followed by a "tailing-off" in the reaction progress. Thus, for the determination of the kinetic parameters the initial linear rate (v_i) was measured. The kinetic parameters (V_{max} and V_{max}/K_m) of the reactions were determined from the Michaelis-Menten equation (eq. VIII.1, where [S] is the initial substrate concentration in the reaction) by using the Hanes linearization method (eq. VIII. 2).

$$v_i = \frac{V_{max} \cdot [S]}{[S] + K_m} \qquad \text{(VIII.1)}$$

$$\frac{[S]}{v_i} = \frac{K_m}{V_{max}} + \frac{[S]}{V_{max}} \qquad \text{(VIII.2)}$$

The choice of the Hanes plot over the more common linearization Lineweaver-Burke method is because the latter is biased towards the values of v_i that possess greatest error.

8.9 Molecular orbital calculation

Structural determination and heats of formation (ΔH_f) for the amides and their postulated intermediate radicals and radical cations, were calculated using the semi-empirical AM1 self-consistent-field molecular-orbital program within the MOPAC package.[15] Radical structures were determined using unrestricted Hartree-Fock calculations. All the structures were geometrically optimised using the Broyden-Fletcher-Goldfarb-Shanno procedure. Computations were performed using a Silicon Graphic Indy workstation computer.

Differences in the heats of formation between the parent amide and the radical intermediates ($\Delta\Delta H_f$) were used as an estimate for the energy of activation Ea, from which relative rate constants could be calculated as follows:

$$K_1 = e^{-E_a^1 / RT} \qquad \text{for amide 1}$$

$$K_2 = e^{-E_a^2 / RT} \qquad \text{for amide 2}$$

So:
$$\frac{K^1}{K^2} = e^{E_a^2 - E_a^1 / RT}$$

or
$$\ln \frac{K_1}{K_2} = \frac{E_a^2 - E_a^1}{RT} = \frac{\Delta\Delta H_f^2 - \Delta\Delta H_f^1}{RT}$$

8.10 References

1 Vedejs E., Engler D.A. and Telschow J.E., (1978); *J.Org. Chem.*; **43**, 2: 188-

2 Dagne E. and Castagnoli N. Jr., (1972); *J. Med. Chem.*; **15**, 4: 356-

3 Constantino L., Rosa E. and Iley J., (1992); *Biochem. Pharmacol.*; **44**: 651-

4 Moreira R., Mendes E., Caldheiros T., Bacelo M.J. and Iley J., (1992); *Tetrahedron Lett.*; **35**, 38: 7107-

5 Rigo B., Fasseur D., Cherapy N. and Couturier D., (1989); *Tetrahedron Lett.*; **30**, 50: 7057-

6 Pirkle W.H., Robertson M.R. and Hyun H., (1984); *J. Org. Chem.*; **49**, 13: 2433-

7 Pirkle W.H. and Sikkenga D.L., (1977); *J. Org. Chem.*; **42**: 1370-

8 Pirkle W.H. and Hoover D., (1982); *Top. Stereochem.*; **13**: 263-

9 Lowry O. H., Rose N.J., Farr A.L. and Randal R.J., (1951); *J. Biol. Chem.*; **193**: 265-

10 Omura T. and Sato R., (1964); *J. Biol. Chem.*; **239**: 2370-

11 Omura T. and Sato R., (1964); *J. Biol. Chem.*; **239**: 2379-

12 PaulK.G., Theorell H. and Akeson A., (1953); *Acta Chem. Scand.*; **7**: 1284-

13 Morrison G.R., (1965); *Anal. Chem.*; **37**: 1124-

14 Falk J.E. (1964); Appendix 1. Absorption spectra. In: *Porphyrins and Metalloporphyrins* (J.E. Falk, Ed.); 231-

15 MOPAC 4.0, quantum chemistry programme exchange; QPCE No 455, Indiana University.